Università degli Studi di Palermo

AREA RICERCA E TRASFERIMENTO TECNOLOGICO
SETTORE DOTTORATI E CONTRATTI PER LA RICERCA
U. O. DOTTORATI DI RICERCA

Corso di Dottorato in Sistemi Agro-Alimentari e Forestali Mediterranei
Dipartimento di Scienze e Agrarie, Alimentari e Forestali
SSD AGR/08

Hydraulic characterization of eco-sustainable growing substrates for urban green infrastructures

LA DOTTORESSA
Dott.ssa Cristina Bondì

IL COORDINATORE
Prof. Vincenzo Bagarello

IL TUTOR
Prof. Massimo Iovino

IL CO TUTOR
Prof. Vincenzo Bagarello

CICLO XXXVII
ANNO CONSEGUIMENTO TITOLO 2023-2024

DOTTORATO

Acknowledgments

My deepest and most heartfelt thanks go to my family. To my mother, for never allowing me to give up during challenging times, you are the guiding light of my life. To my sister, for sharing both my moments of joy and worries, I hope that you can realize all your dreams. To my father, for having faith in my abilities and for his unwavering economic support throughout this long academic journey. To my babies, Polly and Isabella. To my grandfather Angelo and grandmother Zina, I miss you. I am deeply grateful to all of you, I love you.

I extend my sincere gratitude to my colleague and dear friend, Doctor Gaetano Caltabellotta, for his support during the PhD course.

I also thank all the people with whom I have had the pleasure of collaborating during this journey: Doctor Sergio Andri, Doctor Nicolò Auteri, Doctor Dario Autovino, Doctor Mirko Castellini, Professor Filippo Saiano, Professor Riccardo Scalenghe, and Professor Vincenzo Bagarello, co-tutor of my thesis and source of inspiration for research ideas.

Last, but not least, I would like to express my heartfelt thanks to my tutor, Professor Massimo Iovino, for the valuable guidance provided and for believing in me from the first day of my PhD. He has been and will remain, my mentor, imparting to me the passion and knowledge essential to becoming, I hope, a competent and dedicated researcher.

Finally, my thoughts go to all the women who, like me, dreamed as children of studying, attending university, participating in sports, and pursuing their aspirations, but are unable to realize these dreams due to the circumstances of their birthplace and the constraints of their society.
I hope that one day the world will open its eyes and remember you.
Until then, "Woman, Life, Freedom".

Index

Abstract

In highly urbanized contexts, green roofs are increasingly studied and utilized as sustainable solutions for capturing and modulating runoff to achieve hydraulic and hydrological invariance. They reduce the total volume of runoff and mitigate the ridge flow returned to the sewer system through two hydrological processes: rainfall retention, which is the permanent removal of stormwater, and runoff detention, which is the transient storage of rainfall. Both processes are conditioned by the physical and hydraulic properties of the substrate or culture medium, a key aspect that is still little investigated. This thesis represents a contribution to fill the gap of knowledge in the field of hydraulic characterization of substrates for green roofs, with a view to environmental sustainability and circular economy. Through a comprehensive and multi-scalar methodological approach, this thesis assessed: *i*) the effects of adding different organic soil amendments, such as compost, vermicompost, and pruning residues, on the soil water retention curve and the related indicators of soil physical quality (SPQ); *ii*) the assessment of the retention and detention capacities of a volcanic medium suitable for green roof system under intense rainfall events; *iii*) the changes in substrate hydraulic characteristics of a prototype green roof plot throughout the lifecycle The soil water retention curve, $\theta(h)$, was determined by the tension hanging water column apparatus and the pressure plate extractors. Measurements of the hydraulic conductivity fuction, $K(h)$, were conducted by either the evaporation method and the MiniDisk Infiltrometer (MDI). A needle rainfall simulator was applied to determine the retention/detention of green roof microcosms assembled with different drainable layers.) a field assessment of substrate hydraulic changes throughout the lifecycle on a prototype green roof plot. The hydraulic conductivity curves, $K(h)$, were determined by using the MiniDisk Infiltrometer (MDI).

All the amendments applied demonstrated a positive impact on the hydraulic properties of the substrates, significantly enhancing the soil water retention and improving physical quality. The results underscore the potential of organic amendments to improve soil structure and optimize water management, as they increased plant-available water in coarse-textured soils and improved the air/water balance in fine-textured soils. However, soil texture and aging of the substrate proved to influence the soil physical quality, therefore careful consideration must be given to soil texture and the temporal variability of the beneficial effects on the soil physical quality, which tend to diminish over time, when the selecting selection of the amendment, determining its optimal dosage, and planning the application schedule. Moreover, the volcanic medium analyzed has demonstrated a favorable hydrological response, thus encouraging its use in combination with amendments like compost or vermicompost. This establishes it as an effective and sustainable choice for the mineral component of a green roof substrate in Mediterranean climates, especially when it is combined with a well-balanced mixture of organic materials such as compost or vermicompost.

1. Introduction

In recent decades, there has been an exponential growth in the human population. According to recent statistics from the Statistical Office of the European Union (Eurostat), between 2001 and 2020, the population of the European Union (EU) increased from 429 million to 447 million, a growth of 4 %. This led to an increase in urban areas and urbanization processes with the development of impervious surfaces and resulting runoff increase. Soil sealing, caused by covering the ground with artificial impermeable materials such as concrete or asphalt, is one of the main causes of soil degradation in EU territories, negatively affecting the vulnerability of environmental systems and the hydrological cycle (Tobias et al., 2018). The European Environment Agency (EEA) has highlighted that in the past decade, impervious surfaces in the EU have increased by 5%. Soil sealing results in a reduction of the natural hydrological processes of water infiltration into the soil and interception by vegetation, causing a rapid transformation of rainwater into surface runoff that, usually, is entirely loaded on the urban drainage network (Pistocchi, 2017; Scalenghe and Marsan, 2009). These negative effects are particularly evident and disastrous in Mediterranean regions, which are increasingly and frequently affected by intense weather events concentrated in space and time. Recurrent and severe floods have increasingly overloaded the urban drainage systems in recent years with consequent huge damages in densely anthropizated areas.

On July 15, 2020, the city of Palermo was hit by an intense meteoric event that brought about 130 mm of rain over 3 hours, causing extensive damage to homes and people. Between 24 and 26 October 2021, more than 300 mm of rain fell in the city of Catania, causing landslides and flooding. On November 26, 2022, an intense meteoric event, with about 126 mm of rain in 6 hours, hit the island of Ischia, causing 12 victims and countless material damage in the area. From 2 to 5 November 2023, several areas in Tuscany were struck by a devastating flood caused by torrential rains, leading to the overflow of rivers such as the Bisenzio, significant damage, and loss of life, prompting Tuscany to declare a state of national emergency on November 3. Therefore, experts are wondering whether the traditional “grey” urban drainage works will be able to cope the more and more intense rainfall events caused by the future scenario of climate change.

Awareness of the seriousness of these problems has prompted a reconsideration of traditional engineering solutions, aiming, instead, to maintain or reestablish as much as possible the “natural water cycle” to ensure a good level of hydraulic-environmental protection of the

land. Interventions aimed at restoring “natural” drainage conditions, referred to as SUDS (Sustainable Urban Drainage Systems) in English literature and LID (Low Impact Development) in American literature, must aim to achieve both hydraulic and hydrological invariance (figure 1).

According to the hydraulic invariance principle when a new work is constructed, the peak flow rate of storm runoff, discharged into the sewer system, must be less than, or at most equal to, the pre-existing one. Hydrological invariance, on the other hand, is that principle whereby the maximum volume of stormwater runoff, discharged into the sewer system, must be less than or, at most, equal to that returned before the intervention. Hydrological invariance is more complicated to achieve, it can be realized through controlled stormwater storage and release works overtime, associated with infiltration systems.

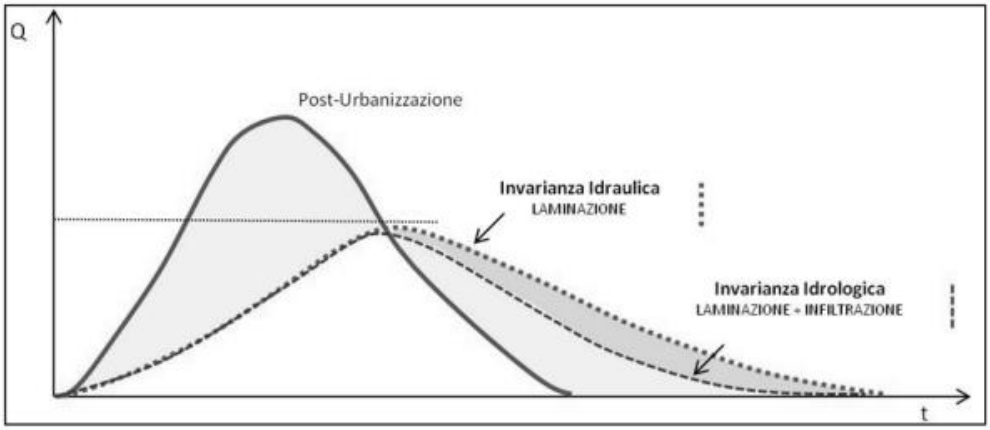

Figure 1. Hydraulic and hydrological invariance.

Among the interventions known as SUDS, green infrastructures, GIs, are particularly significant, representing an increasingly demanded and utilized sustainable solution. GIs play a key role in the capture and modulation of runoff. The scientific literature reports a reduction in water volume input to the urban drainage network of up to 80%, while more uncertain is the effect on flood flow rates where peak hydrogram abatement is strongly influenced by precipitation characteristics and those of the substrate-vegetation system (Gregoire and Clausen, 2011; Stovin et al., 2012).

According to the European Commission (2016), GIs can be defined as “a strategically planned network of natural, semi-natural areas along with other environmental elements, designed and managed to provide a wide range of ecosystem services”. Unlike traditional infrastructures, commonly called Grey Infrastructures, GIs are designed and built to benefit the widest audience of stakeholders according to the *“small loss-big gain”* principle.

Naturalness and biodiversity characterize GIs, which at the same time, have other benefits both of a material order, such as “heat island” mitigation (Santamouris, 2014), runoff regimentation (Li & Babcock, 2014), soil and water pollution remediation (Elliott and Trowsdale, 2007), air quality improvement (Luo et al, 2015), noise pollution mitigation (Van Renterghem and Botteldooren, 2011), and intangible order, such as improving the quality of life through the enjoyment of green areas and promoting urban biodiversity (Wooster et al., 2022).

GIs are a key strategy of European spatial planning policies, constituting a possible “natural” solution to climate change challenges. In highly urbanized contexts, GIs, which improve natural water retention measures (NWRM) and reduce rainfall inputs, are represented by "green roofs" or "vertical gardens", i.e., vegetated plants made on impermeable structural supports, such as floors, roofs, walls of buildings or, in general, in all those cases where there is no ecological continuity between the green and the subsoil down to the parent rock.

The green roof represents an essential tool for environmental mitigation and compensation within the urban fabrics where the high building density and the high anthropogenic disturbance allow little space for natural dynamics (ISPRA, 2016).

The Italian Ministry of the Environment, as part of the 2013 National Conference dedicated to the “green economy,” highlighted the importance of GIs in the management and protection of water resources, calling for a policy of large-scale development and investment of GIs and recognizing the great benefit of these systems to critical environmental and economic-social issues, which are particularly serious in Italy due to the climate crisis, land consumption, and hydrogeological disorder.

The active presence of a soil-plant system promotes, through the processes of infiltration, retention, and evapotranspiration, the capture of water and the return to the atmosphere of an important proportion of precipitation. The water-regulating capacity of GRs and runoff dynamics are influenced by several factors, including construction and design characteristics such as the number of layers and materials, type and thickness of the substrate, slope, location, age of the roof, and roof geometry, as well as weather and climate conditions such as the characteristics of the rainfall event and initial substrate moisture conditions (Berndtsson, 2010). GRs reduce the total volume of runoff and mitigate the ridge flow returned to the sewer system through two hydrological processes: rainfall retention, which is the permanent removal of stormwater, and runoff detention, which is the transient storage of rainfall (De Ville et al., 2017). Both processes are conditioned by the physical and hydraulic properties of the substrate or growing medium. Specifically, the retention capacity

of the substrate is influenced by the pore size distribution while the detention capacity depends on the hydraulic conductivity that defines the aptitude of the substrate to allow water to pass through it. Like natural soil, a GI growing medium provides physical support and essential nutrients for the plant. In the case of green roofs or roof gardens, the optimal growth substrate must ensure lightness so as not to weigh down the building structures while, hydrologically, it must allow rapid drainage of excess water to quickly restore the unsaturated conditions necessary for the plant and to ensure an optimal thermal regime (Charpentier, 2015). Likewise, especially in Mediterranean environments, it is desirable to have a substrate that has good water retention capacity to store enough water to meet crop needs.

An efficient strategy for enhancing the hydraulic and physical properties of soil involves the use of various organic soil amendments derived from agricultural by-products, such as compost, vermicompost, biochar, and other recycled organic materials, which generally enhance water retention capacity, reduce bulk density, and increase overall porosity, while also stabilizing soil structure through particle aggregation and optimizing hydraulic conductivity, offering a sustainable solution for soil health enhancement (Aggelides and Londra, 2000; Eden et al., 2017).

This approach is fully aligned with the principles of the circular economy, as it reduces the reliance on external resources, minimizes waste production, and promotes the sustainable regeneration of natural resources (Chiarelotto et al., 2021).

For stormwater management, it is often assumed that a green roof's ability to retain and detain runoff remains consistent over time. However, much like other natural or artificial porous media, the growing substrate can undergo temporal changes due to a range of biological, chemical, and physical processes, leading to notable alterations in hydraulic properties such as permeability, hydraulic conductivity, and water retention capacity (Cannavo et al., 2014; De-Ville et al., 2018).

The age of a green roof is expected to significantly influence its hydraulic performance, underscoring the importance of ongoing monitoring of the substrate's evolving properties to maintain optimal performance over time (Bouzouidja et al., 2018).

Therefore, in the construction of GIs, one of the most important challenges is represented by the choice of growth medium. However, the aspects related to the physical and hydraulic characteristics of the substrate used for GIs are still little investigated, perhaps due to the limited implementation experiences in the Italian territory.

1.1 Specific objectives

This thesis aims to implement knowledge in the field of hydraulic characterization of substrates for green infrastructure in urban areas, with a view to environmental sustainability and circular economy. The current direction is to develop "engineered soils," which are technical substrates designed to replicate the characteristics of natural soils while enhancing their performance. These innovative and multifunctional substrates are made to balance often antithetical physical and mechanical properties.

The primary focus of the thesis was to investigate the role of the substrate hydraulic properties, i.e. water retention curve and hydraulic conductivity function, in determining the hydrological behavior of a green roof in terms of rainfall retention and detention.

A comprehensive, multi-scale methodological approach was followed, encompassing various levels of analysis to ensure a thorough understanding of the subject. The specific objectives of the thesis (figure 2), in detail, were as:

- Determination of the water retention curve of commercial and innovative substrates for urban green infrastructure. Experimental laboratory tests were performed on substrate microcosms (volume of 100-1000 cm^3) and the effect of adding different organic soil amendment derived from agricultural by-products, such as compost, vermicompost, or pruning residues, on the hydraulic characteristics of the growing mixtures was investigated.

- Determination of the retention and detention capacity of the green roof under intense rainfall events. Simulated rainfall tests were carried out on microcosms of green roofs (volume of 0.004 m^3) arranged in different combinations of substrate and drainage layers.

- Analysis of the functional characteristics of a substrate-vegetation system. A field evaluation of substrate modifications during the life cycle was conducted on the green roof prototype (volume of 2.2 m^3) at the Department of Agricultural, Food and Forestry Sciences (SAAF) of the University of Palermo.

The experimental activity carried out during the Ph.D., is within the framework of the PON “Ricerca e Innovazione” 2014-2020, in priority axis IV “Istruzione e ricerca per lo sviluppo”, action IV.5 “Tematica Green”.

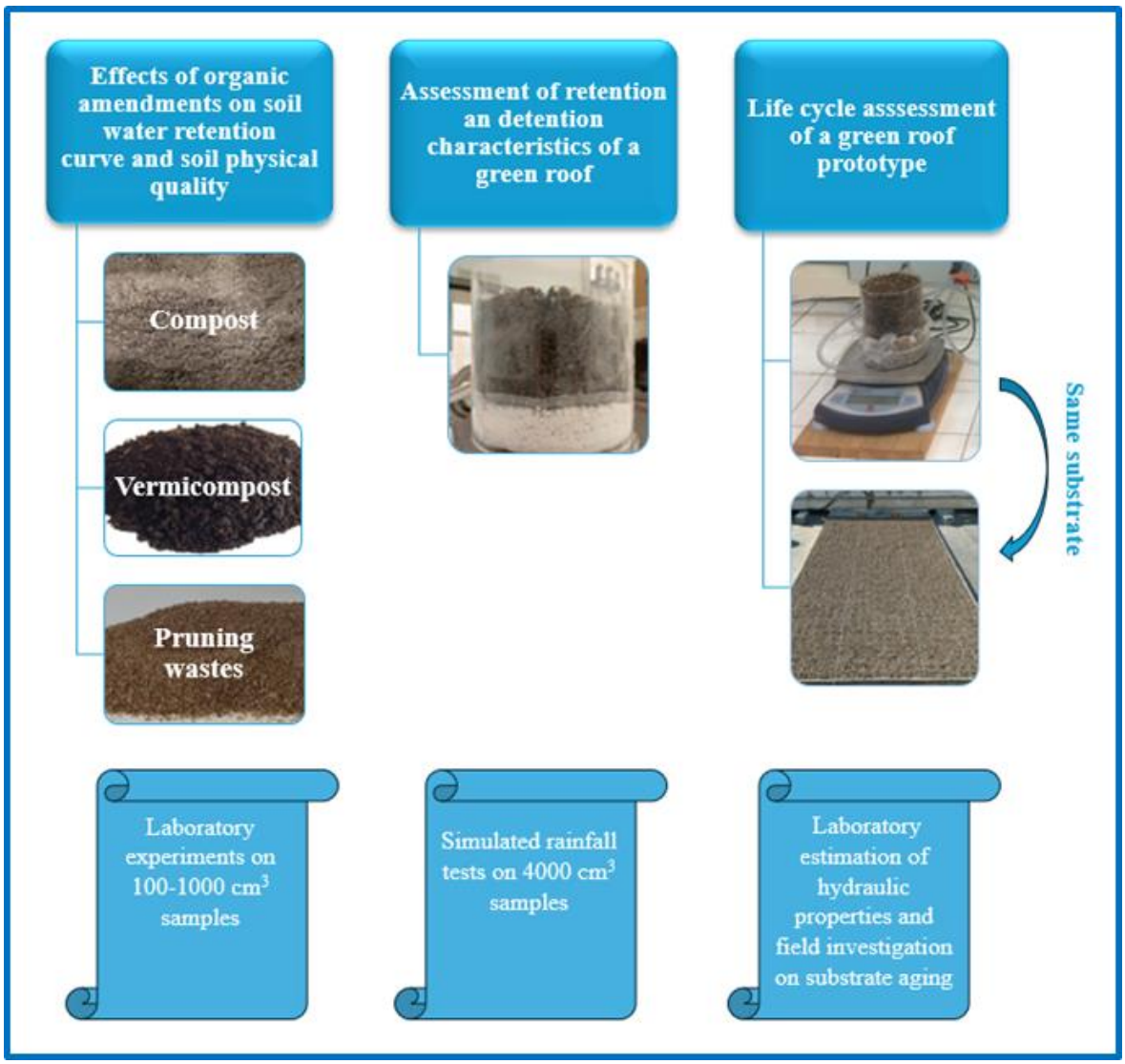

Figure 2. Scheme illustrating the interconnections between the specific objectives of the thesis.

1.2 Historical overview

The use of green infrastructures by man to cover and protect homes dates back to the birth of great civilizations. The archaic prototype of the "green roofs" is the hanging gardens of Babylon (figure 3), which due to their grandeur and majesty were one of the seven wonders of the ancient world. Located in the ancient city of Babylon, near modern-day Baghdad (Iraq), they were commissioned around 590 BC by King Nebuchadnezzar II as a gift for his wife Queen Amytis.

Strabo, a Greek geographer and historian of the I century AD, gave a description of the hanging gardens of Babylon:

"It consists of vaulted terraces raised one above another, and resting upon cube-shaped pillars. These are hollow and filled with earth to allow trees of the largest size to be planted. The pillars, the vaults, and terraces are constructed of baked brick and asphalt. The ascent to the highest story is by stairs, and at their side are water engines, by means of which persons, appointed expressly for the purpose, are continually employed in raising water from the Euphrates into the garden".

Figure 3. The Hanging Gardens of Babylon - Maarten van Heemskerck (1498 – 1574).

Other evidence of the use of green infrastructures in ancient times is the *tumulus tombs* of the Etruscans, built around the IX century BC, in which the soil, removed during the excavation to create the tomb, was reused to cover the pseudo-dome of the tomb itself with vegetation, protecting and isolating the entire sepulchral structure.

This practice was also maintained in Roman times, one thinks of Hadrian's Mausoleum and the Mausoleum of Augustus (130 AD) in Rome. The Romans also employed green

infrastructure as an integral part of their mansions, such as Villa Adriana at Tivoli (92 AD) and Pliny the Younger's Villa Lauretina (I century AD).

During the medieval era, hanging greenery plays a functional role. It is mainly found in monasteries, where the green infrastructure was used as a vegetable garden, and in fortifications, where mounds of soil covered with vegetation were placed adjacent to the city walls to protect the structures and cushion the blows of enemy offensives during battles.

From the XV century to the XIX century, the aesthetic and ornamental connotation prevailed again, and the green roof became an almost exclusive presence of villas and noble palaces. Examples include Villa d'Este in Tivoli (figure 4), Villa Fiesole by Giovanni de' Medici, the Palace of Versailles in Paris, and the Belvedere Gardens in the Vatican.

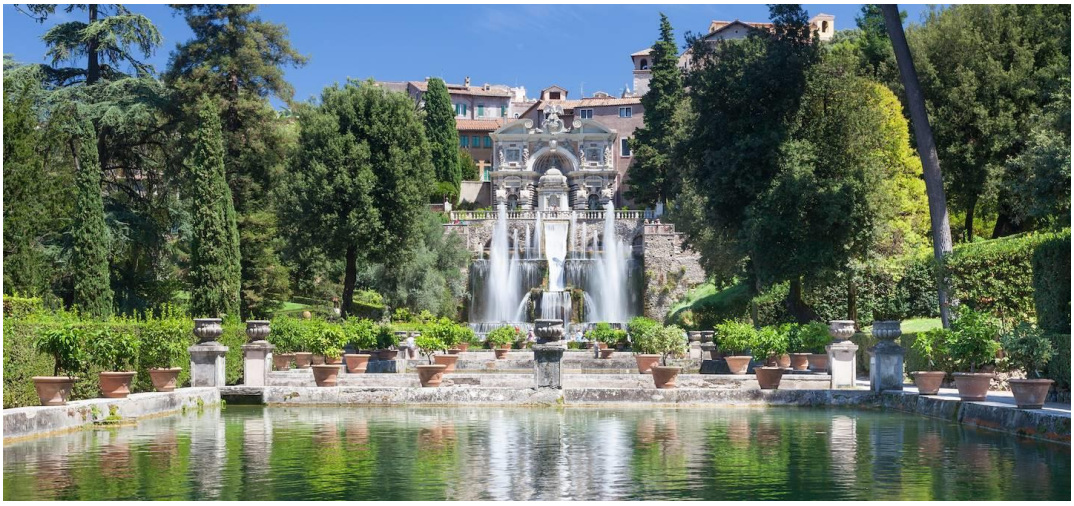

Figure 4. Villa d'Este in Tivoli.

The modern concept of hanging green dates back to 1865, the year in which the German architect Von Rabitz wrote his first work on the subject, a treatise on the use, from a functional and ecological point of view, of hanging green. It is seen as a means to obtain healthy environments even in highly anthropized contexts.

In 1923, the Swiss architect, naturalized French, Le Corbusier enunciated, in his work "Vers une architecture", the five axiomatic points for a modern vision of architecture, among which there is the "roof-garden", described as follows:

"The roof-garden gives back to man the greenery, which is not only under the building but also and especially above it. Soil is placed between the joints of the roofing slabs and grass and plants are sown, which have an insulating function against the lower floors and make the roof lush and livable...".

From this moment, green roofs have become an important element in compensation and mitigation measures in urban areas. Beginning in the 1960s, in a climate of growing interest in environmental issues, it became widespread in Europe, especially in Germany, a country where, following the Second World War (1939-1945), there were vast areas of degraded land that required reclamation. In 1975, FFL (Forschungsgesellschaft Landschaftsentwicklung Landschaftsbau), a scientific network of the green sector to restore and improve the living environment, was founded in Germany. Thanks to the FFL, the first guidelines for the design, construction, and maintenance of green roofs are obtained.

In recent years, the green roof market in Italy appears to be growing, albeit at a slower pace than in other European countries. At the regulatory level, it was only in 2018 that the "Bonus Verde" was established, which allows for benefits and tax breaks for interventions aimed at the renovation of gardens and terraces, and the creation of green infrastructures and roof gardens. At present, vertical gardens are more common in Italy, the best known of which is the "Bosco Verticale," a building-prototype of a green architecture, built in 2014 by architect Stefano Boeri and located in the Milan Business Center (figure 5).

Figure 5. "Bosco verticale" in Milan.

The European project "Clever Cities," co-funded under the Horizon 2020 research program (the European Union's Framework Program for Research and Innovation), aims to test and promote green infrastructure and nature-based solutions (NBS) in Milan, London and Hamburg. NBS are defined by the International Union for Conservation of Nature (IUCN) as "actions to protect, sustainably manage, and restore natural or modified ecosystems that address societal challenges effectively and adaptively while providing benefits for human well-being and biodiversity."

1.3 Types and stratification of green roofs

In Italy, the reference standard for green roof design and management is UNI 11235 "Istruzioni per la progettazione, l'esecuzione, il controllo e la manutenzione di coperture Verdi", issued in May 2007. It constitutes a real guideline for a workmanlike implementation.

Green roofs are classified according to the level of maintenance required by the system during its life cycle. Two categories can be distinguished in this regard:

- Extensive systems
- Intensive systems

Such division is crucial as the two types exhibit distinct patterns of usage and fields of application. Extensive systems, one or two years after implantation require little maintenance consisting of one or two operations per year. These systems are designed so that water and nutrient supply occurs, as much as possible, through natural processes.

Plants with a high capacity for propagation and regeneration, resistant to adverse climatic conditions such as drought or frost, including various species belonging to the genus *Sedum*, are used: *S.album, S. cauticolum, S. floriferum, S. hybridum, S. reflexum, S. sexangulare, S. spurium.* Many other herbaceous perennial species can be used including *Festuca rubra, Lavandula angustifolia* or *Origanum vulgare.*

The substrate consists mainly of mineral components and has a small thickness, less than 15 cm, and a weight between 75 and 150 kg m^{-2} under conditions of maximum saturation.

This type of greening is used on large roofs, such as industrial buildings or parking lots, to replace the impervious roofs made of inert materials (figure 6). Intensive systems require more maintenance that consists of regular irrigation and fertilization but also mowing and weeding. The intensive system makes it possible to create real usable gardens on surfaces such as roofs or garages, having a high bearing capacity (figure 6). Thus, in these systems there can be a variety of wind- and cold-resistant plant species and associations: turf mats, herbaceous perennials, shrubs, or sometimes trees. Intensive systems are made with a deep layer of substrate, usually composed of a balanced mixture of mineral and organic elements. The thickness of the stratifications is between 15 and 60 cm and weights more than 150 kg m^{-2} under conditions of maximum water saturation.

Regardless of the type, the UNI 11235 standard considers green roofs as a "roof system" that, as such, must ensure a set of minimum requirements and performance.

Figure 6. Example of extensive system (left) and intensive system (right).

A “roof system” is composed of the aggregation of elements or layers that are always present, also called primary layers, and secondary layers that are present when there are special conditions of use or climatic context.

The primary layers of a green roof (figure 7), from bottom to top, are: supporting element; sealing element; root protection element (integrated or not); mechanical protection element; draining element; water storage element; filtering element; substrate (or growing media); vegetation layer.

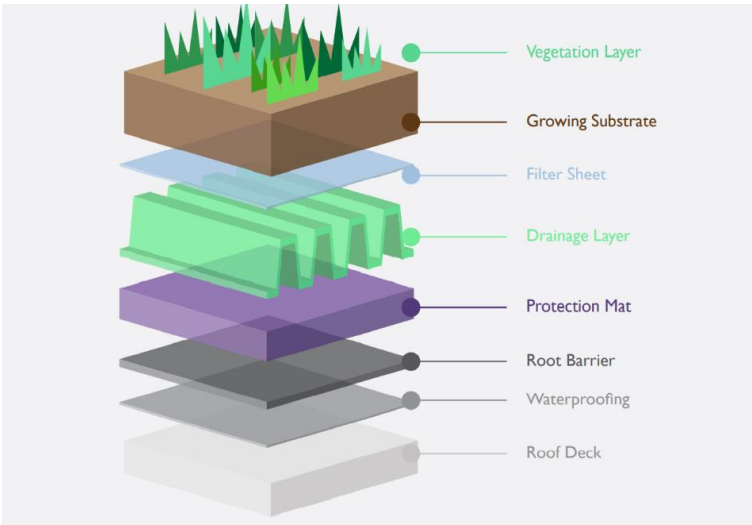

Figure 7. Primary layers of a green roof.

1.4 Substrate: function and characteristics

UNI 11235 defines the substrate, or growing media, as a layer that supports the plant development of a green cover. The substrate constitutes a key component of any green cover; it must ensure optimal plant growth conditions.

A substrate is a three-phase system consisting of a solid phase that performs the function of anchoring plant root systems, a liquid phase that ensures water and nutrient supply, and a gas phase necessary for root aeration and the life of the microorganisms present (Hillel, 1998).

It is characterized by physical parameters such as density, particle size, maximum water volume, and maximum air volume under saturated conditions, and chemical parameters such as pH, electrical conductivity, or the amount of organic matter (OM).

There is no universal growing medium; in the design phase, it is chosen according to the climatic conditions in which it operates and the needs of the desired plants. An optimal growing medium must provide permanent physical support for the plants and ensure a balance between free drainage and adequate retention of available water for the plants and nutrients (Ampim et al., 2010). An incorrect choice of substrate can lead to compaction, asphyxiation of the root system, drainage reduction, and alteration of nutrients (Cascone, 2019).

An optimal growth substrate for green roofs must, therefore, have the following characteristics:

- High draining capacity;
- Good water holding capacity (WHC);
- Low weight even in conditions of maximum saturation;
- Balanced air/water ratio at maximum saturation;
- Stable physical and chemical structure;
- Very good frost resistance;
- Reduced compaction over time;
- No weeds;
- Do not allow the formation of mud in conditions of maximum saturation and during meteoric events;
- Cost-effectiveness, possibly by encouraging the reuse of waste products from production activities;

These characteristics must be maintained over time, constantly guaranteeing the water and nutritional needs of the cultivated plants. WHC can be improved by increasing the volume, depth, and OM content of the substrate. The substrates for the construction of green roofs are porous media obtained by mixing different components, both mineral and organic (Sandoval et al., 2017). The composition of a substrate can vary, for example, depending on the type of green roof (extensive or intensive), the target vegetation, the climatic conditions, and other factors such as availability and cost of components (Ampim et al., 2010). The mineral part of the substrate generally varies between 50% and 90% of its total volume and it is made up of coarse fractions of volcanic materials (pumice, zeolite) or technological products (perlite, expanded clays) chosen not only for their lightness but also for the possibility of retaining water in the intraparticle microporosity (Stanić et al., 2020).

The organic fraction fulfills the primary purpose of fertilizing the substrate but can contribute significantly to increasing the crop's water availability. The basic products used in nurseries, being characterized by lightness, high porosity, good drainage capacity, and accumulation of water and nutrients, are considered good materials (Kazemi e Mohorko, 2017). Inert minerals (expanded clay, lapilli, pumice), recycled materials (bricks, tiles), or the products of industrial processes, are mixed with organic matter in different concentrations depending on the design objectives. Peat has traditionally been used as an organic component in technological substrates (Handreck and Black, 1994; Paquet et al., 1993), however, the focus has recently shifted to eco-friendly products. In the literature, several organic fractions with a lower environmental impact have been proposed, often obtained from waste materials from the agri-food processing industry such as compost, which improves water retention capacity and provides a high nutrient content (Benito et al., 2005), vermicompost or coco coir. Several analyses have been carried out on the improvement of different substrate characteristics including biochar and super-absorbent polymers (Cao et al., 2014, Young et al., 2014).

2. Soil water retention curve (SWRC)

The water content in the soil influences various hydrological processes, such as rainfall infiltration and plant water uptakes, and mechanical properties, such as compactability and penetrability. The soil's water content also regulates air content and gas exchange, thereby influencing root respiration, microbial activity, and the soil's chemical state, e.g., its oxidation-reduction potential (Hillel, 1998).

Soil water content can be expressed on a gravimetric basis or on a volumetric basis. The soil water content, or soil moisture, expressed on a gravimetric basis, U (g g^{-1}), is the ratio of the mass of water present in the soil M_w (g), to the mass of dry soil M_s (g). Thus, moisture on a gravimetric basis, U, is equal to:

$$U = \frac{M_w}{M_s} \tag{1}$$

Instead, volumetric soil water content, θ (m^3 m^{-3}), expresses the amount of water referred to the apparent soil volume unit, and is defined as the ratio of water volume V_w (m^3), to total soil volume, V_t (m^3). Moisture on a volumetric basis, θ, is equal to:

$$\theta = \frac{V_w}{V_t} \tag{2}$$

The soil water matric potential, *h*, is determined by the capillary and adsorption forces that act between the solid soil matrix and the water in the pores. Water is therefore retained in the soil, and its potential is negative (negative pressure or suction), meaning it is lower than that of free water, which is conventionally set to zero. The smaller is the soil moisture, the stronger is the matric potential.

The empirical relationship that links matric potential, *h*, and volumetric water content, θ, is referred to as the "*soil water retention curve*" or soil moisture characteristic curve, SWRC (Hillel, 1998). SWRC describes the ability of soil to store or release water and influences various processes related to water and solute storage in soil, such as water supply to plants, and biological processes such as, for example, seed germination, microbial activity, or degradation of organic matter. So, knowledge of SWRC is critically important to understand and simulate the hydrological processes that take place in a green infrastructure (Huang et al., 2020).

Graphically, the SWRC can be represented by a highly nonlinear sigmoid. It is not unique and varies significantly from soil to soil, as it strongly depends on the grain size, texture, and structural characteristics of the soil (figure 8).

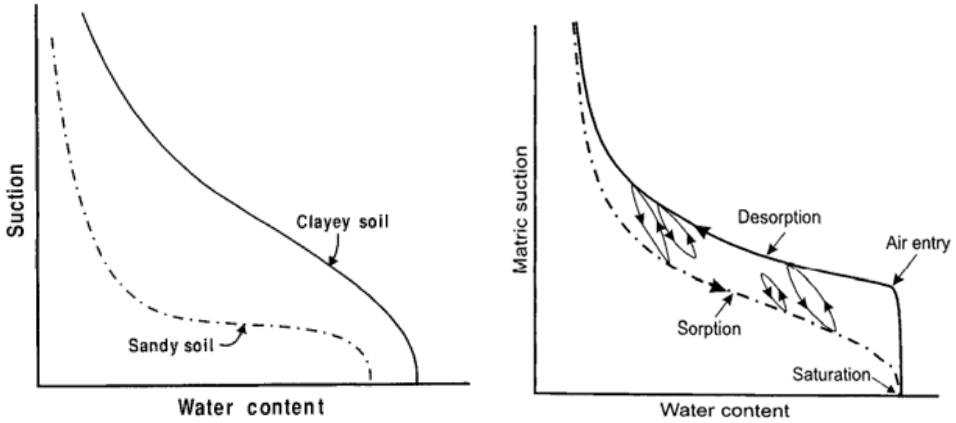

Figure 8. Water retention curves of different textured soils (left) and hysteresis phenomenon (right), from Hillel (1998).

For a given soil, the SWRC obtained during a drying process starting from saturated conditions does not coincide with that obtained by wetting an initially dry soil (figure 8). This phenomenon is called hysteresis (from the Greek ὑστέρησις, meaning "delay") and highlights how the same value of matric potential corresponds to different values of volumetric water content, θ. Specifically, the highest moisture content corresponds to the drying process from saturation, and the lowest is related to the wetting process from the completely dry soil condition. Consequently, two main soil water retention curves can be defined: a main wetting curve, $\theta(h)_w$, that is always below the main drainage curve, $\theta(h)_d$.

Hysteresis can be attributable to multiple causes including, for example, pore size unevenness, the effect of different solid-liquid contact angles during the drying or wetting process, air trapped inside non-conductive pores, and the phenomena of swelling, shrinkage, or aging (Hillel, 1998).

The two limiting curves or main curves of drying and wetting enclose all other possible curves, called secondary curves, which are obtained in cases where the drying or wetting process occurs from partially saturated or partially dry soil.

2.1. Determination of the SWRC

The water retention curves were determined experimentally with the tension hanging water column apparatus (figure 9), in the range of higher values of the matric potential (- 5 cm ≤ h ≤ -100 cm) and with the pressure plate extractors (figure 10) for the lower values of matric potential (-100 cm ≤ h ≤ -15000 cm).

Regardless of the method used, the experiment consists of equilibrating a previously saturated soil sample to a predetermined value of h and then determining its corresponding θ value by the thermogravimetric method. To determine the water retention curve, a succession of h values is applied to the same soil sample. Since the relationship θ(h) is subject to the hysteresis phenomenon, its measurement depends on the increasing or decreasing sequence of applied potentials. By convention, for agronomic purposes, when we refer to the water retention curve, we mean the main retention curve during drying or drainage.

In the tensiometric method (Dane and Hopmans, 2002a), the soil sample to be analyzed, after being placed on the surface of the plate of a tensiometric funnel, is preliminarily saturated from below, to achieve complete saturation of the sample, in four gradual steps of 24 h each, setting three successive values of matric potentials -0.2, -0.1, -0.05, followed by complete saturation by immersion in water. After being saturated, the sample is subjected to a monotonically decreasing sequence of matric potentials, set through the use of a burette hydraulically connected to the funnel. All the experiments for the present study were conducted following the same sequence of h values: -5.0, -7.5, -10.0, -15.0, -20.0 -25.0, -30.0, -40.0, -50.0, -70.0, -100.0 cm.

At equilibrium with each fixed h value, the volume drained into the burette is recorded. When the last potential of the sequence is reached, the sample is removed from the funnel, weighed, and dried in an oven at 105° C for 24 h, to determine its final volumetric water content by the thermogravimetric method. The volumetric water contents corresponding to the revious potentials were determined backward by adding the volumes subsequently drained to the final volumetric moisture.

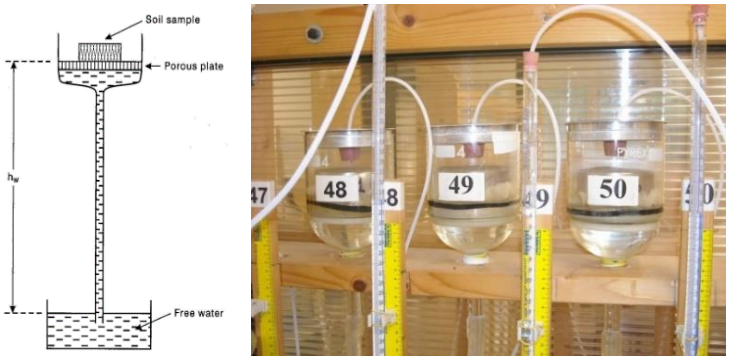

Figure 9. Tensiometric apparatus for determining the soil water retention curve in the range of higher values of the matric potential, - 5 cm ≤ h ≤ -100 cm.

With the pressiometric method (Dane and Hopmans, 2002b) a soil sample is saturated on the top of a ceramic porous septum that is permeable to water and not air (figure 10). The sample is then placed inside a pressure chamber with the bottom of the porous septum directly in contact with external pressure. A pressure greater than atmospheric pressure is established inside the chamber. The pressure difference between the upper and lower surfaces of the porous plate allows the water contained within the pores of the sample to drain until an equilibrium condition in which the soil matric potential, in absolute value, is equal to the applied pressure. The sample is considered at equilibrium when it no longer drains for at least 24 h. When equilibrium is reached, the sample is taken and dried in an oven at 105°C for 24 h to determine, by the thermogravimetric method, the volumetric water content corresponding to the applied pressure head value. With this method, it is possible to derive the points of the retention curve in the range of values of the matric potential of greatest interest for plant water supply (-100 < h ≤ -15000 cm).

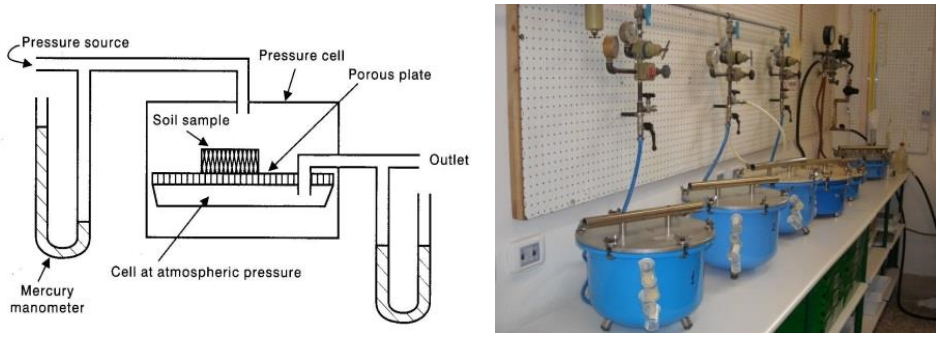

Figure 10. Pressiometric apparatus for determination of soil water retention curve in the range of lower values of the matric potential, -100 ≤ h ≤ -15000 cm.

Multiple empirical and theoretical models have been proposed in the literature to describe the relationship θ(*h*) with continuous functional forms having a specific number of parameters (Brooks and Corey, 1966; Durner, 1994; Fredlung and Xing, 1994; Kosugi, 1996; Van Genuchten, 1980). Constitutive parameters are then estimated by fitting the assumed model to the experimental θ(*h*) data by non-linear fitting algorithms (Seki, 2007; Van Genuchten et al., 1991).

The most popular and widely used model is the unimodal model proposed by Van Genuchten, VG, (1980), the equation for which is given below:

$$S_e = [1 + (\alpha h)^{n}]^{-m} \tag{4}$$

$$S_e = \frac{\theta - \theta_r}{\theta_s - \theta_r} \tag{5}$$

where θ_s (cm^3cm^{-3}) and θ_r (cm^3cm^{-3}) are the saturation volumetric water content and the residual volumetric water content, α (cm^{-1}) is a scale parameter, and *n* and *m* with *m* = 1-1/*n* are two dimensionless shape parameters. The latter constraint has the advantage of reducing to two the number of parameters to be estimated to describe the water retention curve from experimental data.

Parameter α is related to the most frequent pore diameter, parameter n, on the other hand, is a measure of the heterogeneity of the pore size distribution. The latter can be inferred indirectly from the water retention curve and expresses the relative abundance of each pore size in a representative volume of soil. The derivative dθ/d*h*, represented as a function of the average pore radius expressed through the capillarity relation, allows us to know the pore distribution function (Reynolds, 2009). In the case of the function of VG (1980), this relationship has a single maximum at the inflection point of the curve. The corresponding modal diameter corresponds to the class of pores that is most frequently represented in the porous medium. Therefore, the unimodal VG model assumes that the pore distribution in the soil is substantially uniform, or 'monodisperse,' which may be appropriate for coarse soils but is inadequate for describing the behavior of complex structural soils that exhibit both macro- and micro-porosity, also known as bimodal porous media.

Consequently, there is a need to model hydraulic conductivity, *K* ($m\ s^{-1}$) in dual-porosity soils, where the interaction between macropores and micropores significantly influences fluid flow (Gerke and van Genuchten, 1993; Jarvis et al., 1991; Vogel et al., 2000).

Durner (1994) proposed modeling the water retention curve of a bimodal soil by superimposing two characteristic curves, one corresponding to matric porosity (i.e., the smaller pores that form within aggregates between individual soil particles), the other to structural porosity (i.e., the larger pores that form between aggregates and, more generally, the so-called macroporosity). The expression of the water retention curve is, in this case:

$$S_e = w_1[1 + (\alpha_1 h)^{n_1}]^{-m_1} + w_2[1 + (\alpha_2 h)^{n_2}]^{-m_2} \quad (6)$$

where subscripts 1 and 2 refer to matrix and structural porosity, respectively, and w_1 and w_2 with $w_1 + w_2 = 1$.

The experimental data obtained, as part of the different experimental tests, were fitted, with both unimodal and bimodal versions of the Van Genuchten model, using SWRC Fit software (Seki, 2007) or RETC software (Van Genuchten et al., 1991).

The performance of the water retention model used, from time to time, was evaluated through the statisticians commonly used to quantify estimation accuracy: the coefficient of determination, R^2, the root mean square error, RMSE, the maximum deviation, the Akaike information criterion, AIC.

2.2. Soil physical quality

By determining the SWRC, several soil physical quality (SPQ) indices can be inferred. Doran et al., (1996) defined SPQ as "the ability of soil to perform multiple functions within the ecosystem and neighboring areas of differing use to sustain biological productivity, maintain environmental quality, and support plant and animal growth and health." SPQ is affected by various factors, including soil structure, density, porosity, permeability, water retention capacity, pH, and organic matter content (Bondì et al., 2024, **Appendix B**). In turn, it influences the chemical and biological processes occurring in the porous medium (Dexter, 2004). An agricultural soil of good physical quality must stably have a good structure, allow the anchoring of crops, limit erosion and compaction phenomena, promote root development and proliferation of soil fauna, and have a balanced content of air, water and nutrients.

There are several parameters in the literature to assess SPQ. For example, Reynolds et al., (2002, 2003, 2009) proposed bulk density (*BD*), plant available water (*PAWC*), air capacity

(*AC*), macroporosity (P_{mac}), and relative field capacity (*RFC*).

Dexter (2004), on the other hand, determined an index, namely the *S-index*, which is based on the value taken by the slope, *S*, of the soil water retention curve at its inflection point.

The bulk density of dry soil, *BD* (g cm^{-3}), expresses the ratio of the mass of the solid phase to the bulk volume of the sample (Hao et al., 2008).

$$BD = \frac{M_S}{V_b} \tag{7}$$

BD can be used as an indirect indicator of aeration and the ability to store and transmit water (Reynolds et al., 2008). It also influences soil permeability and porosity.

The plant available water capacity, *PAWC* (cm^3 cm^{-3}), is:

$$PAWC = \theta_{FC} - \theta_{PWP} \tag{8}$$

in which θ_{FC} (cm^3 cm^{-3}) and θ_{PWP} (cm^3 cm^{-3}) are, respectively, the volumetric soil water content corresponding to the field capacity, (h = -100 cm), and the volumetric soil water content corresponding to the wilting point (h = -15000 cm).

The air capacity, *AC* (cm^3 cm^{-3}), expresses the ability of the soil to provide the necessary aeration for root systems, and is equal to:

$$AC = \theta_s - \theta_{FC} \tag{9}$$

where θ_s (cm^3 cm^{-3}) represents the saturated soil water content.

Macroporosity, P_{mac} (cm^3 cm^{-3}), expresses the soil's ability to promote drainage processes and root proliferation. It can be defined as:

$$P_{mac} = \theta_s - \theta_m \tag{10}$$

where θ_m (cm^3 cm^{-3}) is the volumetric water content of the soil when only the matrix is saturated.

Relative head capacity, *RFC*, is indicative of the ability of soil to store water and air in relation to overall porosity, expressed through θ_s, and is equal to:

$$RFC = \frac{\theta_{FC}}{\theta_s} \tag{11}$$

Dexter's (2004) *S-index* is the slope of the soil water retention curve at its inflection point (*S* = tan ω, in Figure 11), that is, at the point where the curvature of the SWRC is zero (it changes from convex to concave). *S* is equal to:

$$S = \frac{dw}{d(\ln(h))} \tag{12}$$

The S-*index* theory is based on the premise that the shape of the SWRC is primarily governed by the structural porosity for matric potential values (h) ranging from saturation to the inflection point, and by the matric porosity for lower matric potential values. While the former pore domain can be influenced by soil management practices, including the use of amendments, the latter is largely determined by more stable soil characteristics, such as texture (Bondì et al., 2022, **Appendix A**).

This index is easily and unequivocally determined, as it is based solely on the measurement of SWRC obtained by a drying process. Since *S* has a negative value, for practical purposes it is used in absolute value.

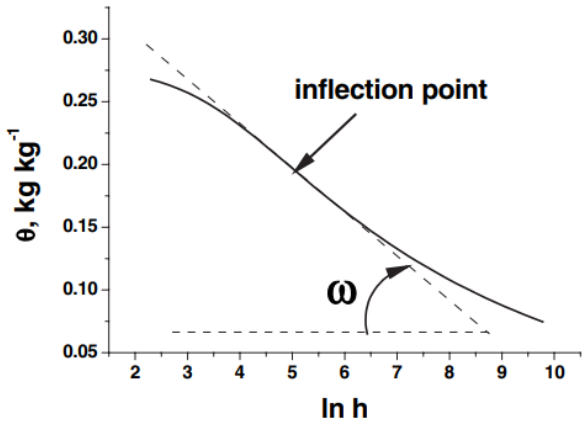

Figure 11. The inflection point of a soil water retention curve (from Dexter and Czyz, 2007).

Considering the VG model for the soil water retention curve, the pore volume distribution function, $S_v(h)$, can be defined as the slope of the SWRC expressed as volumetric water content, θ_v (cm^3cm^{-3}), versus ln(*h*), and plotted against equivalent pore diameter, d_e (μm), on a $\log_{10}$ scale (Reynolds et al., 2009).

$$S_v = \frac{d\theta}{d(\ln h)} = -mn(\theta_s - \theta_r)\alpha^n h^n [1 + (\alpha h)^n]^{-(m+1)} \quad (13)$$

The equivalent pore diameter, d_e, is estimated using the capillary rise equation (Warrick, 2002).

$$d_e = \frac{2980}{h} \; ; h > 0 \text{ (cm)}; \; d_e \text{ (µm)} \quad (14)$$

The pore volume distribution function can be normalized, $S^*(h)$, by dividing $S_v(h)$ by the magnitude of the slope at the inflection point, S_{vi}. The normalized soil pore volume distribution, $S^*(h)$, is not influenced by bulk density or porosity, making it a useful method for comparing pore volume distributions between different porous materials being $0 \leq S^*(h) \leq 1$.

Pore volume distributions can be characterized and compared by analyzing "location" and "shape" parameters (figure 12), where the location parameters include the modal diameter, d_{mode} (µm), the median diameter, d_{median} (µm), and the mean diameter, d_{mean} (µm). The shape parameters include standard deviation, SD (-), that is indicative of the spread, skewness, SK (-), indicative of the asymmetry and kurtosis, KU (-), indicative of the peakedness (Reynolds et al., 2009).

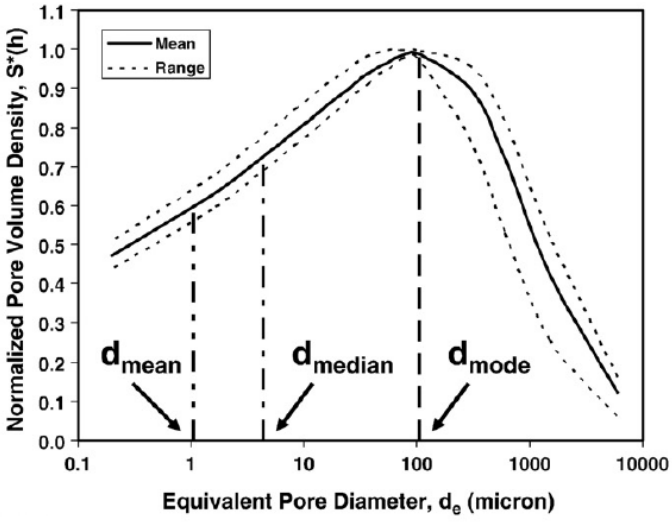

Figure 12. Example of normalized pore volume distribution (from Reynolds et al., 2009).

The location parameters use d_e described in the form:

$$d_\theta = \frac{2980\alpha}{\left(\theta^{-\frac{1}{m}}-1\right)^{\frac{1}{n}}} \quad (15)$$

The median and modal d_e values, valid for the VG model, are given, respectively:

$$d_{mode} = \frac{2980\alpha}{m^{-1/n}} \quad (16)$$

$$d_{median} = \frac{2980\alpha}{\left(0.5^{-1/m}-1\right)^{1/n}} \quad (17)$$

The geometric mean d_e (d_{mean}), standard deviation (SD), skewness, and kurtosis were adapted from the relationships outlined by Blott and Pye (2001) for describing particle size distributions, and are given by:

$$d_{mean} = exp\left(\frac{\ln d_{0.16}+\ln d_{0.50}+\ln d_{0.84}}{3}\right) \quad (18)$$

$$SD = exp\left(\frac{\ln d_{0.84}-\ln d_{0.16}}{4} + \frac{\ln d_{0.95}-\ln d_{0.05}}{6.6}\right) \quad (19)$$

$$SK = \frac{1}{2}\left[\frac{\ln d_{0.16}+\ln d_{0.84}-2(\ln d_{0.50})}{(\ln d_{0.84}-\ln d_{0.16})} + \frac{\ln d_{0.05}+\ln d_{0.95}-2(\ln d_{0.50})}{(\ln d_{0.95}-\ln d_{0.05})}\right] \quad (20)$$

$$Ku = \frac{\ln d_{0.05}-\ln d_{0.95}}{2.44\,(\ln d_{0.25}-\ln d_{0.75})} \quad (21)$$

where m = 1–1/n and $d_{0.05}$, $d_{0.16}$, $d_{0.25}$, $d_{0.50}$, $d_{0.75}$, $d_{0.84}$, $d_{0.95}$, are equivalent pore diameters (μm) that can be obtained from the capillary rise equation (eq. 15) in correspondence with predetermined values of the soil saturation degree.

The SD parameter quantifies the size range of equivalent pore diameters, or the "sorting" of pore diameters and it can take values within the range $1 \leq SD < \infty$. An SD value of 1 indicates that all pores are of the same diameter, while higher SD values reflect a broader range of pore diameters, indicating a lower degree of sorting. SK can take values between $-1 \leq SK \leq +1$, specifically, a SK value of 0 indicates a lognormal distribution, which is symmetrical on the log(d_e) scale. Negative SK values suggest an excess of small pores compared to a lognormal distribution, while positive values indicate an excess of large pores.

Lastly, KU falls within the range of value $0.41 \leq KU < \infty$. KU =1 corresponds to a lognormal distribution, values greater than 1 indicate a "leptokurtic" distribution, characterized by a higher peak at the center and more pronounced tails in the extremes compared to the lognormal curve. Conversely, values less than 1 indicate a "platykurtic" distribution, which is flatter at the center and has less pronounced tails in the extremes than the lognormal curve. The assessment of soil physical quality is based on comparing, for a given parameter, the measured value against one or more threshold values that distinguish between optimal, good, and poor-quality conditions (Reynolds et al., 2002, 2009; Olness et al., 1998; Dexter, 2004), shown in Table 1.

Parameter	Unit	Optimal value	Poor value	References
AC	$cm^3\ cm^{-3}$	>0.14	<0.10	Drewry, 2006 White, 2006
BD	$g\ cm^{-3}$	0.9 - 1.2	>1.30 (inadequate soil aeration) <0.90 (inadequate plant anchoring)	Olness et al., 1998 Reynolds et al., 2007
P_{mac}	$cm^3\ cm^{-3}$	≥ 0.07	≤0.04	Drewry et al., 2001 Drewry and Paton, 2005
PAWC	$cm^3\ cm^{-3}$	≥ 0.20	<0.10	Hall et al., 1977 Cockroft and Olsson, 1997
RFC	-	0.6 - 0.7	<0.6 (“water limited” soil) >0.7 (“aeration limited” soil)	Skopp et al., 1990 Doran et al., 1990
S-index	-	≥ 0.050	≤0.020	Dexter, 2004 Dexter and Czyz, 2007
d_{mode}	µm	60.0 - 140.0	-	Reynolds et al., 2009
d_{median}	µm	3.0 - 7.0	-	Reynolds et al., 2009
d_{mean}	µm	0.7 - 2.0	-	Reynolds et al., 2009
SD	-	400 - 1000	-	Reynolds et al., 2009
SK	-	-0.43 to -0.41	-	Reynolds et al., 2009
Ku	-	1.13 - 1.14	-	Reynolds et al., 2009

Table 1. Optimal and poor values for soil physical quality (SPQ) parameters, as proposed in the literature.

2.3. Effect of soil organic amendments on the SWRC

Soil organic matter (SOM) is a dynamic component of soil, composed of detritus from both animal and plant origins at various stages of decomposition. SOM contributes to vital soil functions such as sustained biological activity, nutrient cycling, and crop productivity

(Veum et al., 2014; Lal, 2021). The quantity and quality of organic matter directly affect numerous physical properties of the soil such as water retention capacity, porosity, and aeration (Dazzi, 2013). “Additionally, SOM is important to both soil structure and the potential for soil erosion, to sorption of mobile plant nutrients and retention of pesticides, and the CO_2 balance between agro-ecosystems and the atmosphere” (Christensen et al., 1997).

Degradation of organic matter can compromise soil fertility and functionality, a phenomenon that can be caused by various anthropogenic disturbances, including intensive agricultural practices, soil tillage and compaction by agricultural machinery, deforestation, and waterproofing interventions (Bedolla-Rivera et al., 2023). This degradation affects the soil's physical, chemical, biological, and ecological components, leading to an overall decline in soil quality and potentially reducing its ability to support essential ecosystem functions and services (Albiach et al., 2001).

To counteract this phenomenon, applying organic amendments could be one of the most effective agronomic practices. Indeed, it has been extensively proven that these amendments positively impact soil quality and improve water availability, which in turn leads to increased crop yields (Eden et al., 2017; Arthur et al., 2011; Kranz et al., 2020). Their application enhances soil structure, nutrient content, and moisture retention, ultimately contributing to more productive and resilient agricultural systems. The literature highlights a wide range of organic soil amendments available to improve soil water availability, including various types of animal manures, crop residues, tree leaves, grass clippings, food processing wastes, and sewage sludges, which can be residues or by-products of both agriculture and industrial processes (Magdof and Weil 2004). Peat, coir fiber dust, compost, and biochar, have been shown to significantly enhance the physical-chemical soil properties (Dong et al., 2022; Ibrahim et al., 2021; Ampim et al., 2010).

Compost types encompass a variety of materials, including sewage sludge and municipal waste (Sadeghi et al., 2014), maize and sewage sludge (Glab et al., 2020), pruning waste (Benito et al., 2006), farm crop residues (Ibrahim and Horton, 2021), yard waste (Curtis and Classen, 2009), orange juice processing by-products (Palazzolo et al., 2019), as well as various mixtures of these materials.

Glab et al. (2018) investigated the impact of adding co-composted mixtures of maize, sewage sludge, and biochar on the hydrological and physical quality of loamy sandy soil. Compared to the untreated control, the amended soil showed significant improvements in

physical properties with beneficial effects that were influenced by the compost application rate and the specific type of feedstock used.

Castellini et al. (2022) evaluated the short- and medium-term effects of compost addition on the physical and hydraulic properties of a clay soil by considering three different compost application rates (T): fertilizer (T2 = 1.5 kg m^{-2}), amending (T3 = 15 kg m^{-2}), and organic (T4 = 75 kg m^{-2}), all compared to a control (T1). Compost application at higher rates (75 kg m^{-2} and 15 kg m^{-2}) improved water retention and reduced bulk density in a clay soil, while at the lower dose (1.5 kg m^{-2}) the effects were not significantly different from the control. Higher compost rates also increased AC and PAWC, while decreasing RFC and BD.

Recently, vermicompost has been increasingly used as an organic soil improver, as it supports sustainable management practices and promotes the recycling of organic waste. Vermicompost, also called worm humus, is the result of the bio-oxidation and stabilization processes of organic material (e.g., food waste, horticultural waste, poultry droppings, food industry sludge, and so on) operated by earthworms, which makes it possible to obtain an organic material that is highly rich in humic acids thus representing a sustainable source of macro- and micro-nutrients. Several positive effects are documented in the literature, such as the constitution of a sustainable source of macro- and micro-nutrients (Zhao et al., 2017), promoting the survival of soil bacteria and reducing the number of soil fungi (Hou et al., 2023), increase in total porosity (Hallam et al., 2021), improvement of water infiltration (Fischer et al., 2014), decrease in bulk density (Baghbani-Arani et al., 2021), improvement of water use efficiency (Ebrahimi et al., 2021). However, only a few studies have fully explored the effects of adding vermicompost on soil water retention (Ma et al., 2022).

Pruning wastes have recently been utilized as organic soil amendment, though practical experience and studies in this area remain limited (Benito et al., 2006; Auteri et al., 2022). The pruning waste from cactus pear (*Opuntia ficus-indica* (L.) Mill.) paddles, resulting from agricultural activities, presents notable advantages due to its local availability, which contributes to its cost-effectiveness and sustainability. This species thrives in many semi-arid regions and is highly widespread in Central America and the Mediterranean basin, currently resulting in the disposal of 13–15 t ha^{-1} of biomass per year (Enea, 2017).

Cactus pear cladodes are succulent plant organs consisting of chlorenchyma, the outer layer in which photosynthesis occurs, and parenchyma, the innermost layer whose main function is to retain water. Both layers contain mucilage, a hydrocolloid that forms stable (honeycomb-like) lattices capable of holding large amounts of water. This feature allows

Cactaceae to thrive in harsh climatic conditions, making cactus pear an interesting and valuable agricultural by-product with potential as an organic soil amendment.

A point that has not been investigated in detail is related to the effect of the soil water retention curve hysteresis on soil pore volume distribution functions and capacitive soil physical quality (SPQ) indicators. Generally, the estimation of these parameters has been conducted based on data $\theta(h)$ obtained from desorption experiments, under the simplified assumption that hysteresis can be neglected in field conditions, as its influence is often masked by heterogeneity and spatial variability (Haverkamp et al., 2002).

The desorption SWRC reflects the soil's ability to store water and transfer it from wet to dry periods, across a relatively long-time scale. Instead, the adsorption SWRC, i.e., the soil water retention curve determined during a wetting process, can provide valuable insights into the soil's capacity to store water over shorter time scales related to the infiltration process. However, to the best of our knowledge, the wetting SWRC has never been employed to determine SPQ.

With this premise, Bondì et al. (2022; **Appendix A**) investigated the reliability of capacity-based indicators of SPQ and pore size distribution parameters in assessing the effectiveness of compost amendments on sandy loam soil. They evaluated the effects of water retention hysteresis on the estimation of SPQ.

A 5-months-aged compost from orange juice processing wastes (75%) and garden cleaning (25%), previously sieved at 2 mm and dried, was mixed to a sandy-loam soil in 7 different proportions by weight: 0% (or soil without amendment), 10%, 20%, 30%, 50%, 75% and 100% (or pure compost). Fourteen samples were prepared, and obtained by compacting the dry mass into metal cylinders with a diameter and height of 5 cm.

A typical hysteretic behavior has been found in the wetting–drainage water retention curves, which has affected the estimation of capacity-based indicators of SPQ and pore volume distribution parameters of a sandy-loam soil amended with compost. Compost amendment was effective in modifying the soil pore distribution system as the water entry potential increased and the air entry potential decreased at increasing the percentage of compost.

Therefore, compost has a positive effect on the hydrological and agronomic response of the soil, as it favors both water infiltration during wetting and water retention during drying, increasing in both cases the availability of water for crops as also detected by *RFC* and *PAWC* that increased with the percentage of compost added to soil.

Understanding the temporal persistence of the benefits of compost amendment is a crucial aspect for planning the most effective soil management practices. At this aim, a further investigation was conducted by Bondì et al., (2024; **Appendix B**) to evaluate the short-term effects of compost amendment on the physical and hydraulic properties of sandy loam soil. A total of forty-two samples were prepared according to the same procedure outlined in Bondì et al. (2022, **Appendix A**). In November 2021, soon after preparation, 14 samples, two for each mixture, were analyzed to determine the soil water retention curve at time M0. The remaining samples were placed directly on the surface of the extensive green roof plot at the University of Palermo, exposing them to atmospheric agents, and analyzed after six (M6) and twelve months (M12).

Temporal variability affected all assessed SPQ indicators, revealing significant differences. The maximum benefits were noted in the first six months. In particular, the compost application dose negatively affected SPQ indicators related to macro- and mesoporosity, such as P_{mac} and *AC*, while positively influenced SPQ indicators linked to plant water availability, such as *PAWC* and *RFC*. Compost also reduced soil compaction and modified the porosity system, resulting in smaller and less heterogeneous pores, thus improving the soil's water retention capacity.

In Castellini et al. (2024, **Appendix C**) the short-term effects of vermicompost addition on the water availability of five different textured soils, from sandy loam to clay loam, were analyzed. Soils were preliminary air-dried and sieved at 2-mm, mixed at 19 different amendment proportions by weight: from 0 (i.e., soil without amendment) to 43%. A total of 95 repacked soil samples were prepared, compacting the dry mass into metal cylinders with a diameter and height of 5 cm. Preliminarily, the hydrophobicity of vermicompost was tested by the water drop penetration time, WDPT, test. It was found that the water repellency depended on the initial moisture conditions, being easily wettable at field capacity but strongly to severely hydrophobic at lower moisture levels. Anyway, soil water repellency was negligibly affected by vermicompost in real field conditions.

Soil physical quality was effectively affected by vermicompost addiction with different results depending on soil texture: greater water availability for plants in coarse soils and a more balanced air/water ratio in fine soil. Minimal effects were found in the intermediate soil.

A further study by Bondì et al. (2024, **Appendix D**) explores the impact of adding powdered cactus pear pruning waste (PCPPW) on the hydraulic properties of benchmark soils, aligning with the principles of a circular economy. Two soils with different textures (sandy loam and

clay loam), previously air-dried and sieved to 2 mm, were mixed in 13 different proportions of amendment by weight: from 0 to 50%. 26 repacked soil samples were prepared, compacting the dry mass into metal cylinders with a diameter and height of 5 cm.

In both soils, bulk density significantly decreased with the increasing percentage of soil conditioner. Similarly, the drainable water content decreased as the amount of soil conditioner increased in both cases. In sandy loam, the PAWC increased to a maximum of 0.26 cm^3cm^{-3} with a content of r = 20%. A similar trend was observed in clay loam, where the maximum PAWC of 0.23 cm^3cm^{-3} corresponded to content of r = 30%.

3. Hydrological cycle: theory and modeling

The water present in the terrestrial globe describes a closed cycle, called the *water cycle* or *hydrological cycle*. It originates from the continuous water flow between the land and the atmosphere, during which it undergoes state transformations and qualitative changes while keeping its global mass constant in practice. The water cycle consists mainly of three phases: precipitation, evapotranspiration, and condensation (Paci, 2011). The energy contribution of solar radiation activates the processes of formation and transport of steam, the formation of runoffs from precipitation is, on the other hand, a process of an essentially gravitational nature.

The hydrological balance constitutes the mathematical schematization of the principle of conservation of mass that is, a quantitative evaluation of natural flows and stocks in the different forms (liquid, solid, gaseous) in which water manifests itself in its cycle on earth, (Munafò, 2022).

Therefore, in a given time interval the change in water content stored in a given volume of soil must be equal to the difference between water inputs and losses:

$$\Delta W = W_{in} - W_{out} \tag{22}$$

The hydrological balance is regulated by several variables (precipitation, atmospheric humidity, solar radiation, wind, soil, vegetation) and can be schematized through the following equation:

$$\Delta W = (P + I + U) - (R + S + E + T) \tag{23}$$

where ΔW is the change in water content in the active layer of soil explored by the roots, P is the precipitation water, I is the water supply through irrigation, U is the capillary rise, R represents the surface runoff, S is the amount of water that is loss by deep percolation (drainage), E is the evaporation from the soil, T is the transpiration by vegetation. All variables are expressed, for the time interval considered, in terms of volume per unit area (mm).

In the traditional approach to soil water balance modeling, the complex dynamics of water movement and distribution within the soil profile are overlooked. This approach typically models the soil as a static reservoir, representing water storage by a simple range between

two fixed limits. The permanent wilting point, generally assumed as the volumetric water content corresponding to h = -150 m, defines the lower boundary, which is the minimum soil moisture level at which plants can no longer extract water, leading to physiological stress and, ultimately, wilting. The upper boundary is determined by the field capacity, generally assumed as the volumetric water content corresponding to h = -1 m, represents the maximum amount of water soil can hold after gravitational drainage ceased. Therefore, this constitutes a one-dimensional approach, in which water flows are predominantly vertical. The Thornthwaite reservoir model (Thornthwaite, 1948) represents the first complete and formalized hydrological balance.

Afterward, the reservoir model gained traction and has been included in the FAO's guidelines for estimating crop evapotranspiration under conditions of water stress, as outlined in FAO Irrigation and Drainage Paper No. 56 (Allen et al., 1998). This approach has also been incorporated into the AquaCrop model, which simulates the effects of water availability on crop growth and performance.

More recently, a reservoir model concept has been adopted by Kasmin et al. (2010), who proposed a process-based rainfall-runoff model for simulating retention and detention in a green roof (figure 13). Rainfall retention refers to the permanent removal of stormwater, while runoff retention refers to the transient storage of rainfall (De Ville et al., 2017).

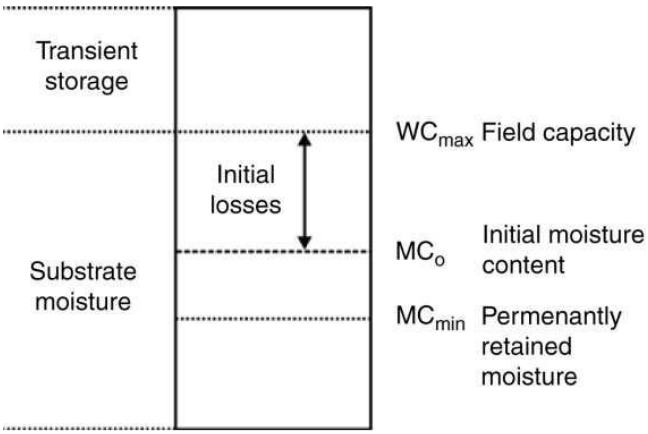

Figure 13. Schematization of the reservoir model (from Kasmin et al., 2010).

The Kasmin model is developed to estimate the temporary water storage capacity of a green roof by employing a straightforward storage routing approach, the equation for which is outlined below:

$$h_t = h_{t-1} + Qin_t \Delta t - Qout_t \Delta t \quad (24)$$

in which Q_{in} and Q_{out} represent, respectively, the flow of rainfall into and out of the growing medium layer, and h represents the stored moisture depth. Q_{out} is given by:

$$Q_{out_t} = kh_{t-1}^{n} \tag{25}$$

in which k and n are the reservoir routing parameters, representing the scale and exponent, respectively. In eqs. (24) and (25), h is expressed in mm, Q in mm min^{-1}, while k is expressed in $mm^{(1-n)}$ min^{-1} and n is a dimensionless parameter.

3.1. Hydrological behavior of a green roof

The hydrological behavior of a green roof is strongly conditioned by the water holding capacity, i.e. the ability to temporarily store incoming rainwater, resulting in a delay and reduction of the peak flood output. The water holding capacity of a green roof is a significant aspect of the potential contribution of green infrastructure to stormwater management (Yio et al.,2013). It is a phenomenon conceptually analogous to that of "lamination" exerted by a storage capacity.

The water holding capacity can be estimated using physically-based models (e.g.: HYDRUS-1D) based on an accurate hydrological parameterization of the stratified system consisting of the crop growth substrate and the underlying drainage element, or it can be determined experimentally through simulated rainfall tests. The latter possibility has been analyzed and studied in the framework of the present thesis.

To this end, several green roof microcosms were constructed using cylindrical samples with a diameter of 20 cm. These were created by combining various commercial substrates with different drainage systems.

The meteoric events were simulated using an experimental installation consisting of two load cells for the continuous monitoring of the water content of the microcosm and for the measurement of the drainage volume and by a needle rain simulator (figure 14).

Figure 14. Experimental installation: at the top the needle simulator, on the counter, and at the bottom the two load cells for measuring the water content and volumes drained from the microcosm of the green roof.

The two load cells (AZ 0-10) used are of the preamplified type with 0-10 Vdc output signal and full scale of 100 kg (measurement error on the f.s. $\leq \pm$ 2%). The signal acquisition was carried out automatically through a CR1000 datalogger, manufactured by Campbell Scientific® (figure 15).

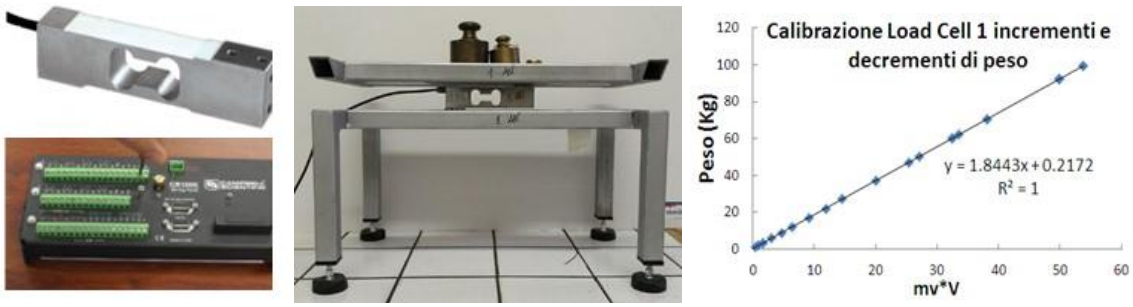

Figure 15. Load cell and acquisition system. On the right the experimental calibration report for cell no. 1.

The calibration report allows the electrical output signal to be transformed into a weight value. For the experimental determination, masses of known weight in the range 0 - 60 kg were used, detecting the corresponding voltage value (mV) at the output of the datalogger.

The relationship between the two quantities was linear with the values of the coefficient of determination $R^2 = 1$ and the value of the Root Mean Square Error (RMSE) less than 0.017 kg. The calibration reports for the two cells were as follows:

Cell n.1 $y = 1.84431x + 0.21724$ (26)

Cell n.2 $y = 1.8881x - 0.0085$ (27)

The rain simulator consists of an airtight chamber, fed by a height-adjustable loading tank (figure 14), on the bottom of which there are n = 45 hypodermic needles, distributed over an area of 314 cm^2. The diameter of the drop can be adjusted by varying the size of the needles. In the case in question, 22 G-type needles with a nominal external diameter of 0.7 mm were chosen.

The calibration of the simulator was carried out preliminarily, to determine the relationship between the rainfall intensity, i (mm h^{-1}), and the water head established in the loading tank, H (cm). The previously calibrated No. 1 load cell was used for the measurement of rainfall intensities.

Several tests were carried out in which increasing/decreasing sequences of water heads ($0 < H < 12$ cm) were applied to explore rainfall intensity values up to 180 mm h^{-1}. The explored range of rainfall intensity includes the maximum rainfall intensity in the duration of 10 min recorded in the period 2002-2021 for the Palermo area (figure 16).

The calibration report was linear with a coefficient of determination, R^2, equal to 0.9986.

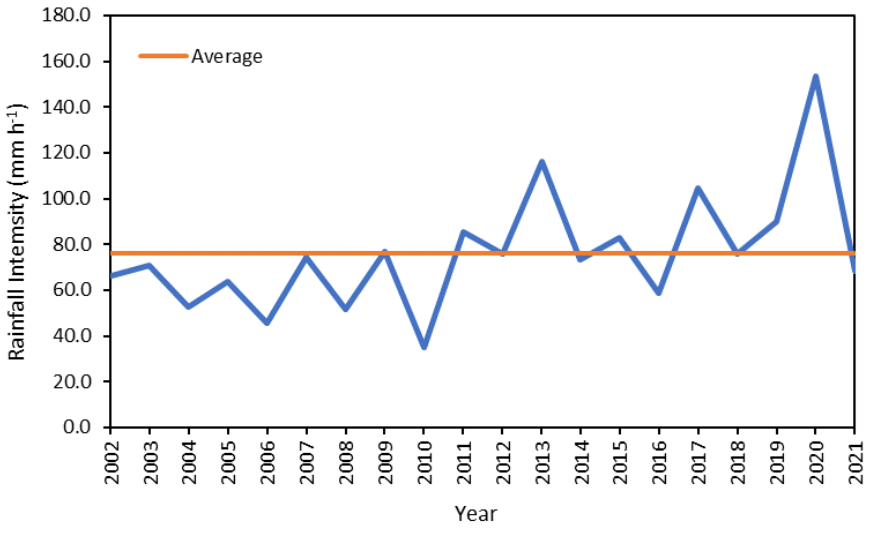

Figure 16. Maximum rainfall intensity (mm h^{-1}) for the duration of 10 min recorded in the period 2002-2021 at Palermo Uditore weather station managed by Sistema Informativo Agrometeorologico Siciliano (SIAS).

Through simulated rainfall experiments, Bondì et al. (2023, **Appendix E**) evaluated the hydrological response of a volcanic medium, VM, derived from ash deposition following recent volcanic eruptions of Mount Etna (Italy). Owing to its lightweight properties and sustainability, this material seems well-suited for the development of "engineered soils" that can serve as substrates for green roofs. Simulated rainfall experiments were carried out on microcosms ($V \approx 3000$ cm^3) to evaluate the detention and retention capacities of the VM under dynamic conditions. Three drainage layers were considered: a preformed stratified system called "MediDrain MD 25" (MD), a layer of expanded clay balls (EC), and a mineral layer consisting of expanded perlite (EP). The microcosms underwent infiltration tests with a constant rainfall intensity of 60 mm h^{-1}, applied for one hour. The first rain event was conducted on an air-dried sample to assess the hydraulic performance of a green roof under very dry summer conditions. A second rain event, conducted 24 hours later, aimed to investigate the hydrological response of the green roof under wet conditions, approaching field capacity. Furthermore, to enhance the physical and hydraulic properties of the VM, the particle size distribution was adjusted by artificially increasing or decreasing the coarse fraction, and the effects on pore size distribution were evaluated from the experimental assessment of SWRC.

Under initial dry conditions, the green roof was able to detain between 19.3% and 46.0% of the total rainfall, consistent with findings reported in the literature. The delay in the runoff formation was found to be maximum, i.e. 0.38 h, for the VM-EC combination. When starting from initially wet conditions, the detention capacity decreased but still accounted for approximately 10% of the total rainfall. Finally, reducing the coarse fraction of the VM decreased macroporosity and increased mesoporosity, thereby improving the drainable water capacity, which positively impacted the substrate's detention capacity.

In conclusion, VM can be considered an effective and sustainable mineral component that, when combined with organic materials such as compost or peat, forms an ideal substrate for extensive green roofs in Mediterranean climates.

4. Hydraulic conductivity of green roof substrates

A crucial property of a green roof substrate is its hydraulic conductivity. Hydraulic conductivity, K (m s^{-1}), expresses the substrate's ability to transmit water.

The saturated hydraulic conductivity of porous media governs the partition of rainfall into infiltration and surface runoff, playing a crucial role in effective stormwater management by directly influencing the substrate's detention capacity and its rate of water absorption and retention.

It primarily depends on the geometry of the pores, including their size, shape, and interconnections, as well as the soil's water content (Hillel, 1998).

When the soil is fully saturated, meaning all pore spaces are filled with water, the hydraulic conductivity reaches its maximum value, known as saturated hydraulic conductivity, K_s. This condition represents the soil's highest potential for water transmission, as the continuous liquid phase allows for the most efficient water flow. Thus, K_s constitutes a key parameter for describing water fluxes and solute transport within the soil (Rienzner and Gandolfi, 2014).

However, in most cases, the soil is only partially saturated. Under these conditions, the conductivity decreases, as air fills some of the pore spaces, disrupting the continuity of the water flow. The hydraulic conductivity of partially saturated soil is thus dependent on its moisture content, which varies with environmental conditions such as rainfall, evaporation, and plant uptake. As the water content decreases, and consequently the soil's matric potential, h, drops, hydraulic conductivity decreases due to the draining of larger pores. Typically, under saturated conditions, K is higher in coarse-textured soils and/or highly porous, or well-aggregated soils, while it is lower in fine-textured, compacted, and dense soils. However, due to the sorting of conductive pores, the unsaturated hydraulic conductivity of a coarse soil may drop well below that of a fine soil at water contents close or below the field capacity.

Accurate estimation of hydraulic conductivity is crucial for simulating water flow by physically based models, like HYDRUS model, which solves the non-linear Richards equation (1931) for water fluxes into the vadose zone (Haverkamp et al., 1994).

4.1. Methods

Among the multiple methods available for measuring soil hydraulic conductivity, which vary on the basis measurement scale (laboratory vs. field), the geometry of flux (1D vs. 3D) and the flow process (steady-state vs. transient), the focus has been put on three techniques: the MiniDisk Infiltrometer (MDI), the evaporation method, and steady-state unit hydraulic gradient (UHG) method.

The MDI, manufactured by Decagon (Decagon Devices, Inc., Pullman, WA), is a simple, cost-effective, portable miniaturized tension infiltrometer, making it highly practical for field use. It enables fast and accurate measurements, providing valuable data on soil water movement without the request for complex equipment or extensive setup. It needs small amounts of water, approximately 135 mL, to function, which makes it particularly efficient and suitable for field settings where water resources may be constrained. The MDI is handy for studying water infiltration in soils, offering insights into the hydrological behavior of various substrates in real-world conditions.

It consists of a single plexiglass tube, approximately 3 cm in diameter and 30 cm in height, divided into two chambers by a sealed partition (figure 17). The upper chamber, or bubble chamber, controls the pressure head via a suction control tube, while the lower chamber, or water reservoir, is designed like a graduated cylinder, and contains 95 mL of water, which infiltrates into the soil at the selected pressure head, h, through a porous sintered stainless-steel disk, with a diameter of 4.5 cm, located at the bottom of the infiltrometer (figure 17).

To ensure proper hydraulic connection between the disk and the soil, a layer of contact fine material is often placed beneath the infiltrometer.

When the MDI is placed on the soil surface, the rise of the first air bubble into the reservoir indicates the start of the infiltration process. Following a transient phase, where the infiltration rate initially decreases, the flow stabilizes, reaching a constant steady-state infiltration rate, i_s (mm h^{-1}). The water flow rate is then monitored by observing the water level on the graduated scale of the reservoir.

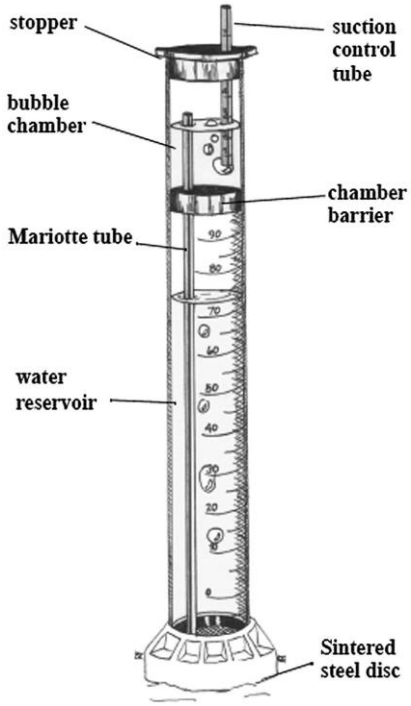

Figure 17. Scheme of MiniDisk Infiltrometer (by Decagon Devices, Inc., Pullman, WA).

The evaporation method, also referred to as the Wind method (Wind, 1968), is a well-established and extensively applied technique for simultaneously determining the hydraulic conductivity and the water retention properties of unsaturated soils in the matric potential range of 0 to -8 m.

The experimental setup consists of a precision balance for determination of the sample's weight, along with two or more porous microtensiometers, with a diameter between 2 and 6 mm, connected to pressure transducers for the measurement of matric potential. Additionally, the system includes an automated data acquisition and recording system, ensuring precise and continuous monitoring of the experimental parameters throughout the testing process (figure 18).

The experiment involves subjecting a soil sample, initially saturated or nearly saturated, to a controlled evaporation process. Following saturation from below, the sample is allowed to drain freely for a minimum of twelve hours, with the upper end covered to prevent evaporation (Bagarello and Iovino, 2010). It is recommended to initiate the experiment at a matric potential slightly below zero, as this ensures the continuity of the air phase within the sample (Wendroth et al., 1993). The sample is sealed at the bottom and placed on the balance, with the top surface exposed to the atmosphere.

It is important to consider that the evaporation process occurs at a rate influenced not only by the hydraulic properties of the soil but also by the environmental conditions under which the test is conducted. For this reason, it is recommended to conduct the experiment under controlled temperature and humidity conditions to make the results from different samples comparable.

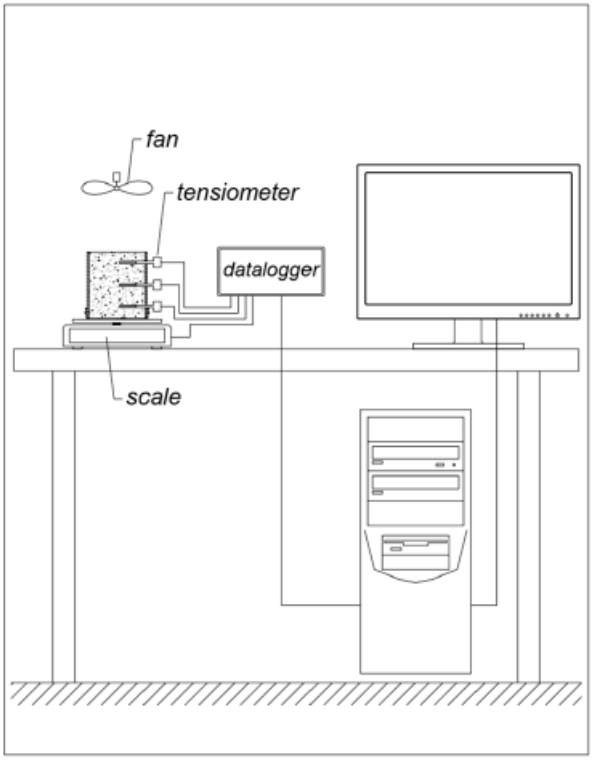

Figure 18. Experimental setup for the Wind evaporation method (from Autovino et al., 2024).

During the transient phase, simultaneous measurements are taken at various time intervals to monitor both the matric potential at different depths and the total water content of the sample. The analysis of the measurements is conducted in two stages: first, the water retention curve, $\theta(h)$, is determined using an iterative procedure considering the sample weight and the average pressure head readings of the microtensiometers, and then the hydraulic conductivity function, $K(h)$, is calculated through a modified version of the instantaneous profile method, which assumes knowledge of the average water content of the entire sample, ensuring a comprehensive characterization of the soil's hydraulic properties.

The steady-state unit hydraulic gradient (UHG) method enables the laboratory determination of hydraulic conductivity near saturation. A steady-state water flow condition is established

in a soil sample which is subjected to the same predetermined pressure head value at both the surface and the bottom of the soil sample.

The equipment described by Bagarello et al., (2007) was utilized. The lower end of the sample is placed in contact with a porous ceramic plate having an air entry value of −400 mm, connected to an outflow tube (figure 19), which can be adjusted in height to ensure a uniform distribution of the pressure potential along the sample, i.e., unitary hydraulic potential gradient. The upper pressure head is maintained by the porous disk of a tension infiltrometer device. As a result, the flow occurs solely due to gravity. Under steady-state conditions, the sample hydraulic conductivity is equal to the flow density measured a the tension infiltrometer reservoir.

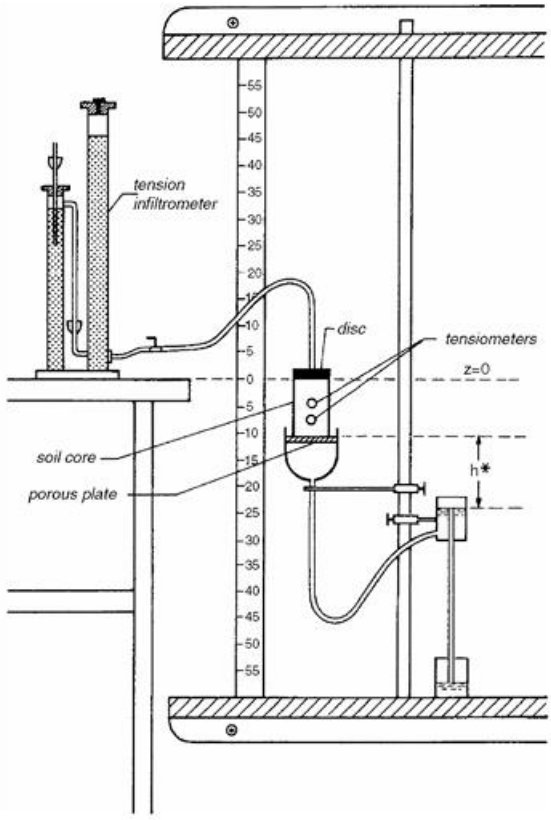

Figure 19. Experimental setup for the steady-state unit hydraulic gradient (UHG) method (from Bagarello et al., 2007).

The assumption is that, under steady-state conditions, the pressure head remains constant along the vertical axis and over time, allowing the measured value of *K* to be associated with an unequivocally determined value of *h*. The knowledge of the soil water retention curve,

independently determined for the same soil, enables the association of the measured *K* value with the corresponding volumetric water content of the soil, θ.

4.2. Hydraulic characterization of commercial substrates for green roofs

Two commercially available substrates for green roof realizations, Terra Mediterranea (TMT) and AgriTERRAMR (ATV), produced respectively by Harpo Verdepensile (Harpo spa, Trieste, Italy) and Perlite Italiana srl (Corsico, Milan, Italy), were hydraulically characterized in a study conducted by Autovino et al. (2024, **Appendix F**). The first substrate is composed of a mixture of 80% mineral materials, including lapillus, pumice, and zeolite, and 20% organic materials, such as peat and compost. The second substrate comprises a mineral fraction (75–80%) that includes lapillus, pumice, and expanded perlite, while the organic fraction (20–25%) consists of peat, bark, coconut fiber, and organic conditioners.

The water retention curve, θ(*h*), and hydraulic conductivity curve, K(*h*), were determined using a laboratory procedure consisting of a transient evaporation experiment combined with a steady-state UHG test.

Both direct and inverse estimations of K(θ) and θ(h) relationships in the form of unimodal or bimodal Van Genuchten (VG) models were performed. For the numerical inversion of the transient evaporation experiments, Hydrus-1D was applied.

The results highlighted that the evaporation method, whether direct or inverse, is inadequate for estimating the near-saturated hydraulic conductivity of heterogeneous pore media like the substrates under study.

A significantly more accurate description of the K(*h*) function was achieved only when the inverse method was coupled with UHG data and the bimodal VG model was considered.

4.3. Effect of aging on a commercial substrate for green roofs

Hydraulic conductivity exhibits significant spatial and temporal variability, even in areas of limited surface extent, stemming from a complex interaction of factors that influence water movement through porous media (Bagarello and Iovino, 2010; Deb and Shukla, 2012). According to Nielsen et al. (1973), hydraulic conductivity is primarily influenced by intrinsic factors related to soil formation, affecting long-term variability, and by extrinsic factors such as land use and management practices, which typically drive short-term changes. Intrinsic

variability, driven by pedogenesis, is often characterized by regionalization, with nearby areas exhibiting greater similarity than those located further apart (Dane and Topp, 2002). In contrast, extrinsic variability can manifest more rapidly and may not follow a regionalized pattern. Among the extrinsic factors, fluctuations in moisture content are significant, as they alter the degree of saturation within the soil or substrate, thereby affecting its permeability. Additionally, changes in pore structure play a crucial role in determining hydraulic conductivity. For instance, root growth can lead to local compaction, thereby reducing pore volume, whereas the decay of dead roots can create channels that increase pore space, enhancing hydraulic conductivity (Schwen et al., 2011). The process of self-filtration, involving the mobilization and re-deposition of particles within the porous medium, can lead to a more compact and less conductive lower layer (Dikinya et al., 2008).

Environmental conditions, such as temperature, precipitation patterns, and seasonal cycles, also contribute to dynamic variations of soil hydraulic conductivity.

Aging of a green roof substrate, marked by the gradual degradation of its physical, chemical, and biological properties, alters its hydraulic conductivity, leading to reduced water retention and detention capacity due to compaction, changes in porosity, nutrient depletion, and organic matter accumulation, ultimately compromising the roof's efficiency in stormwater management (Berndtsson, 2010). In their comprehensive review of green roof literature, Li and Babcock (2014) found that few studies have examined the impact of green roof aging on hydrological performance, a gap partly due to the lack of long-term data and the influence of climatic variability on observed changes.

Therefore, all these factors must be carefully considered when assessing the hydraulic behavior of such systems. An accurate assessment is essential to understand how the substrate performs under different humidity conditions and to optimize its performance in various climates and operative scenarios.

It is in this context that the study conducted by Bondì et al. (2023, **Appendix G**) fits in, aiming to address the knowledge gap regarding the processes underlying the short-term changes in green roof detention capacity. The study was conducted in the extensive green roof plot established at the University of Palermo established in 2019. This plot was constructed using the Terra Mediterranea (TMT) supplied by Harpo Verdepensile (Harpo spa, Trieste, Italy), the same commercial substrate characterized by Autovino et al., (2024, **Appendix F**). Seasonal variations in the saturated and near-saturated hydraulic conductivity, corresponding to h values of -0.5 and -3.0 cm, were investigated using the MiniDisk

Infiltrometer (MDI), which allows for a relatively simple, rapid, and cost-effective measurement of the infiltration rate with minimal disturbance to the surface layer, also preserving the functional connection of the conductive pore system with the surrounding medium.

Field infiltration experiments were conducted on the experimental plot in December 2017 (T0), October 2018 (T1), and summer 2022 (T2) to assess short- and long-term variations in infiltration characteristics. The steady-state infiltration rate, i_s (mm h^{-1}), was estimated from the slope of the regression line fitted to the linear portion of the cumulative infiltration, I (mm), versus time, t (s), curve. A minimum of five consecutive data points for I vs. t were used for the regression. From T0 to T1, i_s increased by a factor of 2.4 under near-saturated conditions and by a factor of 1.9 under quasi-saturated conditions.

From measurements of bulk density and texture carried out at the same time, at different depths of the substrate, it was possible to ascertain that the increase in infiltration speed is attributable to the washing away of the finest particles from the surface of the substrate towards the deeper layer. After five years (T2), the hydraulic characteristics of the substrate continue to evolve, although at a reduced rate. Specifically, the steady-state infiltration rate under unsaturated conditions tends to decrease, approaching values closer to those observed at the beginning (i_s = 51.9 mm h^{-1} for T2 versus i_s = 37.5 mm h^{-1} for T0). In contrast, the steady-state infiltration rate under saturated conditions continues to increase, reaching approximately twice the initial value (i_s = 267.7 mm h^{-1} for T2 versus i_s = 147.8 mm h^{-1} for T0).

The experiment detected changes in the steady-state infiltration characteristics of the growing substrate resulting from particle self-filtration induced by rainfall.

Over the lifespan of the green roof, the contribution to flow from macropores (larger than 1 mm) increases, while that from smaller pores decreases, due to pore occlusion caused by root development and hydrophobicity from vegetation exudates and decaying materials.

5. Conclusions

The increasing spread of soil sealing has significantly disrupted the natural hydrological processes of water infiltration and interception by vegetation. This has led to a rapid transformation of rainfall into surface runoff, typically diverted entirely into urban drainage systems. Soil sealing also contributes to the loss of organic matter, a critical component for maintaining soil health and productivity. In Mediterranean regions, this phenomenon has been a driving force behind disastrous events caused by intense rainfall. Addressing this issue requires urgent attention and the implementation of sustainable urban planning practices to mitigate the environmental and societal risks associated with altered hydrological processes. In urban environments, green infrastructures (GI) are an increasingly sought-after solution for enhancing the resilience of urban areas by capturing and regulating runoff. However, one of the key challenges in its implementation is the selection of an appropriate substrate, which is critical to its overall effectiveness and sustainability.

The main objective of this thesis was to investigate the hydraulic properties of the substrate through a comprehensive, multiscale methodological approach, specifically focusing on the water retention curve and hydraulic conductivity function, both of which influence the hydrological response of green roofs being closely connected to, respectively, the substrate's retention and detention capacities. The retention capacity refers to the substrate's ability to permanently store incoming rainwater whereas the detention capacity pertains to transient storage of rainfall. Both of them contribute to delaying and reducing peak flow of stormwater events.

In the first part of the thesis, the effects of various organic soil amendments derived from agricultural by-products, such as compost, vermicompost, and pruning residues, were evaluated with regard to soil water retention curves and soil physical quality. All the amendments studied demonstrated a positive impact on the hydraulic properties of the substrates. As found in the **Appendix A**, , the incorporation of compost effectively alters, in the short term, the pore distribution of sandy loam soil with an increase of the fraction of structural porosity (i.e.,macropores) and a decrease ofthe fraction of textural porosity (i.e., micropores). This amendment positively impacts the soil's hydrological and agronomic responses by promoting water infiltration during wetting and retention during the drying process, thereby increasing water availability for crops. From **Appendix B** it can be deduced that all SPQ indicators were affected by temporal variability with the maximum benefits that

were obsereved in the first six months of application. Specifically, indicators linked to the macro- and mesoporosity (P_{mac} and AC) decreased with the compost amendment dose whereas indicators linked to plant water availability ($PAWC$ and RFC) increased. Furthermore, compost has reduced, over time, soil compaction and modified the porosity system, resulting in smaller and less heterogeneous pores, thus improving the soil's water retention capacity.

Vermicompost also positively influenced the physical quality of five amended soils of varying textures (from sandy loam to clay loam) studied in **Appendix C**, with effects differing by soil texture. Specifically, it increased water availability in coarse-textured soils and improved the air-to-water ratio in fine-textured soils, while minimal and not statistically significant results were observed in soils of intermediate texture. Vermicompost also exhibited hydrophobicity that depended on the initial moisture conditions; it was found to be wettable at field capacity but strongly hydrophobic when air-dry. However, when incorporated into soil even at the highest application ratio (r = 43%), vermicompost minimally influenced hydrophobicity thus concluding that its effect on water availability can be considered negligible in practice.

As illustrated in **Appendix D**, the amendment with the powdered cactus pear pruning waste was investigated in the perspective of a circular economy approach aiming at reusing the residues of crops widespread in Sicily. It effectively reduced the bulk density of both amended sandy loam and clay loam soils and increased the water availability for plants, enhancing the overall soil quality for cultivation.

The selection of the soil amendment, its optimal dosage, and the timing of applications should carefully consider soil texture and the temporal variability of its beneficial effects, which tend to diminish over time. Furthermore, each soil improver has shown the capacity to enhance one or more physical quality parameters of the soil while potentially being less effective for others.

In conclusion, all these findings underscore the potential of organic amendments to significantly enhance the soil structure and improve water retention.. Their short-term effects offer valuable insights for increasing the fraction of water available for crops in arid environments or during extended dry periods, such as those that occur in the summer months of the Mediterranean regions.

In the second part of the thesis, the hydrological behavior of the green roof substrate was assessed, focusing on its retention and detention capacities. Particular attention was given,

in **Appendix E**, to evaluating the hydrological response of a volcanic medium collected from street sweeping on Mount Etna. This material, which meets the principles of a circular economy, demonstrated a favorable hydrological behavior under different types of drainage layer and initial moisture conditions. Therefore, it can be recommended as an effective and sustainable choice for the mineral component of a green roof substrate in Mediterranean climates, especially when it is combined with a well-balanced mixture of organic materials such as for example, those considered in this thesis: compost and vermicompost.

The last part of the thesis is focused on the laboratory and field determination of the substrate hydraulic conductivity which is closely linked to the detention capacity of a green roof. An accurate experimental determination of the hydraulic conductivity curve, K(h), was found to be highly dependent on the laboratory methodology and the data fitting model applied. In **Appendix F**, it is demonstrated that combining several techniques, in this case, the UHG method with the inverse evaporation method, yields the highest accuracy.

Hydraulic conductivity is a dynamic property of the porous medium that may be influenced by environmental conditions such as temperature, precipitation patterns, and seasonal cycles. The assessment of seasonal variations in saturated and near-saturated hydraulic conductivity, conducted in **Appendix G**, highlighted short-term changes in the steady-state infiltration characteristics of the growing substrate. These changes were attributed to the particle self-filtration induced by rainfall and to the reduction in the bulk density of the upper layer, overall resulting in a more conductive porous medium. After five years of green roof operation, field conductivity did not increase further, indicating that the washout/clogging process was either completed within a season or counteracted by other processes, such as root development and hydrophobicity.

Field monitoring of infiltration is an essential tool for detecting changes in water detention properties, which could compromise the environmental benefits of green roofs by reducing stormwater mitigation and water storage capacity.

In conclusion, the set of results obtained in this thesis contribute to move forward the knowledge on the hydraulic functioning of growing substrates for urban green infrastructure. A thorough assessment is essential to understand the substrate's behavior under varying moisture conditions and optimize its performance across different climates and operational scenarios. Organic amendments have proven to be highly effective in enhancing the overall physical quality of the soil and mitigating the loss of soil organic matter. Their performance

can be further optimized by incorporating strategically selected mineral components to improve the substrate's hydrological response. However, a deeper understanding requires further investigation, particularly on the influence that plants may play in the hydrological response of green roofs.

References

Aggelides, S.M., Londra, P.A., 2000. Effects of compost produced from town wastes and sewage sludge on the physical properties of a loamy and a clay soil. Bioresource Technology 71: 253-259. https://doi.org/10.1016/S0960-8524(99)00074-7

Alagna, V., Bagarello, V., Concialdi, P., Giordano, G., Iovino, M., 2020. Evaluation of Green Roof Ageing Effects on Substrate Hydraulic Characteristics, Lecture Notes in Civil Engineering, pp. 89–97. https://doi.org/10.1007/978-3-030-39299-4_10

Albiach, R., Canet, R., Pomares, F., Ingelmo, F., 2001. Organic matter components and aggregate stability after the application of different amendments to a horticultural soil. Bioresource Technology 76: 125-129. https://doi.org/10.1016/S0960-8524(00)00090-0

Allen, R.G., Pereira, L.S., Raes, D., Smith, M., 1998. Crop evapotraspiration. Guidelines for computing crop water requirements. FAO Irrigation and Drainage Paper (56), Rome, Italy.

Ampim, P.A.Y., Sloan, J.J., Cabrera, R.I., Harp, D.A., Jaber, F.H., 2010. Green roof growing substrates: types, ingredients, composition and properties. J. Environ. Hort, 28(4): 244-252. https://doi.org/10.24266/0738-2898-28.4.244

Arthur, E., Cornelis, W.M., Vermang, J., De Rocker, E., 2011. Amending a loamy sand with three compost types: impact on soil quality. Soil Use Manag. 27, 116–123. https://doi.org/10.1111/j.1475-2743.2010.00319.x

Auteri, N., Saiano, F., Scalenghe, R., 2022. Recycling phosphorus from agricultural streams: grey and green solutions. Agronomy 12: 2938. https://doi.org/10.3390/agronomy12122938

Autovino, D., Alagna, V., Bondì, C., Iovino, M., 2024. Hydraulic Characterization of Green Roof Substrates by Evaporation Experiments. Appl. Sci. 14: 1617. https://doi.org/10.3390/app14041617

Bagarello, V., Castellini, M., Iovino, M., 2007. Comparison of unconfined and confined unsaturated hydraulic conductivity. Geoderma 137: 394–400. https://doi.org/10.1016/j.geoderma.2006.08.031

Bagarello, V., Iovino, M., 2010. Conducibilità idraulica del suolo. Metodi di misura nelle applicazioni idrologiche. Ulrico Hoepli Editore S.p.A., Milano.

Baghbani-Arani, A., Modarres-Sanavy, S.A.M., Poureisa, M., 2021. Improvement the soil physicochemical properties and fenugreek growth using zeolite and vermicompost under water deficit conditions, J. Soil Sci. Plant Nutr., 21: 1213–1228. https://doi.org/10.1007/s42729-021-00434-y

Bedolla-Rivera, H.I., Xochilt Negrete-Rodríguez, M., Gámez-Vázquez, F.P., Álvarez-Bernal, D., Conde-Barajas, E., 2023. Analyzing the Impact of Intensive Agriculture on Soil Quality: A Systematic Review and Global Meta-Analysis of Quality Indexes. Agronomy 13(8), 2166. https://doi.org/10.3390/agronomy13082166

Benito, M., Masaguer, A., De Antonio, R., Moliner, A., 2005. Use of pruning waste compost as a component in soilless growing media. Bioresource Technology, 96: 597-603. https://doi.org/10.1016/j.biortech.2004.06.006

Benito, M., Masaguer, A., Moliner, A., de Antonio, R., 2006. Chemical and physical properties of pruning waste compost and their seasonal variability. Bioresour. Technol., 97: 2071–2076. https://doi.org/10.1016/j.biortech.2005.09.011

Berndtsson, J.C., 2010. Green roof performance towards management of runoff water quantity and quality: A review. Ecological Engineering, 36: 351-360. https://doi.org/10.1016/j.ecoleng.2009.12.014

Blott, S.J., Pye, K., 2001. Gradistat: a grain size distribution and statistics package for the analysis of unconsolidated sediments. Earth Surf. Process. Landforms 26, 1237–1248. https://doi.org/10.1002/esp.261

Bondì, C., Castellini, M., Iovino, M., 2022. Compost Amendment Impact on Soil Physical Quality Estimated from Hysteretic Water Retention Curve. Water, 14: 1002. https://doi.org/10.3390/w14071002

Bondì, C., Concialdi, P., Iovino, M., Bagarello, V., 2023. Assessing short- and long-term modifications of steady-state water infiltration rate in an extensive Mediterranean green roof. Heliyon 9: e16829. https://doi.org/10.1016/j.heliyon.2023.e16829

Bondì, C., Alagna, V., Iovino, M., 2023. Hydrological response of a volcanic medium as a potential substrate for green roofs. 2023 IEEE International Workshop on Metrology for Agriculture and Forestry (MetroAgriFor). https://doi.org/10.1109/MetroAgriFor58484.2023.10424119

Bondì, C., Auteri, N., Saiano, F., Scalenghe, R., D'Acqui, L.P., Bonetti, A., Iovino, M., 2024. Cactus pear pruning residue in agriculture: Unveiling soil-specific responses to enhance water retention. Environmental Technology & Innovation, 34: 103602. https://doi.org/10.1016/j.eti.2024.103602

Bondì, C., Castellini, M., Iovino, M., 2024. Temporal variability of physical quality of a sandy loam soil amended with compost. Biologia. https://doi.org/10.1007/s11756-024-01637-1

Bouzouidja, R., Séré, G., Claverie, R., Ouvrard, S., Nuttens, L., Lacroix, D., 2018. Green roof aging: Quantifying the impact of substrate evolution on hydraulic performances at the lab-scale. Journal of Hydrology 564: 416-423. https://doi.org/10.1016/j.jhydrol.2018.07.032

Brooks, R.H., Corey, A.T., 1966. Properties of porous media affecting fluid flow. J. Irrig. Drain. Div., Am. Soc. Civil Eng., 92(IR2): 61-88. https://doi.org/10.1061/JRCEA4.0000425

Cannavo, P., Vidal-Beaudet, L., Grosbellet, C., 2014. Prediction of long-term sustainability of constructed urban soil: impact of high amounts of organic matter on soil physical properties and water transfer. Soil Use Manag. 30, 272–284. https://doi.org/10.1111/sum.12112

Cao, C.T.N., Farrell, C., Kristiansen, P.E., Rayner, J.P., 2014. Biochar makes green roof substrates lighter and improves water supply to plants. Ecological Engineering, 71: 368-374. https://doi.org/10.1016/j.ecoleng.2014.06.017

Cascone, S., 2019. Green Roof Design: State of the Art on Technology and Materials. Sustainability, 11: 3020. https://doi.org/10.3390/su11113020

Castellini, M., Diacono, M., Preite, A., Montemurro, F., 2022. Short- and Medium-Term Effects of On-Farm Compost Addition on the Physical and Hydraulic Properties of a Clay Soil. Agronomy, 12: 1446. https://doi.org/10.3390/agronomy12061446

Castellini, M., Bondì, C., Giglio, L., Iovino, M., 2024. Impact of vermicompost addition on water availability of differently textured soils. Heliyon, 10: e35699. https://doi.org/10.1016/j.heliyon.2024.e35699

Charpentier, S., 2015. Simulation of Water Regime and Sensible Heat Exchange Phenomena in Green Roof Substrates. Vadose Zone Journal. https://doi.org/10.2136/vzj2014.07.0090

Chiarelotto, M., Salcedo Restrepo, J.C.P., Lorin, H.E.F., Damaceno, F.M., 2021. Composting organic waste from the broiler production chain: A perspective for the circular economy. Journal of Cleaner Production 329: 129717. https://doi.org/10.1016/j.jclepro.2021.129717

Christensen, B.T., Johnston, A.E., 1997. Soil organic matter and soil quality: lessons learned from long-term experiments at Askov and Rothamsted. In Gregorich, E.G., Carter, M.R. (Eds.), *Soil Quality for Crop Production and Ecosystem Health. Developments in Soil Science*, vol. 25. Elsevier, New York, NY, pp. 399 – 430. https://doi.org/10.1016/S0166-2481(97)80045-1

Cockroft, B., Olsson, K.A., 1997. Case study of soil quality in south-eastern Australia: management of structure for roots in duplex soils. In: Gregorich, E.G., Carter, M.R. (Eds.), Soil Quality for Crop Production and Ecosystem Health. In: Developments in Soil Science, vol. 25. Elsevier, New York, NY, pp. 339-350. https://doi.org/10.1016/S0166-2481(97)80043-8

Curtis, M.J., Claassen, V.P., 2009. Regenerating topsoil functionality in four drastically disturbed soil types by compost incorporation. Restor. Ecol.,17: 24–32. https://doi.org/10.1111/j.1526-100X.2007.00329.x

Dane, J.H.; Hopmans, J.W. 3.3.2.2 Hanging water column. In Methods of Soil Analysis, Part 4, Physical Methods, Number 5 in the Soil Science Society of America Book Series; Dane, J.H., Topp, G.C., Eds.; Soil Science Society of America, Inc.: Madison, WI, USA, 2002; pp. 680–683.

Dane, J.H.; Hopmans, J.W. 3.3.2.4 Pressure plate extractor. In Methods of Soil Analysis, Part 4, Physical Methods, Number 5 in the Soil Science Society of America Book Series; Dane,

J.H., Topp, G.C., Eds.; Soil Science Society of America, Inc.: Madison, WI, USA, 2002; pp. 688–690.

Dazzi, C. 2013. Fondamenti di pedogologia. *Le Penseur*.

Deb, S.K., Shukla, M.K., 2012. Variability of hydraulic conductivity due to multiple factors. American Journal of Environmental Science 8 (5): 489-502.

De-Ville, S., Menon, M., Stovin, V., 2018. Temporal variations in the potential hydrological performance of extensive green roof systems. Journal of Hydrology, 558: 564–578. https://doi.org/10.1016/j.jhydrol.2018.01.055

Dexter, A.R., 2004. Soil physical quality Part I. Theory, effects of soil texture, density, and organic matter, and effects on root growth. Geoderma, 120: 201-214. https://doi.org/10.1016/j.geoderma.2003.09.004

Dexter, A.R., CZYŻ, E.A., 2007. Applications of *S*-Theory in the study of soil physical degradation and its consequences. Land Degrad. Develop., 18: 369-381. https://doi.org/10.1002/ldr.779

Dikinya, O., Hinz, C., Aylmore, G., 2008. Decrease in hydraulic conductivity and particle release associated with self-filtration in saturated soil columns, Geoderma 146 (1): 192–200. https://doi.org/10.1016/j.geoderma.2008.05.014

Dong, L., Zhang, W., Xiong, Y., Zou, J., Huang, Q., Xu, X., Ren, P., Huang, G., 2022. Impact of short-term organic amendments incorporation on soil structure and hydrology in semiarid agricultural lands. Int. Soil Water Conserv. Res. 10: 457–469. https://doi.org/10.1016/j.iswcr.2021.10.003

Doran, J.W., Mielke, L.N., Power, J.F., 1990. Microbial activity as regulated by soil waterfilled pore space. Symposium III-3, Ecology of Soil Microorganisms in the Microhabitat Environments III. Transactions of the 14th International Congress of Soil Science, August 12–18, Kyoto, Japan, pp. 94–99.

Doran, J.W., Sarrantoni, M., Liebig, M.A., 1996. Soil health and sustainability, In L.S. Donald (ed.). Adv. Agron. Academic Press, pp. 1-54.

Drewry, J.J., Cameron, K.C., Buchan, G.D., 2001. Effect of simulated dairy cow treading on soil physical properties and ryegrass pasture yield. New Zealand J. Agric. Res., 44: 181–190. https://doi.org/10.1080/00288233.2001.9513476

Drewry, J.J., Paton, R.J., 2005. Soil physical quality under cattle grazing of a winter-fed brassica crop. Aust. J. Soil Res., 43: 525–531. https://doi.org/10.1071/SR04122

Drewry, J.J., 2006. Natural recovery of soil physical properties from treading damage of pastoral soils in New Zealand and Australia: a review. Agric. Ecosys. Environ. 114: 159-169. https://doi.org/10.1016/j.agee.2005.11.028

Durner, W., 1994. Hydraulic conductivity estimation for soils with heterogeneous pore structure. Water Resources Research, 30(2): 211-223. https://doi.org/10.1029/93WR02676

Ebrahimi, M., Souri, M.K., Mousavi, A., Sahebani, N., 2021. Biochar and vermicompost improve growth and physiological traits of eggplant (*Solanum melongena* L.) under deficit irrigation, Chem. Biol. Technol. Agric., 8:19. https://doi.org/10.1186/s40538-021-00216-9

Eden, M., Gerke, H.H., Houot, S., 2017. Organic waste recycling in agriculture and related effects on soil water retention and plant available water: a review. Agron. Sustain. Dev. 37: 11. https://doi.org/10.1007/s13593-017-0419-9

Elliott, A.H., Trowsdale, S.A., 2007. A review of models for low impact urban stormwater drainage. Environmental Modelling & Software, 22: 394-405. https://doi.org/10.1016/j.envsoft.2005.12.005

Fischer, C., Roscher, C., Jensen, B., Eisenhauer, N., Baade, J., Attinger, S., Hildebrandt, A., 2014. How do earthworms, soil texture and plant composition affect infiltration along an experimental plant diversity gradient in grassland? PLoS One, 9 (6): e98987. https://doi.org/10.1371/journal.pone.0098987

Fredlung, D.G., Xing, A., 1994. Equations for the soil-water characteristic curve. Canadian Geotechnical Journal**,** 31(4).

Gerke, H.H., van Genuchten, M.Th., 1993. A dual-porosity model for simulating the preferential movement of water and solutes in structured porous media. Water Resources Research 29(2): 305-319. https://doi.org/10.1029/92WR02339

Glab, T., Zabinski, A., Sadowska, U., Gondek, K., Kopec, M., Mierzwa-Hersztek, M., Tabor, S., 2018. Effects of co-composted maize, sewage sludge, and biochar mixtures on hydrological and physical qualities of sandy soil. Geoderma, 315: 27–35. https://doi.org/10.1016/j.geoderma.2017.11.034

Głab, T., Zabinski, A., Sadowska, U., Gondek, K., Kopec´, M., Mierzwa-Hersztek, M., Tabor, S., Stanek-Tarkowska, J., 2020. Fertilization effects of compost produced from maize, sewage sludge and biochar on soil water retention and chemical properties. Soil Tillage Res., 197: 104493. https://doi.org/10.1016/j.still.2019.104493

Gregoire, B.G., Clausen, J.C., 2011. Effect of a modular extensive green roof on stormwater runoff and water quality. Ecological Engineering, 37: 963‑969. https://doi.org/10.1016/j.ecoleng.2011.02.004

Hall, D.G.M., Reeve, M.J., Thomasson, A.J., Wright, V.F., 1977. Water retention, porosity and density of field soils. Soil Survey Tech. Monog. No. 9, Rothamsted, Harpenden, U.K

Hallam, J., Holden, J., Robinson, D.A., Hodson, M.E., 2021. Effects of winter wheat and endogeic earthworms on soil physical and hydraulic properties, Geoderma, 400: 115126. https://doi.org/10.1016/j.geoderma.2021.115126

Handreck, K.A., Black, D., 1994. Growing Media for Ornamental Plants and Turf. University of New South Wales Press (UNSWP). Randwick, Australia.

Hao, X., Ball, B.C., Culley, J.L.B., Carter, M.R., Parkin, G.W., 2008. Soil Density and Porosity. In Soil Sampling and Methods of Analysis. Boca Raton, FL: CRC Press, pp. 743-749.

Haverkamp, R., Ross, P.J., Smettem, K.R.J., Parlange, J.Y. 1994. Threedimensional analysis of infiltration from the disc infiltrometer. 2. Physically based infiltration equation. Water Resources Research, 30: 2931-2935. https://doi.org/10.1029/94WR01788

Haverkamp, R., Reggiani, P., Ross, P.J., Parlange, J.Y., 2002. SoilWater Hysteresis Prediction Model Based on Theory and Geometric Scaling. Environ. Mech. 129: 213–246.

Hillel, D., 1998. Environmental soil physics. Academic Press.

Hou, S., Zhang, R., Zhang, C., Wang, L., Wang, H., 2023. Role of vermicompost and biochar in soil quality improvement by promoting *Bupleurum falcatum* L. nutrient absorption, Soil Use Manag., 39 (4):1600–1617, https://doi.org/10.1111/sum.12955

Huang, S., Garg, A., Mei, G., Huang, D., Chandra, R.B., Sadasiv, S.G., 2020. Experimental study on the hydrological performance of green roofs in the application of novel biochar. Hydrological Processes. 1-14. https://doi.org/10.1002/hyp.13881

Jarvis, N., Jansson, P.E., Dik, P.E., Messing, I., 1991. Modeling water and solute transport in macroporous soil, I, Model description and sensitivity analysis, *J. Soil Sci.* **42**: 59–70. https://doi.org/10.1111/j.1365-2389.1991.tb00091.x

Ibrahim, A., Horton, R., 2021. Biochar and compost amendment impacts on soil water and pore size distribution of a loamy sand soil. Soil Sci. Soc. Am. J., 85: 1021–1036. https://doi.org/10.1002/saj2.20242

Ibrahim, A., Marie, H.A.M.E., Elfaki, J., 2021. Impact of biochar and compost on aggregate stability in loamy sand soil. Agric. Res. J. 58: 34–44. DOI No. 10.5958/2395-146X.2021.00005.3

ISPRA, 2016. Rapporto Consumo di suolo in Italia 2016.

Kasmin, H., Stovin, V.R., Hathway, A., 2010. Towards a generic rainfall-runoff model for green roofs. Water Science & Technology—WST, 62.4. https://doi.org/10.2166/wst.2010.352

Kazemi, F., Mohorko, R., 2017. Review on the roles and effects of growing media on plant performance in green roofs in world climates. Urban Forestry & Urban Greening, 23: 13-26. https://doi.org/10.1016/j.ufug.2017.02.006

Kosugi, K., 1996. Lognormal distribution model for unsaturated soil hydraulic properties. Water Resources Research, 32: 2697-2703. https://doi.org/10.1029/96WR01776

Kranz, C.N., McLaughlin, R.A., Johnson, A., Miller, G., Heitman, J.L., 2020. The effects of compost incorporation on soil physical properties in urban soils – A concise review. J. Environ. Manag. 261, 110209. https://doi.org/10.1016/j.jenvman.2020.110209

Lal, R., 2021. Soil Organic Matter and Feeding the Future: Environmental and Agronomic Impacts, first ed., CRC Press. https://doi.org/10.1201/9781003102762

Li, Y., Babcock, R.W.J., 2014. Green roof hydrologic performance and modeling: a review. Water Science & Technology, 69(4). https://doi.org/10.2166/wst.2013.770

Luo, H., Wang, N., Chen, J., Ye, X., Sun, Y.F., 2015. Study on the Thermal Effects and Air Quality Improvement of Green Roof. Sustainability, 7(3): 2804-2817. https://doi.org/10.3390/su7032804

Ma, H., Zhao, S., Hou, J., FeYissa, T., Duan, Z., Pan, Z., Zhang, K., Zhang, W., 2022. Vermicompost improves physicochemical properties of growing medium and promotes plant growth: a meta-analysis, J. Soil Sci. Plant Nutr., 22: 3745–3755. https://doi.org/10.1007/s42729-022-00924-7

Magdof, F., Weil, R.R., 2004. Soil organic matter in sustainable agriculture. 1st edn. CRC Press, Boca Raton. https://doi.org/10.1201/9780203496374

Munafò, M. (a cura di), 2022. Consumo di suolo, dinamiche territoriali e servizi ecosistemici. Edizione 2022. Re-port SNPA 32/22.

Nielsen, D.R., Biggar J.W., Erh, K.T., 1973. Spatial variability of field-measured soil-water properties. Hilgardia, 42: 215-259. Olness, A., Clapp, C.E., Liu, R., Palazzo, A.J., 1998. Biosolids and their effects on soil properties, In Wallace A. and Terry R.E. (eds.), Handbook of Soil Conditioners, Marcel Dekker, New York, NY, pp. 141-165.

Paci, M., 2011. Ecologia forestale. Elementi di conoscenza dei sistemi forestali applicati alla selvicoltura. Edagricole, 288 p.

Palazzolo, E., Laudicina, V.A., Roccuzzo, G., Allegra, M., Torrisi, B., Micalizzi, A., Badalucco, L., 2019. Bioindicators and nutrient availability through whole soil profile under orange groves after long-term different organic fertilizations. SN Appl. Sci., 1: 468. https://doi.org/10.1007/s42452-019-0479-3

Paquet, J.M., Caron, J., Banton, O., 1993. In situ determination of the water desorption characteristics of peat substrates. Can. J. Soil Sci., 73: 329-339. https://doi.org/10.4141/cjss93-035

Pistocchi, A., 2017. Hydrological impact of soil sealing and urban land take. Urban expansion, land cover and soil ecosystems services, Routledge, 1st edition.

Reynolds, W.D., Bowman, B.T., Drury, C.F., Tan, C.S., Lu, X., 2002. Indicators of good soil physical quality: density and storage parameters. Geoderma, 110: 131-146. https://doi.org/10.1016/S0016-7061(02)00228-8

Reynolds W.D., Yang X.M, Drury C.F., Zhang T.Q., Tan, C.S., 2003. Effects of selected conditioners and tillage on the physical quality of a clay loam soil. Canadian Journal of Soil Science, 83: 381-393. https://doi.org/10.4141/S02-066

Reynolds, W.D., Drury, C.F., Yang, X.M., Fox, C.A., Tan, C.S., Zhang, T.Q., 2007. Land management effects on the near-surface physical quality of a clay loam soil. Soil Till. Res. 96: 316-330. https://doi.org/10.1016/j.still.2007.07.003

Reynolds, W.D., Drury, C.F., Yang, X.M., Tan, C.S., 2008. Optimal soil physical quality inferred through structural regression and parameter interactions. Geoderma, 146: 466-474. https://doi.org/10.1016/j.geoderma.2008.06.017

Reynolds, W.D., Drury, C.F., Tan, C.S., Fox, C.A., Yang, X.M., 2009. Use of indicators and pore volume-function characteristics to quantify soil physical quality. Geoderma, 152: 252-263. https://doi.org/10.1016/j.geoderma.2009.06.009

Richards, L.A., 1931. Capillary conduction of liquids through porous medium. Physics 1, 318–333.

Rienzner, M., Gandolfi, C., 2014. Investigation of spatial and temporal variability of saturated soil hydraulic conductivity at the field-scale. Soil and Tillage Research 135: 28-40. https://doi.org/10.1016/j.still.2013.08.012

Sadeghi, S., Ebrahimi, S., Zakerinia, M., 2014. The Study of the Parametric Changes inWater Potential Points by Using Waste Manuciple Compost in Three Kinds of Soils. Int. J. Basic Sci. Appl. Res. 3: 254–260.

Sandoval, V., Bonilla, C.A., Gironás, J., Vera, S., Victorero, F., Bustamante, W., Rojas, V., Leiva, E., Pastén, P., Suárez, F., 2017. Porous Media Characterization to Simulate Water and Heat Transport through Green Roof Substrates. Vadose Zone J., 16(4): 1-14.

Santamouris, M., 2014. Cooling the cities – A review of reflective and green roof mitigation technologies to fight heat island and improve comfort in urban environments. Solar Energy, 103: 682-703. https://doi.org/10.1016/j.solener.2012.07.003

Scalenghe, R., Marsan, F.A., 2009. The anthropogenic sealing of soils in urban areas. Landscape and Urban Planning, 90: 1-10. https://doi.org/10.1016/j.landurbplan.2008.10.011

Schwen, A., Bodner, G., Scholl, P., Buchan, G.D., Loiskandl, W., 2011. Temporal dynamics of soil hydraulic properties and the water-conducting porosity under different tillage, Soil Tillage Res. 113 (2): 89–98. https://doi.org/10.1016/j.still.2011.02.005

Seki, K., 2007. SWRC fit - a nonlinear fitting program with a water retention curve for soils having unimodal and bimodal pore structure. Hydrol. Earth Syst. Sci. Discuss., 4: 407-437. https://doi.org/10.5194/hessd-4-407-2007

Skopp, J., Jawson, M.D., Doran, J.W., 1990. Steady-state aerobic microbial activity as a function of soil water content. Soil Sci. Soc. Am. J., 54:1619–1625. https://doi.org/10.2136/sssaj1990.03615995005400060018x

Stanić, F., Cui, Y., Delage, P., De Laure, E., Versini, P., Schertzer, D., Tchiguirinskaia, I., 2020. A device for the simultaneous determination of the water retention properties and the hydraulic conductivity function of an unsaturated coarse material; Application to a green-roof volcanic substrate. Geotechnical Testing Journal, 43(3): 547-564. https://doi.org/10.1520/GTJ20170443

Stovin, V., Vesuviano, G., Kasmin, H., 2012. The hydrological performance of a green roof test bed under UK climatic conditions. Journal of Hydrology, 414: 148‑161. https://doi.org/10.1016/j.jhydrol.2011.10.022

Thornthwaite, C.W., 1948. An approach toward a rational classification of climate. Geogr Rev 38(1): 55–94.

Tobias, S., Conen, F., Duss, A., Wenzel, L.M., Buser, C., Alewell, C., 2018. Soil sealing and unsealing: State of the art and examples. Land Degradation & Development, 29(6): 2015-2024. https://doi.org/10.1002/ldr.2919

Topp, G.C., Reynolds, W.D., Cook, F.J., Kirby, J.M., Carter, M.R., 1997. Chapter 2. Physical attributes of soil quality. p: 21-58. In E.G. Gregorich e M.R., Carter (eds.), Soil Quality for Crop Production and Ecosystem Health, Developments in Soil Science 25, Elsevier, Amsterdam. https://doi.org/10.1016/S0166-2481(97)80029-3

Van Genuchten, M.Th., 1980. A closed-form equation for predicting the hydraulic conductivity of unsaturated soils. Soil Science Society of America Journal, 44: 892-898. https://doi.org/10.2136/sssaj1980.03615995004400050002x

Van Genuchten, M.Th., Leij, F.J., Yates, S.R., 1991. The RETC Code for Quantifying the Hydraulic Functions of Unsaturated Soils, Version 1.0. EPA Report 600/2-91/065, U.S. Salinity Laboratory, USDA, ARS, Riverside, California.

Van Renterghem, T., Botteldooren, D., 2011. In-situ measurements of sound propagating over extensive green roofs. Building and Environment, 46: 729-738. https://doi.org/10.1016/j.buildenv.2010.10.006

Veum, K.S., Goyne, K.W., Kremer, R.J., Miles, R.J., Sudduth, K.A., 2014. Biological indicators of soil quality and soil organic matter characteristics in an agricultural management continuum. Biogeochemistry 117: 81–99. https://doi.org/10.1007/s10533-013-9868-7

Vogel, T., Gerke, T.T., Zhang, R., Van Genuchten, M.Th., 2000. Modeling flow and transport in a two-dimensional dual-permeability system with spatially variable hydraulic properties. Journal of Hydrology 238(1-2): 78-89. https://doi.org/10.1016/S0022-1694(00)00327-9

Warrick, A.W., 2002. Soil Physics Companion. CRC Press LLC, Boca Raton, USA.

Wendroth, O., Ehlers, W., Hopmans, J.W., Kage, H., Halbertsma, J., Wosten, J.H.M., 1993. Reevaluation of the evaporation method for determining hydraulic functions in unsaturated soils. Soil Science Society of America Journal, 57: 1436-1443. https://doi.org/10.2136/sssaj1993.03615995005700060007x

White, R.E., 2006. Principles and Practice of Soil Science, 4th edition. Blackwell Publishing, Oxford, UK.

Wind, G.P., 1968. Capillary conductivity data estimated by a simple method. p.181-191. IN P.E. Rijtema e H. Wassink (co-eds.I, Water in the Unsuturated Zone, Proc. Wageningen Symp., June 1966, Vol.1.IASAH, Gentbrugge, Belgium.

Wooster, E.I.F., Fleck, R., Torpy, F., Ramp, D., Irga, P.J., 2022. Urban green roofs promote metropolitan biodiversity: A comparative case study. Building and Environment, 207: 108458. https://doi.org/10.1016/j.buildenv.2021.108458

Yio, M.H.N., Stovin, V., Werdin, J., Vesuviano, G., 2013. Experimental Analysis of Green Roof Substrate Detention Characteristics. Water Sci Technol, 68 (7): 1477–1486. https://doi.org/10.2166/wst.2013.381

Young, T., Cameron, D.D., Sorrill, J., Edwards, T., Phoenix, G.K., 2014. Importance of different components of green roof substrate on plant growth and physiological performance. Urban Forestry & Urban Greening, 13: 507-516. https://doi.org/10.1016/j.ufug.2014.04.007

Zhao, H.T., Li, T.P., Zhang, Y., Hu, J., Bai, Y.C., Shan, Y.H., Ke, F., 2017. Effects of vermicompost amendment as a basal fertilizer on soil properties and cucumber yield and quality under continuous cropping conditions in a greenhouse, J. Soils Sediments, 17(12): 2718–2730. https://doi.org/10.1007/s11368-017-1744-y

water

MDPI

Article

Compost Amendment Impact on Soil Physical Quality Estimated from Hysteretic Water Retention Curve

Cristina Bondì [1,*], Mirko Castellini [2] and Massimo Iovino [1]

[1] Department of Agricultural, Food and Forest Sciences, University of Palermo, 90128 Palermo, Italy; massimo.iovino@unipa.it
[2] Council for Agricultural Research and Economics–Research Center for Agriculture and Environment (CREA–AA), Via C. Ulpiani 5, 70125 Bari, Italy; mirko.castellini@crea.gov.it
* Correspondence: cristina.bondi@unipa.it

Abstract: Capacity-based indicators of soil physical quality (SPQ) and pore distribution parameters were proposed to assess the effects of compost amendment but their determination was limited to desorption water retention experiments. This study also considered the pore size distribution obtained from adsorption experiments to establish the effectiveness of compost amendment in modifying the physical and hydrological attributes of a sandy loam soil. Repacked soil samples with different compost to soil ratios, *r*, were subjected to a wetting–drying cycle, and the water retention data were fit to the van Genuchten model to obtain the pore volume distribution functions. The soil bulk density was minimally affected by the wetting–drying cycle but a significant negative correlation with *r* was obtained. The sorption process involved larger and more heterogeneous pores than the desorption one thus resulting in an estimation of the air capacity SPQ indicators (P_{mac} and *AC*) that were higher for the wetting–water retention curve (WWRC) than the drying one (DWRC). The opposite result was found for the water storage SPQ indicators (*PAWC* and *RFC*). In general, SPQ indicators and pore distribution parameters were generally outside the optimal range but estimates from the DWRC were closer to the reference values. The water entry potential increased and the air entry potential decreased with an increase in the compost rate. Significant correlations were found between the SPQ indicators estimated from the DWRC and *r* but the same result was not obtained for the WWRC. It was concluded that compost addition could trigger positive effects on soil hydrological processes and agronomic service as both water infiltration during wetting and water storage during drying are favored. However, the effectiveness of the sorption process for evaluating the physical quality of soils needs further investigation.

Keywords: soil structure; pore volume distribution function; bulk density; macroporosity; air capacity; plant available water capacity; relative field capacity; S-index

Citation: Bondì, C.; Castellini, M.; Iovino, M. Compost Amendment Impact on Soil Physical Quality Estimated from Hysteretic Water Retention Curve. *Water* **2022**, *14*, 1002. https://doi.org/10.3390/w14071002

Academic Editor: Jan Wesseling

Received: 23 February 2022
Accepted: 20 March 2022
Published: 22 March 2022

1. Introduction

Application of compost is one efficient way to increase soil organic matter level and indirectly improve soil structure and hydrological functions [1,2]. A large number of studies have documented positive effects of compost application on different soil physical and hydrological attributes: total porosity [3], bulk density [4], soil resistance to penetration [5], pore size distribution [6], aggregation and aggregate stability [1,7,8], water retention capacity [9,10], and saturated and unsaturated hydraulic conductivity [11,12]. As a consequence of improved water retention capacity, compost addition increases the plant available water capacity (PAWC) of soils [13]. Comparative analysis of twenty-five studies showed that compost incorporation had positive effects on degraded urban soils in terms of reduced compaction, enhanced infiltration and hydraulic conductivity, and increased water content and PAWC [14].

The above-mentioned positive effects depend on the compost application rate but also on the feedstock type, compost maturity, and compost quality. Application rate usually

ranges from 30 to 150 Mg ha^{-1} [3,6,10] but values up to 750 Mg ha^{-1} have been reported [12]. A variety of organic wastes have been proposed as soil amendment materials, also with the aim to find sustainable disposal for urban and agricultural byproducts. Compost types include sewage sludge and municipal waste [15,16], maize and sewage sludge [9], pruning waste [17], farm crop residues [18], yard waste [3,19], orange juice processing wastes [20], and mixtures of these materials. As an example, Glab et al. [21] reported the effects of co-composted maize, sewage sludge, and biochar mixtures addition on the hydrological and physical quality of a loamy sandy soil. Compared with the control soil, the physical properties of the amended soil were significantly improved with beneficial effects that were dependent on the rate of compost application and the type of feedstock. Likewise, Rivier et al. [22] investigated the effect of compost and vermicompost on soil structure, water retention, aggregate stability, and plant water use efficiency, compared with that of mineral fertilizers and food-waste digestate.

Binding primary particles into stable aggregates, organic matter influences attributes of soil pores such as size, distribution, shape, and connectivity [18]. The soil–water retention curve (SWRC), relating volumetric water content, θ, to pressure head, h, provides an indirect method to estimate soil porosity and, therefore, to assess the effectiveness of compost for improving the conditioning of soil. A complete description of the pore volume distribution function can be obtained by fitting appropriate semi-empirical functions to θ(h) data [23,24]. Reynolds et al. [25] classified pore size distribution on the basis of selected "location" and "shape" parameters and proposed optimal ranges for each parameter. Another approach relies on estimation of capacity-based indicators of soil physical quality (SPQ) accounting for soil ability to store air and water [23,26]. In any case, comparison of measured pore distribution parameters and SPQ indicators with optimal ranges deduced from literature allows a straightforward assessment of compost application effects [27,28]. To date, such an approach has proved useful for studying different agro-environments and evaluating their sustainability [29–34].

The SWRC is not unique because of hysteresis [35]. Briefly, hysteresis is a phenomenon depending on several factors, including non-uniformity in pore cross-sections, variation of dynamic contact angles in the advancing or receding water–air interface menisci, and entrapped air effects, air volume changes, and aging phenomena [36]. Due to hysteresis, the soil water content at a given pressure head is higher during the drying than the wetting process. Nevertheless, estimation of pore distribution parameters and capacitive SPQ indicators has been generally conducted from θ(h) data obtained from desorption experiments under the simplified assumption that hysteresis can be neglected in field conditions because its influence is often masked by heterogeneities and spatial variability [37]. Another reason for using desorption SWRC is that capacity-based SPQ indicators are generally associated with the soil's ability to store water and transfer it from wet to dry periods, i.e., across a relatively long temporal scale. Adsorption SWRC, i.e., the water retention curve determined for a wetting process, can give additional information on the soil's ability to store water over the shorter time scale related to the infiltration process. However, to the best of our knowledge, wetting SWRC was never used to determine SPQ nor the effects of compost addition on water retention hysteresis evaluated.

The study investigates the reliability of capacity-based indicators of SPQ and pore size distribution parameters for assessing the effectiveness of compost amendment on a sandy loam soil. With the aim to move forward from the traditional approach based on the analysis of the desorption SWRC, the effects of water retention hysteresis on the estimation of soil physical quality were evaluated. The assumed hypothesis was that analysis of the pore distribution system obtained from the wetting SWRC could complete our knowledge of active porosity under different hydrological processes.

2. Materials and Methods

2.1. Sample Preparation and SWRC Measurement

Soil samples were collected in a citrus orchard at the Department of Agriculture and Forestry Sciences of the University of Palermo, Italy (UTM 33S 355511E-4218990N). The soil (Typic Rhodoxeralf) was classified as sandy loam with a relatively high gravel content (13% by weight) [38] and moderate organic carbon content at the time of sampling (Table 1). The soil samples were air-dried, gently crushed, and passed through a 2 mm sieve before mixing with compost.

Table 1. Physicochemical attributes of soil and compost.

Soil		Compost	
Clay (%)	17.6	pH	7.2
Silt (%)	29.8	EC (dS/m)	0.54
Sand (%)	52.6	C (%)	9.91
OM (%)	2.1	N (%)	0.64
pH	7.8	P (%)	0.45
EC (dS/m)	0.48	Ash (%)	82.5
CEC (cmol Kg^{-1})	25.31	C/N ratio	15:1

The amending compost consisted of 5-months-aged compost from orange juice processing wastes (75%) and garden cleaning (25%) [20]. Agro-industrial wastes were composed of about 60% peel, 30% pulp, and 10% pips, while garden cleaning contained triturated pruning residues and mown grasses. The characteristics of the used compost are reported in Table 1. Compost was preliminarily screened through a 2 mm sieve to eliminate large vegetal residues.

Air-dried compost was mixed with soil in five different proportions by weight: 10% (M10); 20% (M20); 30% (M30); 50% (M50); and 75% (M75). For comparative purposes, the two unmixed matrices, i.e., 100% soil (M0) and 100% compost (M100), were also considered. It is worth noting that the highest compost to soil ratios, *r*, are far above the maximum usually applied in the field [3,39]. However, the choice to also use high compost application rates was considered reasonable given the ash content of the compost is above and the total carbon content is below the average values for usual food waste and/or dairy animal manure composts [3,18].

Replicate samples of each mixture were obtained by compacting into 5 cm diameter by 5 cm height cylinders a dry mass of the two constituents given by:

$$M_s = \frac{V\ BD_c BD_s}{BD_c + rBD_s} \qquad M_c = rM_s \tag{1}$$

in which M_c (g) and M_s (g) are the dry masses of compost and soil, respectively, BD_s (g cm^{-3}) and BD_c (g cm^{-3}) are the dry bulk densities of the two constituents [40], V (cm^3) is the sample volume, and r is the compost to soil ratio. The air-dried masses were corrected to account for the initial soil water content and then gently mixed for 5 min by means of a mechanical sieve to obtain a homogeneous mixture. Sample compaction was conducted in four successive steps by beating the mixture with five strokes from a height of 5 cm followed by five rotations with a pestle at each increment. The same treatment was applied to M0 and M100 to avoid any artifacts due to sample preparation. The samples were then weighted to check that the measured initial bulk density was the same as the theoretical one determined from Equation (1). This sample preparation procedure allowed to obtain highly replicable results even with a limited sample number ($n = 2$).

The water retention curve was determined by the tension hanging water column apparatus [41] for pressure head, h (m), values ranging from −0.01 to −1 m, and the pressure plate extractors [42] for h values ranging from −1 to −150 m. Each sample was placed on the porous plate of a glass funnel and saturated from the bottom by progressively

raising the water level in a graduated burette that allowed to measure the volume of water adsorbed by or drained from the sample. Initial saturation was obtained in four equilibrium steps of 24 h each at h values of −0.2, −0.1, and −0.05 m followed by submersion. Then, the sample was drained by lowering h in several successive steps of 24 h each and finally equilibrated at h = −1 m.

The water retention curve was measured by applying a wetting/drainage cycle consisting of a sequence of 14 h values applied in ascending/descending order (h = −0.01 m, −0.02 m, −0.03 m, −0.05 m, −0.075 m, −0.10 m, −0.15 m, −0.20 m, −0.25 m, −0.30 m, −0.40 m, −0.50 m, −0.70 m, and −1 m). At each h level, the volume of water adsorbed or drained from/into the burette was recorded. The volumetric water content, θ (m^3m^{-3}), at each equilibrium stage was calculated by adding the drained or adsorbed volumes to the final θ_{-1} value determined at h = −1 m by weighting the sample after oven-drying at 105 °C for 24 h. The sample height was measured at the end of the experiment (h = −1 m) and the sample dry soil bulk density, BD (g cm^{-3}) was calculated from the oven-dried weight of the soil sample [43]. Additional replicate samples (n = 3), prepared by the same procedure using only soil (M0) and compost (M100), were intensively monitored during the water retention experiment to evaluate changes in bulk density due to swelling or consolidation processes. At this aim, the sample height was measured at nine fixed points of the sample surface by using a gauge with a precision of 0.5 mm and an average value was determined by the arithmetic mean. Measurements were conducted after sample preparation (H0), at initial saturation (HS), at the initial equilibrium pressure head h = −1 m (H1), at the end of the wetting process when the sample was equilibrated at h = −0.01 m (H2), and at the end of the drainage process for the final equilibrium pressure head h = −1 m (H3).

Water retention data at pressure heads of −1 m, −3.3 m, −10 m, −30 m, and −150 m were determined in pressure plate extractors on three replicated samples of 5 cm diameter by 1 cm height. For each of the seven considered mixtures, the dry masses of compost and soil were calculated from Equation (1) to obtain the same theoretical bulk density value of the 5 cm by 5 cm samples. Determination of volumetric water content at h = −1 m was included in pressure plate experiments for comparison with the θ value measured at the same potential in the tension apparatus. All the measurements were conducted under temperature-controlled conditions at 22 ± 1 °C.

2.2. SWRC Parameterization

Experimental data were fitted by the van Genuchten [24] model (VGN):

$$\theta(h) = \theta_r + (\theta_s - \theta_s)\left(1 + |\alpha h|^n\right)^{-m} \quad (2)$$

in which θ_s (m^3m^{-3}) and θ_r (m^3m^{-3}) are the saturated and residual volumetric water contents, respectively, α is a scale parameter, and n and m with $m = 1-1/n$ are shape parameters. Equation (2) was fitted to experimental data by the SWRC Fit software [44]. Separate fitting was conducted for the two replicates of a given mixture and for the wetting (WWRC) and drainage (DWRC) water retention data. In the second case (DWRC), both the tension and the pressure plate data (n = 19) were considered given the latter were obtained for a drainage process. The VGN model shape and scale parameters (α, n, θ_s, and θ_r) were estimated without any constraint to their possible range. For the WWRC, only the tension data (n = 14) were considered and the VGN model was fitted to the data with θ_r fixed at the value determined for the DWRC. The reliability of estimates was evaluated by the coefficient of correlation, R, the mean error, ME, and the root mean square error, $RMSE$ [45]:

$$R = \frac{\sum(O_i - \overline{O})(P_i - \overline{P})}{\sum(O_i - \overline{O})^2 \sum(P_i - \overline{P})^2} \quad (3)$$

$$ME = \frac{\sum_{i=1}^{n}(P_i - O_i)}{N} \quad (4)$$

$$RMSE = \sqrt{\frac{\sum_{i=1}^{n}(P_i - O_i)^2}{N}} \quad (5)$$

in which P_i is the value of the volumetric water content at a given pressure head estimated from Equation (2), O_i is the corresponding measured value, and $\overline{P}$ and $\overline{O}$ are, respectively, the mean of estimated and measured θ values. Only the van Genuchten model was considered in this investigation as a preliminary visual analysis of the θ(*h*) data highlighted a typical S-shaped curve that could be adequately fitted by a unimodal water retention curve model.

2.3. Estimation of Soil Physical Quality

The fitted VGN water retention curves were used to estimate the following capacity-based indicators of soil physical quality [25,27,28,46]:

$$Macroporosity \quad Pmac = Ts - Tm \quad (6)$$

where θ_m (m^3m^{-3}) is the saturated volumetric water content of the soil matrix ($h = -0.1$ m). The P_{mac} parameter gives the volume of large (macro) pores (i.e., >300 μm equivalent pore diameter) indirectly indicating the soil's ability to quickly drain excess water:

$$Air\ capacity \quad AC = Ts - TFC \quad (7)$$

where θ_{FC} (m^3m^{-3}) is the field capacity water content ($h = -1$ m). The *AC* parameter is an indicator of soil aeration:

$$Plant - available\ water\ capacity \quad PAWC = TFC - TPWP \quad (8)$$

where θ_{PWP} (m^3m^{-3}) is the permanent wilting point corresponding to $h = -150$ m:

$$Relative\ field\ capacity \quad RFC = TFCTs \quad (9)$$

that expresses the soil's capacity to store water (and air) relative to the soil's total pore volume (as represented by θ_s):

$$S - index \quad Sindex = -n(Us - Ur)[1 + 1m] - (m + 1) \quad (10)$$

where U_s (g g^{-1}) and U_r (g g^{-1}) are the gravimetric saturated and residual water content that, under the assumption of rigid soil, can be calculated from θ_s and θ_r. The S_{index} represents the magnitude of the slope of the SWRC at the inflection point when the curve is expressed as gravimetric water content versus a natural logarithm of the pressure head [23]. The theory of the S_{index} is based on the premise that the shape of the SWRC is controlled primarily by structure pores for *h* values from saturation to the inflection point and by matrix pores for lower *h* values. While the former can be modified by soil management (including amendments), the latter mainly depends on more stable soil properties, such as texture.

Optimal soil physical quality conditions require [25,31,47]: $P_{mac} \geq 0.07$ m^3m^{-3}, $AC \geq 0.14$ m^3m^{-3}, $PAWC \geq 0.20$ m^3m^{-3}, and $0.60 \leq RFC \leq 0.70$; $S \geq 0.050$.

The pore volume distribution function, $S_v(h)$, may be defined as the slope of the SWRC expressed as volumetric water content versus ln(*h*), and plotted against equivalent pore diameter, d_e (μm) [25]:

$$S_v = \frac{d\theta}{d(lnh)} = -mn(\theta_s - \theta_r)\alpha^n h^n \left[1 + (\alpha h)^n\right]^{-(m+1)} \quad (11)$$

The capillary rise equation was used to estimate the equivalent diameter $d_e = 2980/h$ (μm) with *h* expressed in cm. The pore volume distribution function was normalized by dividing S_v by the magnitude of the slope at the inflection point, S_{vi}. Note

that S_{vi} is given by $S_{vi} = (BD \times S_{index})$ for a rigid soil. The normalized soil pore volume distribution, $S^*(h)$, provides a means for comparing among different porous materials being $0 \leq S^*(h) \leq 1$. Pore volume distributions can be characterized and compared using "location" and "shape" parameters, where the location parameters include the modal diameter, d_{mode} (µm), the median diameter, d_{median} (µm), and mean diameter, d_{mean} µm). The shape parameters include standard deviation, SD (-), skewness, SK (-), and kurtosis, KU (-). For brevity reasons, the expressions for estimating the location and shape parameters are not given here but the reader is referred to Reynolds et al. [25]. The optimal ranges for these indicators are: d_{median} = 3–7 µm; d_{mode} = 60–140 µm; d_{mean} = 0.7–2 µm; SD = 400–1000; SK: from −0.43 to −0.41; and KU = 1.13–1.14.

The flow chart in Figure 1 depicts the procedures and the calculations used to estimate the SPQ indicators and the pore volume distribution functions.

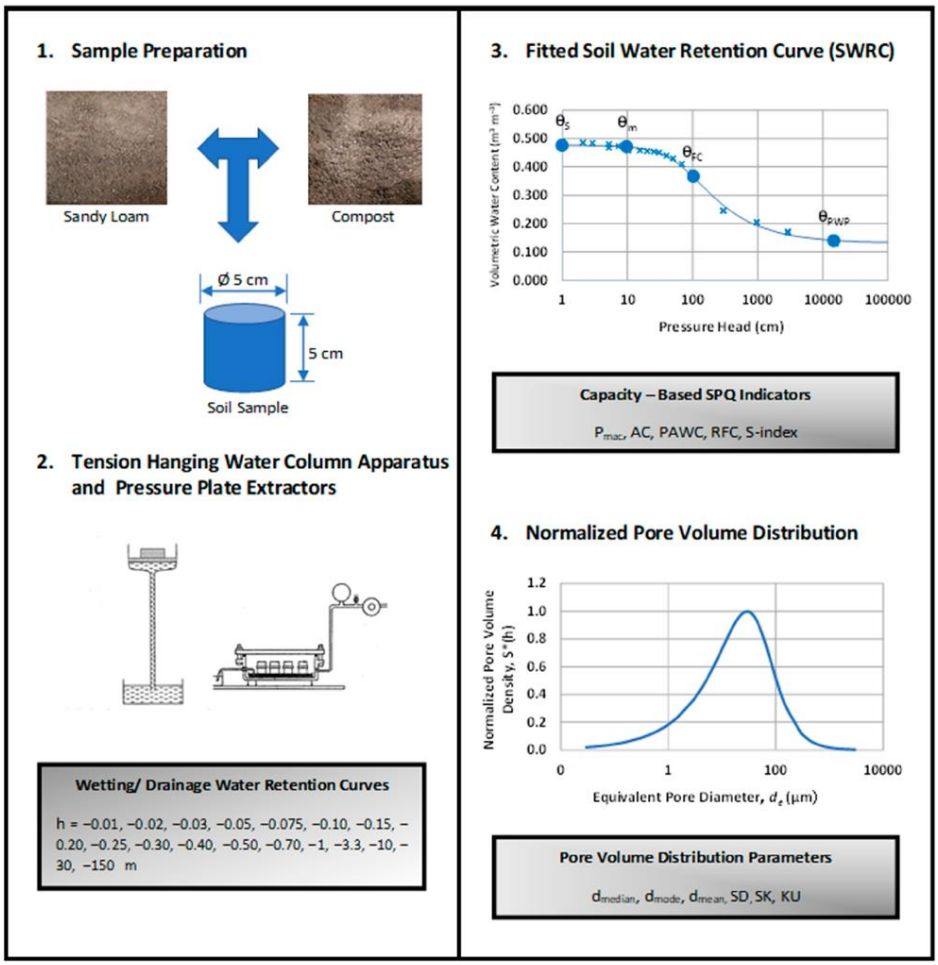

Figure 1. Flow chart of the procedural steps to estimate capacity-based indicators of SPQ and pore distribution parameters.

2.4. Data Analisys

For each considered variable and soil property, mean and associated coefficients of variation (CV) were calculated according to the assumed cumulative frequency distribution. Specifically, sample height, *BD*, P_{mac}, *AC*, *PAWC*, *RFC*, S_{index}, d_{mode}, and d_{median}, were assumed to be normally distributed whereas, according to Reynolds et al. [25], the other data (d_{mean}, *SD*, *SK*, and *KU*) were assumed to be ln distributed.

Comparison of means was conducted by the HSD Tukey test ($p = 0.05$). The influence of compost addition was investigated by assessing the significance of the regression coefficients between the considered soil variables (i.e., BD, VGN parameters, SPQ indicators, and pore distribution parameters) and the compost to soil ratio, r ($p = 0.05$).

3. Results and Discussion

3.1. Soil Bulk Density

The average height of the samples after preparation under air-dried conditions, H0, varied between 3.99 cm for M0 and 3.92 cm for M100 (Figure 2). The corresponding bulk density values were characterized by the coefficient variations (CV) of 0.29% and 2.14% that are far below the limit of 15% considered acceptable for the properties of this soil [48], thus confirming the reliability of the sampling preparation procedure. Following initial saturation (HS), the mean sample height increased to 4.21 cm for M0 (+5.6%) and 4.49 cm (+14.4%) for M100. Moreover, the CV of the M100 increased following saturation thus showing a higher susceptibility of the amended soil to undergo particle rearrangement as a consequence of the saturation process. According to an HSD Tukey test, the difference in sample heights between preparation and saturation was significant ($p = 0.05$) for both M0 and M100. After equilibration at the initial pressure head of $h = -1$ m (H1), the mean sample height significantly decreases to 4.09 cm (M0) and 4.26 cm (M100). Therefore, initial saturation followed by the first drainage cycle modified the original bulk density of the laboratory packed samples probably as a consequence of inter-particle bonds relaxation during wetting followed by settling during drainage. The M100 samples showed higher and more variable heights than M0 samples thus indicating a greater sensitivity to such modifications (Figure 2).

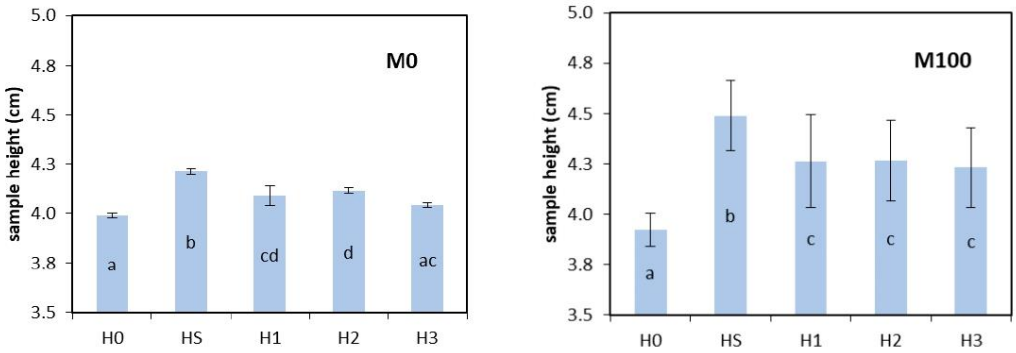

Figure 2. Sample height measured for M0 and M100 samples after preparation (H0), at initial saturation (HS), at the beginning of wetting (H1), at the end of wetting (H2), and at the end of drainage (H3).

In the subsequent wetting–drainage cycle, the samples were subjected to much fewer height modifications. For M0, height increased by a not significant 0.6% during wetting and decreased by 1.75% during drainage. The height after the wetting–drainage loop (H3 = 4.04 cm) was not statistically different from H1 measured at the same equilibrium pressure head, and it slightly increased only for the higher pressure head of the sequence

(H2). For M100, the mean height was practically the same (H1 = 4.26 cm, H2 = 4.27 cm, and H3 = 4.23 cm) being the differences well within the precision of the measurement technique (Figure 2). Therefore, provided a preliminary wetting–drainage cycle had been performed, the sample bulk density was not influenced by subsequent sorption–desorption processes and the soil samples can be considered rigid independently of the applied pressure head in the range $-1 \leq h \leq -0.01$ m. It is worth noting that the mean height of the M100 samples is on average 1.04 times the mean height of the M0 samples. The results of this preliminary investigation allow us to conclude that the laboratory repacked samples may undergo changes in particle configuration as a consequence of the applied sequence of pressure head values. These changes, however, tend to be negligible after the first wetting–drainage loop, at least in the range of h values that are requested for estimating the SPQ indicators. Therefore, the hypothesis of rigid porous medium was considered reasonable and, following the suggestion by Reynolds et al. [25], the *BD* measured at $h = -1$ m was assumed to assess the effects of compost amendment.

The *BD* values measured at the end of the wetting–drainage cycle (H3) ranged from 1.03 to 1.14 g cm^{-3} with a mean value of 1.08 g cm^{-3} (CV = 3.10%). Independently of the compost to soil ratio, the soil *BD* was always within the range of *BD* values considered as optimal for field crop production ($0.90 \leq BD \leq 1.2$ g cm^{-3}) [31,43]. A significant negative correlation ($p < 0.005$) was found between the sample bulk density and the compost percentage (Figure 3). Similar results were reported by Khaleel et al. [49] and Eden et al. [39] in their review articles on the long-term effects of organic waste recycling in agriculture. Mandal et al. [4] obtained a linear decreasing *BD* relationship for a silt loam soil amended with composted poultry litter up to 40% *v/v*. However, a closer examination of the plot also highlights that a threshold type behavior for *BD* vs. *r* relationship could be supposed. In particular, compost addition seems to have no effect on *BD* until a threshold value of $r = 30\%$ is reached. Afterward, the soil *BD* decreases at increasing *r* value. Such a different soil response was observed, among others, by Reynolds et al. [26] for the short-term effects of a single high rate addition of yard waste compost to a clay loam soil. They found significant differences only at the highest compost rate application, i.e., 300 t ha^{-1}, whereas 75 t ha^{-1} and 150 t ha^{-1} produced negligible or small improvements relative to the control. Similarly, Brown and Cotton [50] observed significant changes of a loamy soil *BD* only for application rates higher than 168 t ha^{-1}.

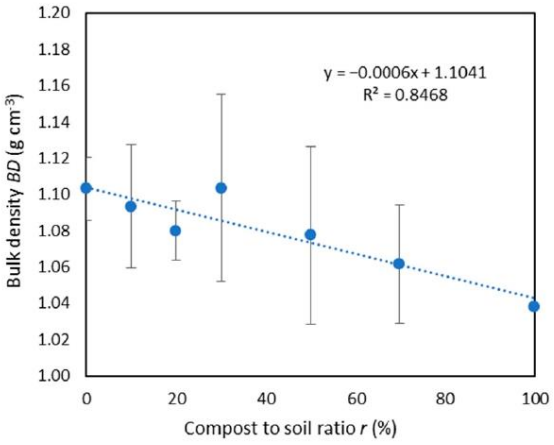

Figure 3. Relationship between soil bulk density and compost to soil ratio.

3.2. Soil Water Retention and Pore Volume Distribution

The wetting–drainage water retention curves exhibited a typical hysteretic behavior with volumetric water content at a given pressure head that was always lower for the wetting curve, θ_W, than the draining one, θ_D. As an example, Figure 4 compares the wetting (WWRC) and draining (DWRC) water retention curves obtained for M20 and M75 mixtures. The two curves were practically coincident close to saturation ($h \geq -0.05$ m). At lower h values, the differences between θ_D and θ_W first increased up to a maximum 0.156 m^3m^{-3} at h = 0.50 m and then tended to decrease but remained as high as 0.135 m^3m^{-3} at the lowest h value measured with the tension apparatus ($h = -1$ m).

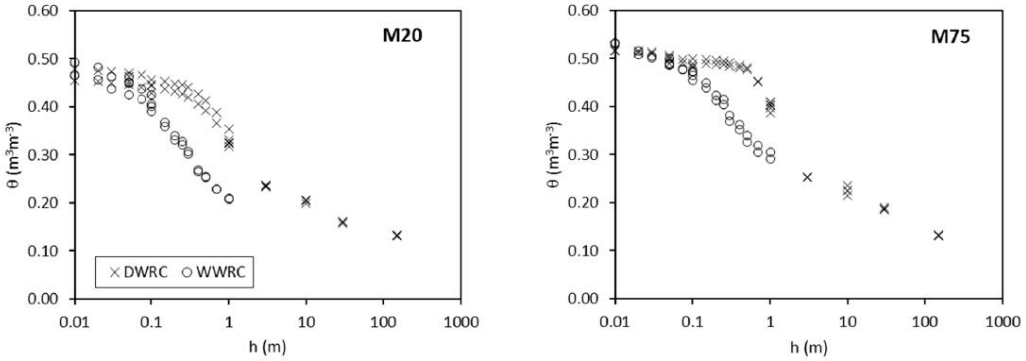

Figure 4. Measured water retention data for the wetting (WWRC) and draining (DWRC) curves of M20 and M75 mixtures.

The statistics of the estimated VGN model parameters and the indices of the fitting quality (*R*, *ME*, and *RMSE*) for both the wetting and the drainage WRC are listed in Table 2. A complete dataset of the estimated parameters is provided in the Supplementary Materials, Table S1.

Table 2. Minimum, maximum, and mean value of the estimated van Genuchten parameters for the wetting and draining water retention curve. The statistics of coefficient of correlation, *R*, mean error, *ME*, and root mean square error, *RMSE*, for the estimated water retention curves are also listed.

	α	n	θ_s	θ_r	R	*ME*	*RMSE*
			Wetting water retention curve WWRC				
Min	0.0613	1.406	0.457	0.110	0.9954	-6.54×10^{-4}	6.00×10^{-3}
Max	0.1203	1.894	0.536	0.161	0.9976	3.83×10^{-4}	9.00×10^{-3}
Mean	0.0871	1.639	0.500	0.138	0.9962	-3.14×10^{-6}	7.57×10^{-3}
			Draining water retention curve DWRC				
Min	0.0088	1.458	0.443	0.110	0.9931	-4.70×10^{-5}	5.90×10^{-3}
Max	0.0231	1.998	0.508	0.161	0.9985	1.13×10^{-4}	1.58×10^{-2}
Mean	0.0149	1.726	0.479	0.138	0.9959	2.62×10^{-5}	1.11×10^{-2}

The VGN model adequately fitted the water retention data as detected by the high *R* and low *ME* and *RMSE* values. The mean α value for the WWRC was 5.8 times higher than for the DWRC. This α_W/α_D value is above those usually reported ($\alpha_W/\alpha_D \approx 2$) [35]. The mean n parameter of the WWRC was 0.95 times that of the DWRC (Table 2). A significant negative correlation ($R^2 = 0.544$) was found between n_W and n_D thus indicating that, for the considered soil–compost mixture, estimation of the n parameter for one of the two branches of the water retention curve is also able to retrieve information for the other one. The estimated saturated water contents for the wetting, θ_{sW}, and drying, θ_{sD}, branches were

highly correlated (R^2 = 0.917) but the slope of the regression line was significantly different from one thus indicating that the water contents close to saturation for the WWRC were higher than for the DWRC (Figure 3, Table 2). The reason for the observed discrepancies between θ_{sW} and θ_{sD} is unknown but could be associated to the observed variability of sample height during the sorption and desorption processes (Figure 2). In any case, these differences can be considered negligible for the aims of estimating the SPQ given they were always lower than 0.033 m^3m^{-3} and equal to 0.020 m^3m^{-3} on average.

The scale parameter α decreased and the shape parameter n increased in the passage from the WWRC to the DWRC (Table 2). Generally, the α and n parameters are positively correlated (e.g., [51,52]); therefore, the observed inverse relationship is a sign that active soil pore classes are different in the two processes. Comparison between the pore volume distribution functions confirms that the sorption process (WWRC) involves larger and more heterogeneous pores (Figure 5). Therefore, different information is provided by the two soil water retention curves and, consequently, by the respective estimates of the SPQ indicators.

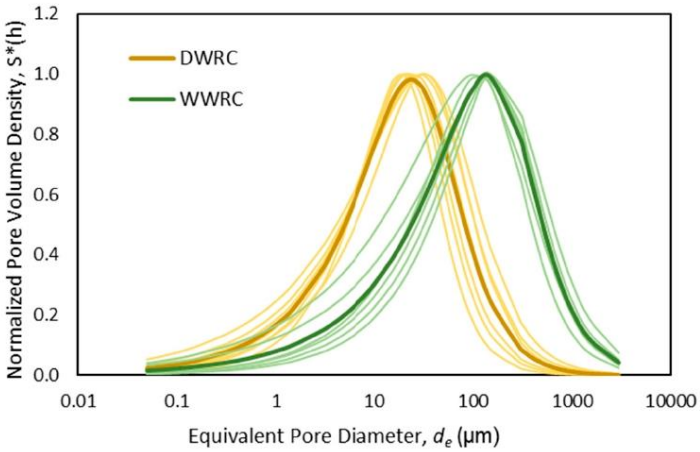

Figure 5. Normalized pore volume distribution functions for the wetting and draining processes.

3.3. Influence of Hysteresis on Soil Physical Quality

The capacity-based indicators linked to the macro- and mesoporosity (P_{mac} and AC) calculated for the WWRC were generally higher than for the DWRC (Table 3). In particular, the maximum values of P_{mac} and AC obtained from the DWRC (P_{mac} = 0.012 m^3m^{-3} and AC = 0.146 m^3m^{-3}) were lower than the minimum values of the same parameters obtained from the WWRC (P_{mac} = 0.047 m^3m^{-3} and AC = 0.224 m^3m^{-3}). Differences were also observed for indicators linked to the plant water availability (*PAWC* and *RFC*) but, in this case, the WWRC yielded lower values than the DWRC one. According to these results, use of the WWRC in spite of the DWRC yielded larger estimates of SPQ indicators related to soil aeration and lower estimation of those related to water storage. These findings were not entirely predictable and, to the best of our knowledge, they were experimentally assessed for the first time in this study. Similar estimates of the S_{index} were obtained by the two sets of water retention data (Table 3), probably because of the observed compensation between the two domains (macro- and micropores) involved in its calculation.

Table 3. Statistics of the considered SPQ indicators obtained from wetting and draining SWRC and correlation coefficients between SPQ indicators and the compost ratio *r*. The suggested optimal range for each SPQ indicator is also shown.

SPQ	Units	Wetting Water Retention Curve				Draning Water Retention Curve				Optimal Range
		Min	Max	Mean	*R*	Min	Max	Mean	*R*	
P_{mac}	m^3m^{-3}	0.047	0.087	0.072	0.1439	0.001	0.012	0.006	***−0.8508***	≥0.07
AC	m^3m^{-3}	0.224	0.306	0.267	−0.2528	0.085	0.146	0.116	***−0.9505***	≥0.14
PAWC	m^3m^{-3}	0.051	0.272	0.102	***0.6419***	0.185	0.255	0.216	***0.9580***	≥0.20
RFC	-	0.354	0.571	0.464	0.5322	0.696	0.831	0.756	***0.9790***	0.60–0.70
S-index	-	0.077	0.125	0.101	−0.4651	0.074	0.132	0.104	***0.8001***	≥0.05
d_{median}	µm	51.4	130.9	94.7	−0.3660	15.1	24.1	17.8	***−0.7754***	3–7
d_{mode}	µm	102.3	168.4	142.8	−0.1191	18.5	33.1	25.7	***−0.9523***	60–140
d_{mean}	µm	36.8	116.9	78.3	−0.4141	12.1	20.7	15.0	***−0.5329***	0.7–2
SD	-	3.7	11.7	6.1	0.5079	3.3	9.2	5.1	***−0.6303***	400–1000
SK	-	−0.29	−0.17	−0.22	***−0.5725***	−0.27	−0.16	−0.21	***0.7285***	−0.43 to −0.41
KU	-	1.14	1.16	1.15	***0.5919***	1.14	1.16	1.15	***−0.7699***	1.13–1.14

Values in bold indicate statistically significant correlation ($p = 0.05$).

According to the observed differences between the pore volume distribution curves, the location parameters (d_{median}, d_{mode}, and d_{mean}) obtained from the WWRC were larger than the DWRC. In particular, the median diameter of water-filled pores during sorption (d_{median} = 95 µm) is larger than the draining ones (d_{median} = 18 µm) in agreement with the hysteresis theory (Figure 5). Indeed, during a drainage process, the soil holds water in relatively smaller pores whereas the water entry process takes place, on average, at lower suction heads (i.e., larger pores). The shape parameters of the pore volume distribution functions were more similar but a tendency to increase *SD* and decrease *SK* for the WWRC was observed (Table 3). The mean pore volume distribution function was in both cases skewed towards small pores ($SK < 0$) whereas the two curves were classified as leptokurtic, i.e., more peaked in the center and more tailed in the extremes than the lognormal curve ($KU > 1$) [25].

According to the literature suggestions for optimal soil physical quality [23,25,31], the mean values of capacity-based SPQ indicators and pore distribution parameters were generally outside the optimal range but estimates from the DWRC were closer to the reference values (Table 3). The only exception was for P_{mac} and *AC* estimated from the WWRC that fell in the optimal range whereas the corresponding indicators estimated from the DWRC signaled an aeration deficit for soil. Location and shape parameters of pore volume distribution were always non-optimal. The observed discrepancies were not surprising given the soil samples considered in this investigation were laboratory repacked (i.e., structureless) whereas the literature guidelines for optimal SPQ were generally obtained from undisturbed soil samples. A recent study conducted on repacked soil samples of a loamy sand amended with crop residues and dairy manure compost [18] yielded location parameters, d_{median}, d_{mode}, and d_{mean}, of 21–26 µm, 28–32 µm, and 19–23 µm, respectively, and shape parameters, *SD*, *SK*, and *KU* of 3.1–3.9, −0.18 to −0.15 and 1.14, respectively. These values were outside the optimal range reported by Reynolds et al. [25] and closer to the mean values obtained in the present study from the DWRC (d_{median} = 17.8 µm, d_{mode} = 25.7 µm, d_{mean} = 15.0 µm, SD = 5.1, SK = −0.21, and KU = 1.15) thus confirming that the existing guidelines for optimal pore size distribution parameters need to be applied with caution to repacked soil samples. Furthermore, estimation of the SPQ indicators, as well as the definition of their optimal intervals, was almost exclusively conducted considering desorption data and our results show that different information can be obtained if sorption data are considered. Providing specific experimental information on the effect of water retention hysteresis on repacked soil samples is essential to fill the knowledge gap and provide recalibrated values for the current optimal SPQ guidelines.

3.4. Influence of Compost Amendment on Soil Water Retention and Physical Quality

The lack of reference values for the SPQ indicators obtained from the WWRC does not allow drawing of definitive conclusions about the reliability of such an approach. However, an indirect validation could be gathered from the analysis of compost amendment effects on the VGN model parameters as well as the related capacity-based SPQ indicators and pore size distribution parameters obtained by the two approaches (i.e., WWRC and DWRC).

Compost amendment influenced the shape and the scale parameters of the SWRC to different extents depending on the considered wetting or draining process (Table 4). In particular, α increased with r for the WWRC and decreased for the DWRC. However, only the latter relationship was statistically significant. Symmetrically, the n parameter decreased with r for the WWRC and increased for the DWRC. The α parameter is related to the inverse of the water or air entry potential. As expected from the hysteresis theory, the absolute value of the water entry potential (i.e., the inverse of α_W) is lower than the air entry potential (i.e., the inverse of α_D) (Table 2). However, at increasing the compost content, the water entry potential tended to decrease (Table 4) thus meaning that the compost amendment facilitates the water entry into the soil during a wetting process or, in other words, that infiltration is favored. On the contrary, the air entry potential tended to increase, that is, water loss is impeded during the soil drainage. The observed modifications have positive effects on soil hydrological and agronomic response under dryland agriculture as either infiltration is promoted during rainfall periods or storage enhanced during dry periods, in both cases, increasing the water availability for crops.

Table 4. Correlation coefficients between the van Genuchten model parameters (i.e., α, n, θ_s, and θ_r) and compost ratio r.

	α	n	θ_s	θ_r
WWRC	0.3376	**−0.5773**	**0.8188**	n.d.
DWRC	**−0.8909**	**0.7785**	**0.7905**	**0.7367**

Values in bold indicate statistically significant correlation ($p = 0.05$).

Compost addition tended to decrease the shape parameter n for the WWRC and to increase it for the DWRC. As the n parameter is related to the slope of the water retention curve at the inflection point, it means that due to amendment, the WWRC tended to be less S-shaped and the DWRC more S-shaped. In other words, not only did the wetting or the draining processes activate different pore systems but the compost addition seems to influence them in a different way, i.e., increasing the active pore assortment for the WWRC and decreasing it for the DWRC. Independently of the considered process (wetting or draining), θ_{sW}, θ_{sD}, and θ_{rD} were positively correlated with r indicating that the compost amendment was effective in increasing the water content of the considered sandy loam soil at, or close to, saturation as well as at the dry end of the SWRC (Table 4).

The significant correlations between the capacity-based SPQ indicators estimated from the DWRC and the compost ratio, r, strengthened the reliability of the procedure that estimates the soil physical quality from the water release experiments (Table 3). A significant reduction in P_{mac} and AC and an increase in $PAWC$, RFC, and S_{index} was observed (Figure 6) that was attributed to an increase in micropores and a decrease in macropores associated to the modification of pore volume distribution. Similar results were observed in literature with PAWC that increased [18] or was practically unaffected by compost addition [3]. On the other hand, many studies showed long-term benefits on AC that increased up to 26% in a fine-textured soil [26] and 15% in a loamy sand [3] when food waste compost was used. Our results lead to the conclusion that short-term organic matter incorporation probably increased micropore volume as a consequence of compost mineral residue (13.7% of particles less than 2 µm in diameter) but had negative effects on macroporosity.

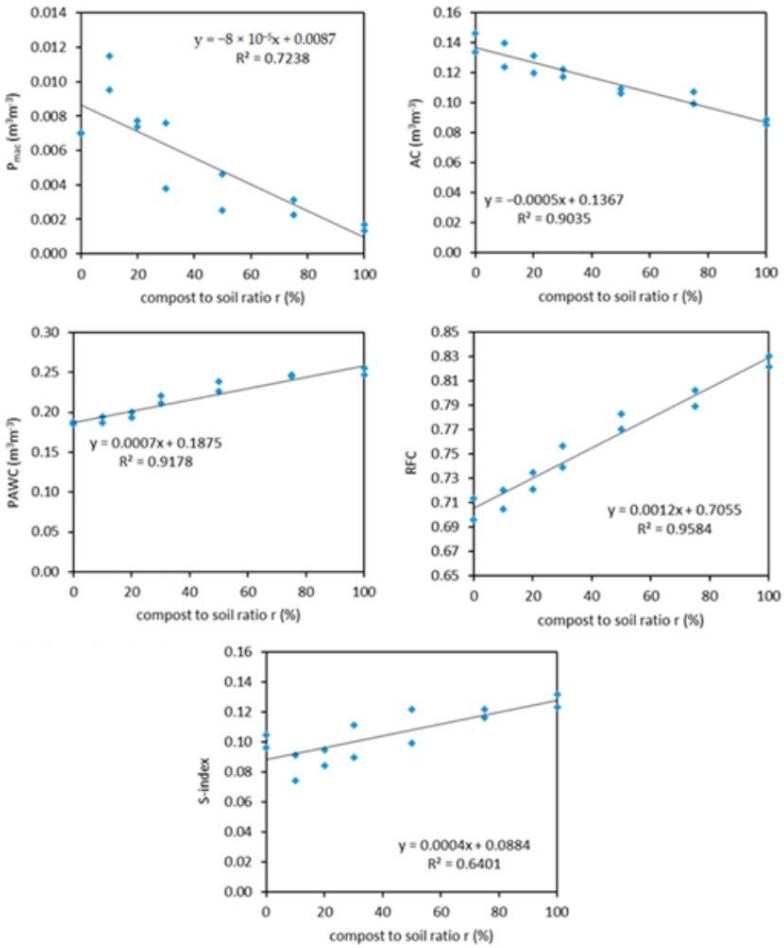

Figure 6. Regressions between the capacity-based SPQ indicators derived from the DWRC and the compost ratio.

The highly significant negative correlation observed for d_{median}, d_{mode}, and d_{mean} (Table 3) confirmed that amending was effective in modifying the pore systems. Ibrahim and Horton [18] reported a similar result that was also attributed to filling of loamy sand pore spaces by amendment material. Shape parameters were likewise significantly affected by compost amendment (Table 3). In particular, as the compost percentage increased, the pore distributions were less sorted (decreasing *SD*) and shifted toward large soil pores (increasing *SK*). Moreover, *KU* was affected by compost addition even if the range of variation was limited (Table 3). Al-Omran et al. [53] showed that *SD* and *SK* increased by 18% and 12%, respectively, whereas *KU* values were practically unaffected by compost amendment.

The results obtained from the DWRC data clearly show that compost had a positive effect on soil water storage. These results are in agreement with the extensive literature showing how the use of compost improves the physical properties of the soil. However, information is lacking for hysteretic soil water retention. Our data showed that, in most

cases, correlations between SPQ indicators obtained from the WWRC and r were not significant indicating that the sorption process is probably less recommended for the aim of SPQ evaluation. The only exception was for the PAWC that exhibited a positive, even less strong (R = 0.642), correlation with r (Table 3). Determination of the wetting branch of the SWRC is more affected by experimental errors due, for example, to soil hydrophobicity [54], air entrapment [55], and slaking or swelling of soil aggregates [56]. Therefore, it is possible that one, or all these factors, hampered the sensitivity of the estimated SPQ to compost addition. On the other hand, there are signs that also support the use of the WWRC for soil physical quality evaluation. For example, the circumstance that a negative, despite not significant, trend with r was observed for AC and the location parameters. It is also worth to note, that the relationship between S_{index} and r (Table 3) followed the same trend found for the shape parameter n (Table 4). Skewness and kurtosis had a contrasting behavior with compost amendments, that is, a negative correlation was found for the WWRC when it was positive for the DWRC and vice versa.

Dynamic indicators of SPQ were not considered in this investigation, but our results suggest that the use of compost could also affect them, depending on the wetting or drainage phase considered. More in-depth analysis is therefore desirable to investigate the effect of hysteresis on dynamic indicators of SPQ, including number and volume of the hydraulically active pores [32,57]. As an example, Bagarello et al. [58] identified a clear hysteresis effect on soil water retention of a sandy loam soil that also affected soil hydraulic conductivity data [59]. Consequently, different estimates of the dynamic indicators are expected, depending whether the wetting or drying process is considered.

Another point that requires further investigation is the use of repacked soil samples that could be non-representative of field conditions. Many researchers hypothesized that incorporation of compost would influence soil structure and, consequently, soil hydraulic properties in the short term (among others, [1,22]). The addition of compost to sieved soil, to obtain a repacked laboratory sample, can be likened, to some extent, to the real soil shortly after compost incorporation followed by tillage. Further investigations are necessary to test the adopted methodology after several wetting–drainage cycles with the aim to study the combined effects of compost and the soil structural restoration.

4. Conclusions

Hysteresis of the water retention curve affected the estimation of capacity-based indicators of SPQ and pore volume distribution parameters of a sandy loam soil amended with compost obtained from orange juice processing wastes and garden cleaning. The sorption process involved larger and more heterogeneous pores thus resulting in capacity-based indicators linked to soil aeration (P_{mac} and AC) that were generally higher and plant water availability indicators ($PAWC$ and RFC) were generally lower than those determined from desorption data. The SPQ indicators estimated from the DWRC were closer to the reference literature values that were usually retrieved from the same desorption process.

The absolute value of the water entry potential decreased and the air entry potential increased at increasing the percentage of added compost. In terms of the SPQ response to compost amendment, all the selected indicators estimated from the DWRC were sensitive to compost amendment. The same result was not obtained for the SPQ indicators estimated from the WWRC. In this case, the correlations with compost percentage were generally not significant thus indicating that the sorption process is probably less recommended than the desorption one for evaluating the physical quality of soils.

Overall, the results showed that compost amendment was effective in modifying the soil pore distribution system and the related SPQ indicators. In particular, compost addition could trigger positive effects on soil hydrological processes and agronomic services as both water infiltration during wetting and water storage during drying are favored. It is necessary to extend this investigation to other soils exploring to what extent the observed modification in pore volume distribution could also affect hydrodynamic indicators of soil quality directly related to the soil's ability to transmit water down into the profile.

The perspectives opened by these studies could help to improve our understanding of the effects of organic matter (compost) incorporation on soil structure, hydrological functions, and physical quality.

Supplementary Materials: The following supporting information can be downloaded at: https://www.mdpi.com/article/10.3390/w14071002/s1, Table S1: Estimated values of the van Genuchten parameters for the wetting and draining water retention curve and corresponding fitting statistics.

Author Contributions: Conceptualization, M.C. and M.I.; methodology, M.C. and M.I.; formal analysis, M.C., C.B. and M.I.; investigation, C.B.; data curation, C.B. and M.I.; writing—original draft preparation, C.B. and M.I.; writing—review and editing, M.C. and M.I. All authors have read and agreed to the published version of the manuscript.

Funding: This work was supported by the project WATER4AGRIFOOD, contratto "Tetto Verde", Codice Progetto: CON-0375, CUP B94I20000300005.

Informed Consent Statement: Not applicable.

Data Availability Statement: The data presented in this study are available on request from the corresponding author.

Conflicts of Interest: The authors declare no conflict of interest.

References

1. Dong, L.; Zhang, W.; Xiong, Y.; Zou, J.; Huang, Q.; Xu, X.; Ren, P.; Huang, G. Impact of short-term organic amendments incorporation on soil structure and hydrology in semiarid agricultural lands. *Int. Soil Water Conserv. Res.* **2021**, *in press*. [CrossRef]
2. Reynolds, W.D.; Drury, C.F.; Yang, X.M.; Fox, C.A.; Tan, C.S.; Zhang, T.Q. Land management effects on the near-surface physical quality of a clay loam soil. *Soil Tillage Res.* **2007**, *96*, 316–330. [CrossRef]
3. Arthur, E.; Cornelis, W.M.; Vermang, J.; de Rocker, E. Amending a loamy sand with three compost types: Impact on soil quality. *Soil Use Manag.* **2011**, *27*, 116–123. [CrossRef]
4. Mandal, M.; Chandran, R.; Sencindiver, J. Amending Subsoil with Composted Poultry Litter-I: Effects on Soil Physical and Chemical Properties. *Agronomy* **2013**, *3*, 657–669. [CrossRef]
5. Negiş, H.; Şeker, C.; Gümüş, I.; Manirakiza, N.; Mücevher, O. Effects of Biochar and Compost Applications on Penetration Resistance and Physical Quality of a Sandy Clay Loam Soil. *Commun. Soil Sci. Plant Anal.* **2020**, *51*, 38–44. [CrossRef]
6. Aggelides, S.M.; Londra, P.A. Effects of compost produced from town wastes and sewage sludge on the physical properties of a loamy and a clay soil. *Bioresour. Technol.* **2000**, *71*, 253–259. [CrossRef]
7. Annabi, M.; Houot, S.; Francou, C.; Poitrenaud, M.; Bissonnais, Y.L. Soil Aggregate Stability Improvement with Urban Composts of Different Maturities. *Soil Sci. Soc. Am. J.* **2007**, *71*, 413–423. [CrossRef]
8. Ibrahim, A.; Marie, H.A.M.E.; Elfaki, J. Impact of biochar and compost on aggregate stability in loamy sand soil. *Agric. Res. J.* **2021**, *58*, 34–44. [CrossRef]
9. Głąb, T.; Żabiński, A.; Sadowska, U.; Gondek, K.; Kopeć, M.; Mierzwa-Hersztek, M.; Tabor, S.; Stanek-Tarkowska, J. Fertilization effects of compost produced from maize, sewage sludge and biochar on soil water retention and chemical properties. *Soil Tillage Res.* **2020**, *197*, 104493. [CrossRef]
10. Zemánek, P. Evaluation of compost influence on soil water retention. *Acta Univ. Agric. Silvic. Mendel. Brun. LIX* **2011**, *3*, 227–232. [CrossRef]
11. Schneider, S.; Coquet, Y.; Vachier, P.; Labat, C.; Roger-Estrade, J.; Benoit, P.; Pot, V.; Houot, S. Effect of Urban Waste Compost Application on Soil Near-Saturated Hydraulic Conductivity. *J. Environ. Qual.* **2009**, *38*, 772–781. [CrossRef] [PubMed]
12. Whelan, A.; Kechavarzi, C.; Coulon, F.; Sakrabani, R.; Lord, R. Influence of compost amendments on the hydraulic functioning of brownfield soils. *Soil Use Manag.* **2013**, *29*, 260–270. [CrossRef]
13. Şeker, C.; Manirakiza, N. Effectiveness of compost and biochar in improving water retention characteristics and aggregation of a sandy clay loam soil under wind erosion. *Carpathian J. Earth Environ. Sci.* **2020**, *15*, 5–18. [CrossRef]
14. Kranz, C.N.; McLaughlin, R.A.; Johnson, A.; Miller, G.; Heitman, J.L. The effects of compost incorporation on soil physical properties in urban soils—A concise review. *J. Environ. Manag.* **2020**, *261*, 110209. [CrossRef] [PubMed]
15. Sadeghi, S.; Ebrahimi, S.; Zakerinia, M. The Study of the Parametric Changes in Water Potential Points by Using Waste Manuciple Compost in Three Kinds of Soils. *Int. J. Basic Sci. Appl. Res.* **2014**, *3*, 254–260. Available online: http://www.isicenter.org (accessed on 22 February 2022).
16. Paradelo, R.; Basanta, R.; Barral, M.T. Water-holding capacity and plant growth in compost-based substrates modified with polyacrylamide, guar gum or bentonite. *Sci. Hortic.* **2019**, *243*, 344–349. [CrossRef]
17. Benito, M.; Masaguer, A.; Moliner, A.; de Antonio, R. Chemical and physical properties of pruning waste compost and their seasonal variability. *Bioresour. Technol.* **2006**, *97*, 2071–2076. [CrossRef]

18. Ibrahim, A.; Horton, R. Biochar and compost amendment impacts on soil water and pore size distribution of a loamy sand soil. *Soil Sci. Soc. Am. J.* **2021**, *85*, 1021–1036. [CrossRef]
19. Curtis, M.J.; Claassen, V.P. Regenerating topsoil functionality in four drastically disturbed soil types by compost incorporation. *Restor. Ecol.* **2009**, *17*, 24–32. [CrossRef]
20. Palazzolo, E.; Laudicina, V.A.; Roccuzzo, G.; Allegra, M.; Torrisi, B.; Micalizzi, A.; Badalucco, L. Bioindicators and nutrient availability through whole soil profile under orange groves after long-term different organic fertilizations. *SN Appl. Sci.* **2019**, *1*, 468. [CrossRef]
21. Glab, T.; Zabinski, A.; Sadowska, U.; Gondek, K.; Kopec, M.; Mierzwa-Hersztek, M.; Tabor, S. Effects of co-composted maize, sewage sludge, and biochar mixtures on hydrological and physical qualities of sandy soil. *Geoderma* **2018**, *315*, 27–35. [CrossRef]
22. Rivier, P.-A.; Jamniczky, D.; Nemes, A.; Makó, A.; Barna, G.; Uzinger, N.; Rékási, M.; Farkas, C. Short-term effects of compost amendments to soil on soil structure, hydraulic properties, and water regime. *J. Hydrol. Hydromech.* **2022**, *70*, 74–88. [CrossRef]
23. Dexter, A.R. Soil physical quality Part I. Theory, effects of soil texture, density, and organic matter, and effects on root growth. *Geoderma* **2004**, *120*, 201–214. [CrossRef]
24. Van Genuchten, M.T. A Closed-form Equation for Predicting the Hydraulic Conductivity of Unsaturated Soils. *Soil Sci. Soc. Am. J.* **1980**, *44*, 892–898. [CrossRef]
25. Reynolds, W.D.; Drury, C.F.; Tan, C.S.; Fox, C.A.; Yang, X.M. Use of indicators and pore volume-function characteristics to quantify soil physical quality. *Geoderma* **2009**, *152*, 252–263. [CrossRef]
26. Reynolds, W.D.; Drury, C.F.; Tan, C.S.; Yang, X.M. Temporal effects of food waste compost on soil physical quality and productivity. *Can. J. Soil Sci.* **2015**, *95*, 251–268. [CrossRef]
27. Reynolds, W.D.; Bowman, B.T.; Drury, C.F.; Tan, C.S.; Lu, X. Indicators of good soil physical quality: Density and storage parameters. *Geoderma* **2002**, *110*, 131–146. [CrossRef]
28. Topp, G.C.; Reynolds, W.D.; Cook, F.J.; Kirby, J.M.; Carter, M.R. Physical attributes of soil quality. In *Development in Soil Science; Soil Quality for Crop Production and Ecosystem Health*; Gregorich, E.G., Carter, M.R., Eds.; Elsevier: New York, NY, USA, 1997; Volume 25, pp. 21–58.
29. Manici, L.M.; Castellini, M.; Caputo, F. Soil-inhabiting fungi can integrate soil physical indicators in multivariate analysis of Mediterranean agroecosystem dominated by old olive groves. *Ecol. Indic.* **2019**, *106*, 105490. [CrossRef]
30. Stellacci, A.M.; Castellini, M.; Diacono, M.; Rossi, R.; Gattullo, C.E. Assessment of soil quality under different soil management strategies: Combined use of statistical approaches to select the most informative soil physico-chemical indicators. *Appl. Sci.* **2021**, *11*, 5099. [CrossRef]
31. Agnese, C.; Bagarello, V.; Baiamonte, G.; Iovino, M. Comparing physical quality of forest and pasture soils in a Sicilian watershed. *Soil Sci. Soc. Am. J.* **2011**, *75*, 1958–1970. [CrossRef]
32. Iovino, M.; Castellini, M.; Bagarello, V.; Giordano, G. Using static and dynamic indicators to evaluate soil physical quality in a Sicilian area. *Land Degrad. Dev.* **2016**, *27*, 200–210. [CrossRef]
33. Cullotta, S.; Bagarello, V.; Baiamonte, G.; Gugliuzza, G.; Iovino, M.; La Mela Veca, D.S.; Maetzke, F.; Palmeri, V.; Sferlazza, S. Comparing Different Methods to Determine Soil Physical Quality in a Mediterranean Forest and Pasture Land. *Soil Sci. Soc. Am. J.* **2016**, *80*, 1038–1056. [CrossRef]
34. Shahab, H.; Emami, H.; Haghnia, G.H.; Karimi, A. Pore Size Distribution as a Soil Physical Quality Index for Agricultural and Pasture Soils in Northeastern Iran. *Pedosphere* **2013**, *23*, 312–320. [CrossRef]
35. Kutilek, M.; Nielsen, D.R. Soil Hydrology. In *GeoEcology Textbook*; Catena Verlag: Cremlingen, Germany, 1994; 370p, ISBN 3-923381-26-3.
36. Zhao, Y.; Wen, T.; Shao, L.; Chen, R.; Sun, X.; Huang, L.; Chen, X. Predicting hysteresis loops of the soil water characteristic curve from initial drying. *Soil Sci. Soc. Am. J.* **2020**, *84*, 1642–1649. [CrossRef]
37. Haverkamp, R.; Reggiani, P.; Ross, P.J.; Parlange, J.Y. Soil Water Hysteresis Prediction Model Based on Theory and Geometric Scaling. *Environ. Mech.* **2002**, *129*, 213–246.
38. Alagna, V.; Bagarello, V.; Cecere, N.; Concialdi, P.; Iovino, M. A test of water pouring height and run intermittence effects on single-ring infiltration rates. *Hydrol. Processes* **2018**, *32*, 3793–3804. [CrossRef]
39. Eden, M.; Gerke, H.H.; Houot, S. Organic waste recycling in agriculture and related effects on soil water retention and plant available water: A review. *Agron. Sustain. Dev.* **2017**, *37*, 11. [CrossRef]
40. Gugliuzza, G.; Verduci, A.; Iovino, M. Water retention characteristics of substrates containing biochar and compost as peat and perlite replacements for ornamental plant production. *Acta Hortic.* **2021**, *1305*, 507–511. [CrossRef]
41. Dane, J.H.; Hopmans, J.W. 3.3.2.2 Hanging water column. In *Methods of Soil Analysis, Part 4, Physical Methods, Number 5 in the Soil Science Society of America Book Series*; Dane, J.H., Topp, G.C., Eds.; Soil Science Society of America, Inc.: Madison, WI, USA, 2002; pp. 680–683.
42. Dane, J.H.; Hopmans, J.W. 3.3.2.4 Pressure plate extractor. In *Methods of Soil Analysis, Part 4, Physical Methods, Number 5 in the Soil Science Society of America Book Series*; Dane, J.H., Topp, G.C., Eds.; Soil Science Society of America, Inc.: Madison, WI, USA, 2002; pp. 688–690.
43. Reynolds, W.D.; Drury, C.F.; Yang, X.M.; Tan, C.S. Optimal soil physical quality inferred through structural regression and parameter interactions. *Geoderma* **2008**, *146*, 466–474. [CrossRef]

44. Seki, K. SWRC fit—A nonlinear fitting program with a water retention curve for soils having unimodal and bimodal pore structure. *Hydrol. Earth Syst. Sci.* **2007**, *4*, 407–437.
45. Castellini, M.; Iovino, M. Pedotransfer functions for estimating soil water retention curve of Sicilian soils. *Arch. Agron. Soil Sci.* **2019**, *65*, 1401–1416. [CrossRef]
46. Reynolds, W.D.; Yang, X.M.; Drury, C.F.; Zhang, T.Q.; Tan, C.S. Effects of selected conditioners and tillage on the physical quality of a clay of a clay loam soil. *Can. J. Soil Sci.* **2003**, *83*, 381–393. [CrossRef]
47. Dexter, A.R.; Czyz, E.A. Applications of s-theory in the study of soil physical degradation and its consequences. *Land Degrad. Dev.* **2007**, *18*, 369–381. [CrossRef]
48. Warrick, A.W. Appendix 1: Spatial variability. In *Environmental Soil Physics*; Hillel, D., Ed.; Academic Press: San Diego, USA, 1998; pp. 655–675.
49. Khaleel, R.; Reddy, R.; Overcash, M.R. Changes in Soil Physical Properties Due to Organic Waste Applications: A Review. *J. Environ. Qual.* **1981**, *10*, 133–141. [CrossRef]
50. Brown, S.; Cotton, M. Changes in soil properties and carbon content following compost application: Results of on-farm sampling. *Compost Sci. Util.* **2011**, *19*, 88–97. [CrossRef]
51. Carsel, R.F.; Parrish, R.S. Developing Joint Probability-Distributions of Soil-Water Retention Characteristics. *Water Resour. Res.* **1988**, *24*, 755–769. [CrossRef]
52. Haverkamp, R.; Leij, F.J.; Fuentes, C.; Sciortino, A.; Ross, P.J. Soil water retention: I. Introduction of a shape index. *Soil Sci. Soc. Am. J.* **2005**, *69*, 1881–1890. [CrossRef]
53. Al-Omran, A.; Ibrahim, A.; Alharbi, A. Effects of Biochar and Compost on Soil Physical Quality Indices. *Commun. Soil Sci. Plant Anal.* **2021**, *52*, 2482–2499. [CrossRef]
54. Doerr, S.H.; Shakesby, R.A.; Walsh, R.P.D. Soil water repellency: Its causes, characteristics and hydro-geomorphological significance. *Earth Sci. Rev.* **2000**, *51*, 33–65. [CrossRef]
55. Kaluarachchi, J.J.; Parker, J.C. Effects of hysteresis with air entrapment on water flow in the unsaturated zone. *Water Resour. Res.* **1987**, *23*, 1967–1976. [CrossRef]
56. DeBano, L.F. *Water Repellent Soils: A State-of-the-Art*; General Technical Report, PSW-46; United States Department of Agriculture, Forest Service: Berkeley, CA, USA, 1981; 21p.
57. Castellini, M.; Ventrella, D. Impact of conventional and minimum tillage on soil hydraulic conductivity in typical cropping system in southern Italy. *Soil Tillage Res.* **2012**, *124*, 47–56. [CrossRef]
58. Bagarello, V.; Castellini, M.; Iovino, M. Influence of the pressure head sequence on the soil hydraulic conductivity determined with the tension infiltrometer. *Appl. Eng. Agric.* **2005**, *21*, 383–391. [CrossRef]
59. Bagarello, V.; Castellini, M.; Iovino, M. Comparison of unconfined and confined unsaturated hydraulic conductivity. *Geoderma* **2007**, *137*, 394–400. [CrossRef]

Biologia
https://doi.org/10.1007/s11756-024-01637-1

ORIGINAL ARTICLE

Temporal variability of physical quality of a sandy loam soil amended with compost

Cristina Bondì[1] · Mirko Castellini[2] · Massimo Iovino[1]

Received: 6 September 2023 / Accepted: 5 February 2024

Abstract

Compost can enhance the soil's ability to retain water, resulting in an overall improvement of soil physical quality (SPQ). The purpose of this study was to evaluate the temporal variability of physical and hydraulic properties of a sandy loam soil amended with a compost obtained from orange juice processing wastes and garden cleaning. The soil water retention curve of repacked soil samples at varying compost to soil ratios, r, was determined at the time of compost embedding (M0) and after six months (M6), and twelve months (M12). Indicators of SPQ linked to soil water retention curve such as air capacity (AC), macroporosity (P_{mac}), plant available water capacity ($PAWC$), relative field capacity (RFC) and Dexter S-index (S), were estimated. The effect of compost addiction of the pore volume distribution function was also evaluated.

The elapsed time from compost application influenced all SPQ indicators but the maximum beneficial effects of compost amendment were achieved within approximately the first six months. Indicators linked the macro- and mesoporosity (P_{mac} and AC) decreased with r whereas indicators linked to plant water availability ($PAWC$ and RFC) increased with r. The combined effect of time and rate was statistically observed only for P_{mac}, $PAWC$ and S.

Compost addiction reduced the soil compaction and modified the pore system, as the fraction of structural porosity (i.e., macropores) decreased and the fraction of textural porosity (i.e., micropores) increased. It was concluded that even a single application of compost could have a significant impact on soil water retention and microstructure with positive implications for soil health, precision agriculture and crop productivity.

Keywords Compost amendment · Soil physical quality (SPQ) · Soil water retention · Temporal variability

Introduction

In sandy soils, organic amendments are mainly used for enhancing the organic matter levels of the soil and improving its physical and chemical properties (Garbowski et al. 2023).

In this regard, compost is undoubtedly an effective and sustainable organic soil amendment that can increase humus content, improve soil fertility, and boost the soil's ability to retain water and nutrients, thereby enhancing the soil physical quality (SPQ) (Ampim et al. 2010; Paradelo et al. 2019; Wang et al. 2022). Compost is the result of the composting process, i.e., the aerobic, thermophilic decomposition of organic wastes by different species of microorganisms under controlled conditions (Parr et al. 1978). The process of decomposition transforms potentially toxic organic matter into a stabilized state that can be used to improve soil condition for plant growth.

Regarding the soil physical properties, numerous studies have highlighted various benefits of using compost as an organic soil amendment, such as: improvement of aggregation and aggregate stability (Annabi et al. 2007; Dong et al. 2021; Sarker et al. 2022), increase in total porosity (Arthur et al. 2011; Wallace et al. 2019), decrease in bulk density (Somerville et al. 2018; McGrath et al. 2020), improvement of pore size distribution (Aggelides and Londra 2000), increase in water retention capacity (Logsdon et al. 2017; Schmid et al. 2017; Gląb et al. 2020). Compost can also enhance soil air permeability, reduce compaction, and provide a favorable environment for plant root growth (Olson et al. 2013; Maškova et al. 2021). Apart from the specific

✉ Cristina Bondì
cristina.bondi@unipa.it

[1] Department of Agricultural, Food and Forest Sciences, University of Palermo, 90128 Palermo, Italy

[2] Council for Agricultural Research and Economics–Research Center for Agriculture and Environment (CREA–AA), Via C. Ulpiani 5, 70125 Bari, Italy

Published online: 01 March 2024

climatic characteristics of each environment which drive the degradation rate of the soil organic matter, the impact of compost can vary over time depending on various factors such as the quality and the quantity of the compost used, the soil texture and the soil management adopted (Rupasinghe and Leelamanie 2020; Kranz et al. 2023).

The soil physical properties play a crucial role in determining the interactions between soil, water, and plants, thereby influencing the growth and germination of plants (Dexter 2004). The physical, chemical, and biological processes occurring in the plant root zone are mainly driven by the SPQ. It primarily refers to soil strength, water and air transmission, and storage characteristics (Topp et al. 1997). Physical quality is closely related to the soil water retention curve, which expresses the volumetric water content, θ, as a function of the pressure head, *h*. The soil water retention curve provides an indirect method for estimating pore size distribution (Hillel 1998) and can be used to determine capacity based SPQ indicators directly linked to the soil's ability to retain and supply water and air to plants. These indicators, that can be used in practical applications, include air capacity (*AC*), macroporosity (P_{mac}), plant available water capacity (*PAWC*), relative field capacity (RFC) (Reynolds 2002, 2003). Dexter (2004) introduced a conceptually different SPQ indicator, namely the S-index, which provides information on the distribution of soil pore sizes.

SPQ is affected by various factors, including soil structure, density, porosity, permeability, water retention capacity, pH, and organic matter content. Soil quality worldwide has been declining due to multiple reasons, including improper land use, poor agricultural management, excessive use of pesticides and fertilizers, soil compaction due to machinery, erosion, loss of organic matter, and climate change (Mojiri et al. 2012; Ferreira et al. 2022). Soils with poor physical characteristics generally exhibit high compaction or low porosity with limited water retention and slowed fluid transmission (Dexter 2004). This can result in inadequate root development and reduced soil aeration, both of which can hinder plant growth and productivity. Conversely, excessively high porosity can cause anchoring problems for crops or plants. Accordingly, the rational use of compost can be a valuable support to cultivation techniques for improving SPQ.

The duration of beneficial effects of compost amendment is not fully investigated as most of the studies focused the long-term effects that implies repeated inputs, generally every year, whereas very few studies have addressed the effects of a single input of organic matter (Cannavo et al. 2014; Sax et al. 2017). To the best of our knowledge, there is a limited number of studies focused on the use of SPQ indicators for evaluating the effects of compost amendment (Reynolds et al. 2009, 2015). Arthur et al. (2011) quantified the long-term effects of adding three different types of compost on the physical properties of a sandy soil by SPQ indicators. Castellini et al. (2022) evaluated the short- and medium-term effects of a compost addition on the physical and hydraulic properties of a clay soil. They reported that soil water retention and bulk density can be enhanced when high rates of compost, equal to 15 and 75 kg m^{-2}, were used. Bondì et al. (2022) assessed the reliability of SPQ indicators and pores size distribution parameters to evaluate the effectiveness of compost amendment on a sandy loam soil. They found that the addition of compost effectively altered the soil pore distribution system and associated SPQ indicators, resulting in possible positive effects on soil hydrological processes and agronomic services. Existing studies proved that SPQ indicators can be valuable tools for assessing the impacts of compost on soil.

The objective of this study was to assess the short-term effects of compost amendment on the physical and hydraulic properties of sandy loam soil. In particular, the temporal effect of a single application of compost at different rates was evaluated through measurements of SPQ indicators conducted at the time of embedding and after six and twelve months. Information on the temporal persistence of the benefits of compost amendment is crucially important for planning the most effective soil management practices.

Materials and Methods

Sample preparation

A sandy loam soil was amended with 5-months-aged compost derived from orange juice processing waste (75%) and garden cleaning (25%). Orange juice processing waste were composed of about 60% peel, 30% pulp and 10% pips, while garden cleaning contained triturated pruning residues and mown grasses (Palazzolo et al. 2019).

The sandy loam soil, classified by Alagna et al. (2018) as a Typic Rhodoxeralf, was sampled in a citrus orchard at the Department of Agriculture and Forestry Sciences of the University of Palermo, Italy (UTM 33S 355511E, 4218990N). Physicochemical attributes of soil and compost are shown in Table 1, taken from Bondì et al. (2022). Both components, before being mixed, were sieved through a 2 mm sieve, and air-dried.

Compost was blended with soil in five different rates by weight: $r = 10\%, 20\%, 30\%, 50\%$, and 75%. Additionally, for comparative purposes, the two unmixed matrices were also considered: i.e., the not amended soil ($r = 0$) and pure compost ($r = 100\%$). In total, 42 samples were prepared, with two replicates for each compost rate and each duration of the compost embedment. The samples were prepared by compacting the dry mass of soil and compost into metal cylinders having diameter and height of 5 cm with a porous nylon

Table 1 Physicochemical attributes of soil and compost (from Bondì et al. 2022)

Soil		Compost	
Clay (%)	17.6	pH	7.2
Silt (%)	29.8	EC (dS m^{-1})	0.54
Sand (%)	52.6	C (%)	9.91
OM (%)	2.1	N (%)	0.64
pH	7.8	P (%)	0.45
EC (dS m^{-1})	0.48	Ash (%)	82.5
CEC (cmol kg^{-1})	25.31	C/N ratio	15.1

cloth at the bottom. The packing methodology described by Bondi et al. (2022) was used that proved to be effective in obtaining replicable results as showed by coefficients of variation, *CV*, for bulk density and water retention far below the acceptable limit of 15% (Warrick 1998).

Use of a limited number of replicates (i.e., $N = 2–3$) is a frequent option when operating with repacked soil cores (Arthur et al. 2011; Reynolds et al. 2015; Ibrahim and Horton 2021) given the variability due to natural aggregation is loss in these samples. On the other hand, using repacked samples is preferable in studies aimed at estimating the effects of soil amendments rate as they allow to compare soil physical and hydraulic characteristics associated to exactly the same amendment dose.

In November 2021, soon after preparation, 14 samples, two for each mixture, were analyzed to determine the soil water retention curve at time M0. The remaining samples were placed directly on the surface of the extensive green roof plot at the University of Palermo and analyzed after six (M6) and twelve months (M12). The samples were subjected to meteoric events, thus undergoing natural drainage and wetting cycles, with variation of soil moisture content, which also caused swelling and shrinkage phenomena in the samples.

Rainfall and temperature data, during the embedding period were recorded by a weather station of the Servizio Informativo Agrometeorologico Sicialiano (SIAS), located about 3 km far from the green roof. The thermopluviometric chart for the study period is showed in Fig. 1.

In May 2022 and in November 2022, i.e., respectively after six and twelve months from compost embedding, determination of soil water retention curve were repeated, following the same experimental procedure.

Soil water retention curve measurement and parameterization

The soil water retention curve was determined experimentally by the hanging water column apparatus (Dane and Hopmans 2002a), for pressure head, h (m), values ranging from −0.01 to −1 m, and by the pressure extractor method (Dane and Hopmans 2002b) for lower h values ranging from −1 to −150 m. With the hanging water column technique, the soil samples were placed on the surface of the porous plate of a glass funnel and saturated from below by applying four successive equilibrium steps of 24 h each at h values of −0.2, −0.1, and −0.05 m followed by submersion (i.e., $h = 0$). Starting from saturation, soil samples were drained by imposing a decreasing sequence of 11 h values: −0.05, −0.075, −0.10, −0.15, −0.20, −0.25, −0.30, −0.40, −0.50, −0.70 and −1 m. For each equilibrium h value, the volume of water drained was recorded and these volumes were added backwards to the equilibrium volumetric water content, θ ($m^3 m^{-3}$), determined at $h = -1$ m by weighting the sample after oven-drying at 105 °C for 24 h.

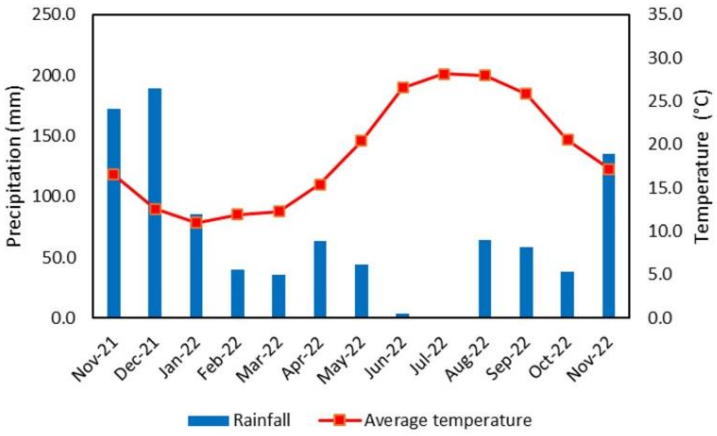

Fig 1 Thermopluviometric chart of the weather station in Palermo (50 m a.s.l., UTM ED50 353448E, 4221667N)

At the end of the experiment ($h = -1$ m), the height of the sample was measured at nine fixed points on sample surface by using a gauge with a precision of 0.5 mm and an average value was determined through the application of the arithmetic mean. This value was used to calculate the sample volume, V (cm^3), and, consequently, the sample dry soil bulk density, BD ($g\ cm^{-3}$).

For the pressure head values of −1, −10, −30 and −150 m, the water retention data were determined in pressure plate extractors on two replicated samples of 5-cm-diameter by 1-cm-height, prepared at the same bulk density value of the larger samples. Determination of volumetric water content at $h = -1$ m was included in pressure plate experiments for comparison with the θ value measured at the same potential in the tension apparatus. All the measurements were conducted under temperature-controlled conditions at 22 ± 1 °C. The van Genuchten's empirical unimodal model (1980) was used to fit the experimental water retention data:

$$\theta(h) = \theta_r + \left(\theta_s - \theta_r\right)(1 + |\alpha h|^n)^{-m} \quad (1)$$

where θ_s ($m^3\ m^{-3}$) and θ_r ($m^3\ m^{-3}$) are the saturated and residual volumetric water contents, respectively, α (m^{-1}) is a scale parameter, and n and m with $m = 1-1/n$ are shape parameters. The water retention data were fitted separately for the two replicates of each mixture by using SWRC fit software (Seki 2007). The shape and scale parameters (α, n, θ_s, and θ_r) were estimated without any constraint to their possible range. The reliability of the estimates was assessed by common statistical indicators such as the correlation coefficient, R, the mean error, ME and the root mean square error, $RMSE$ (Bondì et al. 2022).

Estimation of SPQ indicators

Bulk density, BD ($g\ cm^{-3}$), is an indirect indicator of aeration, strength, and ability to store and transmit water (Reynolds et al. 2008):

$$Bulk\ density\ BD = \frac{M_s}{V_b} \quad (2)$$

where M_s (g) is oven-dry soil mass and V_b (cm^3) is the corresponding bulk soil volume.

From the fitted van Genuchten water retention curves, the following capacity-based indicators of SPQ were calculated (Reynolds et al. 2002, 2003):

$$Air\ capacity\ AC = \theta_s - \theta_{FC} \quad (3)$$

$$Macroporosity\ P_{mac} = \theta_s - \theta_m \quad (4)$$

$$Plant\ available\ water\ capacity\ PAWC = \theta_{FC} - \theta_{PWP} \quad (5)$$

$$Relative\ field\ capacity\ RFC = \frac{\theta_{FC}}{\theta_s} \quad (6)$$

where θ_{FC} ($m^3\ m^{-3}$) is the volumetric water content corresponding to so-called field capacity (h = -1 m), θ_m ($m^3\ m^{-3}$) is the volumetric water content of the soil matrix (h = -0.1 m), and θ_{PWP} ($m^3\ m^{-3}$) is the volumetric water content corresponding to the permanent wilting point (h = -150 m).

Air capacity, AC ($m^3\ m^{-3}$), is expressive of the ability of the soil to ensure the necessary aeration to the root systems. Macroporosity, P_{mac} ($m^3\ m^{-3}$), is representative of the volume of macropores (i.e., >l300 µm equivalent pore diameter) of the soil and, indirectly, provides an indication of the soil's ability to favor the drainage processes and the root proliferation. Plant available water capacity, $PAWC$ ($m^3\ m^{-3}$), is expressive of the soil's ability to store and provide water that is available to plant roots. Relative field capacity, RFC (-), indicates the soil's ability to store water and air in relation to the total porosity which is assumed to be expressed by θ_s.

Dexter (2004) proposed to evaluate SPQ from the slope of the retention curve at the inflection point when the curve is expressed as gravimetric water content, U ($g\ g^{-1}$), versus the natural logarithm of h.

$$S - index\ S = -n\left(U_s - U_r\right) \cdot \left[1 + \frac{1}{m}\right]^{-(1+m)} \quad (7)$$

where U_s ($g\ g^{-1}$) and U_r ($g\ g^{-1}$) are the gravimetric saturated and residual water contents that, under the assumption of rigid soil, can be calculated from θ_s and θ_r.

The judgment on SPQ is made comparing the measured value of a given SPQ indicator with the classification range proposed in the literature (Olness et al. 1998; Reynolds et al. 2002, 2009; Dexter 2004).

The pore volume distribution function, $S_v(h)$, may be defined as the slope of the soil water retention curve expressed as volumetric water content versus ln(h), and plotted against the equivalent pore diameter, d_e (µm). To allow comparison of different porous materials, Reynolds et al. (2009) proposed a normalized soil pore volume distribution, $S^*(h)$ being $0 \le S^*(h) \le 1$.

Evaluation of SPQ involves comparison of "location" and "shape" parameters, derived from the normalized pore volume distribution, with optimal values suggested by Reynolds et al. (2009).

Location parameters are the mode diameter, d_{mode} (µm), the median diameter, d_{median} (µm), and mean diameter, d_{mean} (µm), shape parameters are standard deviation, SD (-), skewness, SK (-), and kurtosis, KU (-). For brevity reasons, the expressions for estimating the location and shape parameters are not given here but the reader is referred to Reynolds et al. (2009).

Statistical analysis

A pairwise t-test was applied to establish statistical comparisons between two datasets corresponding to different times from compost application date. The influence of compost addition on the considered SPQ indicators was evaluated by analyzing the significance of Pearson correlation coefficient, *R*, calculated between each SPQ indicator and the compost to soil ratio, *r*. A two-way ANOVA was employed to assess the individual and combined effects of time and compost rate on the SPQ indicators. All statistical tests were carried out with Microsoft Excel at a significance level $p = 0.05$.

Results and discussion

Influence of time from compost application on SPQ indicators

The water retention data were adequately fitted by the unimodal model of van Genuchten as showed by the high values of *R* and the low values of *ME* and *RMSE* (Table 2).

The average values of SPQ indicators obtained at the three sampling dates are reported in Table 3 whereas mean and standard deviation values corresponding to the different soil-compost rates are listed in Table S1 (supplementary material). The coefficients of variations for the soil bulk density and the capacity-based indicators of SPQ were generally within the limit of 15% considered acceptable for these soil properties (Warrick 1998) with the only exception of P_{mac} and *AC* that were respectively characterized by mean *CV* values in the range 20.9–36.8% and 5.0–17.3%, depending on the sampling time. Variability of replicated measurements also tended to increase with time from compost application (Table S1).

For all the considered indicators, statistically significant differences were observed between the value at the time of compost embedment and the values measured after six (M6) and twelve (M12) months, respectively. This indicated a clear temporal effect that influences the soil's physical properties and pore distribution, which ultimately impact plant growth and overall soil health.

In particular, the SPQ indicators associated to total porosity or macro-porosity (*BD*, *AC*, P_{mac}) decreased whereas SPQ indicators associated to the smaller pore size domain (*PAWC* and *RFC*) increased. Also, the S-index, which is representative of the entire pore size distribution, increased. No statistically significant differences were observed in the mean values of *PAWC* and *RFC* between M6 and M12. The other indicators showed significant differences between M6 and M12 that, however, were of opposite sign compared to the differences observed between M0 and M6. This result indicates that the maximum benefits of compost amendment was achieved within six months whereas the soil physical quality remained unchanged or regressed in the following six months. Our results are consistent with those of Weber et al. (2007) who observed short-term beneficial effects of compost on soil water retention. Specifically, they observed that total porosity and plant available water increased only within the first five months after compost application. The short-term effects of adding compost to the soil were evaluated in another study by Guo et al. (2019) on a tomato crop in China that showed improved soil structure, increased water retention capacity, and enhanced soil fertility six months after the compost application. Therefore, it can be inferred that the positive effects of compost on soil water availability may not last for more than approximately six months and it will require regular application to maintain the benefits over time. The temporal effects of a single compost application on soil bulk density and water retention were modelled by simple asymptotic and exponential functions by Cannavo et al. (2014). According to their published data for a compost made of sewage sludge and wood chips applied at 40% v/v rate to an urban soil, *BD* is expected to increase by 7.2% after 6 months, P_{mac} and *AC* to decrease by 18% and 5%. Our results are in good agreement with the short-term effects observed by Cannavo et al. (2014). However, while their results suggest that the soil physical properties are monotonically increasing or decreasing even after the first six months, signs of inverted trends were observed in the present study. A possible factor of discrepancy could be the influence of root system that, under field conditions, could contrast the effects of soil compaction and compost

Table 2 Statistics of coefficient of correlation, *R*, mean error, *ME*, and root mean square error, *RMSE*, for the estimated water retention curves

	R	*ME*	*RMSE*
Min	0.9307	-1.52×10^{-3}	4.04×10^{-3}
Max	0.9996	1.26×10^{-3}	1.03×10^{-2}
Mean	0.9930	3.40×10^{-5}	7.12×10^{-3}

Table 3 Mean values of SPQ indicators obtained for M0, M6 and M12. Mean values followed by the same letter did not differ significantly according to Student's t-test ($p < 0.05$). Values in parentheses were standard deviations ($N = 2$)

	M0	M6	M12
BD	1.07a (0.02)	1.17c (0.04)	1.13b (0.05)
AC	0.12c (0.02)	0.09a (0.03)	0.10b (0.02)
P_{mac}	0.006c (0.003)	0.001a (0.001)	0.003b (0.002)
PAWC	0.22a (0.03)	0.29b (0.04)	0.30b (0.03)
RFC	0.76a (0.04)	0.82b (0.006)	0.80b (0.05)
S-index	0.10a (0.02)	0.16c (0.03)	0.13b (0.01)

decomposition thus extending over time the benefits of soil amendment.

Compost rate effect on SPQ indicators

Table 4 shows the Pearson's correlation coefficients, *R*, between the SPQ indicators and the compost to soil ratio, *r*. In Fig. 2 the regression lines between the SPQ indicators and *r,* are plotted together with classification ranges according to criteria found in the literature (Reynolds et al. 2002, 2009; Dexter 2004; Agnese et al. 2011).

The soil *BD* showed a significant negative correlation with *r* only at M6 and M12 sampling dates. At M0, the compost rate did not statistically influenced *BD* as the densities of the compost and the soil were similar (i.e, soil *BD* = 1.07 g cm^{-3}, compost *BD* = 1.04 g cm^{-3}, see supplementary material Table S1). Differently, at M6 and M12, compost amendment was effective in contrasting the soil compaction due to the mechanical effects of rainfall that was observed for low compost rates (r < 20%) (Fig. 2a). For both dates, the *BD* decreased at increasing the compost rate thus indicating that less compacted conditions were maintained over time in amended soils. This result is in line with the conclusions of Khaleel et al. (1981), Sax et al. (2017), Somerville et al. (2018) and Castellini et al. (2022), who suggested that the use of compost decreases the soil bulk density and, consequently, reduces soil compaction.

Specifically, the dry *BD* values ranged from 1.04 to 1.12 g cm^{-3} with a mean value of 1.07 g cm^{-3} (coefficient of variation, *CV* = 2.09%). After six months (M6), *BD* increased with values ranging from 1.12 to 1.24 g cm^{-3} and mean value equal to 1.17 g cm^{-3} (*CV* = 3.40%). After twelve months (M12), the *BD* values decreased slightly, although remaining greater than the initial values (M0), with a range of values between 1.06 to 1.21 g cm^{-3} with a mean value of 1.13 g cm^{-3} (*CV* = 4.53%). Differences in *BD* values observed across the three sampling dates were mainly due to compaction phenomena caused by the impacts of raindrops that break soil aggregates (Vaezi et al. 2017). Indeed, a seasonal trend could be observed in *BD* with compaction mainly occurring in the first six rainy months (M0-M6) followed by a partial recovery during the dry season (M6-M12) (Fig. 1). It is worth to be remarked that the study neglects the role of vegetation that can contribute to maintain a loose soil structure due to the effect of roots system as well as to protect soil surface by raindrop compaction (Curtis and Claassen 2009). However, regardless of the time period and *r*, the soil *BD* values remained, generally, within the range considered optimal for field crop production, i.e., 0.9–1.2 g cm^{-3}, as suggested by Agnese et al. (2011).

Table 4 Pearson's correlation coefficients between SPQ indicators and the compost to soil ratio, *r*. Values in bold indicate statistically significant correlation ($p < 0.05$)

	M0	M6	M12
BD	-0.467	**-0.578**	**-0.682**
AC	**-0.951**	-0.498	**-0.774**
P_{mac}	**-0.851**	-0.232	**-0.667**
PAWC	**0.958**	**0.874**	**0.723**
RFC	**0.979**	**0.623**	**0.775**
S-index	**0.800**	0.319	**0.566**

At M0 and M12, the capacity-based indicators linked to the macro- and mesoporosity (P_{mac} and *AC*), exhibited significant negative correlations with *r*. At the intermediate sampling date (M6), the correlations were similarly negative despite not significant. In any case, classification of soil physical quality according to P_{mac} and *AC* was always non-optimal (Fig. 2). This finding was not unexpected since the soil samples used in this study were repacked in the laboratory, resulting in a structureless samples.

The plant available water capacity (*PAWC*) was always positively correlated with *r* (Table 4) thus showing that, independently of the sampling date, the compost amendment determined more favorable conditions for plant as already showed by several studies (Celik et al. 2004; Sax et al. 2017; Seker et al. 2020; Rivier et al. 2022) that reported how compost addition can increase soil water retention, thereby increasing the *PAWC*. For a sandy loam soil amended at 25% by volume with a windrowed yard waste compost, Curtis and Claassen (2009) observed a *PAWC* increase of 32% compared to 21% estimated from the regression line in Fig. 2 (M0). Overall, the results of the present study further support previous findings showing that compost application yielded *PAWC* values that were all above the optimal threshold suggested in the literature (Fig. 2).

The relative field capacity (*RFC*) was significantly influenced by the compost rate with *RFC* values that, independently of the sampling date, increased at increasing *r*. The values of this SPQ indicator remained always outside the optimal range recommended in the literature (Fig. 2), indicating that the soil has a relatively high field capacity compared to total porosity. Given the results were obtained on repacked structure less samples, this condition highlights how the loose of natural aggregation may lead to limited soil aeration with negative impact on plant growth.

The values of *S* always increased at increasing the compost rate (Fig. 2) and were consistently above the optimal threshold value of 0.05 indicating the presence of a well-defined microstructure as suggested by Dexter (2004).

Overall, the rate of compost application tended to decrease the macro- and mesoporosity and to increase the microporosity thus improving the availability of water for plant. At the time of compost embedment (M0), the

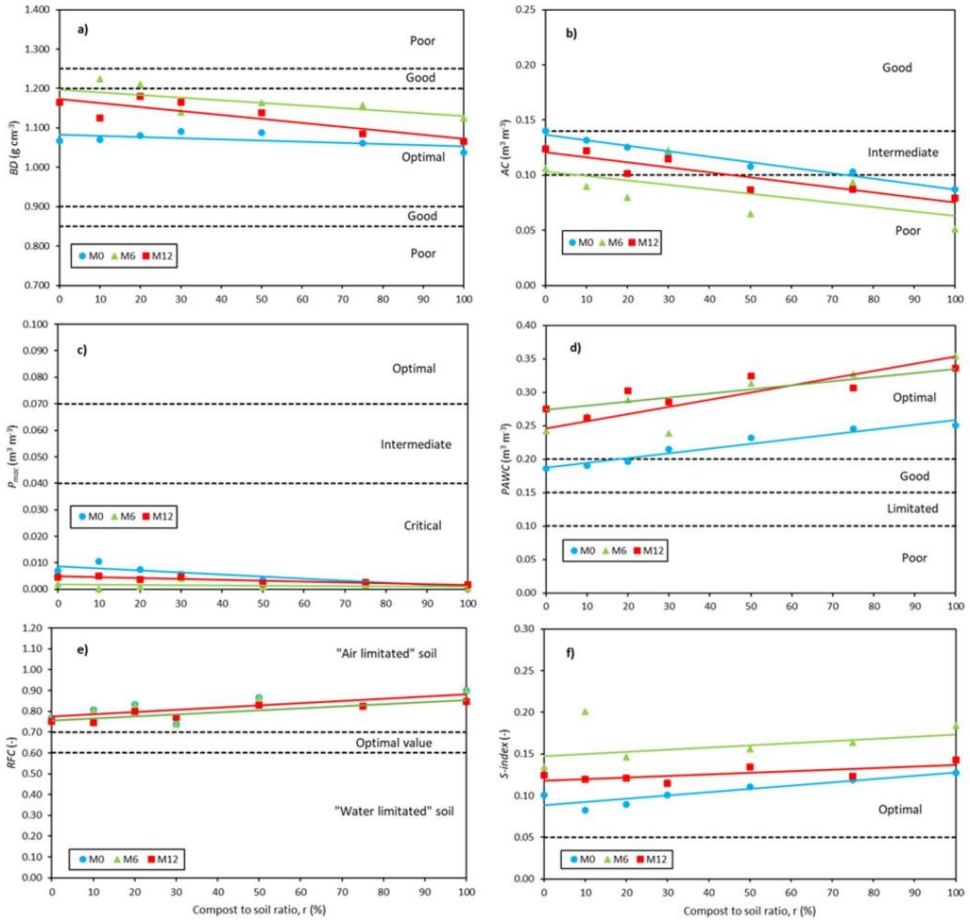

Fig 2 Regression lines between the SPQ indicators and the compost to soil ratio, *r*, with corresponding classification ranges according to criteria found in the literature. **a**) bulk density; **b**) air capacity; **c**) macroporosity; **d**) plant available water capacity; **e**) relative field capacity; **f**) *S*-index

strength of the correlation between SPQ indicators and *r* was maximum whereas *R* decreased, and also became not significant, with time. This result confirm that the effects of compost are short-term effects and frequent applications of compost are necessary to maintain the benefits over time.

Two-way ANOVA

For each considered SPQ indicator, the two-way ANOVA (time, rate, time x rate) was used to analyze the effects of time elapsed from compost embedment and added dose of compost. Table 5 reports the results of ANOVA. A significant separated effect ($p < 0.05$) of each individual factor on all the considered SPQ indicators was observed. The combined effect was found to be statistically significant only for P_{mac}, *PAWC* and *S* indicators, which means that the effect of

Table 5 Two-way ANOVA of time and compost rate effects on the SPQ indicators

	Sum of square	*Df*	*Mean Square*	*F*	*p-Value*	*F crit.*
			BD			
Time	0.070	2	0.035	36.996	<0.050	3.467
Rate	0.026	6	0.004	4.547	<0.050	2.573
Time x Rate	0.016	12	0.001	1.388	0.246	2.250
Within	0.020	21	0.001			
Total	0.131	41				
			AC			
Time	0.006	2	0.003	12.177	<0.050	3.467
Rate	0.012	6	0.002	8.210	<0.050	2.573
Time x Rate	0.003	12	2.18×10^{-4}	0.870	0.586	2.250
Within	0.005	21	2.52×10^{-4}			
Total	0.026	41				
			$\boldsymbol{P_{mac}}$			
Time	1.14×10^{-4}	2	5.74×10^{-5}	37.314	<0.050	3.467
Rate	9.16×10^{-5}	6	1.53×10^{-5}	9.935	<0.050	2.573
Time x Rate	7.19×10^{-5}	12	5.99×10^{-6}	3.898	<0.050	2.250
Within	3.23×10^{-5}	21	1.54×10^{-6}			
Total	3.10×10^{-4}	41				
			PAWC			
Time	0.057	2	0.029	132.471	<0.050	3.467
Rate	0.034	6	0.006	26.126	<0.050	2.573
Time x Rate	0.006	12	0.001	2.407	<0.050	2.250
Within	0.005	21	2.15×10^{-4}			
Total	0.101	41				
			RFC			
Time	0.028	2	0.014	17.295	<0.050	3.467
Rate	0.069	6	0.011	13.921	<0.050	2.573
Time x Rate	0.012	12	0.001	1.252	0.315	2.250
Within	0.017	21	0.001			
Total	0.127	41				
			S-index			
Time	0.020	2	0.010	105.272	<0.050	3.467
Rate	0.007	6	0.001	11.718	<0.050	2.573
Time x Rate	0.007	12	0.001	6.404	<0.050	2.250
Within	0.002	21	9.56×10^{-5}			
Total	0.036	41				

an individual factor depends on the level of the other individual factor. For *BD*, *AC* and *RFC* no statistically significant combined effect was found, i.e., the differences in the levels of factors time and rate, taken together, do not have a significant impact on these SPQ indicators. This may be due to an antagonistic effect of the two factors that showed opposite influence on these SPQ indicators.

Effect of compost addition on the pore size distribution

To investigate the influence of compost amendment, the trend of the location and shape parameters of the normalized pore volume distribution curves as a function of the compost dose was analysed. Except for *SK*, all the examined parameters exhibited a negative correlation with r (Table 6), with statistically significant R values ($p < 0.05$) for the location parameters, namely d_{mode}, d_{median} and d_{mean}. Compost amendment significantly affected shape parameters only at the time of application (M0) thus suggesting that the effects of compost on the shape parameters are probably weak or, alternatively, that these parameters are less sensitive to compost rate.

Figure 3 shows the mean values of the location parameters for the three sampling dates. The mode diameter, d_{mode}, which represents the most frequently occurring equivalent

Table 6 Pearson's correlation coefficients between the location and the shape parameters and *r*. Values in bold indicate statistically significant correlation ($p < 0.05$)

	M0	M6	M12
d_{mode}	**-0.952**	**-0.680**	**-0.722**
d_{median}	**-0.775**	**-0.749**	**-0.711**
d_{mean}	**-0.533**	**-0.748**	**-0.685**
SD	**-0.630**	-0.099	-0.482
SK	**0.728**	0.053	**0.579**
KU	**-0.770**	-0.037	-0.526

pore diameter, decreased from M0 to M6 and then remained roughly constant in M12. Castellini et al. (2022) identified a positive, and significant, relationship between saturated hydraulic conductivity and d_{mode}, therefore reporting a similar result. Differently, the median, d_{median}, and the mean, d_{mean}, equivalent diameters progressively decreased from M0 to M12. Also, Al-Omran et al. (2021) found that application of date palm biochar and compost, both separately or in combination, reduced the equivalent pore diameters and the locations parameters, and this resulted in improved water retention and water use efficiency of sandy soils. Therefore, embedment of compost yielded a porous medium characterized by smaller pore size and lower heterogeneity as detected by the negative correlation with location and shape parameters. Such effects are not to be considered entirely positive, unless the pores system established is well interconnected, ensuring adequate hydrodynamic soil properties. These effects continued over time with reference to location parameters but not to the shape ones. Our findings agree with the results obtained by Ibrahim and Horton (2021), demonstrating that the application of compost led to a decrease in soil pore equivalent diameters, resulting in altered soil pore distributions. In agreement with the results obtained for capacitive SPQ indicators, it can be hypothesized that the addition of compost caused a relocation of pore size distribution from structural porosity (i.e., macropores), that decreased, to textural porosity (i.e., micropores), that increased.

Conclusions

The SPQ of a sandy loam soil was influenced by a single application of compost obtained from orange juice processing wastes and garden cleaning, dosed at different rates. The study revealed a clear influence of the elapsed time from compost application as significant differences were observed for all SPQ indicators between M0 and, respectively, M6 and M12. Between M6 and M12, SPQ indicators showed no significant differences (*PAWC* and *RFC*) or even an opposite sign as compared to the differences observed between M0 and M6. It was concluded that the maximum benefits of compost embedding were achieved within approximately the first six months of application. Consequently, to maintain these benefits over time, regular compost application would be necessary.

At the time of application (M0), the soil bulk density was not influenced by the compost rate. Interestingly, a negative correlation with *r* was observed at M6 and M12 that was attributed to the effective role of compost in reducing soil compaction due to rainfall impact thus showing a seasonal influence on porosity and related indicators of SPQ. Compost application dose negatively affected the SPQ indicators linked the macro- and mesoporosity, such as P_{mac} and *AC*, and positively influenced SPQ indicators linked to plant water availability, such as *PAWC* and *RFC*.

The two-way ANOVA showed a significant separated effect of both time and rate on all the considered SPQ indicators. The combined effect was significant only for P_{mac},

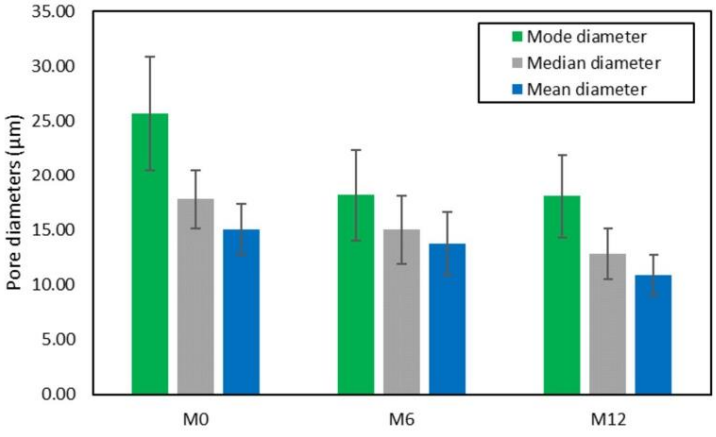

Fig 3 Mean values of the location parameters (d_{mode}, d_{median} *and* d_{mean}) obtained for M0, M6 and M12. Error bars indicate standard deviation

PAWC and *S*, while for the remaining indicators an antagonistic effect of the two factors was observed.

The pore size distribution was affected by compost rate as, at M0, both location and shape parameters decreased with *r*. Compost addiction involved a smaller and less heterogeneous pore system, thereby influencing the soil water retention capacity as the fraction of structural porosity (i.e., macropores) decreased and the fraction of textural porosity (i.e., micropores) increased. However, these modifications generally tended to vanish with time from compost application.

Overall, it can be concluded that a single application of compost has a significant impact on soil water retention and pore system of a sandy loam soil for at least six months from compost embedding. A possible downside of this investigation is that it neglects the influence of vegetation in maintaining a stable and interconnected porosity and protecting the soil form compaction due to raindrop impact. Given the important implications that these results bear for soil health, precision agriculture and crop productivity further field investigations are necessary to investigate the role of soil natural aggregation and root system on the physical quality of soils amended with compost of different characteristics.

Supplementary Information The online version contains supplementary material available at https://doi.org/10.1007/s11756-024-01637-1.

Author contributions Conceptualization: MC, MI; Methodology: CB, MC; Formal analysis and investigation: CB; Writing - original draft preparation: CB; Writing - review and editing: MC, MI; Funding acquisition: MC, MI; Supervision: MI

Funding Open access funding provided by Università degli Studi di Palermo within the CRUI-CARE Agreement. This study was supported by WATER4AGRIFOOD, contratto "Tetto Verde", Codice Progetto: CON-0375, CUP B94I20000300005 and PRIN 2022 PNRR "NBS4STORWATER", Next Generation EU, M4C2, CUP B53D23023760001.

Declarations

The authors have no relevant financial or non-financial interests to disclose.

Conflicts of Interest The authors declare no conflict of interest.

References

Aggelides SM, Londra PA (2000) Effects of compost produced from town wastes and sewage sludge on the physical properties of a loamy and a clay soil. Bioresour Technol 71:253–259. https://doi.org/10.1016/S0960-8524(99)00074-7

Agnese C, Bagarello V, Baiamonte G, Iovino M (2011) Comparing physical quality of forest and pasture soils in a Sicilian watershed. Soil Sci Soc Am J 75:1958–1970. https://doi.org/10.2136/sssaj2011.0044

Alagna V, Bagarello V, Cecere N, Concialdi P, Iovino M (2018) A test of water pouring height and run intermittence effects on single-ring infiltration rates. Hydrol Proc 32:3793–3804. https://doi.org/10.1002/hyp.13290

Al-Omran A, Ibrahim A, Alharbi A (2021) Effects of Biochar and Compost on Soil Physical Quality Indices. Commun Soil Sci Plant Anal 52(20):2482–2499. https://doi.org/10.1080/00103624.2021.1949461

Ampim PAY, Sloan JJ, Cabrera RI, Harp DA, Jaber FH (2010) Green roof growing substrates: types, ingredients, composition and properties. J Environ Hort 28(4):244–252. https://doi.org/10.24266/0738-2898-28.4.244

Annabi M, Houot S, Francou C, Poitrenaud M, Bissonnais YL (2007) Soil Aggregate Stability Improvement with Urban Composts of Different Maturities. Soil Sci Soc Am J 71:413–423. https://doi.org/10.2136/sssaj2006.0161

Arthur E, Cornelis WM, Vermang J, De Rocker E (2011) Amending a loamy sand with three compost types: Impact on soil quality. Soil Use Manag 27:116–123. https://doi.org/10.1111/j.1475-2743.2010.00319.x

Bondì C, Castellini M, Iovino M (2022) Compost Amendment Impact on Soil Physical Quality Estimated from Hysteretic Water Retention Curve. Water 14:1002. https://doi.org/10.3390/w14071002

Cannavo P, Vidal-Beaudet L, Grosbellet C (2014) Prediction of long-term sustainability of constructed urban soil: impact of high amounts of organic matter on soil physical properties and water transfer. Soil Use Manage 30:272–284. https://doi.org/10.1111/sum.12112

Castellini M, Diacono M, Preite A, Montemurro F (2022) Short- and Medium-Term Effects of On-Farm Compost Addition on the Physical and Hydraulic Properties of a Clay Soil. Agronomy 12:1446. https://doi.org/10.3390/agronomy12061446

Celik I, Ortas I, Kilic S (2004) Effects of compost, mycorrhiza, manure and fertilizer on some physical properties of a Chromoxerert soil. Soil Tillage Res 78:59–67. https://doi.org/10.1016/j.still.2004.02.012

Curtis MJ, Claassen VP (2009) Regenerating Topsoil Functionality in Four Drastically Disturbed Soil Types by Compost Incorporation. Restor Ecol 17(1):24–32. https://doi.org/10.1111/j.1526-100X.2007.00329.x

Dane JH, Hopmans JW (2002a) 3.3.2.2 Hanging water column. In: Methods of Soil Analysis, Part 4, Physical Methods, Number 5 in the Soil Science Society of America Book Series; Dane, JH, Topp GC, Eds.; Soil Science Society of America, Inc: Madison, WI, USA, pp 680–683

Dane JH, Hopmans JW (2002b) 3.3.2.4 Pressure plate extractor. In: Methods of Soil Analysis, Part 4, Physical Methods, Number 5 in the Soil Science Society of America Book Series; Dane JH, Topp GC, Eds.; Soil Science Society of America, Inc.: Madison, WI, USA, pp 688–690

Dexter AR (2004) Soil physical quality Part I. Theory, effects of soil texture, density, and organic matter, and effects on root growth. Geoderma 120:201–214. https://doi.org/10.1016/j.geoderma.2003.09.004

Dong L, Zhang W, Xiong Y, Zou J, Huang Q, Xu X, Ren P, Huang G (2021) Impact of short-term organic amendments incorporation on soil structure and hydrology in semiarid agricultural lands. Int Soil Water Conserv Res in press. https://doi.org/10.1016/j.iswcr.2021.10.003

Ferreira CSS, Seifollahi-Aghmiuni S, Destouni G, Ghajarnia N, Kalantari Z (2022) Soil degradation in the European Mediterranean region: Processes, status and consequences. Sci Total Environ 805:150106. https://doi.org/10.1016/j.scitotenv.2021.150106

Garbowski T, Bar-Michalczyk D, Charazinska S, Grabowska-Polanowska B, Kowalczyk A, Lochynski P (2023) An overview of natural soil amendments in agriculture. Soil Tillage Res 225:105462. https://doi.org/10.1016/j.still.2022.105462

Głąb T, Zabi´nski A, Sadowska U, Gondek K, Kope´c M, Mierzwa-Hersztek M, Tabor S, Stanek-Tarkowska J (2020) Fertilization effects of compost produced from maize, sewage sludge and biochar on soil water retention and chemical properties. Soil Tillage Res 197:104493. https://doi.org/10.1016/j.still.2019.104493

Guo Z, Han J, Li J, Xu Y, Wang X (2019) Effects of short-term fertilization on soil organic carbon mineralization and microbial community structure. PLoS ONE 14(4). https://doi.org/10.1371/journal.pone.0216006

Hillel D (1998) Environmental soil physics. Academic Press

Ibrahim A, Horton R (2021) Biochar and compost amendment impacts on soil water and pore size distribution of a loamy sand soil. Soil Sci Soc Am J 85:1021–1036. https://doi.org/10.1002/saj2.20242

Khaleel R, Reddy KR, Overcash MR (1981) Changes in Soil Physical Properties Due to Organic Waste Applications: A Review. J Environ Qual 10:133–141. https://doi.org/10.2134/jeq1981.00472425001000020002x

Kranz CN, McLaughlin RA, Amoozegar A, Heitman JL (2023) Influence of compost amendment rate and level compaction on the hydraulic functioning of soils. J Am Water Resour Assoc 00:1–13. https://doi.org/10.1111/1752-1688.13119

Logsdon SD, Sauer PA, Shipitalo MJ (2017) Compost Improves Urban Soil and Water Quality. J Water Resour Prot 9:345–357. https://doi.org/10.4236/JWARP.2017.94023

Mašková L, Simmons RW, Deeks LK, De Baets S (2021) Best Management Practices to Alleviate Deep-Seated Compaction in Asparagus (Asparagus officinalis) Interrows (UK). Soil Tillage Res 213:105124. https://doi.org/10.1016/j.still.2021.105124

McGrath D, Henry J, Munroe R, Williams C (2020) Compost improves soil properties and tree establishment along highway roadsides. Urban For Urban Green 55:126851. https://doi.org/10.1016/j.ufug.2020.126851

Mojiri A, Aziz HA, Ramaji A (2012) Potential decline in soil quality attributes as a result of land use change in a hillslope in Lordegan. Western Iran. Afr J Agric Res 7(4):577–582. https://doi.org/10.5897/AJAR11.1505

Olness A, Clapp CE, Liu R, Palazzo AJ (1998) Biosolids and their effects on soil properties, In: Wallace A and Terry RE, Handbook of Soil Conditioners, Marcel Dekker, New York, pp 141–165

Olson NC, Gulliver JS, Nieber JL, Kayhanian M (2013) Remediation to improve infiltration into compact soils. J Environ Manage 117:85–95. https://doi.org/10.1016/j.jenvman.2012.10.057

Palazzolo E, Laudicina VA, Roccuzzo G, Allegra M, Torrisi B, Micalizzi A, Badalucco L (2019) Bioindicators and nutrient availability through whole soil profile under orange groves after long-term different organic fertilizations. SN Appl Sci 1:468. https://doi.org/10.1007/s42452-019-0479-3

Paradelo R, Basanta R, Barral MT (2019) Water-holding capacity and plant growth in compost-based substrates modified with polyacrylamide, guar gum or bentonite. Sci Hortic 243:344–349. https://doi.org/10.1016/j.scienta.2018.08.046

Parr JE, Willson GB, Chaney RL, Sikora LJ and Tester CE (1978) Effect of certain chemical and physical factors on the composting process and product quality. In: Proceedings of National Conference on Design of Municipal Sludge Compost Facilities. Hazardous Materials Control Research.

Reynolds WD, Bowman BT, Drury CF, Tan CS, Lu X (2002) Indicators of good soil physical quality: density and storage parameters. Geoderma 110:131–146. https://doi.org/10.1016/S0016-7061(02)00228-8

Reynolds WD, Yang XM, Drury CF, Zhang TQ, Tan CS (2003) Effects of selected conditioners and tillage on the physical quality of a clay of a clay loam soil. Can J Soil Sci 83:381–393. https://doi.org/10.4141/S02-066

Reynolds WD, Drury CF, Yang XM, Tan CS (2008) Optimal soil physical quality inferred through structural regression and parameter interactions. Geoderma 146:466–474. https://doi.org/10.1016/j.geoderma.2008.06.017

Reynolds WD, Drury CF, Tan CS, Fox CA, Yang XM (2009) Use of indicators and pore volume-function characteristics to quantify soil physical quality. Geoderma 152:252–263. https://doi.org/10.1016/j.geoderma.2009.06.009

Reynolds WD, Drury CF, Tan CS, Yang XM (2015) Temporal effects of food waste compost on soil physical quality and productivity. Can J Soil Sci 95:251–268. https://doi.org/10.4141/cjss-2014-114

Rivier PA, Jamniczky D, Nemes A, Makó A, Barna G, Uzinger N, Rékási M, Farkas C (2022) Short-term effects of compost amendments to soil on soil structure, hydraulic properties, and water regime. J Hydrol Hydromech 70:74–88. https://doi.org/10.2478/johh-2022-0004

Rupasinghe ISU, Leelamanie DAL (2020) Comparison of municipal and agriculture-based solid waste composts: short-term crop-yield response and soil properties in a tropical Ultisol. Biologia 75:809–818. https://doi.org/10.2478/s11756-020-00464-4

Sarker TC, Zotti M, Fang Y, Giannino F, Mazzoleni S, Bonanomi G, Cai Y, Chang SX (2022) Soil Aggregation in Relation to Organic Amendment: a Synthesis. J Soil Sci Plant Nutr 22:2481–2502. https://doi.org/10.1007/s42729-022-00822-y

Sax MS, Bassuk N, van Es H, Rakow D (2017) Long-term remediation of compacted urban soils by physical fracturing and incorporation of compost. Urban Urban Green 24:149–156. https://doi.org/10.1016/j.ufug.2017.03.023

Schmid CJ, Murphy JA, Murphy S (2017) Effect of tillage and compost amendment on turfgrass establishment on a compacted sandy loam. J Soil Water Conserv 72(1):55–64. https://doi.org/10.2489/jswc.72.1.55

Seker C, Manirakiza N (2020) Effectiveness of compost and biochar in improving water retention characteristics and aggregation of a sandy clay loam soil under wind erosion. Carpathian J Earth Environ Sci 15:5–18

Seki K (2007) SWRC fit—A nonlinear fitting program with a water retention curve for soils having unimodal and bimodal pore structure. Hydrol Earth Syst Sci 4:407–437. https://doi.org/10.5194/hessd-4-407-2007

Somerville PD, May PB, Livesley SJ (2018) Effects of deep tillage and municipal green waste compost amendments on soil properties and tree growth in compacted urban soils. J Environ Manage 227:365–374. https://doi.org/10.1016/j.jenvman.2018.09.004

Topp GC, Reynolds WD, Cook FJ, Kirby JM, Carter MR (1997) Physical attributes of soil quality. In: Gregorich EG, Carter MR (Eds), Soil Quality for Crop Production and Ecosystem Health. Developments in Soil Science, vol 25, Elsevier, New York, pp 21 – 58. https://doi.org/10.1016/S0166-2481(97)80029-3

Vaezi AR, Ahmadi M, Cerdà A (2017) Contribution of raindrop impact to the change of soil physical properties and water erosion under

semi-arid rainfalls. Sci Total Environ 583:382–392. https://doi.org/10.1016/j.scitotenv.2017.01.078
Van Genuchten MT (1980) A Closed-form Equation for Predicting the Hydraulic Conductivity of Unsaturated Soils. Soil Sci Soc Am J 44:892–898. https://doi.org/10.2136/sssaj1980.03615995004400050002x
Wallace D, Almond P, Carrick S, Thomas S (2019) Targeting changes in soil porosity through modification of compost size and application rate. Soil Res 58(3):268–276. https://doi.org/10.1071/SR19170
Wang D, Lin JY, Sayre JM, Schmidt R, Fonte SJ, Rodrigues JLM, Scow KM (2022) Compost amendment maintains soil structure and carbon storage by increasing available carbon and microbial biomass in agricultural soil – A six-year field study. Geoderma 427:116117. https://doi.org/10.1016/j.geoderma.2022.116117
Warrick AW (1998) Appendix 1: Spatial variability. In: Hillel D (ed) Environmental Soil Physics. Academic PressSan Diego, USA, pp 655–675
Weber J, Karczewska A, Drozd J, Licznar M, Licznar S, Jamroz E, Kocowicz A (2007) Agricultural and ecological aspects of a sandy soil as affected by the application of municipal solid waste composts. Soil Biol Biochem 39:1294–1302. https://doi.org/10.1016/j.soilbio.2006.12.005

Heliyon 10 (2024) e35699

Contents lists available at ScienceDirect

Heliyon

journal homepage: www.cell.com/heliyon

Research article

Impact of vermicompost addition on water availability of differently textured soils

Mirko Castellini [a], Cristina Bondì [b,*], Luisa Giglio [a], Massimo Iovino [b]

[a] Council for Agricultural Research and Economics–Research Center for Agriculture and Environment (CREA–AA), Via C. Ulpiani 5, 70125, Bari, Italy

[b] Department of Agricultural, Food and Forest Sciences, University of Palermo, 90128, Palermo, Italy

ARTICLE INFO

Keywords:
Organic amendments
Soil water repellency
Soil bulk density
Soil water retention
Soil physical quality indicators
Pore volume distribution

ABSTRACT

Vermicompost is an organic material that is abundant in humic acids and nutrients. It is obtained through the bio-oxidation and stabilization processes carried out by earthworms. It has been proven to bring several benefits to different soil properties, including bulk density, soil structure, and plant available water capacity (*PAWC*). This investigation was conducted to fill the knowledge gap in some critical factors related to vermicompost application, specifically the short-term influence of a single vermicompost application with increasing doses on soil wettability and physical quality of differently textured soils. Water repellency of vermicompost and soil/vermicompost mixtures was investigated at different moisture contents by the water drop penetration time test, whereas physical quality was assessed by 35 soil indicators related to bulk density, soil water retention curve, and pore size distribution function.

Despite vermicompost showed from strong to severe hydrophobicity at moisture content lower than the field capacity, amended soils were at the most slightly water repellent thus indicating that, under field conditions, the hydrophobicity attributable to soil amendment with vermicompost could be considered negligible. Soil physical quality was effectively affected by vermicompost addiction with different outcomes depending on soil texture. Indicators linked to *PAWC* generally increased at increasing the vermicompost rate in the coarse soils whereas no significant effect was observed for intermediate and fine soils. For example, plant available water capacity of coarse-textured soils increased from an average initial value of 0.056 cm^3 cm^{-3} to an optimal value of 0.15 cm^3 cm^{-3} when a vermicompost addition dose of about one-third by volume (34 %) was applied. In the finest soil, drainable porosity significantly increased from an initial value of 0.09 cm^3 cm^{-3} to 0.23 cm^3 cm^{-3} when the maximum vermicompost dose (43 %) was applied thus indicating that amendment could be effective in enhancing water and air circulation.

1. Introduction

Soil organic matter is a dynamic soil component that represents a main source for several ecosystem services critically important for human well-being and nature conservancy [1]. It is well known that intensive agriculture can be a major cause of fertility loss and soil degradation [2]. By worsening the physical, chemical, biological, and ecological components of the soil, soil degradation implies an overall decline in soil quality and a possible consequent reduction in ecosystem functions and services [2,3]. Several technological

* Corresponding author.
E-mail address: cristina.bondi@unipa.it (C. Bondì).

https://doi.org/10.1016/j.heliyon.2024.e35699
Received 25 January 2024; Received in revised form 31 July 2024; Accepted 1 August 2024
Available online 3 August 2024

options were suggested in the literature for soil organic matter management and, therefore, for improving soil quality [4]. Practically, they consist of controlling the organic carbon losses by reducing soil erosion, decreasing leaching, and minimizing soil organic matter decomposition or, alternatively, increasing soil organic matter content through the use of amendments [4–6]. It has been widely proven that amendments have beneficial effects on soil quality and water availability, thus resulting in higher crop yields [7–9]. Depending on the agricultural sectors considered (i.e., conventional open-field or greenhouse agriculture) or plant type (food crops or ornamental plants), several organic soil amendments are available to increase soil water availability [10]. For example, coconut fiber, sphagnum, and peat represent the basis for substrates creation in nursery, and for high-income ornamental crops [11–13]. On the other hand, under extensive field crops, traditional amendments such as aged manure and compost, or more innovative ones such as biochar, are generally reported in the literature as effective in improving the physical-chemical soil properties [14–17].

Recently, the use of vermicompost as an organic soil conditioner has progressively increased also due to its contribution to sustainable management and recycling of organic waste [6–18]. Vermicompost, or called worm humus, is the product of the bio-oxidation and stabilization processes of organic material (e.g., food waste, horticultural waste, poultry droppings, food industry sludge, and so on) by earthworms, to obtain an organic material highly rich in humic acids and nutrients. In terms of benefits for crops, vermicompost is considered a sustainable source of macro- and micro-nutrients, because it is a source of mineral nutrient elements that are easily available for plants growth [19]. Application of vermicompost favored the survival of soil bacteria and actinomycetes and reduced the number of soil fungi [20]. Earthworms act as a natural bioreactor. Their activity stimulates the rate of decomposition of organic residues but, thanks to their motion into the soil, improves its structure and aeration, resulting in increased porosity, infiltration, and water retention [21,22]. Therefore, vermicompost is usually considered a natural and sustainable soil improver [23,24]. Several investigations reported the benefits of vermicompost application on different soil properties, including bulk density [25] or water use efficiency [26], but little literature has considered thoroughly the impact of vermicompost addition on soil water retention [27]. For two different soils, for example, Rivier et al. [28] evaluated the effect of compost and vermicompost addition on soil structure, soil water retention and water use efficiency. They reported that the application of both organic amendments improved soil water holding capacity, increased the macro-aggregates, and reduced soil bulk density, even at small application rates. Liu et al. [29] reported that vermicompost can significantly improve soil water permeability and retention thus ultimately improving the available water content.

Using vermicompost could be recommended to improve the water retention of coarse-intermediate textured soils or, more generally, to balance the water-to-air ratio in intermediate-fine textured ones [30]. However, to our knowledge, few in-depth evaluations of vermicompost effect on agricultural soils are available, and none of them aimed to compare the effects on contrasting soil texture. In fact, most studies have considered the impact on one-two soil's physical properties, e.g., stability of soil aggregates [31,32], bulk density [32–34] soil porosity [33–35] or water content at field capacity and wilting point [25–32], but there are no studies that simultaneously evaluated the effects on several physical soil properties as a function of both different soil textures and increasing amendment rates. A possible drawback of vermicompost amendment, not adequately considered in the available literature, could be related to the reduced soil wettability given it is commonly accepted that soil water repellency (SWR) is caused by organic compounds derived from living or decomposing plants or microorganisms [36]. However, the composition of organic matter rather than its total amount was found to influence SWR [37,38]. Furthermore, evaluating the short-term impact of amendment deserves interest given the soil wettability and the related physical properties can be modified, even immediately after vermicompost incorporation, with unpredictable effects on the soil hydrological processes. A simple assessment of SWR can be conducted by the water drop penetration time (WDPT) test which consists of placing a drop of water on the soil surface and measuring the time for it to penetrate [39]. Despite the WDPT test has been criticized [40,41] it still remains the most widely applied option for SWR assessment [42,43].

Evaluation of the effects of organic amendments on soil physical properties and water retention, can be made by estimating several soil indicators from the soil water retention curve [5,44–46]. For instance, Reynolds et al. [5] suggested using some capacity-based indicators accounting for the soil's ability to store and provide water and air to the crops, such as macroporosity, air capacity, relative field capacity, and plant available water capacity. On the other hand, when the entire soil water retention curve is available, it is possible to derive the pore volume distribution function and its related "location" and "shape" parameters [5]. The aforementioned soil physical indicators were widely and profitably used also to evaluate the impact of soil organic matter on the soil water retention of natural [15–45] and repacked [13–47] soil samples. A third approach for water retention curve analysis is based on the S-theory proposed by Dexter [44]. The S-index represents the magnitude of the slope of the soil water retention curve at the inflection point when such curve is expressed as gravimetric water content vs. the natural logarithm of the pressure head. According to Dexter [44], the inflection point should be able to discriminate the non-capillary from capillary porosity. Han et al. [48] suggested estimating some inflection point indicators from the soil water retention curve parameters expressed by the van Genuchten [49] model, including the effective porosity and a pore distribution index.

This investigation was conducted to evaluate the impact of increasing levels of vermicompost addition on the physical properties of five soils with different textures, from coarse to intermediate and fine. Specifically, hydrophobicity of vermicompost and soil/vermicompost mixtures was preliminarily evaluated in the range of moisture content from field capacity to oven-dry. Then, the impact of amendment rates up to about 50 % was evaluated in terms of modification of soil bulk density, water retention, and 15 indicators of soil physical quality. Therefore, the investigation structure can be summarized by the following steps: i) selection of five soils with different physical properties, with particular attention to the water retention capacity; ii) preparation of soil/vermicompost mixtures, until relatively high levels of soil amendment are achieved (0–43 %); iii) evaluation of soil/vermicompost mixtures effects on soil properties, including hydrophobicity, bulk density, macroporosity, air capacity, relative field capacity, plant available water capacity, indicators from the pore volume distribution function and from the inflection point of the water retention curve; iv) discussion about the practical impact of soil amendment on water availability for plants growth.

2. Material and methods

2.1. Soils and experimental materials

Five soils of different textures were collected in Sicily and Apulia, namely at Palermo Orleans (OR), Bari CREA (CR), Palermo Campus UNIPA (UN), Taranto Ginosa (GI) and Taranto Castellaneta (CA). Soil use of the selected fields was fallow, grass lawn, or orchard (Table 1). For each site, about 20 kg of soil was taken in the upper layer of soil profile (up to 20 cm) and stored in the laboratory, where it was air-dried and sieved to a diameter of 2 mm. Soils were characterized by standard laboratory techniques to determine the particle distribution [50] and the main chemical soil properties, including organic matter, pH, electrical conductivity, cation exchange capacity, and nitrogen content.

The vermicompost used in this investigation is a by-product of the digestion of cow manure by earthworms (*Eisenia foetida*) manufactured by CONITALO, Italian Lombrichi Breeding Consortium. The physico-chemical characteristics of the vermicompost were conducted using standard laboratory techniques. In particular, after oven dried at 70 °C for 24 h, vermicompost was grounded to pass a <1-mm sieve. Total organic carbon (TOC) and N contents were determined through the Dumas method (dry combustion method), using a CHNS Analyzer (Flash EA 1112-CHNS, Thermo Electron Corporation). For the determination of total contents of Ca, K, Mg, Na, P, Fe, Mn, Cu and Zn the samples were mineralized using microwave assisted pressure digestion and quantified by an ICP-OES optical spectrometer (Varian Inc., Vista MPX). The remaining parameters listed in Table 2 were retrieved from the manufacturer's technical sheet.

2.2. Soil/vermicompost mixtures

Soils and vermicompost were preliminary air-dried and sieved at 2-mm- sieve to remove coarse fragments and large vegetal residues and then mixed at 19 amendment different proportions by weight: 0 (i.e., soil without amendment), 0.5, 1, 2, 4, 5, 6, 6.5, 7, 8, 9, 10, 12, 13, 15, 17, 22, 33, 43 %. Therefore, a total of 95 repacked soil samples (19 concentrations x 5 soils) were prepared. Samples of each soil/amendment mixture were obtained by compacting into 5 cm diameter by 5 cm height metal cylinders a dry mass of the two constituents given by the following relationships [47]:

$$M_s = \frac{V\,\rho_{b,v}\rho_{b,s}}{\rho_{b,v} + r\rho_{b,s}} \tag{1}$$

$$M_v = rM_s \tag{2}$$

where M_v (g) and M_s (g) are the dry masses of vermicompost and soil, respectively, $\rho_{b,v}$ (g cm^{-3}) and $\rho_{b,s}$ (g cm^{-3}) are the dry bulk densities of the two constituents, V (cm^3) is the sample volume, and r is the ratio between dry masses of amendment and soil. Sample preparation was conducted by filling the cylinder with the mixture in four successive steps and, for each step, by lightly pressing the sample surface with a twisting motion using a pestle [47]. A flow chart explaining the procedural steps for determining soil physical quality indicators is reported in Fig. 1. Considering steps 1–3 of the flow chart (i.e., starting from the preparation of the samples, going through their saturation phase, and the subsequent water retention curve determination), the incubation time of soil samples was less than approximately two months. When transferred to field conditions, the amendment rates considered in this investigation corresponded to an air-dried vermicompost dose between 3-4 and 176–213 t ha^{-1}, depending on the considered soil, for an application depth of 5 cm.

Table 1
Sampling sites and main physical and chemical characteristics of the considered soils.

	OR	CR	UN	GI	CA
Site	Palermo Orleans	Bari CREA	Palermo Campus UNIPA	Taranto Ginosa	Taranto Castellaneta
Latitude, Longitude	38.107208N 13.349832 E	41.110366N 16.877836 E	38.107184N 13.351942E	40.461383N 16.84105 E	40.51246N 16.886826 E
Land use	Grass lawn	Fallow	Citrus orchard	Vineyard	Citrus orchard
Clay, Cl (%)	30	17	18	16	6
Silt, Si (%)	34	40	30	13	21
Sand, Sa (%)	36	43	52	71	73
Texture USDA	clay loam	loam	sandy loam	sandy loam	sandy loam
Texture group	fine	intermediate	coarse	coarse	coarse
Organic Matter, OM (%)	3.65	4.57	6.15	1.55	0.60
pH	7.69	7.53	7.99	7.90	7.35
EC (dS m^{-1})	0.29	0.42	0.34	0.13	0.20
CEC (cmol kg^{-1})	28.7	11.76	25.31	6.14	5.40
N (%)	0.21	0.24	0.32	0.099	0.029
C (%)	2.12	2.65	3.57	0.90	0.35
C/N ratio	10.10	11.04	11.16	9.09	12.07
WRB classification [51]	Chromic Cambisol (Loamic)	Chromic Cambisol (Loamic)	Terric Chromic Cambisol (Loamic)	Chromic Cambisol (Loamic)	Terric Chromic Cambisol (Loamic)

Table 2
Chemical characteristics of the considered vermicompost.

Water content (%)	Ash content (%)	pH (-)	EC (dS/m)	TOC (%)	N (%)	Ca (g/kg)	K (g/kg)	Mg (g/kg)	Na (g/kg)	P (g/kg)	Fe (g/kg)	Cu (mg/kg)	Mn (mg/kg)	Pb (mg/kg)	Zn (mg/kg)
7.6	56.7	7.5	3.1	19.7	15.6	39.9	15.2	12.7	3.7	9.5	14.2	67.0	718.4	*n.f.*	265.6

EC = electric conductivity; TOC = total organic carbon; N = total nitrogen; Ca = total calcium; K = total potassium; Mg = total magnesium; Na = total sodium; P = total phosphorus; Fe = total iron; Cu = total copper; Mn = total manganese; Pb = total lead; Zn = total zinc (*n.f.* = not found).

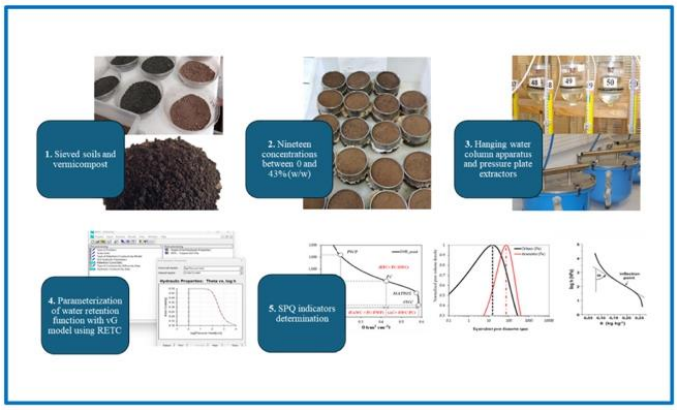

Fig. 1. Flow chart of the procedural steps for soil physical quality (SPQ) indicators determination: 1. Preparation of sieved soil and vermicompost, 2. Soil/vermicompost mixture in cylindrical samplers, 3. Soil water retention determination, 4. Parameterization of soil water retention function and 5. Determination of the three groups of SPQ indicators, i.e., capacitive indicators, location and shape parameters of pore volume distribution function, and related to the inflection point of soil water retention function.

2.3. Assessment of vermicompost wettability

The water drop penetration time (WDPT) test [36–50,52] was applied to evaluate the hydrophobicity of vermicompost at four reference water content values. Specifically, sieved vermicompost was compacted to a height of approximately 1 cm into metallic trays having dimensions of 10.5 × 17.0 cm^2. Two samples were established at air-dried (AD) and oven-dried (OD) conditions. In the latter case, the sample was dried for 24 h at 105 °C and then cooled for 2 h in a silica gel desiccator before conducting the WDPT test. Two samples were preliminary saturated and equilibrated into a pressure plate apparatus (Soil Moisture Equipment Corp., Santa Barbara, CA) at pressure head values of $h = -100$ and -15000 cm, i.e., at field capacity (FC) and permanent wilting point (WP). For each pressure head value, the soil water content was determined by the thermogravimetric method after subtracting the total weight of water added for the WDPT test. For each vermicompost sample, 20 drops of distilled water, each having a 60 ± 5 μL volume, were placed on the sample surface, and the time for complete infiltration was recorded. Drops were placed according to a square grid of 20 × 20 mm^2 by micropipette from a height of 10 mm to avoid excessive kinetic energy.

To evaluate the influence of vermicompost on the wettability of the amended soils, five 10.5 × 17.0 × 1.0 cm^3 repacked samples of air-dried soil/vermicompost mixtures at 43 % proportion by weight were prepared and the WDPT test conducted according to the same experimental procedure. Given all the considered soils were not hydrophobic under air-dried conditions (WDPT ≈ 0), only the highest concentration was considered to assess the maximum possible effect of vermicompost in trigging soil water repellency.

The SWR classification suggested by Bisdom et al. [53] was used to classify soils according to different WDPTs, that is < 5 s (wettable, W), 5–60 s (slightly hydrophobic, SLH), 60–600 s (strongly hydrophobic, STH), 600–3600 s (severely hydrophobic, SEH) and >3600 s (extremely hydrophobic, EXH). The repellency class was determined for each of the 20 droplets and the frequency distribution of the repellency classes for each sample was calculated [54].

2.4. Soil water retention curve and bulk density determination

Soil water retention curve in the range of soil pressure head (h) values $-100 \leq h \leq -5$ cm was determined by a hanging water column apparatus [55]. The apparatus consisted of a sintered porous plate with an air entry value of −200 cm connected to a graduated burette that may move vertically allowing to set different pressure head values and to measure the water drained from the sample. After preparation, each soil sample was placed on the porous plate surface and progressively wetted by capillary rise until full

saturation. Saturation was carefully completed in four successive equilibrium steps of 24 h each at h values of −20, −10, and −5 cm followed by sample submersion ($h = 0$). Then, the samples were subjected to a drainage cycle consisting of a sequence of 11 decreasing pressure head values ($h = -5$, −7.5, −10, −15, −20, −25, −30, −40, −50, −70, and −100 cm) and the volume of water drained into the burette at equilibrium recorded. The volumetric water content, θ ($cm^3\ cm^{-3}$), at each equilibrium stage was calculated by adding the drained volumes to the final θ value determined at $h = -100$ cm by weighting the sample after oven-drying at 105 °C for 24 h. The sample dry soil bulk density, ρ_b ($g\ cm^{-3}$) was also calculated from the oven-dried weight [56]. For each vermicompost/soil mixture considered, the water retention data at pressure heads in the range $-15000 \leq h \leq 330$ cm were determined in pressure plate extractors on three replicated samples of 5-cm-diameter by 1-cm-height [57]. Therefore, 15 pairs of volumetric soil water content-soil pressure head, θ-h values were measured for each soil/vermicompost mixture.

The unimodal van Genuchten (vG) water retention function [49] was fitted to the data by the RETC software [58]. To accurately estimate the water retention curve, model fitting was performed by optimizing all the parameters (i.e., θ_r, θ_s, α and n) of the vG model [59].

2.5. Soil physical quality indicators

Three groups of soil physical quality indicators, derived from the measured soil water retention curve, were considered in this investigation [15–50,52–60]. The first group consists of widely used soil indicators accounting for the soil's ability to store and provide water and air to the crops [5], such as macroporosity, air capacity, relative field capacity, and plant available water capacity. The second group includes "location" and "shape" parameters of the pore volume distribution function, as suggested by Reynolds et al. [5]. The third group includes indicators related to the inflection point of the water retention function: soil pressure head, soil water content, slope of the water retention curve, soil porosity, and pore distribution index. According to Dexter [44] and Han et al. [48], the inflection discriminates the non-capillary (macropores) from capillary porosity. Overall, a total of 15 soil indicators were therefore considered. The specific characteristics of the considered soil physical quality indicators are given below.

2.5.1. Capacitive-based indicators

Four capacitive indicators of soil physical quality, that account for the water-air ratio into the soil, were considered in this first group, namely macroporosity, P_{MAC} ($cm^3\ cm^{-3}$), air capacity, AC ($cm^3\ cm^{-3}$), relative field capacity, RFC, and plant available water capacity, $PAWC$ ($cm^3\ cm^{-3}$):

$$P_{MAC} = \theta_s - \theta_m \tag{3}$$

$$AC = \theta_s - \theta_{fc} \tag{4}$$

$$RFC = \frac{\theta_{fc}}{\theta_s} \tag{5}$$

$$PAWC = \theta_{fc} - \theta_{pwp} \tag{6}$$

where θ_s, θ_m, θ_{fc} and θ_{pwp} are the volumetric water contents ($cm^3\ cm^{-3}$) corresponding to a pressure head h = 0, −10, −100 and −15000 cm, respectively [5].

2.5.2. Pore volume distribution indicators

Location parameters (modal, d_{mod} (μm), median, d_{med} (μm), and mean, d_m (μm) diameters) indicative of central tendency, and shape parameters (standard deviation, SD (μm), skewness, Sk, and kurtosis, Ku) indicative of spread, asymmetry, and peakedness, respectively, of the soil pore volume distribution function, were calculated as follows [5]:

$$d_{mod} = \frac{2980\alpha}{m^{-1/n}} \tag{7}$$

$$d_{med} = \frac{2980\alpha}{\left(0.5^{-1/m} - 1\right)^{1/n}} \tag{8}$$

$$d_m = exp\left(\frac{\ln d_{0.16} + \ln d_{0.50} + \ln d_{0.84}}{3}\right) \tag{9}$$

$$SD = exp\left(\frac{\ln d_{0.84} - \ln d_{0.16}}{4} + \frac{\ln d_{0.95} - \ln d_{0.05}}{6.6}\right) \tag{10}$$

$$Sk = \frac{1}{2}\left[\frac{\ln d_{0.16} + \ln d_{0.84} - 2(\ln d_{0.50})}{(\ln d_{0.84} - \ln d_{0.16})} + \frac{\ln d_{0.05} + \ln d_{0.95} - 2(\ln d_{0.50})}{(\ln d_{0.95} - \ln d_{0.05})}\right] \tag{11}$$

$$Ku = \frac{\ln d_{0.05} - \ln d_{0.95}}{2.44(\ln d_{0.25} - \ln d_{0.75})} \tag{12}$$

where $m = 1–1/n$ and $d_{0.05}$, $d_{0.16}$, $d_{0.25}$, $d_{0.50}$, $d_{0.75}$, $d_{0.84}$, $d_{0.95}$, are equivalent pore diameters (μm) obtained from the capillary rise equation for given normalized water content values. The reader is referred to Reynolds et al. [5] for further details.

2.5.3. Inflection point indicators

Considering the vG model for the soil water retention curve, the soil parameters at the inflection point, i.e., pressure head value, h_{inf} (cm), water content, θ_{inf} (cm^3 cm^{-3}), slope of the water retention curve, S, porosity from saturation to infection point, POR_{inf} (cm^3 cm^{-3}) and pore distribution index, λ_{inf} were calculated according to Han et al. [48]:

$$h_{inf} = \frac{1}{\alpha}\left(\frac{1}{m}\right)^{\frac{1}{n}} \tag{13}$$

$$\theta_{inf} = (\theta_s - \theta_r)\left[1 + \frac{1}{m}\right]^{-m} + \theta_r \tag{14}$$

$$S = n(\theta_s - \theta_r)\left[\frac{2n-1}{n-1}\right]^{\left(\frac{1}{n-2}\right)} \tag{15}$$

$$POR_{inf} = \left(\theta_s - \theta_{inf}\right) \tag{16}$$

$$\lambda_{inf} = S/\theta_{inf} \tag{17}$$

2.6. Data analysis

For each soil, a linear regression analysis was performed between each considered soil variable and the vermicompost application rate, r. Specifically, the considered soil variables were: volumetric soil water content at selected pressure head values (i.e., θ_5, $\theta_{7.5}$, θ_{10}, θ_{15}, θ_{20}, θ_{25}, θ_{30}, θ_{40}, θ_{50}, θ_{70}, θ_{100}, θ_{330}, θ_{1030}, θ_{3060}, and θ_{15300}), parameters of vG model (θ_r, θ_s, α and n), soil bulk density (ρ_b), capacitive-based indicators (P_{MAC}, AC, RFC, $PAWC$), location and shape parameters of pore volume distribution function (d_{mod}, d_{med}, d_m, SD, Sk, Ku) and inflection point indicators (h_{inf}, θ_{inf}, S, POR_{inf}, λ_{inf}). Therefore, 175 correlations (35 soil indicators x 5 soils) were considered. The influence of vermicompost addiction was investigated by assessing the significance of the regression coefficients between the considered soil variables and the vermicompost to soil ratio, r ($p = 0.05$). Furthermore, for the significant correlations, the range of variability of each considered variable was calculated in the range between zero (non-amended soil or control) and the maximum vermicompost application rate (i.e., $r = 43$ %).

3. Results

3.1. Soil and vermicompost characteristics

According to the USDA classification, the five soils were sandy-loam (Castellaneta, CA, Ginosa, GI, and UNIPA, UN), loam (CREA, CR), and clay-loam (Orleans, OR) (Table 1). The percentage of fine particles, i.e., the sum of clay and silt content, ranged from 26 to 64 % following the order CA < GI < UN < CR < OR. According to common and practical criteria for soil textural grouping e.g., [61], three soils (CA, GI, UN) were coarse-textured soils and the remaining intermediate (CR) or fine (OR) textured soils. The selected soils belong to the Reference Soil Group of the Chromic Cambisols, according to the classification of the IUSS WRB Working Group [62].

Overall, the soils had very low organic matter (OM) contents (Table 1). With the only exception of the coarse soil at the UN site (OM = 6.14 %), the coarse soils showed lower organic matter contents (OM = 0.6–1.6 %) than the intermediate-fine soils (OM = 3.7–4.6 %). According to literature references suggesting a lower critical threshold of OM equal to 4 %, and optimal values in the range of 5–9% [5, 51], only UN and CR soils had adequate levels of organic matter, while the other soils were poorly rated. The soil pH ranged from neutral to moderately alkaline (7.3–8.0) and electrical conductivity was in general very low (<0.42 dS m^{-1}).

The vermicompost had levels of moisture and ash contents of 7.6 and 56.7 %, respectively, and a pH of 7.5; also, TOC and N contents were equal to 20 % and 16 %, respectively (Table 2). Therefore, due to oxidative processes, it has lost some organic matter, as compared both to the values reported in the manufacturer's technical sheet and the references (i.e., European standard NF U44-051 sets minimum thresholds of C/N at 8 and dry matter at 30 %). In accordance with the European law for "organic soil improvers-designations, specifications and marking", threshold limits for metallic trace elements (e.g., Cu and Pb) were always below the limits (Table 2). Likewise, P, K, and N were lower than the references, i.e., not higher than 3 % [24].

3.2. Influence of vermicompost on soil wettability

For the vermicompost, the median water drop penetration time was minimum at field capacity (FC) (WDPT = 3 s) and maximum under air-dried (AD) conditions (WDPT = 778 s). Intermediate median values of WDPT were obtained at permanent wilting point (WP) (WDPT = 169 s) and after oven-drying (OD) (WDPT = 250 s) (Table 3). According to the soil water repellency classification by Bisdom

et al. [53], 95 % of the individual WDPT values fell in the non-repellent class (WDPT <5 s) when the vermicompost was wetted at FC (h = −100 cm) (Fig. 2a). Vermicompost wettability decreased at WP (h = −15000 cm), given all individual droplets fell in the strongly hydrophobic class (60 ≤ WDPT <600 s), and was minimum for AD in which 95 % of the droplets showed severe hydrophobicity (600 ≤ WDPT <3600 s). Therefore, our results agree with literature that generally reported that dry soils exhibit the highest level of SWR whereas, above a critical moisture content, soils appear to be wettable [63]. In the case of vermicompost, the critical moisture threshold is located between FC and WP. It is not surprising that under OD condition vermicompost hydrophobicity was lower than under AD one. Indeed, it is likely that the organic matter content was partially volatilized during oven-drying treatment thus resulting in a lower hydrophobicity. For instance, reusing the same sample after oven-drying at 105 °C resulted in a decrease of the soil water repellency of two forest soils with similar OM content [54].

The median WDPT of soil/vermicompost mixtures ranged from 9 s (CA) to 33 s (OR) and generally increased following the same order of the percentage of fine particles, i.e. CA < UN < GI < CR < OR (Table 3). According to Bisdom et al. [53] classification, 100 % of the individual WDPT values for all the considered soils fell in the slightly repellent class (Fig. 2b). Therefore, addiction of vermicompost at the highest proportion rate determined the occurrence of a limited hydrophobicity in the tested soils. However, given the water repellency of vermicompost was maximum under air-dried conditions and declined as the vermicompost wetted, it can be argued that, under normal operative conditions, i.e., for lower vermicompost proportions and higher soil water contents, the hydrophobicity attributable to soil amendment with vermicompost could be considered negligible.

3.3. Vermicompost effects on water retention curve parameterization and soil bulk density

The vG unimodal model for the water retention curve adequately fitted the experimental data, with maximum average error (MAE) and root mean square error (RMSE) that were in the range 0.005–0.0022 $cm^3\ cm^{-3}$ for MAE, and 0.010–0.0018 $cm^3\ cm^{-3}$ for RMSE. Practically, individual maximum discrepancies between measured and estimated values were at most equal to 0.04 $cm^3\ cm^{-3}$ (only at a single soil pressure head value for UN).

For each considered soil and amendment rate, the results of water retention curves parameterization, carried out with vG model, are reported in Fig. 3. As expected, the retention curve scale parameter, n, of non-amended (control) soils increased from finer to coarser soils, ranging from 1.38 (OR) to 2.06 (GI). No particular trend was observed for θ_s, θ_r, and α parameters of control soils even if the former increased, as expected, from coarse soils to intermediate ones. The residual water content, θ_r, should be considered as a fitting parameter without a clear physical meaning.

Regardless of the considered soil, θ_r and θ_s significantly increased as the vermicompost to soil ratio increased, with determination coefficients (R^2) of the regression lines that generally increased from finer to coarser soils (Fig. 3). The same increasing and significant trend was detected for the α parameter of CA and GI soils but not for the other soils. Both increasing and decreasing trends, depending on the soil texture class, were obtained for n parameter (Fig. 3). A singular feature was observed for this parameter with a significantly increasing (o decreasing) trend for vermicompost concentrations up to about 15–17 % (R^2 = 0.86–0.88) followed by a plateau that highlights how higher vermicompost concentrations were no more effective in modifying the shape of the water retention curve. It was therefore concluded that vermicompost amendment had a significant general effect on the water retention curve of the considered soils.

A highly significant decreasing relationship between soil bulk density (ρ_b) and vermicompost to soil ratio was observed for the five soils with coefficients of determination in the range of 0.80–0.95 (Fig. 4). The soil ρ_b decrease is an expected consequence of the lower weight of the amended soils when an increasing percentage of vermicompost (ρ_b = 0.409 g cm^{-3}) is added.

The volumetric water content generally increased with increasing the vermicompost dose with the only exception of the OR soil at very low soil pressure head values (i.e., between −330 and −15300 cm), where a decreasing trend was detected. Table 4 reports the coefficients of determination for the linear regressions between the volumetric water content, θ, at three reference values of applied pressure head (h = −10, −100, and −15000 cm) and the vermicompost to soil ratio, r. The generally observed positive correlation between θ and r highlights that the vermicompost addiction was effective in increasing the water retained by the soils. The reliability of the regression model was affected by soil texture and the considered pressure head value, given the coefficients of determination changed depending on these variables (Fig. 5). On average, the coefficients of determination were highest for CA and lowest for UN soils (i.e., 0.73 and 0.13, respectively). A minimum R^2 value was always detected that fell in the range from −20 to −100 cm of soil water pressure head (Fig. 5a). According to capillary law, this range of h corresponds to the size of the largest pores that are full of

Table 3
Statistics of water drop penetration time, WDPT, test (s), of vermicompost at different reference water content and the soil/vermicompost mixture at 43 % proportion by weight (OD = oven dried; AD = air dried; WP = wilting point; FC = field capacity; OR = Orleans; CR = CREA; UN = Campus UNIPA, GI = Ginosa; CA = Castellaneta).

	Vermicompost				Soil/vermicompost mixtures				
	OD	AD	WP	FC	OR	CR	UN	GI	CA
min	182	588	90	2	25	16	6	12	8
max	369	888	527	7	44	27	15	16	11
mean	256	756	210	3	34	21	11	14	9
median	250	778	169	3	33	19	11	14	9
CV%	22	12	64	37	18	17	25	11	12

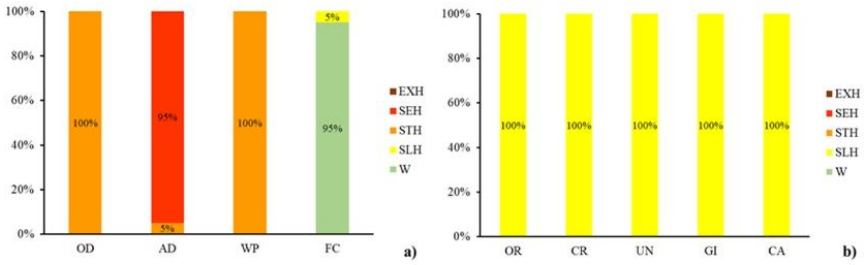

Fig. 2. Classification of SWR for a) the vermicompost at different reference water contents and b) the soil/vermicompost mixtures at 43 % proportion by weight (W = wettable; SLH = slightly hydrophobic; STH = strongly hydrophobic; SEH = severely hydrophobic; EXH = extremely hydrophobic; OD = oven dried; AD = air dried; WP = wilting point; FC = field capacity; OR = Orleans; CR = CREA; UN = Campus UNIPA, GI = Ginosa; CA = Castellaneta).

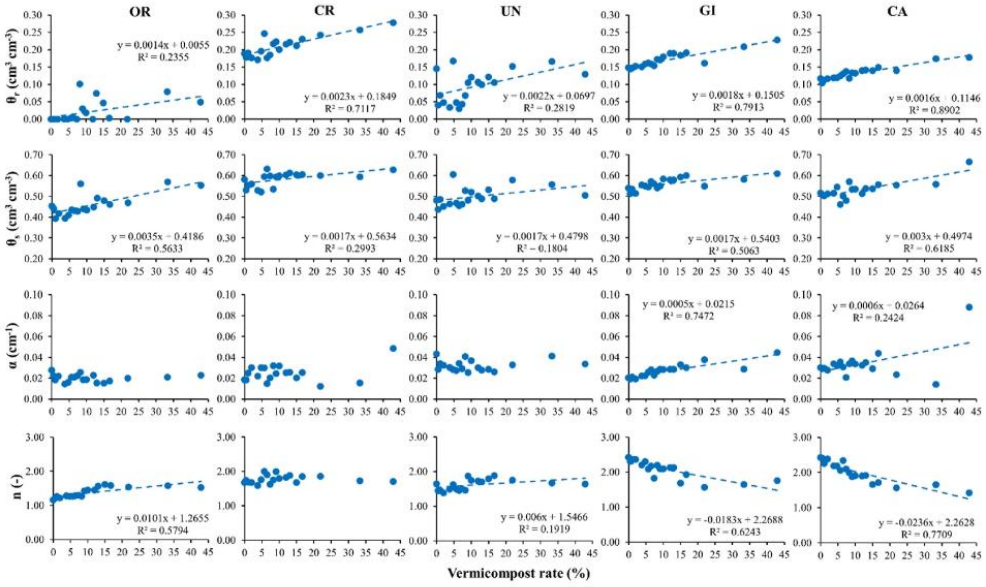

Fig. 3. Linear correlation between parameters of water retention curve vG model and vermicompost application rate. For a given soil and vG-parameter, only significant regression lines were depicted (p = 0.05) (OR = Orleans; CR = CREA; UN = Campus UNIPA, GI = Ginosa; CA = Castellaneta).

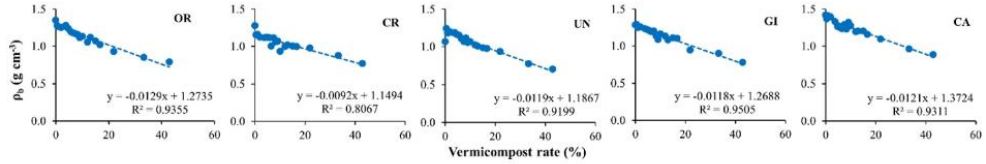

Fig. 4. Linear regressions between soil bulk density (ρ_b) and vermicompost application rate. For a given soil, significant regression lines were depicted (P = 0.05) (OR = Palermo Orleans; CR = Bari CREA; UN = Palermo Campus UNIPA, GI = Taranto Ginosa; CA = Taranto Castellaneta).

water between 30 and 150 μm thus indicating that vermicompost addiction is less effective in determining modification of water retention in this pore size class. The pressure head h value corresponding to the minimum R^2 value increased as the clay content of soil increased (but similar findings were obtained when the percentage of fine particles was considered), suggesting that the effectiveness of vermicompost addiction also depended on the soil texture (Fig. 5b).

3.4. Vermicompost effects on soil physical quality indicators

3.4.1. Capacitive-based indicators

For coarse (GI and CA) and fine (OR) soils, macroporosity (P_{MAC}) significantly increased as the vermicompost dose increased while no trend was observed for the remaining soils (CR and UN) (Table 5). The increase in soil macroporosity was larger for coarse than fine soils, given P_{MAC} increased from 0 to 0.03 $cm^3\ cm^{-3}$ and from 0.01 to 0.05 $cm^3\ cm^{-3}$ for GI and CA, respectively, as a consequence of vermicompost addiction at a rate of 43 % while, for the same application dose, the increase in P_{MAC} was only of 0.004 $cm^3\ cm^{-3}$ for OR soil.

Vermicompost amendment determined an increase in air capacity (AC) for OR and UN soils and a decrease in AC for CA soil (Table 5). The increase in soil air capacity was larger for the fine OR ($\Delta_{AC} = 0.14\ cm^3\ cm^{-3}$) than the coarse UN soil ($\Delta_{AC} = 0.05\ cm^3\ cm^{-3}$). The capacity-based indicators P_{MAC} and AC (eqs. (3) and (4)) are expressive of the water retained in pores with equivalent diameter higher than, respectively, 300 and 30 μm. Therefore, vermicompost addiction was effective in increasing the relative volume of both the porosity classes in the fine OR soil, of only the smaller porosity class in the intermediate UN soil, whereas it increased the larger class (P_{MAC}) and decreased the smaller one (AC) in the coarse CA soil. Independently of the statistical significance, it is worth noting that P_{MAC} trend was always positive with r, i.e., it increased with vermicompost addiction, whereas the AC trend inverted its sign in the passage from fine to coarse soils. Indeed, the highest positive correlation coefficient was obtained for OR soil (percentage of fine particles, Si + Cl = 64 %) and the lowest negative correlation coefficient for CA soil (Si + Cl = 26 %) (Table 5).

The relative field capacity (RFC; eq. (5)) significantly increased with vermicompost for the coarse soils (CA, GI) and significantly decreased for the fine one (OR), showing no trend for the remaining soils. Modeled data suggested that RFC increased from 0.41 to 0.72 for CA and from 0.52 to 0.63 for GI, while it decreased from 0.78 to 0.57 for OR. Considering that the optimal balance between the root-zone soil water capacity and the soil air capacity occurs in the range $0.6 \leq RFC \leq 0.7$ [64], amendment with vermicompost resulted effective in correcting the water-limited or the air-limited conditions occurring, respectively, in coarse and fine soils.

Plant available water capacity ($PAWC$; eq. (6)) significantly increased only for coarse soils (GI and CA) with a more marked effect on the coarsest soil given that, compared to the control, $PAWC$ increased by 0.24 $cm^3\ cm^{-3}$ (Table 5). The ideal condition for maximal root growth and function corresponds to $PAWC \geq 0.20\ cm^3\ cm^{-3}$ [64]. Thus, vermicompost amendment yielded a remarkable improvement of the soil physical quality classification according to this indicator that shifted from "poor" ($PAWC < 0.10\ cm^3\ cm^{-3}$) to optimal for coarse-textured soils.

3.4.2. Pore volume distribution indicators

The location parameters of the pore volume distribution function, d_{mod}, d_{med} and d_m (eqs. (7)–(9)), always increased significantly with the vermicompost rate for OR and UN soils; the former soil showed the largest increments in d_{mod}, d_{med} and d_m, that increased by a factor 2, 6 and 10, respectively, from $r = 0$–43 % (Table 5). The opposite result was found for the CA soil that showed d_{med} and d_m values that significantly decreased with the vermicompost rate and a negative, but not significant, trend for d_{mod}. No correlation was in general observed between the location parameters and r for the CR and GI soils. Lastly, d_{mod} always significantly increased, except for CA and CR soils for which a significant relationship was not observed (Table 5). The effect of vermicompost addiction on shape indicators SD and Sk (eqs. (10) and (11)) agreed with those obtained for capacitive indicators, with an opposite behaviour between coarse and fine soils (Table 5). Finally, kurtosis (Ku; eq. (12)) was found to significantly increase for the two coarsest soils (GI and CA) while no significant relationships were observed for the other soils (CR, UN and OR).

In agreement with the optimal values proposed in the literature for these indicators [5], results suggested that improvements in modal diameter were obtained only for coarse soils (UN and GI) because d_{mod} exceeded the suggested minimum optimal value of 60 μm only when the highest dose was applied. The other indicators related to central values of the pore size distribution (d_{med} and d_m) generally exceeded the literature references suggested for agricultural soils [5]. Parameter SD quantifies the size range of equivalent pore diameters, i.e., the sorting of pore diameters, with $SD = 1$ indicating no variation in pores diameter (pores with the same size). Therefore, increasing SD indicates an increasing range in pore diameters [5]. This occurred only for coarse soils (GI and CA), while the opposite result was detected for UN and OR sites. Negative Sk values indicate a pore size distribution shifted to small pores whereas positive Sk values shifted to large pores. Therefore, the observed significant correlations suggested that the addition of vermicompost

Table 4
Coefficients of determination (R^2) for the correlations between modeled soil water retention values and vermicompost application doses for three selected pressure head values corresponding to matrix capacity (θ_{10}), field capacity (θ_{100}) and permanent wilting point (θ_{15300}). R^2 values with the minus sign indicate decreasing correlations. The significant correlations were marked with asterisks (**p < 0.01; *p < 0.05).

	Orleans (OR)	CREA (CR)	UNIPA (UN)	Ginosa (GI)	Castellaneta (CA)
θ_{10}	0.5597**	0.2255*	0.1795	0.3188*	0.5566**
θ_{100}	0.0013	0.1862	0.0200	0.6316**	0.8263**
θ_{15300}	−0.1498	0.7486**	0.2450*	0.8584**	0.9580**

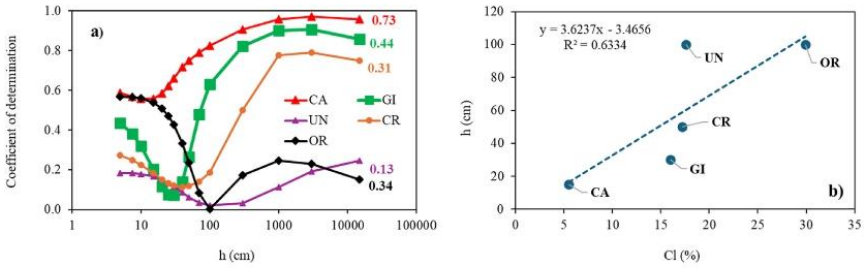

Fig. 5. Values of the coefficient of determination (R^2) for the linear regression between soil water content and vermicompost application rate as a function of soil pressure head values h (a) (curve labels indicate the mean R^2 over the entire h range), and relationship between the h values corresponding to the minimum R^2 values in figure a) and the soil clay fraction (Cl) (b) (OR = Orleans; CR = CREA; UN = Campus UNIPA, GI = Ginosa; CA = Castellaneta).

Table 5
Coefficients of determination (R^2) for the correlation between soil physical indicators and vermicompost rate. R^2 values with the minus sign indicate decreasing correlations. The significant regressions were marked with asterisks (**p < 0.01; *p < 0.05). For each significant regression, the calculated values between minimum and maximum vermicompost concentration (r = 0 and 43 %) are reported in brackets.

	Orleans (OR)	CREA (CR)	UNIPA (UN)	Ginosa (GI)	Castellaneta (CA)
P_{MAC} (cm^3 cm^{-3})	0.2525* (0.01–0.014)	0.1170 (n.a.)	0.0115 (n.a.)	0.7809** (0–0.03)	0.3924** (0.01–0.05)
AC (cm^3 cm^{-3})	0.8542** (0.09–0.23)	0.0001 (n.a.)	0.2652* (0.20–0.25)	−0.0621 (n.a.)	−0.2813* (0.29–0.18)
RFC (−)	−0.6625** (0.78–0.57)	0.0266 (n.a.)	−0.1394 (n.a.)	0.3424** (0.52–0.63)	0.5933** (0.41–0.72)
$PAWC$ (cm^3 cm^{-3})	0.0013 (n.a.)	0.1862 (n.a.)	0.0200 (n.a.)	0.6316** (0.08–0.18)	0.8263** (0.002–0.24)
d_{mod} (μm)	0.7747** (16–38)	0.0787 (n.a.)	0.2138* (46–65)	0.3833** (50–72)	−0.0005 (n.a.)
d_{med} (μm)	0.7554** (4–26)	0.0681 (n.a.)	0.2705* (28–49)	0.0251 (n.a.)	−0.3511** (61–28)
d_m (μm)	0.7454** (2–21)	0.0615 (n.a.)	0.2709* (22–42)	−0.0018 (n.a.)	−0.5343** (57–18)
SD (−)	−0.2116* (62 to −36)	−0.0126 (n.a.)	−0.2446* (13–8)	0.5222** (3–6)	0.8521** (2–9)
Sk (−)	0.5755** (−0.6 to −0.3)	0.0059 (n.a.)	0.2223* (−0.4 to −0.3)	−0.5953** (−0.2 to −0.4)	−0.8699** (−0.2 to −0.5)
Ku (−)	0.0346 (n.a.)	−0.0035 (n.a.)	−0.1868 (n.a.)	0.6153** (1.13–1.15)	0.8145** (1.13–1.16)
h_{inf} (cm)	−0.6001** (181–50)	−0.0002 (n.a.)	−0.2616* (66–43)	−0.2929* (59–41)	0.1569 (n.a.)
θ_{inf} (cm^3 cm^{-3})	0.8326** (0.22–0.46)	0.3911** (0.35–0.62)	0.7913** (0.26–0.54)	0.9300** (0.28–0.57)	0.8492** (0.23–0.52)
S (−)	0.9123** (0.04–0.18)	0.2202* (0.10–0.14)	0.7288** (0.08–0.17)	−0.0514 (n.a.)	−0.2518* (0.13–0.10)
POR_{inf} (cm^3 cm^{-3})	−0.0182 (n.a.)	<0.0001 (n.a.)	−0.0584 (n.a.)	−0.3351** (0.37–0.32)	−0.3972** (0.35–0.31)
λ_{inf} (−)	0.5791** (0.22–0.51)	0.0026 (n.a.)	0.1968 (n.a.)	−0.6231** (0.81–0.38)	−0.7850** (0.81–0.24)

P_{MAC}, macroporosity; AC, air capacity; RFC, relative field capacity; $PAWC$, plant available water capacity; d_{mod}, modal diameter; d_{med} median diameter; d_m, mean diameter; SD, standard deviation, Sk, asymmetry, Ku, kurtosis of soil pores distribution; h_{inf}, soil pressure head at the water retention curve inflection point; θ_{inf}, soil water content at the inflection point; S, Dexter's S index; POR_{inf}, soil porosity at the inflection point; λ_{inf}, pore distribution index.

improved the relatively higher proportion of larger pores of UN and OR soils (Table 5). It is interesting to note that, for OR soil, a threshold behaviour was identified because, starting from a value of −0.65 (control), Sk values linearly increased to about −0.37 (vermicompost rate of about 17 %) to remain stable up to the highest vermicompost concentrations. Since this value approached the optimal values suggested for this soil indicator (Sk = −0.43 to −0.41), the positive impact of the amendment is confirmed. The pore distributions were leptokurtic (Ku > 1) for coarse soils (GI and CA), namely more peaked in the center and more tailed in the extremes than the lognormal curve [5], with Ku values that were optimal (Ku = 1.13–1.14) approximately up to 20 % of vermicompost rate, depending on the considered soil.

3.4.3. Inflection point indicators

Soil pressure head, h_{inf} (eq. (13)), at the inflection point of the water retention curve decreased significantly as the vermicompost rate increased for GI, UN, and OR, while no trend was observed for the other soils. In particular, greater changes were detected for the fine (about 130 cm) than coarse or intermediate (about 20 cm) textured soils (Table 5). Similarly to the θ-h results earlier reported, the water content θ_{inf} corresponding to the inflection point (eq. (14)) always significantly increased with vermicompost rate. According to the soil texture, the improvements in estimated θ_{inf}, i.e., differences between max and min values, increased from fine soils ($\Delta_{\theta inf}$ = 0.24 cm^3 cm^{-3} for OR), to intermediate ($\Delta_{\theta inf}$ = 0.27 and 0.28 cm^3 cm^{-3}, respectively, for CR and UN) to coarse soils ($\Delta_{\theta inf}$ = 0.29 cm^3 cm^{-3} for both CA and GI); this confirms that the assumed sequence for soil texture groupings reasonably explains the effects of vermicompost addiction with the higher improvements observed for coarse soils (Table 5). The slope of the water retention curve at the inflection point (eq. (15)), increased as the vermicompost rate increased for OR, CR and UN and decreased only for CA soil. It is worth noting that the regression equation shifted its slope by increasing the fine particle content from significantly negative (R^2 = 0.25) for CA to significantly positive (R^2 = 0.91) for OR (Table 5). Soil porosity from saturation to infection point, POR_{inf} (eq. (16)) significantly

decreased as the vermicompost rate increased only for the coarsest soils (GI and CA), suggesting an impoverishment in soil porosity (up to 4–5%) when these soils amended with the highest dose of vermicompost. The pore distribution index, λ_{inf} (eq. (17)), significantly decreased with the vermicompost rate for coarse soils (GI and CA) and increased significantly for fine (OR) soil (Table 5). In agreement with the coarse texture of the GI and CA soils, λ_{inf} started from a common value of 0.81 for the control ($r = 0$), to reach 0.38 or 0.24 for GI and CA, respectively, when amended at $r = 43$ %. Overall, references of literature for this indicator suggest that it may decrease from coarser to finer sandy soils [48]. Therefore, a decrease of λ_{inf} as a function of amendment rate appears plausible, as a consequence of the reduction in soil porosity. On the other hand, for the fine OR soil λ_{inf} significantly increased from 0.22 of the control to 0.51 at $r = 43$ %. It is worth noting that the pore distribution index of a not amended fine soil could be comparable with that of sandy soil amended at the higher vermicompost concentrations, as very similar results were detected between CA and OR (Table 5).

4. Discussion

According to literature findings, vermicompost addition can significantly mitigate the loss of organic carbon due to soil tillage [65]. However, the scientific literature relating to this soil amendment is particularly lacking regarding the overall effect on the main soil physical and hydraulic properties, and a very limited literature reports its effects in the short-term. Specifically, most studies have considered one or, at the most, two soil properties (i.e., bulk density, porosity, or aggregates stability), but there are no studies that simultaneously evaluated the effects on several soil physical properties as a function of both different soil textures and increasing amendment rates. For instance, Albiach et al. [31] evaluated the effect of 2.4 t ha^{-1} yr^{-1} of a commercial vermicompost on the aggregates structural stability of a medium textured soil. They found that vermicompost did not produce any significant change in stability of soil aggregates, suggesting that rates recommended by the producers are too low to be effective. Arabi et al. [34] evaluated the effects of 2–6 t ha^{-1} of vermicompost on the bulk density of a silty clay loam. According to their results, vermicompost significantly improved the soil bulk density (already at the minimum rate of 2 t ha^{-1}) and enhanced the water retention in aggregates compared with the not amended soil. Mengistu et al. [33] studied the effects of 3.7–15 t ha^{-1} of vermicompost on the bulk density and porosity of a sandy clay loam. The independently determined soil bulk density and porosity tended to decrease and increase, respectively, with an increased rate of vermicompost application. However, such response was significant only when the vermicompost was applied at a relatively higher rate ($\geq$11.25 t ha^{-1}). Consistent effects on soil porosity were reported by Azarmi et al. [35] for a loamy soil amended with rates of 5–15 t ha^{-1}. Baghbani-Arani et al. [25] concluded that the treatments with vermicompost (2.7 t ha^{-1}) were able to alleviate water deficit stress. Vermicompost improved the biological yield of fenugreek by improving the physicochemical conditions of the soil (e.g., water contents at field capacity and wilting point), especially in the water deficit stress conditions, thus reducing the usage of chemical fertilizers in line with the goals of sustainable agriculture. An investigation on the effects of vermicompost on multiple soil variables (i.e., water holding capacity, infiltration rate, bulk density, aggregate stability, and water use efficiency) for a sandy clay loam soil was conducted by Sharma et al. [32], although they considered a biochar-vermicompost mixture for which the vermicompost rate was selected only according to the recommended nitrogen dose.

Evaluating the short, or very short-term, effects of soil amendment could be decisive for water availability assessment in arid environments or, more generally, during prolonged dry periods. However, although the medium-long-term effect on soil physical and hydraulic properties is well documented, as reported for example by the review of Kranz et al. [6], the short-term impact has been poorly considered. For example, Black et al. [66] reported that the effect on *PAWC* should be assessed within a few months of implementation. Indeed, they studied the effects of compost at several application rates and showed that the *PAWC* of amended plots was greater than not amended plots, but much of such increase was lost within about 6 months. Even shorter response times were sometimes considered when the effect on soil bulk density was studied [6]. For instance, Somerville et al. [67] compared the amendment effects on three textured soils after 3 months, showing a reduction in bulk density values of 15–25 % in amended soils. A significant reduction of bulk density after 7 months of investigation was reported by Mohammadshirazi et al. [68] when they compared tillage with and without compost application to a compacted control soil. Consequently, the present research accounts for the effects on multiple soil indicators in the very short-time after amendment (<1–2 months), providing findings that fill a gap of knowledge in this field of research.

Generally, the agronomic practice aimed at improving the soil physical properties using organic amendments also considers the induced effects on soil fertility. In this case, the amendment rate for field application is more calibrated to improve the availability of chemical elements than to improve the soil physical properties. For instance, Khalifa et al. [30] applied 5 and 10 t ha^{-1} of vermicompost to reduce the water stress impact on some soil properties and on water productivity in terms of barley yield. The results showed that vermicompost improved the physical and chemical properties of soils, as compared with compost, because soil bulk density decreased by 2.2 %; also, there was a significant increase in soil organic carbon, available nitrogen, and field capacity by 44 %, 14 %, and 19 %, respectively [30]. However, to our knowledge, the amendment rate is never diversified according to the considered soil texture or the expected effects. In their review on the effects of compost incorporation on soil physical properties in urban soils, Kranz et al. [6] emphasized the fact that, among the current research gaps on this topic, the rates and depths of compost incorporation were not experimentally determined or optimized using laboratory or field experiments.

In this investigation we considered two of the most critical experimental factors reported in the literature, namely the soil texture and the amendment rate, to investigate the vermicompost effects on the soil water/air relationship and learn from the findings obtained how far the estimates suggested for field amendments differ from those obtained in the laboratory. Since compost can have hydrophobic behaviour, the amendment effects on the soil retention were evaluated in the very short-term, especially to account for the possible negative implications when periods of prolonged dryness occur.

The selected soils included three relatively coarse-textured (sandy loam) soils (i.e., sand content between 53 and 74 %), as such

soils are the most deficient in water retention and, consequently, they could mostly benefit from amendment. The minimum level of *PAWC* should be at least equal to 0.15 $cm^3\ cm^{-3}$ [5], being considered "poor" or "arid" those soils that can store, and provide, less than 0.10 $cm^3\ cm^{-3}$ of water to plant roots. The three sandy loam soils had poor characteristics as, on average, they had *PAWC* of about 0.056 $cm^3\ cm^{-3}$ far below the optimal range (Fig. 6). This means that, referring to rainfed agriculture, they would need a vermicompost addition dose of about one-third by volume (34 %) in the root zone to reach the goal of $PAWC = 0.15\ cm^3\ cm^{-3}$. Conversely, incorporating an average vermicompost amount of 15 t ha^{-1}, as suggested in many applications, would not have a substantial impact, as *PAWC* would increase only by about 0.066 $cm^3\ cm^{-3}$ (Fig. 6).

Reynolds et al. [5] applied 75 e 300 t ha^{-1} of compost in the first 10 cm of a clay loam soil to assess the impact in terms of physical quality and productivity. Regarding *PAWC*, they showed a lack of improvement ($PAWC = 0.13\ cm^3\ cm^{-3}$) when they considered the lowest amendment rate and an optimal improvement ($PAWC = 0.22\ cm^3\ cm^{-3}$) when considered the highest level. Compared to the control, the maize yield increased, respectively, by 1.4 or 2.1 t ha^{-1} when the lowest and highest compost rates were added [5].

Our laboratory data for the sandy loam soils agreed with those by Reynolds et al. [5] because, concerning the first 5 cm of the soil, it is expected to reach an acceptable level of *PAWC* by implementing about 146 t ha^{-1} of vermicompost. However, such effect of organic amendment should be limited to a soil condition shortly after the main tillage, because the effect due to soil consolidation was not considered in this investigation. Moreover, such estimation does not take into account the effect of hysteresis of the soil water retention curve. For the UN sandy loam soil, Bondì et al. [47] showed that *PAWC* is strongly influenced by hysteresis with an average *PAWC* value measured during the drainage that was 112 % higher than during wetting. Therefore, this effect could be easily considered by determining, for example, the mean changes between the two main processes.

As expected, different soil physical quality parameters were affected by vermicompost addiction in the fine OR soil. The macropore and drainable porosity increased as also confirmed by the central diameters of the pore size distribution function. Conversely, the *PAWC* was practically unaffected. The decrease of *SD* and *Ku* and the shift of *S* highlighted that the pore size distribution tended to become more uniform and skewed towards the larger pore diameters. The physical quality of the intermediate CR soil was minimally affected by the vermicompost amendment. Therefore, the results unequivocally show that vermicompost influenced different soil physical qualities depending on the soil texture, i.e., mostly water availability for plants in sandy loam soils and water/air circulation capacity in clay loam soil. For the intermediate loam CR soil, addiction of vermicompost was less effective, and further investigation is needed in these soils.

Another point that deserves further investigation is related to the temporal persistence of the amendment benefits. Overall, a reduction in the soil water retention in larger pores could be expected some months (between 6 and 12) after organic amendment, as reported for both coarse [69] and fine [15] textured soils. In both cases, soil reconsolidation determined an increase of soil bulk density with a corresponding decrease of the capacitive indicators related to drainable porosity (*AC* and P_{MAC}) and an increase of those related to water availability for plants (*PAWC*). Consistent results were obtained also with specific reference to the GI soil amended with 5 % vermicompost (unpublished data). In this case, nine months after amendment, soil water content significantly reduced by 6 % at saturation and 5 % at field capacity, thus determining a reduction of *AC* (from 0.02 to 0.01 $cm^3\ cm^{-3}$) and P_{MAC} (from 0.26 to 0.25 $cm^3\ cm^{-3}$), and an increase of *PAWC* (from 0.16 to 0.24 $cm^3\ cm^{-3}$).

5. Conclusions

The application of vermicompost can effectively improve the physical quality of soils in terms of increased plant water availability and equilibrate air-to-water ratio in the root zone. However, a possible drawback of vermicompost amendment could be related to the induced soil hydrophobicity.

Despite being the subject of several studies, thorough evaluations of the impact of vermicompost addition on the soil hydrophobicity and water retention under different application rates and contrasting soil textures are lacking in the literature. This investigation was conducted to fill the knowledge gap in these factors related to vermicompost application. At this aim, hydrophobicity of vermicompost and soil/vermicompost mixtures and 35 soil physical indicators related to bulk density, soil water retention curve and pore size distribution functions were calculated for five differently textured soils (from sandy loam to clay loam) amended with vermicompost rates up to 43 % by weight that, for an application depth of 5 cm, corresponded to field doses up to 176–213 t ha^{-1}.

Vermicompost was wettable at field capacity but showed strong to severe hydrophobicity for lower moisture contents. However, even under the most severe conditions of moisture content (air dried condition) and application rate ($r = 43$ %), all the soil/vermicompost mixtures were slightly water repellent thus indicating that, for lower vermicompost doses and higher soil water contents, the hydrophobicity attributable to soil amendment with vermicompost could be considered negligible.

An expected decrease in soil bulk density was observed as a consequence of the lower weight of the amended soils when an increasing percentage of vermicompost was applied. This resulted in increased water retained in the entire range of the explored pressure head values for the two coarsest soils (GI and CA) and in an increase of the water content only at higher h values (i.e., for larger pores) for the finest OR soil. A limited effectiveness of vermicompost in improving water retained at intermediate pressure head values (i.e., for h values between −20 and −100 cm) was also detected.

Consequently, different effects in terms of soil physical indicators were observed depending on the soil texture. In the coarse soils, indicators linked to water availability for plants (*PAWC* and *RFC*) generally increased whereas the location indicators of pore size distribution decreased, thus indicating that the most frequent pore diameter shifted towards lower sizes. The opposite result was observed for the fine OR soil whereas no apparent effect of vermicompost addiction was observed for the intermediate CR soil. For the three sandy loam soils, vermicompost application at rates of about 34 % allowed to improve the poor plant available water capacity ($PAWC < 0.10\ cm^3\ cm^{-3}$) up to values close to optimal conditions recommended in the literature ($PAWC \geq 0.15\ cm^3\ cm^{-3}$). In the fine

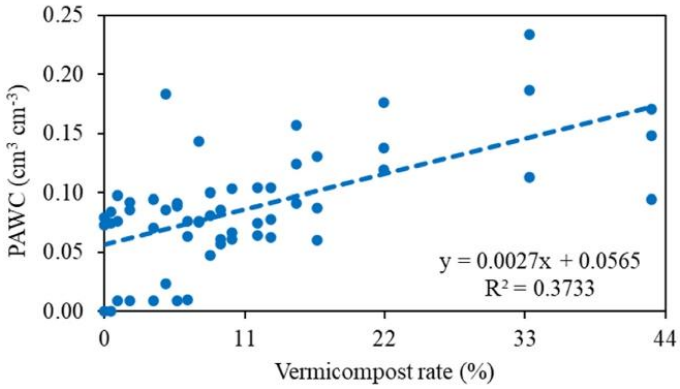

Fig. 6. Relationship between the plant available water capacity (*PAWC*) and the dose of vermicompost added to the sandy loam soils.

OR soil, the *PAWC* was unaffected by vermicompost amendment but macropores and drainable porosity increased thus determining more favourable conditions for air and water circulation.

There is still a need for verification in actual agricultural field conditions because a variety of factors, including vermicompost properties and site-specific climate, may influence the temporal persistence of the amendment benefits. However, the present study, despite being conducted at a laboratory scale, can be considered a first comprehensive step towards understanding the role of vermicompost in soil physical quality improvement under different application rates and textural classes. Moreover, the results are novel as, to our knowledge, a throughout assessment of short-term effects of vermicompost addition on soil hydrophobicity, water retention, and related soil physical quality indicators, involving five differently textured soils and a range of amendment from 3 up to 200 t ha^{-1} has never been conducted before. Applying the same experimental approach, further steps could be made, for example, to quantify the possible amendment effects after a longer period, typically after about a year, to check the residual effects on water retention and hydrophobicity and the improvements due to structural restoration of the soil.

Data availability statement

The entire raw database has been uploaded to Zenodo. Available at http://doi.org/10.5281/zenodo.11198042.

CRediT authorship contribution statement

Mirko Castellini: Writing – review & editing, Writing – original draft, Supervision, Resources, Methodology, Funding acquisition, Formal analysis, conceptualization. **Cristina Bondì:** Writing – review & editing, Writing – original draft, Resources, Methodology, Investigation, Formal analysis, Data curation. **Luisa Giglio:** Investigation, Formal analysis, Data curation. **Massimo Iovino:** Writing – review & editing, Supervision, Methodology, Funding acquisition, Conceptualization.

Declaration of competing interest

The authors declare that they have no known competing financial interests or personal relationships that could have appeared to influence the work reported in this paper.

Acknowledgements

The work was supported by the project "Water4AgriFood, Miglioramento delle produzioni agroalimentari mediterranee in condizioni di carenza di risorse idriche", PNR 2015–2020", funded by MIUR, PON ARS01_00825 "Ricerca e Innovazione" 2014–2020 and by the project PRIN 2022.

PNRR "NBS4STORWATER", Next Generation EU, M4C2, CUP B53D23023760001, funded by Ministero dell'Univerisità e della Ricerca of Italy. This work is part of the experimental activities of the GENFORAGRIS project "Fenotipizzazione di genotipi di olivo resistenti a Xylella fastidiosa e messa a punto di un modello di gestione agronomica ad elevata sostenibilità", funded by MASAF, D.M. n. 664538 del 28/12/2022 and the project "Indagine di laboratorio e di pieno campo sull'uso di Ammendanti naturali dei Suoli per strategie di Conservazione dell'Acqua e dei Nutrienti" (ASCAN) - National Research Centre for Agricultural Technologies, Codice progetto CN00000022, Bando a Cascata Spoke n. 6, CUP D13C22001330005".

Authors wish to thank Carolina Vitti e Marcello Mastrangelo for laboratory chemical analyses.

References

[1] R. Lal, Soil Organic Matter and Feeding the Future: Environmental and Agronomic Impacts, first ed., CRC Press, 2021 https://doi.org/10.1201/9781003102762.
[2] R. Lal, Restoring soil quality to mitigate soil degradation, Sustainability 7 (2015) 5875–5895, https://doi.org/10.3390/su7055875.
[3] M. Castellini, M. Iovino, M. Pirastru, M. Niedda, V. Bagarello, Use of BEST procedure to assess soil physical quality in the Baratz Lake catchment (Sardinia, Italy), Soil Sci. Soc. Am. J. 80 (2016) 742–755, https://doi.org/10.2136/sssaj2015.11.0389.
[4] R. Lal, Challenges and opportunities in soil organic matter research, Eur. J. Soil Sci. 60 (2) (2009) 158–169, https://doi.org/10.1111/j.1365-2389.2008.01114.x.
[5] W.D. Reynolds, C.F. Drury, C.S. Tan, C.A. Fox, X.M. Yang, Use of indicators and pore volume-function characteristics to quantify soil physical quality, Geoderma 152 (2009) 252–263, https://doi.org/10.1016/j.geoderma.2009.06.009.
[6] C.N. Kranz, R.A. McLaughlin, A. Johnson, G. Miller, J.L. Heitman, The effects of compost incorporation on soil physical properties in urban soils – a concise review, J. Environ. Manag. 261 (2020) 110209, https://doi.org/10.1016/j.jenvman.2020.110209.
[7] S.K. Lam, L. Xia, D. Chen, Boosting the benefits of compost, Nat Food 3 (2022) 682–683, https://doi.org/10.1038/s43016-022-00597-6.
[8] J. Viaene, J. Van Lancker, B. Vandecasteele, K. Willekens, J. Bijttebier, G. Ruysschaert, B. Reubens, Opportunities and barriers to on-farm composting and compost application: a case study from northwestern Europe, Waste Manag. 48 (2016) 181–192, https://doi.org/10.1016/j.wasman.2015.09.021.
[9] M. Ros, S. Klammer, B. Knapp, K. Aichberger, H. Insam, Long-term effects of compost amendment of soil on functional and structural diversity and microbial activity, Soil Use Manag. 22 (2006) 209–218, https://doi.org/10.1111/j.1475-2743.2006.00027.x.
[10] T. Garbowski, D. Bar-Michalczyk, S. Charazińska, B. Grabowska-Polanowska, A. Kowalczyk, P. Lochyński, An overview of natural soil amendments in agriculture, Soil Tillage Res. 225 (2023) 105462, https://doi.org/10.1016/j.still.2022.105462.
[11] P.A.Y. Ampim, J.J. Sloan, R.I. Cabrera, D.A. Harp, F.H. Jaber, Green roof growing substrates: types, ingredients, composition and properties 1, J. Environ. Hortic. 28 (4) (2010), https://doi.org/10.24266/0738-2898-28.4.244, 244 -242.
[12] L.J.M. Githinji, J.H. Dane, R.H. Walker, Physical and hydraulic properties of inorganic amendments and modeling their effects on water movement in sand-based root zones, Irrigat. Sci. 29 (1) (2011) 65–77, https://doi.org/10.1007/s00271-010-0218-4.
[13] G. Gugliuzza, A. Verduci, M. Iovino, Water retention characteristics of substrates containing biochar and compost as peat and perlite replacements for ornamental plant production, Acta Hortic. 1305 (2021) 507–511, https://doi.org/10.17660/ActaHortic.2021.1305.67.
[14] A. Ibrahim, R. Horton, Biochar and compost amendment impacts on soil water and pore size distribution of a loamy sand soil, Soil Sci. Soc. Am. J. 85 (4) (2021) 1021–1036, https://doi.org/10.1002/saj2.20242.
[15] M. Castellini, M. Diacono, A. Preite, F. Montemurro, Short- and medium-term effects of on-farm compost addition on the physical and hydraulic properties of a clay soil, Agronomy 12 (2022) 1446, https://doi.org/10.3390/agronomy12061446.
[16] L. Dong, W. Zhang, Y. Xiong, J. Zou, Q. Huang, X. Xu, P. Ren, G. Huang, Impact of short-term organic amendments incorporation on soil structure and hydrology in semiarid agricultural lands, Int. Soil Water Conserv. Res. 10 (2022) 457–469, https://doi.org/10.1016/j.iswcr.2021.10.003.
[17] C. Védère, M. Lebrun, P. Biron, S. Planchais, M. Bordenave-Jacquemin, N. Honvault, C. Rumpel, The older, the better: ageing improves the efficiency of biochar-compost mixture to alleviate drought stress in plant and soil, Sci. Total Environ. 856 (2023) 158920, https://doi.org/10.1016/j.scitotenv.2022.158920.
[18] D. Das, K. Abbhisheka, P. Banik, P. Bhattacharyac, A valorisation approach in recycling of organic wastes using low-grade rock minerals and microbial culture through vermicomposting, Environ. challenges 5 (2021) 100225, https://doi.org/10.1016/j.envc.2021.100225.
[19] H.T. Zhao, T.P. Li, Y. Zhang, J. Hu, Y.C. Bai, Y.H. Shan, F. Ke, Effects of vermicompost amendment as a basal fertilizer on soil properties and cucumber yield and quality under continuous cropping conditions in a greenhouse, J. Soils Sediments 17 (12) (2017) 2718–2730, https://doi.org/10.1007/s11368-017-1744-y.
[20] S. Hou, R. Zhang, C. Zhang, L. Wang, H. Wang, Role of vermicompost and biochar in soil quality improvement by promoting ***Buplaurum falcatum*** L. nutrient absorption, Soil Use Manag. 39 (4) (2023) 1600–1617, https://doi.org/10.1111/sum.12955.
[21] C. Fischer, C. Roscher, B. Jensen, N. Eisenhauer, J. Baade, S. Attinger, A. Hildebrandt, How do earthworms, soil texture and plant composition affect infiltration along an experimental plant diversity gradient in grassland? PLoS One 9 (6) (2014) e98987 https://doi.org/10.1371/journal.pone.0098987.
[22] J. Hallam, J. Holden, D.A. Robinson, M.E. Hodson, Effects of winter wheat and endogeic earthworms on soil physical and hydraulic properties, Geoderma 400 (2021) 115126, https://doi.org/10.1016/j.geoderma.2021.115126.
[23] M. Blouin, J. Barrere, N. Meyer, S. Lartigue, S. Barot, J. Mathieu, Vermicompost significantly affects plant growth. A meta-analysis, Agron. Sustain. Dev. 39 (2019) 34, https://doi.org/10.1007/s13593-019-0579-x.
[24] V. Ducasse, Y. Capowiez, J. Peigné, Vermicomposting of municipal solid waste as a possible lever for the development of sustainable agriculture. A review, Agron. Sustain. Dev. 42 (2022) 89, https://doi.org/10.1007/s13593-022-00819-y.
[25] A. Baghbani-Arani, S.A.M. Modarres-Sanavy, M. Poureisa, Improvement the soil physicochemical properties and fenugreek growth using zeolite and vermicompost under water deficit conditions, J. Soil Sci. Plant Nutr. 21 (2021) 1213–1228, https://doi.org/10.1007/s42729-021-00434-y.
[26] M. Ebrahimi, M.K. Souri, A. Mousavi, N. Sahebani, Biochar and vermicompost improve growth and physiological traits of eggplant (*Solanum melongena* L.) under deficit irrigation, Chem. Biol. Technol. Agric. 8 (2021) 19, https://doi.org/10.1186/s40538-021-00216-9.
[27] H. Ma, S. Zhao, J. Hou, T. FeYissa, Z. Duan, Z. Pan, K. Zhang, W. Zhang, Vermicompost improves physicochemical properties of growing medium and promotes plant growth: a meta-analysis, J. Soil Sci. Plant Nutr. 22 (2022) 3745–3755, https://doi.org/10.1007/s42729-022-00924-7.
[28] P.A. Rivier, D. Jamniczky, A. Nemes, A. Makó, G. Barna, N. Uzinger, C. Farkas, Short-term effects of compost amendments to soil on soil structure, hydraulic properties, and water regime, J. Hydrol. Hydromechanics 70 (1) (2022) 74–88, https://doi.org/10.2478/johh-2022-0004.
[29] X.N. Liu, J. Zhang, Q. Wang, H. Shaghleh, T.T. Chang, Y.A. Hamoud, Modification of soil physical properties by maize straw biochar and earthworm manure to enhance hydraulic characteristics under greenhouse condition, Sustainability 14 (20) (2022) 13590, https://doi.org/10.3390/su142013590.
[30] T.H. Khalifa, S.A. Mariey, Z.E. Ghareeb, I.A. Khatab, A. Alyamani, Effect of organic amendments and nano-zinc foliar application on alleviation of water stress in some soil properties and water productivity of barley yield, Agronomy 12 (2022) 585, https://doi.org/10.3390/agronomy12030585.
[31] R. Albiach, R. Canet, F. Pomares, F. Ingelmo, Organic matter components and aggregate stability after the application of different amendments to a horticultural soil, Bioresour. Technol. 76 (2) (2001) 125, https://doi.org/10.1016/S0960-8524(00)00090-0.
[32] P. Sharma, V. Abrol, V. Sharma, S. Chadda, C.S. Rao, A.Q. Gaine, D.I. Hefft, M.A. El-Sheikh, S. Mansoor, Effectiveness of biochar and compost on improving soil hydro-physical properties, crop yield and monetary returns in inceptisol subtropics, Saudi J. Biol. Sci. 28 (12) (2021), https://doi.org/10.1016/j.sjbs.2021.09.043, 7549-7549.
[33] T. Mengistu, H. Gebrekidan, K. Kibret, K. Woldetsadik, B. Shimelis, H. Yadav, The integrated use of excreta-based vermicompost and inorganic NP fertilizer on tomato (Solanum lycopersicum L.) fruit yield, quality and soil fertility, Int. J. Recycl. Org. Waste Agric. 6 (2017) 63–77, https://doi.org/10.1007/s40093-017-0153-y.
[34] Z. Arabi, A. Moghaddam, M. Hoseini, A. Faraji, Effects of vermicompost and biochar on yield and yield components of maize line AR68 and on some soil physicochemical properties, Arabian J. Geosci. 16 (2023) 677, https://doi.org/10.1007/s12517-023-11774-7.
[35] Rasool Azarmi, M.T. Giglou, R.D. Taleshmikail, Influence of vermicompost on soil chemical and physical properties in tomato (Lycopersicum esculentum) field, Afr. J. Biotechnol. 7 (14) (2008) 2397–2401. http://www.academicjournals.org/AJB.
[36] S.H. Doerr, R.A. Shakesby, R.P.D. Walsh, Spatial variability of soil hydrophobicity in fire-prone eucalyptus and pine forests, Portugal, Soil Sci. 163 (1998) 313–324.
[37] E.S. Vogelmann, J.M. Reichert, J. Prevedello, C.O.B. Consensa, A.É. Oliveira, G.O. Awe, J. Mataix-Solera, Threshold water content beyond which hydrophobic soils become hydrophilic: the role of soil texture and organic matter content, Geoderma 209–210 (2013) 177–187, https://doi.org/10.1016/j.geoderma.2013.06.019.
[38] V. Alagna, M. Iovino, V. Bagarello, J. Mataix-Solera, L. Lichner, Application of minidisk infiltrometer to estimate water repellency in Mediterranean pine forest soils, J. Hydrol. Hydromechanics 65 (3) (2017) 254–263, https://doi.org/10.1515/johh-2017-0009.

[39] C.L. Watson, J. Letey, Indices for characterizing soil-water repellency based upon contact angle-surface tension relationships, Soil Sci. Soc. Am. J. 34 (6) (1970) 841–844, https://doi.org/10.2136/sssaj1970.03615995003400060011x.
[40] V. Alagna, M. Iovino, V. Bagarello, J. Mataix-Solera, L. Lichner, Alternative analysis of transient infiltration experiment to estimate soil water repellency, Hydrol. Process. 33 (4) (2019) 661–674, https://doi.org/10.1002/hyp.13352.
[41] B. Ebel, J.A. Moody, Rethinking infiltration in wildfire-affected soils, Hydrol. Process. 27 (10) (2013) 1510–1514, https://doi.org/10.1002/hyp.9696.
[42] L.W. Dekker, C.J. Ritsema, K. Oostindie, D. Moore, J.G. Wesseling, Methods for determining soil water repellency on field-moist samples, Water Resour. Res. 45 (4) (2009), https://doi.org/10.1029/2008WR007070.
[43] I. Tinebra, V. Alagna, M. Iovino, V. Bagarello, Comparing different application procedures of the water drop penetration time test to assess soil water repellency in a fire affected Sicilian area, Catena 177 (2019) 41–48, https://doi.org/10.1016/j.catena.2019.02.005.
[44] A.R. Dexter, Soil physical quality: Part I. Theory, effects of soil texture, density, and organic matter, and effects on root growth, Geoderma 120 (2004) 201–214, https://doi.org/10.1016/j.geoderma.2003.09.004.
[45] A.M. Stellacci, M. Castellini, M. Diacono, R. Rossi, C.E. Gattullo, Assessment of soil quality under different soil management strategies: combined use of statistical approaches to select the most informative soil physico-chemical indicators, Appl. Sci. 11 (2021) 5099, https://doi.org/10.3390/app11115099.
[46] J. Pranagal, A. Wozniak, 30 years of wheat monoculture and reduced tillage and physical condition of Rendzic Phaeozem, Agric. Water Manag. 243 (2021) 106408, https://doi.org/10.1016/j.agwat.2020.106408.
[47] C. Bondì, M. Castellini, M. Iovino, Compost amendment impact on soil physical quality estimated from hysteretic water retention curve, Water 14 (2022) 1002, https://doi.org/10.3390/w14071002.
[48] H. Han, D. Giménez, A. Lilly, Textural averages of saturated soil hydraulic conductivity predicted from water retention data, Geoderma 146 (2008) 121–128, https://doi.org/10.1016/j.geoderma.2008.05.017.
[49] M.T. van Genuchten, A closed form equation for predicting the hydraulic conductivity of unsaturated soils, Soil Sci. Soc. Am. J. 44 (1980) 892–898, https://doi.org/10.2136/sssaj1980.03615995004400050002x.
[50] G.W. Gee, D. Or, Particle size analysis, in: J.H. Dane, G.C. Topp (Eds.), Methods of Soil Analysis, Part 4, Physical Methods, Soils Science Society of America, Madison, WI, 2002, pp. 255–293, https://doi.org/10.2136/sssabookser5.4.c12.
[51] P.J. Craul, Urban Soils: Applications and Practices, Wiley, Toronto, 1999.
[52] J. Letey, M.L.K. Carrillo, X.P. Pang, Approaches to characterize the degree of water repellency, J. Hydrol. 231–232 (2000) 61–65, https://doi.org/10.1016/S0022-1694(00)00183-9.
[53] E.B.A. Bisdom, L.W. Dekker, J.F.T. Schoute, Water repellency of sieve fractions from sandy soils and relationships with organic material and soil structure, Geoderma 56 (1993) 105–118, https://doi.org/10.1016/B978-0-444-81490-6.50013-3.
[54] G. Caltabellotta, M. Iovino, V. Bagarello, Intensity and persistence of water repellency at different soil moisture contents and depths after a forest wildfire, J. Hydrol. Hydromechanics 70 (4) (2022) 410–420, https://doi.org/10.2478/johh-2022-0031.
[55] J.H. Dane, J.W. Hopmans, 3.3.2.2 Hanging water column. p.680-683, in: J.H. Dane, G.C. Topp (Eds.), Methods of Soil Analysis, Part 4, Physical Methods, Number 5 in the Soil Science Society of America Book Series, Soil Science Society of America, Inc., Madison, WI, USA, 2002.
[56] V. Bagarello, M. Castellini, M. Iovino, Influence of the pressure head sequence on the soil hydraulic conductivity determined with tension infiltrometer, Appl. Eng. Agric. 21 (3) (2005) 383–391, https://doi.org/10.13031/2013.18457.
[57] J.H. Dane, J.W. Hopmans, 3.3.2.4 Pressure plate extractor. p.688-690, in: J.H. Dane, G.C. Topp (Eds.), Methods of Soil Analysis, Part 4, Physical Methods, Number 5 in the Soil Science Society of America Book Series, Soil Science Society of America, Inc., Madison, WI, USA, 2002.
[58] M.T. van Genuchten, F.J. Leij, S.R. Yates, The RETC Code for Quantifying the Hydraulic Functions of Unsaturated Soils, Riverside (CA): U.S. Department of Agriculture, Agricultural Research Service. U.S. Salinity Laboratory, 1991. EPA/600/2-91/065.
[59] M. Castellini, M. Iovino, Pedotransfer functions for estimating soil water retention curve of Sicilian soils, Arch. Agron Soil Sci. 65 (2019) 1401–1416, https://doi.org/10.1080/03650340.2019.1566710.
[60] L.M. Manici, M. Castellini, F. Caputo, Soil-inhabiting fungi can integrate soil physical indicators in multivariate analysis of Mediterranean agroecosystem dominated by old olive groves, Ecol. Indicat. 106 (2019) 105490, https://doi.org/10.1016/j.ecolind.2019.105490.
[61] J.P. Amsili, H.M. van Es, R.R. Schindelbeck, Cropping system and soil texture shape soil health outcomes and scoring functions, Soil Security 4 (2021) 100012, https://doi.org/10.1016/j.soisec.2021.100012.
[62] IUSS Working Group WRB, World Reference Base for Soil Resources. International Soil Classification System for Naming Soils and Creating Legends for Soil Maps, fourth ed., International Union of Soil Sciences (IUSS), Vienna, Austria, 2022.
[63] L.W. Dekker, C.J. Ritsema, How water moves in a water repellent sandy soil: 1. Potential and actual water repellency, Water Resour. Res. 30 (9) (1994) 2507–2517.
[64] W.D. Reynolds, C.F. Drury, X.M. Yang, C.S. Tan, Optimal soil physical quality inferred through structural regression and parameter interactions, Geoderma 146 (2008) 466–474, https://doi.org/10.1016/j.geoderma.2008.06.017.
[65] Z. Ding, A.M. Kheir, O.A. Ali, E.M. Hafez, E.A. ElShamey, Z. Zhou, M.F. Seleiman, A vermicompost and deep tillage system to improve saline-sodic soil quality and wheat productivity, J. Environ. Manag. 277 (2021) 111388, https://doi.org/10.1016/j.jenvman.2020.111388.
[66] R.J. Black, G. Kidder, D.A. Graetz, G.L. Miller, B. Dehgan, Evaluation of Composted Materials to Be Utilized in Florida Roadside and Median Plantings, WPI-0520743, Final Report. Department of Environmental Horticultural, Soil and Water Sciences Department, University of Florida, 1999.
[67] P.D. Somerville, P.B. May, S.J. Livesley, Effects of deep tillage and municipal green waste compost amendments on soil properties and tree growth in compacted urban soils, J. Environ. Manag. 227 (2018) 365–374, https://doi.org/10.1016/j.jenvman.2018.09.004.
[68] F. Mohammadshirazi, R.A. McLaughlin, J.L. Heitman, V.K. Brown, A multi-year study of tillage and amendment effects on compacted soils, J. Environ. Manag. 203 (2017) 533–541, https://doi.org/10.1016/j.jenvman.2017.07.031.
[69] C. Bondì, M. Castellini, M. Iovino, Temporal variability of physical quality of a sandy loam soil amended with compost, Biologia (2024), https://doi.org/10.1007/s11756-024-01637-1.

Environmental Technology & Innovation 34 (2024) 103602

Contents lists available at ScienceDirect

Environmental Technology & Innovation

journal homepage: www.elsevier.com/locate/eti

Cactus pear pruning residue in agriculture: Unveiling soil-specific responses to enhance water retention

C. Bondì [a], N. Auteri [a,*], F. Saiano [a], R. Scalenghe [a], L.P. D'Acqui [b], A. Bonetti [b], M. Iovino [a]

[a] Dipartimento Scienze Agrarie, Alimentari e Forestali, Università degli Studi di Palermo, Italy
[b] Istituto di Ricerca sugli Ecosistemi Terrestri – IRET, Consiglio Nazionale delle Ricerche - CNR, Firenze, Italy

ARTICLE INFO

Keywords:
Soil water retention
Bulk density
Vertisols
Cambisols

ABSTRACT

This study examines the effects of incorporating powdered cactus pear pruning waste (PCPPW) on the hydraulic properties of benchmark soils, in line with circular economy principles. The cultivation of cactus pear generates substantial amounts of pruning residues, which offer the potential for nutrient recovery and reuse. Our findings reveal that amending soils with this material has a positive impact on water retention, but it requires a substantial volume, exceeding 20%, which may not be practical for open-field applications. However, this presents promise for the horticultural and floricultural sectors. These results challenge previous assumptions about soil density, plant-available water capacity, and swelling potential, contributing to our understanding of agronomic applications. Notably, the enhancement of drainable water capacity is most significant in less clayey soils, while highly clayey soils experience fewer benefits. These results highlight the importance of considering specific soil conditions when implementing circular economy principles, particularly in soil amendment practices.

1. Introduction

Arid and semi-arid regions, constituting over forty per cent of the global land area, are key production areas for grains, fruits, and cash crops. Unfortunately, in these regions, agricultural development is limited by water shortages and poor soil fertility (Myers et al., 2017). So, water management in these soils is the key to agronomic success. In this regard, the use of amendments might be one of the most effective agronomic practices (Kranz et al., 2020, Ullah et al., 2021). For instance, biopolymers are ecologically friendly soil improvers that have been commonly employed to increase soil quality (Wang et al., 2023). Organic amendments contribute to the enrichment of soil fertility by increasing soil organic matter (SOM), thereby enhancing crop yield (Bastida et al., 2012, Larney and Angers, 2012). They also indirectly improve hydrological functions and soil structure (Dong et al., 2022; Reynolds et al., 2007) ameliorating the spatial arrangement, shape, and size of solid particles, voids, and SOM (Almendro-Candel et al., 2018). Amendments modify soil water status, evaporation, flow, and retention (Jury and Horton, 2004) despite the positive effects of organic matter on water holding capacity might be less than thought previously (Minasny and McBratney, 2018). Organic amendments can be residues or

Abbreviations: BD, bulk density; BS, black soil Vertisol; DWC, drainable water capacity; PAWC, plant available water capacity; PCPPW, powdered cactus pear pruning waste; PSD, particle size distribution; PTF, pedotransfer functions; RS, red soil *Terra Rossa*; SOM, soil organic matter; SWRC, soil water retention curve.

* Corresponding author.
E-mail address: nicolo.auteri@unipa.it (N. Auteri).

https://doi.org/10.1016/j.eti.2024.103602
Received 18 October 2023; Received in revised form 10 January 2024; Accepted 18 March 2024
Available online 19 March 2024

by-products from both agricultural and industrial processes. However, by-product availability cannot be the only selection criterion to use as several other factors, including quality, applicability, sustainability, cost, and positive impacts on the soil, should be considered (Siedt et al., 2021). Diverse organic wastes have been suggested as possible soil amendment, with various characteristics and locally available in different regions (Larney and Angers, 2012). Examples of fines include biochar (Guo et al., 2024; Ni et al., 2020), municipal waste and sewage sludge (Sadeghi et al., 2014; Paradelo et al., 2019), corn and sewage sludge (Głab et al., 2020), yard waste (Arthur et al., 2011; Curtis and Claassen, 2009), agricultural crop residues (Ibrahim and Horton, 2021), pruning waste (Benito et al., 2006; Auteri et al., 2022), or mixtures of these materials. Among the different types of soil improvers, pruning waste from agricultural activities is interesting as they are locally available and, therefore, generally sustainable in terms of costs. However, the large variability in the composition of pruning makes results hardly generalizable and studies conducted for a specific waste composition in a given pedoclimatic condition should be transferred with caution to other conditions.

Among the low-cost and large-available pruning waste, the residues of cactus pear (*Opuntia ficus-indica* (L.) Mill.), which thrives in most semi-arid countries and is greatly widespread in Central America and the Mediterranean basin, currently leads to the disposal of 13–15 t ha^{-1} of biomass per year (Enea, 2017). Cactus pear cladodes are succulent plant organs consisting of chlorenchyma, the outer layer in which photosynthesis occurs, and parenchyma, the innermost layer whose main function is to retain water. Both are composed of mucilage, which is a hydrocolloid forming stable (honeycomb-like) lattices capable of retaining large amounts of water. The presence of hydrocolloids explains the ability of Cactaceae to grow even in the most unfavorable climatic conditions. This characteristic makes it an interesting agricultural by-product. In addition to its potential as a soil amendment, some authors have evaluated dried and powdered cladodes of cactus pear as adsorbents for eliminating heavy metals or synthetic dyes from aqueous solutions (Nouri et al., 2021; Aziam et al., 2021).

Soil water retention curve (SWRC) expresses the empirical relationship between the matric potential and the volumetric water content of the soil, describing the ability of a given soil to store and release water. Its knowledge is important for agro-environmental modelling or irrigation scheduling and optimization (*e.g.*, Hillel, 1998; Angulo-Jaramillo et al., 2016). The experimental assessment of the SWRC is extremely time-consuming, thus attention has increased towards pedotransfer functions (PTFs) (Bouma, 1989). PTFs have the merit of predicting SWRC from easily measured and/or common soil data, such as bulk density (BD), SOM and particle size distribution (PSD) (Weynants et al., 2009; Castellini and Iovino, 2019). The extreme simplification with which the hydraulic properties are estimated by the existing PTFs considers soils mostly composed by mineral fraction while the effect of large amount of SOM added as soil conditioners is not specifically accounted for. Furthermore, PTFs neglect the presence of plants and the rhizospheric environment. Lateral thinking is that these amendments, even if grossly, can mimic a rhizospheric environment. Considering that 75% of the root mass for all vegetation and biome types is in the upper 40 cm, (Schenk and Jackson, 2002), neglecting the different properties of this layer of soil, especially in an agricultural environment, could be misleading.

The primary purpose of this research is to examine the impact of the amendment of powdered pruning waste from cactus pear (PCPPW) on the water retention characteristics of two contrasting soils widely diffused through the Mediterranean basin. The challenge of transferring our findings lies in the uncertain application to open field crops, whereas the transfer of knowledge proves feasible in plant nurseries, floriculture, or horticulture.

2. Materials and methods

2.1. Benchmark mediterranean soils

The Mediterranean Sea basin covers a surface of seven million square kilometres, encompasses latitude 30° to 40°N and extents from longitude 10°W to 40°E. Its soils are a quite disordered layer of evaporitic deposits originated during the Messinian Salinity Crisis, five and seven million years ago. These soils show analogous characteristics, including a specific climate in which the seasonal distribution of precipitation, rather than the total amount, is the main determinant, a contour of mountains, an abundance of desert dust, accumulations of secondary calcium carbonate or more soluble salts, and a millennial anthropogenic setting. Such a climate provokes the re-precipitation, in the form of nodules, of the partially dissolved carbonates (Carrubba and Scalenghe, 2012; Yaalon, 1997). In Mediterranean landscapes, two categories of soil stand out as archetypal: *terra rossa* (from Italian, red soils) and *terra fusca* (from Latin, black soils). Red soils form through the rubefication process of iron oxides, while black soils originate from the weathering of silicates (which leads to the formation of new inter-layered phyllosilicates) and the simultaneous dissolution of calcareous parent material (Peña and Torrent, 1990). Furthermore, a continuous provision of allochthonous (wind-transported) fine particles works together with pedogenesis, imparting a high water-holding capacity (Bilsel, 2004; Nettleton, 1991; Simonson, 1995).

We have chosen two contrasting soils, well-studied previously. The red soil (RS) is an Ap horizon from a Terric Chromic Cambisol (Loamic) (IUSS WG WRB, 2022; Alagna et al., 2018). The black soil (BS) is a Byss horizon from a Calcic Gypsic Vertisol (Hypereutric) soil (IUSS WG WRB, 2022; Laudicina et al., 2013 and, 2021; Scalenghe et al., 2016) (Table S1). The rationale for this choice depends on the different purposes of organic amendment with soil texture. In the case of coarse soils, organic amendments are frequently employed to augment the humus content and enhance the physical and chemical properties of coarse soils. Likewise, when applied to clayey or fine-textured soils, organic amendments enhance permeability, reduce the risk of soil surface crusting, improve air-water relations, and mitigate surface runoff in agricultural areas (Garbowski et al., 2023).

2.2. Characteristics of cactus pear (Opuntia ficus indica (L.) Mill.)

The cladodes of the cactus pear *cv* Gialla used in the study were collected during the fall season in Roccamena (IT) (472 m a.s.l.;

37°50'17"88 N, 13°9'20"16 E). We collected cladodes of different ages (1–3 years) and sizes (34.2 ± 2.1 ×21.3 ± 3.7 ×2.2 ± 0.3 cm), which would have been removed by normal annual pruning. The thornless cladodes, removed with a knife after collection, were underwent a washing process with tap water, followed by rinsing with deionized water, and were subsequently air-dried. Sequentially, the cladodes were manually dissected (≈ 35 min kg^{-1} cladode) and then dried at 105°C for 48 hours. The dried cladodes were grounded using a laboratory blender, obtaining particles of size $Ø \leq 2$ mm, and stored at room temperature. The grain size distribution of powdered pruning cladodes was determined by manually sieving 50 g of PCPPW at a series of five sieves having diameters of 75, 106, 250, 425 and 860 µm and associating the percentage by mass to the mean geometric diameter in each class. The powder is rich in calcium but contains other elements, particularly manganese (Table S2).

2.3. Soil water retention curve (SWRC) measurement

Air-dried PCPPW was mixed with air-dried 2-mm sieved soil, in twelve different percentages by weight: 1, 2, 4, 6, 8, 10, 12, 15, 20, 30, 40, and 50%. Two control samples, i.e., not amended soil samples (100% RS and 100% BS), were also considered, thus resulting in a total of 26 repacked soil samples. Each sample was prepared by compacting a dry mass of the two constituents (soil and PCPPW), calculated using the following expressions, into cylinders with a diameter of 5 cm and a height of 4 cm:

$$Ms = \frac{V \quad BDp \quad BDs}{BDp + rBDs} Mp = rMs \tag{1}$$

in which M_p (g) and M_s (g) are, respectively, the oven-dried mass of PCPPW and soil, BD_p (Mg m^{-3}) and BD_s (Mg m^{-3}) are the oven-dry bulk densities of the two constituents, V (cm^3) is the sample volume (V = 78.5 cm^3), and r is the ratio between the oven-dry mass of PCPPW and the oven-dry mass of soil. The initial water content of both constituents was considered to calculate the corresponding oven-dried mass. The sample compaction procedure involved four consecutives increments of approximately 1 cm height. At each step a mass of mixture corresponding to one quarter of the calculated mass of the sample was poured into the cylinder and subjected to five strokes of beating from a height of 5 cm, followed by five rotations with a pestle. Finally, the sample bulk density was checked to ensure that it was the same as the theoretical one determined from Eq.(1). This sample preparation procedure was already adopted in former study on compost amendment (Bondì et al., 2022) allowing to obtain highly replicable samples. It is worth noting that the bulk density of the PCPPW (BD = 0.515 g cm^{-3}) was approximately 2.0 and 2.5 times lower than the dry BD of RS and BS (Table S1) thus, at the higher r values, the mixtures contained more amendment than soil on volume basis. These amendment levels could be unpractical for open field crops but are frequent for nursery and greenhouse application.

Laboratory determination of SWRC was conducted by the tension hanging water column apparatus (Dane and Hopmans, 2002a), for matric head values, h, between 0 and −1 m, and by the pressure plate extractor for lower h values down to −150 m (Dane and Hopmans, 2002b).

Soil samples, placed on the surface of the porous plate of a glass funnel, were saturated from below by applying four successive steps of $h = -0.20$, −0.10, and −0.05 m at 24 hr intervals followed by submersion (i.e., $h = 0$) for 2 hr. Starting from saturation, soil samples were subjected to desorption by applying a sequence of twelve decreasing matric head values: −0.025, −0.05, −0.075, −0.10, −0.15, −0.20, −0.25, −0.30, −0.40, −0.50, −0.70 and −1 m. Water drained from the sample was collected in a graduated burette that could be moved in height to regulate the imposed h values. Equilibrium was assumed when the reading at the burette graduate scale did not change during a time spell of 2 hr. It took from 6 to 72 hr to reach equilibrium depending on the soil type and the applied pressure head value. To avoid water losses due to evaporation, the funnel and burette were maintained sealed during the experiment. At each equilibrium h value, the drained water volume from the sample was noted and these volumes backwards added to the equilibrium volumetric water content, θ (m^3 m^{-3}), determined at the end of the drainage sequence ($h = -1$ m) by oven-drying the sample at 105°C for 24 h.

Bulk density variations were monitored by measuring the height of the samples by a gauge at three steps: i) after preparation, i.e., under initial air-dried condition (H0), ii) at the end of the saturation process (HS), and iii) at the end of the desorption process (HF).

Water retention data corresponding to the matric heads of −1, −30, and −150 m were collected using pressure plate extractors on three replicated samples measuring 5 cm in diameter and 1 cm in height, with the same bulk density as the 5 cm by 4 cm samples. In addition, the volumetric content of water at a matric head of −1 m was also determined on pressure plate to compare it with the same value measured in the tension apparatus. All measurements were performed under temperature-controlled conditions at 22 ± 1 °C.

2.4. Pore size distribution by mercury intrusion

Pore size distribution of samples with different PCPPW percentages (i.e., r = 0%, 20%, and 50%) for both RS and BS was measured by mercury intrusion (Pascal 140, Fison and Porosimeter 2000, Carlo Erba, Milan) in the range 0.007–200 µm equivalent cylindrical diameter. Pore volume is expressed on mass basis (mm^3 g^{-1}). The surface tension of mercury and contact angle used for calculation were 0.480 Nm^{-1} and 141.3°, respectively.

3. Results

3.1. Swelling and soil bulk density

Following saturation, the sample height increased for the control samples ($r = 0\%$) of both RS and BS (Fig. 1). As expected, the increase of sample height was more marked for the BS due to the higher clay percentage that promoted soil swelling. In particular, the sample height increased from 39 to 42 mm for the RS and from 38 to 44 mm for the BS. During the subsequent desorption process (from saturation to $h = -1$ m), the height of the RS did not change (HF = 42 mm) whereas continued to increase for the BS (HF = 46 mm). Saturation promoted a more marked increase in the sample height when the different mixtures with variable proportions of PCPPW were considered. In Fig. 1 the effect for the 50% PCPPW addition to soil is reported only, with the notation that all the intermediate PCPPW percentages determined swelling heights comprised between the control samples (i.e., 100% RS or 100% BS) and the corresponding 50% PCPPW mixtures. For the latter, following saturation, the height of the amended samples increased to 52–53 mm. Once saturated, the amended samples maintained the swelling height, or a little reduced it, during the following desorption phase. It is worth noting that the two mixtures (50% RS - 50% PCPPW and 50% BS - 50% PCPPW) followed a similar trend thus showing that the characteristics of the amended soils are mostly controlled by the properties of the PCPPW.

For both RS and BS, the soil dry BD significantly decreased at increasing the percentage of PCPPW (Fig. 2a). Due to the lower BD of the PCPPW (Table S1), the dry BD of the mixtures decreased from 1.032 to 0.698 Mg m^{-3} for RS and from 1.260 to 0.689 Mg m^{-3} for BS, when the percentage of PCPPW increased from 0% to 50% by weight (Fig. 2a). In other words, the dry BD decrease is an expected consequence of the lower weight of the amended soils when an increasing percentage of lighter material is added.

Under wet conditions, the BD was always lower than under dry conditions. Furthermore, no perceivable difference was observed for wet BD measured at saturation ($h = 0$) and field capacity ($h = -1$ m) (Fig. 2b). Under saturated conditions, BD decreased from 0.958 to 0.540 Mg m^{-3} for RS and from 1.088 to 0.530 Mg m^{-3} for BS. At field capacity ($h = -1$ m), BD decreased from 0.958 to 0.550 Mg m^{-3} for RS and from 1.041 to 0.530 Mg m^{-3} for BS. Significant linear regressions with the percentage of PCPPW were also found for wet BD (Fig. 2b). It is worth to be noted that, for both soils, the wet BD decreased to a greater extent than the dry BD at increasing the percentage of PCPPW, as depicted in Fig. 2a-b.

The difference between dry and wet bulk densities can be considered as an index of the swelling susceptibility induced by PCPPW. Indeed, if the swelling capacity of PCPPW were lower or equal to that of the control soils, the substitution of an increasing fraction of swelling soil with PCPPW would determine less (or equal) total swelling susceptibility. Therefore, the wet BD would decrease less than the dry BD at increasing the amending dose and the differences between the two BDs tend to reduce. The opposite is if the swelling capacity of PCPPW is greater than that of the considered soils.

Fig. 2c shows that the relative differences between dry and wet bulk densities were always positive and increased with increasing the PCPPW proportion. For both RS and BS, these differences were significantly correlated to the PCPPW to soil ratio. Compared to the control ($r = 0\%$), for which the differences between wet and dry BDs are exclusively due to swelling of clay particles, addition of PCPPW promoted increased swelling that can be attributed to hydration of the dried powdered cladodes of the cactus pear. For a given value of the PCPPW dose, the BS mixture generally showed larger relative differences between dry and wet BD than the RS because of the higher clay fraction. However, these differences tended to reduce for the highest values of the PCPPW ratio given the sample swelling was mostly controlled by the cactus pear hydration.

3.2. Soil water retention

Water retention data of the control samples of RS and BS soils provided different information (Fig. 3a). The two soils showed equivalent volumetric water content, θ, values for $h = -0.25$ m. For higher values of h, i.e., relatively wet conditions, the volumetric water content of BS was lower than that of RS. An opposite trend was observed at lower h values, i.e., relatively dry conditions, as BS

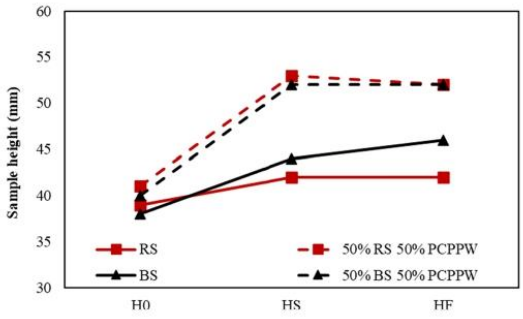

Fig. 1. Sample heights for the initial air-dried conditions (H0), at the end of the saturation process (HS), and at a water content corresponding to matric head $h = -1$ m (HF) for the red soil (RS) and the black soil (BS) and the mixtures of 50% soil and 50% PCPPW.

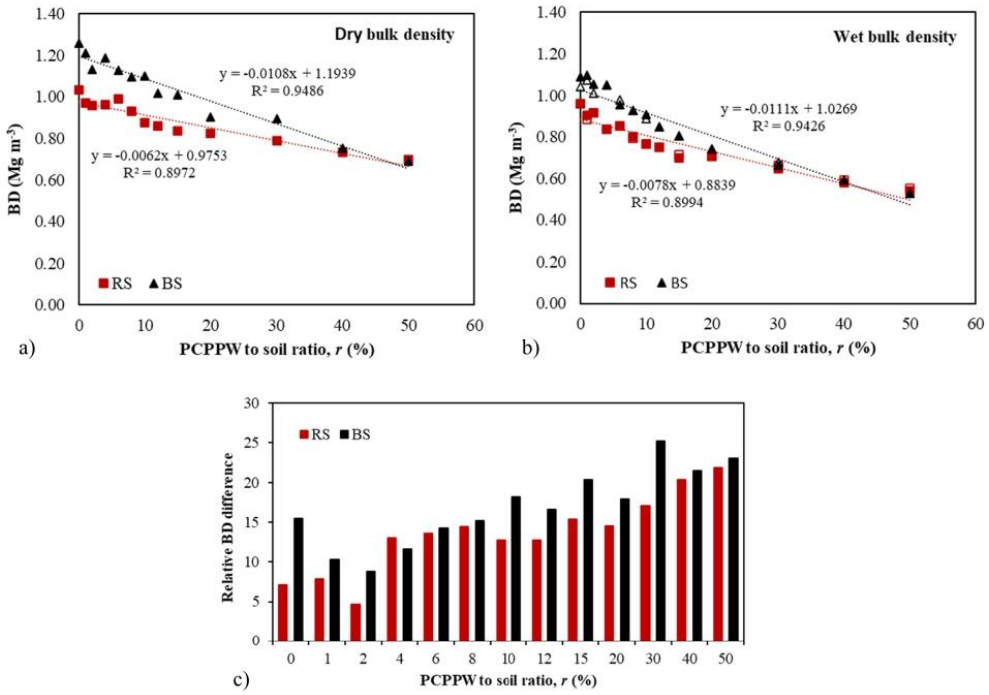

Fig. 2. Sample bulk density under dry (a), and wet (b), conditions as a function of percentages of PCPPW. For wet BD, filled and empty symbols represent saturated ($h = 0$) and field ($h = -1$ m) conditions, respectively. (c) Relative differences between the dry and wet BD for soil mixtures with different percentages of PCPPW. RS = red soil; BS = black soil. Regression lines are shown for saturated conditions only.

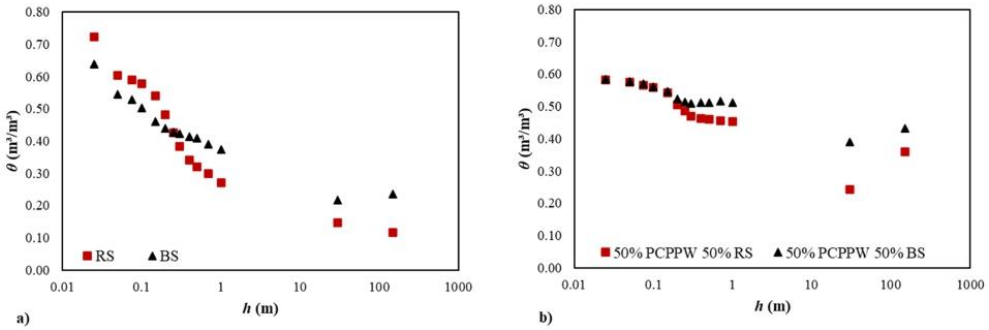

Fig. 3. Soil water retention data for a) the non-amended RS and BS soils and b) the 50% PCPPW to 50% soil mixtures.

showed a higher water retention capacity compared to RS (Fig. 3a). The observed behavior agrees with the different PSD of the two non-amended soils as BS, having a higher clay fraction, is likely characterized by a pore size distribution shifted towards relatively smaller diameters (Table S1). Thus, more water is retained in small pores than in large ones in BS. The opposite is for RS where the large pores predominate over the small ones (Nasta et al., 2009).

Comparison between non-amended soils and PCPPW-soil mixtures showed that soil water retention differed with PCPPW dose and soil type. In particular, the addition of 50% of PCPPW to the RS, resulted in increased θ values for $h < -0.15$ m whereas for higher matric head values (i.e., less negative), the volumetric water content slightly decreased (Fig. 3b). The maximum increase of θ

(0.018 m^3m^{-3}) was observed for $h = -1$ m. For the 50% PCPPW to 50% BS mixture, a generalized increase in the capacity to store water was observed and the volumetric water content increased, as compared to the non-amended BS, by a quantity variable from 0.032 m^3m^{-3} at $h = -0.05$ m to 0.196 m^3m^{-3} at $h = -150$ m. Therefore, our results showed that for both soils the powdered cactus pear improved the water retention capacity for relatively dry soil moisture conditions, which is for soil water content ranging from above the field capacity to the wilting point. However, for relatively wet conditions, the two soils did not show the same response to PCPPW addition. Indeed, for the RS soil a decrease in the water content corresponding to a given matric head was observed whereas, for BS, the addition of PCPPW increased the stored water.

Amending effects were confirmed by Pearson's correlation coefficients between θ values at a given matric head and the PCPPW dose (Table 1). Significant negative correlations were observed for RS at matric heads close to the upper range of matric pore domain ($h = -0.1$ m). For low h values ($h < -0.25$ m) an opposite sign of the correlation was observed with θ values that always increased at increasing the percentage of PCPPW. For BS, the volumetric water content always significantly increased with PCPPW in the range from $h = -0.1$ to -150 m (Table 1).

For both soils, correlations were significant at the matric head values of −0.1, −1.0, and −150 m, which correspond, respectively, to the volumetric water content equivalent to matric capacity, θ_m, field capacity, θ_f, permanent wilting point, θ_w, yielding the following regression lines:

Matric capacity, $h = -0.10$ m

RS: $\theta_m = 0.584 - 0.00121r$ BS: $\theta_m = 0.517 + 0.00101r$

Field capacity, $h = -1.0$ m

RS: $\theta_f = 0.350 + 0.00286r$ BS: $\theta_f = 0.424 + 0.00227r$

Wilting point, $h = -150$ m

RS: $\theta_w = 0.095 + 0.00478r$ BS: $\theta_w = 0.221 + 0.00390r$

A representation of the observed trends is given in Fig. 4, which shows how soil matric capacity is distributed between drainable water capacity (DWC) and plant available water capacity (PAWC). The first, given by difference $\theta_m - \theta_f$, is the water retained in pores that, according to the capillary law, have pore diameters in the range from 300 down to 30 μm. Such fraction corresponds to the soil water that is expected to drain below the root zone due to the synergistic impact of capillary and gravity flows. The latter, given by difference $\theta_f - \theta_w$, is the water retained in pores with a diameter from 30 down to 0.2 μm, and corresponds to the soil water available for crop growth (Reynolds et al., 2002).

For both soils, DWC tended to decrease at increasing the percentage of PCPPW, thus showing that amendment is expected to slow down the drainage below the root zone. A contrasting result (increasing DWC) was observed for RS only for very limited amending doses (*i.e.*, few per cent of PCPPW). The PAWC was to a less extent affected by PCPPW addition (Fig. 4). For the RS, PAWC tended to increase from 0.15 $m^3\ m^{-3}$ for $r = 0\%$ to a maximum of 0.26 $m^3\ m^{-3}$ for $r = 20\%$ and then it decreased to PAWC = 0.20 $m^3\ m^{-3}$ for $r =$ 50%. A comparable trend was noted for BS with the only difference that the maximum PAWC = 0.23 $m^3\ m^{-3}$ corresponded to $r = 30\%$.

3.3. Pore size distribution by mercury intrusion

Fig. 5 displays the pore size distribution in the range of pore size diameter from 0.007 to 200 μm of the control sample ($r = 0\%$), the 20% and 50% mixtures of PCPPW of both RS and BS soil.

The RS pore size distribution (Fig. 5a) displays a pattern with a shoulder with the maximum at around 1.5 μm of pore size diameter

Table 1
Pearson's correlation coefficients and corresponding p-values for the regression between volumetric water content at a given matric head and the PCPPW dose. Bold values indicate significant correlations.

h (m)	Red soil - RS		Black soil - BS	
	Pearson R	p-value	Pearson R	p-value
−0.025	−0.5487	0.0525	−0.1577	0.6085
−0.05	**−0.6216**	0.0235	0.3510	0.2396
−0.075	**−0.6393**	0.0187	0.5424	0.0555
−0.10	**−0.6357**	0.0197	**0.7103**	0.0065
−0.15	−0.4165	0.1574	**0.8014**	0.0010
−0.20	0.1531	0.6178	**0.7677**	0.0022
−0.25	**0.5736**	0.0404	**0.8052**	0.0009
−0.30	**0.6712**	0.0120	**0.8347**	0.0004
−0.40	**0.7156**	0.0060	**0.8657**	0.0001
−0.50	**0.7241**	0.0051	**0.8788**	0.0001
−0.70	**0.7441**	0.0035	**0.8736**	0.0001
−1	**0.7476**	0.0033	**0.8643**	0.0001
−30	**0.8816**	0.0001	**0.9798**	<.00001
−150	**0.9749**	<.00001	**0.9847**	<.00001

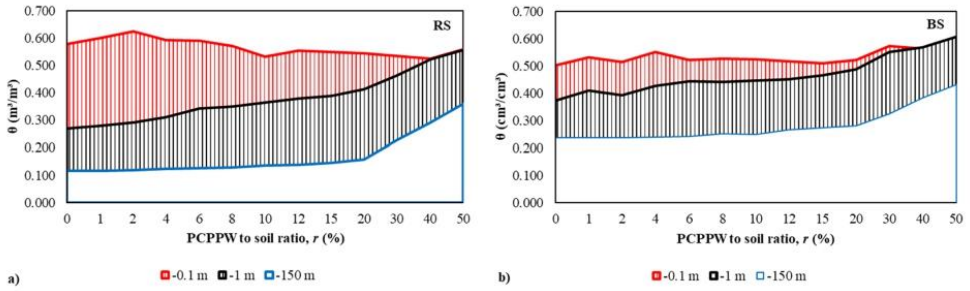

Fig. 4. Volumetric water content retained by PCPPW-soil mixtures for matric head values of −0.1 m (matric capacity), −1 m (field capacity) and −150 m (permanent wilting point). (a) RS (b) BS.

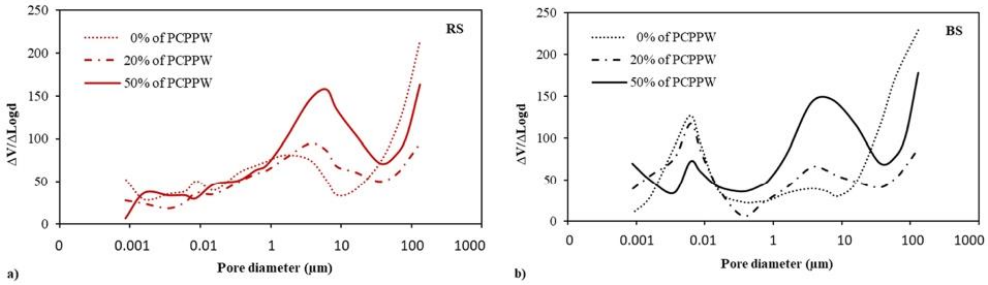

Fig. 5. Pore size distribution by mercury intrusion of a) RS and b) BS samples amended with different PCPPW doses (0%, 20%, and 50%).

for the control ($r = 0\%$) that shifts to higher values (2.5 μm and 5 μm for $r = 20\%$ and 50%, respectively) exhibiting more sharped peaks. Successively all the curves rise toward larger pores >75 μm. In the pore size range 0.007–25 μm, the samples with $r = 20\%$ and 50% increased the pores volume by 13% and 61%, respectively, as compared to the control (Fig. 6).

The BS pore size distribution (Fig. 5b) shows a bimodal pattern with *i*) a maximum of the first peak at around 0.05 μm of pore size diameter in the range of pores 0.007 – 0.25 μm for all samples. Instead, the pore volume in this region is similar for both control and $r =$ 20% mixture but reduced (14%) for the $r = 50\%$ mixture (Fig. 6); *ii*) a maximum of the second peak at around 2.5 μm of pore size diameter for the mixtures and the control in the range of pores 0.25 – 7.5 μm. In this range, the pore volume increased by 78% for the r $= 20\%$ mixture and 315% for the $r = 50\%$ mixture (Fig. 6). Successively, as for RS, all the curves rise toward larger pores >75 μm. The addition of PCPPW promoted the increase of porosity especially in the range of pore diameters around 5 μm with a detrimental effect on the volume of pores with diameter larger than 75 μm. This effect was slightly for $r = 50\%$ mixture but marked for $r = 20\%$ mixture in both soils.

Soils are porous media, notably. Voids are sometimes measured as 'full of air' and other times derived from the measurement of the liquids they contain. In Fig. 6, both methods are considered. The results of both provide unique answers. One of the most important aspects is that the addition of PCPPW 'shifts' the porosity range (including the diameter size of the highest peak) towards regions where liquids are more available for plants. This has considerable relevance in the case of Vertisol, even if the total porosity does not vary significantly (probably because total porosity is mostly ruled by PCPPW addition), the water availability at the rhizospheric level increases. From these results, indications in terms of agronomic management can be extrapolated.

The total pore volume (Table 2), in the range of pores from 0.007 μm to 200 μm, after the amendment with 50% PCPPW increased by 18% in RS and 24% in BS. By contrast, with the $r = 20\%$ mixture the total pore volume reduced by 18% and 16% for RS and BS, respectively.

4. Discussion

Addition of powdered pruning waste of cactus pear to a loamy red soil and a clay black soil determined a decrease in soil BD under dry conditions. Significant negative correlations were found between dry BD and the PCPPW dose indicating that BD decreases at a rate of 0.062–0.078 Mg m^{-3}%$PCPPW^{-1}$. Similarly, Arvidsson (1998) showed that BD was largely dependent on SOM, with which it exhibited a strong negative correlation. Decreasing dry BD could be beneficial in fine-textured compacted or degraded soils showing BD values > 1.3 Mg m^{-3} in which root elongation may be impeded and soil aeration reduced (Reynolds et al., 2007). Instead, BD values

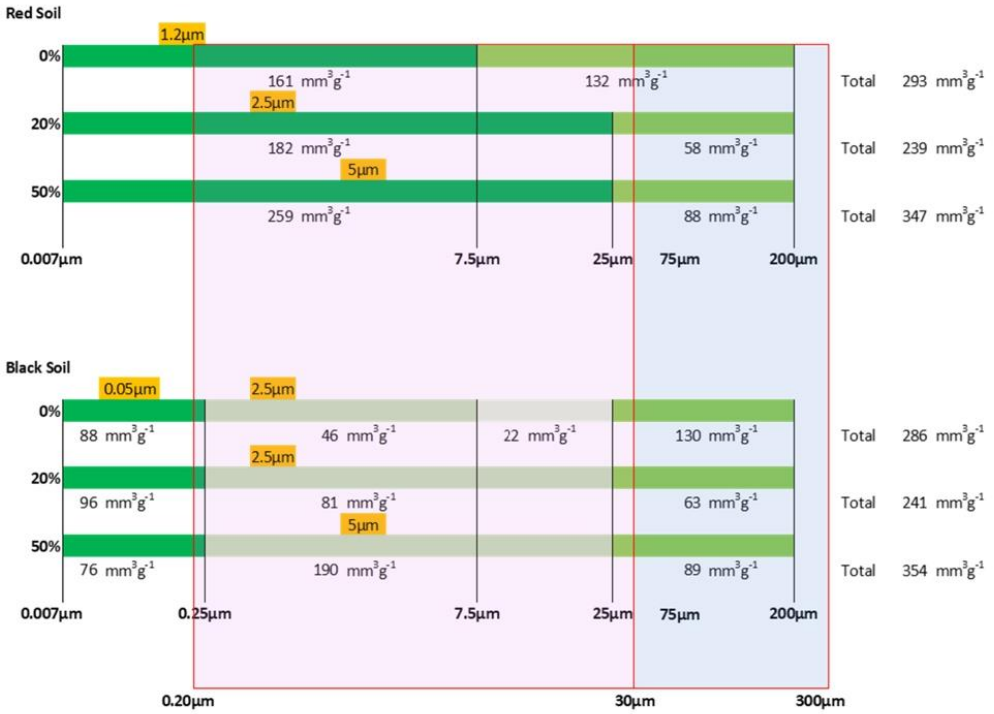

Fig. 6. Pore volume distributions as measured by Hg intrusion method in the different ranges determined based on the cumulative pore volume curve. Superimposition with the ranges measured by the volumetric water content corresponding to the selected matric heads of −0.1 m (300 µm), −1 m (30 µm) and −150 m (0.2 µm), respectively (see Fig. 4). Diameter size of the highest peak in each range (orange) and limits of the respective range (red inset). Figure not to scale.

Table 2
Total pore volume measured by mercury intrusion in the range of pore size diameter from 0.007 to 200 µm of the control (0% of PCPPW), the 20% and 50% mixtures of PCPPW of both RS and BS.

PCPPW	0%	20%	50%
	$mm^3\ g^{-1}$	$mm^3\ g^{-1}$	$mm^3\ g^{-1}$
RS	293	239	347
BS	286	241	354

below 0.8–0.9 Mg m^{-3} might result in inadequate root-soil contact and insufficient plant anchoring (Fan et al., 2021). Despite the present investigation was conducted on laboratory-repacked soil cores with limited compaction compared to natural soils, the observed relationships appear usable to predict the effect of the addition of a given quantity of PCPPW on the BD of natural soils. Furthermore, the two considered soils are widely diffused in the Mediterranean environment and, thus, the range defined by the two linear regression lines can be considered representative of the benefits expected when medium to fine-textured Mediterranean soils are amended with PCPPW.

Being a closed system, the powdered cactus pear had a relatively high swelling effect as, when added to the RS and BS, determined an additional decrease of the wet BD besides that determined by the soil clay particle swelling. The swelling capacity of the PCPPW is a consequence of the chemical structure of polysaccharides of the cactus pear (Amaya-Cruz et al., 2019). Cactus pear cladodes contain mucilage that is rich in galacturonic acid, contributing to improved water retention capabilities (Matsuhiro et al., 2006). The high swelling capacity that characterizes the PCPPW-soil mixtures should be considered with attention given that under constrained conditions, i.e., when the soil is not free to swell, may determine reduced soil porosity with negative effects on air and water circulation. For a limited percentage of PCPPW, the observed increased difference between dry and wet BD is probably positive as it increases the soil water retention.

Indeed, a significant positive correlation was found for water content at a given matric head and the PCPPW dose with the only exception of the matric capacity for the RS. In this last case, θ_m unexpectedly decreased at increasing r. It was hypothesized that the observed trend could be a consequence of specific interactions between PCPPW and RS at low matric head. In particular, the water drop penetration time test (Bisdom et al., 1993), conducted on the PCPPW, showed a slight repellency occurrence as the applied droplets ($N = 5$) infiltrated in time between 12 and 17 s. Therefore, it could be expected that addition of PCPPW hampered wettability particularly when the capillary forces are low (i.e., close to field capacity) and for high organic matter doses (Caltabellotta et al., 2022). However, this effect was not observed for BS. Another possible effect is related to PSD of PCPPW in relation to that of the two considered soils. Fig. 7 shows the percentage distribution by mass of PCPPW, particles compared to those of non-dispersed RS and BS soils. It is worth noting that the PCPPW particles prevailed for larger diameter classes ($d \geq 605$ μm), whereas the soil particles (both RS and BS) prevailed for $d \leq 163$ μm. The singularity is for $d = 326$ μm where the proportion of PCPPW particles prevailed over BS but not over RS ones. Given such particle diameter is very close to the sizes of pores that are saturated at matric capacity ($h = -0.1$ m), it could be supposed that PCPPW addition reduced the number of soil pores falling in that class for the RS thus determining the reduction of θ_m at increasing the PCPPW dose. An opposite trend, i.e.,θ_m increasing with the PCPPW dose, is justified for BS. However, the analyses conducted at the micrometric pore scale by Hg porosimetry similarly displayed the reduction of total pore volume after the addition of the 20% of PCPPW but, in this case, for both RS and BS soils with the successive volume increasing after further PCPPW addition (i.e., 50%) when compared with the respective controls (i.e, 0% of PCPPW).

The estimation of soil porosity has been achieved through two distinct methods: wet soil water retention and dry soil Hg intrusion. It is important to note that these approaches refer to wet and dry soil, respectively. As a result, the swelling effect that occurs in moist soil masks the displacement of the size pores from the smallest to the coarsest pores. This phenomenon is not observed when analyzing dry soil. In terms of retained water, a limited addition of PCPPW (few per cent units) seemed to increase the drainable water capacity (DWC) of the RS and did not affect BS. For higher PCPPW doses a decrease of DWC was observed for both soils, thus confirming that amending medium- to fine-textured soils with swelling PCPPW may hamper soil capacity to drain water and limit air circulation. Although the above statement holds true, the presence of water in the soil tends to mask the true size of the pores. This would explain some of the apparent discordances found between the two methods. The organic particles in the amended soil are larger in size (Fig. 7), and the addition promotes a dominating coarser porosity of the system, especially after 50% of PCPPW addition. This behavior is a result of the final architecture of the particles organization and is influenced by the intrinsic porosity of both soils.

The PAWC was also influenced by PCPPW addition, but observable benefits require very large PCPPW proportions (unlikely under field conditions), up to 20% in RS and even larger in BS. More in general, a redistribution between DWC and PAWC can be supposed with the average energy level of the retained water that becomes more and more negative and drainable water is transformed in plant available water up to a transition threshold of PCPPW dose of around 20% at which PAWC is maximum. Behind that threshold, DWC disappears, and PAWC reduces while most of the soil water is retained below the minimum soil matric head ($h = -150$ m) applicable by crops. For agronomic purposes, that threshold should be not overpassed, at least for these benchmark Mediterranean soils, rather heavily textured.

The ability of soil to retain water significantly affects plant growth, impacting carbon allocation, nutrient cycling, and photosynthesis rates. Research indicates that in various regions globally, soil water-holding capacity dictates crop yield and its stability. Yet, Minasny and McBratney (2018) drawing on data from 60 studies (50,000 measurements) have shown that a 1% increase in soil organic carbon, on average, results in a 1.16% volumetric increase in available water capacity, indicating a minor influence on soil water retention. They showed that overall, there are modest increases in θ when considering all textures. However, when categorized by texture, the rise is significantly greater in coarse-textured soil, followed by medium-textured soil, and least in fine-textured soil.

The significant linear regressions deduced for BD and the characteristic water retention points could help in selecting the most appropriate PCPPW dose to be applied to these soils. Despite the absolute values of BD, θ_m,$\theta\theta_f$ and θ_w can be affected by the empirical setup that made use of laboratory-repacked soil samples, it could be supposed that the relative effects, that is the gradient by which the selected soil property changes because of PCPPW addition, is not affected by the sample preparation. Therefore, if the soil properties under field conditions are known from other investigations, the short-term effect of a given PCPPW dose on bulk density, drainable water capacity and plant available water capacity can be predicted. In particular, the proposed relationships offer a large potentiality to be embedded into PTFs specifically developed for Mediterranean soils with the aim to predict the effects of PCPPW amending on the SWRC (Castellini and Iovino, 2019). A point that needs further investigation is the time stability of the modifications induced by PCPPW addition. In particular, it is expected that the physical and chemical properties of the PCPPW will change over time after soil embedment. However, to the best of our knowledge, no data on PCPPW degradation is available and, thus, long-term modifications could be learned only from studies conducted on similar organic amendment materials (i.e., compost) that showed how the maximum benefits regressed within approximately six months (Bondì et al., 2023; Cannavo et al., 2014; Guo et al., 2019; Weber et al., 2007).

In soil, the rhizospheric environment is complex and difficult to model and thus it is frequently overlooked. However, it is precisely at the level of the rhizosphere that it would be useful to be able to know, for example, the dynamics of water through the soil porous system. Currently, the knowledge of soils is extended to all parts of the world also thanks to the introduction of pedotransfer functions. Pedotransfer functions (PTFs) are used for converting existing data into data that we need but do not have available (Bouma, 1989). Regarding soil hydraulic properties, PTFs are generally based on PSD, BD, SOM, and cation exchange capacity (Tóth et al., 2015; Román Dobarco et al., 2019). For example, in Europe, EU-SoilHydroGrids offers data on soil hydraulic properties up to 2 m depth at 250 m resolution (Tóth et al., 2017). Despite being a powerful tool for planning and land management, most soil databases include the percent of clay and sand only as PTFs predictor variables (e.g., Román Dobarco et al., 2019). They necessarily simplify the complexity of the soil in an extreme manner, excluding the presence of plants. Plants that live in the soil, anchored by their root architecture, modify their intrinsic properties, in particular, the dynamics of liquids and gases. For example, roots secrete mucilage. Polymeric gels

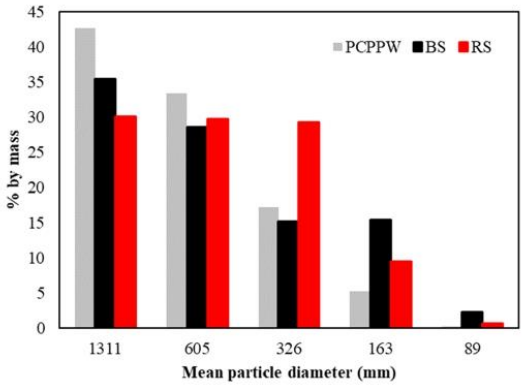

Fig. 7. Particle size distribution among selected diameter sizes in the range from 75 to 2000 μm.

known as mucilages, which are secreted by the cap cells of the root tip, have a crucial role in facilitating root-soil interactions (Ahmed et al., 2015). The physical and chemical properties of mucilage, along with their interactions, are essential in defining its diverse functions and playing a crucial role in hydraulic processes within the rhizosphere (Benard et al., 2019; Rosskopf et al., 2021). Adding plant biomass enhances soil physical properties through the development and stabilization of aggregates (Ansari et al., 2022). Soil macroaggregates (i.e., > 0.250 mm) are stabilized by roots, hyphae, and mucilages, particularly polysaccharides (Machado Vezzani et al., 2018).

The mucilages contained in cactus pear pruning, examined in this work with their potential as a soil conditioner, certainly mimic a rhizospheric environment, albeit oversimplified. Our results, limited to a Mediterranean environment, having chosen two extreme soils, can be used to improve the predictivity of PTFs, considering the presence of plants.

5. Synopsis and conclusions

We tested a by-product of a particular type of Mediterranean cultivation, the cactus pear, and its incorporation effect in benchmark soils. The amendment of powdered pruning waste of cactus pear (PCPPW) exhibited favorable impacts on the physical properties of two contrasting soils, (red soil, RS, and black soil, BS). In both soil types, the incorporation of the amendment led to a reduction in soil BD under dry conditions, which could be advantageous in fine-textured compacted or degraded soils, having BD values > 1.3 Mg m^{-3}, in which root elongation may be prevented and soil aeration reduced. However, PCPPW has a relatively high swelling effect that needs to be considered as, when the soil is confined, it can result in lower soil porosity, which negatively affects air and water circulation. Regarding soil water retention, a limited dose of PCPPW (a few percentage units) seemed to increase the drainable water capacity (DWC) of RS and did not affect BS. Instead, for higher doses of PCPPW, a decrease in DWC was observed for both soils, thus confirming that the emendation of medium to fine-textured soils with swelling PCPPW can hinder the drainage water from the soil and limit air circulation. Plant available water capacity (PAWC) was also found to be affected by the addition of PCPPW, however, observable benefits require very high PCPPW proportions, up to 20% in RS and even more in BS. It is reasonable to assume that a redistribution between DWC and PAWC occurs, with the average energy level of retained water becoming increasingly negative and drainable water converting into plant available water up to a transitional threshold of the PCPPW dose of about 20%, at which PAWC is maximum. Beyond this threshold, DWC disappears and PAWC also decreases, since most of the water is hygroscopic ($h > -150$ m) and not available for plants. For agronomic purposes, this threshold should not be exceeded, at least for these rather heavy textured Mediterranean reference soils. Overall, the findings indicated that the addition of PCPPW, in both soil types, could trigger benefits on hydrological processes and agronomic services by promoting the increase of PAWC, while maintaining the PCPPW content below 20%, and the infiltration of plant roots in the absence of swelling constraint conditions. In conclusion, PCPPW application, as a soil improver, can contribute to efficient water management in arid and semi-arid regions, characterized by limited water availability and low soil fertility.

Despite the general objective of the paper, emphasizing the need for tailored allochthonous material additions to specific soil types, the uncertain applicability of our results to open field crops is acknowledged. However, a potential avenue for knowledge transfer exists within controlled environments like plant nurseries, floriculture, or protected horticulture, where tested ratios are often exceeded, and some crops thrive in pure amendment conditions.

Funding sources

No specific grant was provided for this research from public, commercial, not-for-profit sectors.

CRediT authorship contribution statement

Bondì C.: Conceptualization, Investigation, Writing - original draft, Formal analysis. **Auteri N.:** Conceptualization, Investigation, Writing - original draft, Formal analysis. **Saiano F.:** Conceptualization, Writing - review & editing, Supervision. **Scalenghe R.:** Conceptualization, Writing - review & editing, Supervision. **D'Acqui L.P.:** Writing - review & editing, Formal analysis. **Bonetti A.:** Writing - review & editing, Formal analysis. **Iovino M.:** Conceptualization, Methodology, Resources, Writing - review & editing, Supervision.

Declaration of Competing Interest

The authors declare that they have no known competing financial interests or personal relationships that could have appeared to influence the work reported in this paper.

Data availability

The data have been uploaded to Zenodo. Available at DOI 10.5281/zenodo.7930425. Supplementaty material content related to this article was uploaded at the article submission.

Acknowledgements

We express our gratitude to Cristina Cavallo who composed the infographics.

Appendix A. Supporting information

Supplementary data associated with this article can be found in the online version at doi:10.1016/j.eti.2024.103602.

References

Ahmed, M.A., Holz, M., Woche, S.K., Bachmann, J., Carminati, A., 2015. Effect of soil drying on mucilage exudation and its water repellency: a new method to collect mucilage. J. Soil Sci. Plant Nutr. 178, 821–824. https://doi.org/10.1002/jpln.201500177.

Alagna, V., Bagarello, V., Cecere, N., Concialdi, P., Iovino, M., 2018. A test of water pouring height and run intermittence effects on single-ring infiltration rates. Hydrol. Process. 32, 3793–3804. https://doi.org/10.1002/hyp.13290.

Almendro-Candel, M.B., Lucas, I.G., Navarro-Pedreño, J., Zorpas, A.A., 2018. Physical properties of soils affected by the use of agricultural waste. In: Aladjadjiyan, A. (Ed.), Agricultural waste and residues. IntechOpen. https://doi.org/10.5772/intechopen.77993.

Amaya-Cruz, D.M., Pérez-Ramírez, I.F., Delgado-García, J., Mondragón-Jacobo, C., Dector-Espinoza, A., Reynoso-Camacho, R., 2019. An integral profile of bioactive compounds and functional properties of cactus pear (Opuntia ficus indica L.) peel with different tonalities. Food Chem. 278, 568–578. https://doi.org/10.1016/j.foodchem.2018.11.031.

Angulo-Jaramillo, R., Bagarello, V., Iovino, M., 2016. Infiltration Measurements for Soil Hydraulic Characterization. Springer, Cham. https://doi.org/10.1007/978-3-319-31788-5.

Ansari, M.A., Choudhury, B.U., Layek, J., Das, A., Lal, R., Mishra, V.K., 2022. Green manuring and crop residue management: Effect on soil organic carbon stock, aggregation, and system productivity in the foothills of Eastern Himalaya (India). Soil . Res. 218, 105318 https://doi.org/10.1016/j.still.2022.105318.

Arthur, E., Cornelis, W.M., Vermang, J., De Rocker, E., 2011. Amending a loamy sand with three compost types: impact on soil quality. Soil Use Manag. 27, 116–123. https://doi.org/10.1111/j.1475-2743.2010.00319.x.

Arvidsson, J., 1998. Influence of soil texture and organic matter content on bulk density, air content, compression index and crop yield in field and laboratory compression experiments. Soil . Res. 49, 159–170. https://doi.org/10.1016/S0167-1987(98)00164-0.

Auteri, N., Saiano, F., Scalenghe, R., 2022. Recycling phosphorus from agricultural streams: grey and green solutions. Agronomy 12, 2938. https://doi.org/10.3390/agronomy12122938.

Aziam, R., Boukarma, L., Zaghloul, A., Benhiti, R., Eddaoudi, E., Zerbet, M., Chiban, M., 2021. Factor design methodology for modelling and optimization of carcinogenic acid dye adsorption onto Moroccan cactus pear cactus peel. E3S Web Conf. 240, 02005. https://doi.org/10.1051/e3sconf/202124002005.

Bastida, F., Jindo, K., Moreno, J.L., Hernandez, T., García, C., 2012. Effects of organic amendments on soil carbon fractions, enzyme activity and humus–enzyme complexes under semi-arid conditions. Eur. J. Soil. Biol. 53, 94–102. https://doi.org/10.1016/j.ejsobi.2012.09.003.

Benard, P., Zarebanadkouki, M., Carminati, A., 2019. Physics and hydraulics of the rhizosphere network. J. Plant Nutr. Soil Sci. 182, 5–8. https://doi.org/10.1002/jpln.201800042.

Benito, M., Masaguer, A., Moliner, A., De Antonio, R., 2006. Chemical and physical properties of pruning waste compost and their seasonal variability. Bioresour. Technol. 97, 2071–2076. https://doi.org/10.1016/j.biortech.2005.09.011.

Bilsel, H., 2004. Hydraulic properties of soils derived from marine sediments of Cyprus. J. Arid Environ. 56, 27–41. https://doi.org/10.1016/S0140-1963(02)00319-1.

Bisdom, E.B.A., Dekker, L.W., Schoute, J.F.Th, 1993. Water repellency of sieve fractions from sandy soils and relationships with organic material and soil structure. Geoderma 56 (1), 105–118. https://doi.org/10.1016/B978-0-444-81490-6.50013-3.

Bondì, C., Castellini, M., Iovino, M., 2022. Compost amendment impact on soil physical quality estimated from hysteretic water retention curve. Water 14, 1002. https://doi.org/10.3390/w14071002.

Bondì, C., Castellini, M., Iovino, M., 2023. Temporal variability of physical quality of a sandy loam soil amended with compost. Submitt. Biol.

Bouma, J., 1989. Using soil survey data for quantitative land evaluation. Adv. Soil Sci. 9, 177–213. https://doi.org/10.1007/978-1-4612-3532-3_4.

Caltabellotta, G., Iovino, M., Bagarello, V., 2022. Intensity and persistence of water repellency at different soil moisture contents and depths after a forest wildfire. J. Hydrol. Hydromech. 70 (4), 410–420. https://doi.org/10.2478/johh-2022-0031.

Cannavo, P., Vidal-Beaudet, L., Grosbellet, C., 2014. Prediction of long-term sustainability of constructed urban soil: impact of high amounts of organic matter on soil physical properties and water transfer. Soil Use Manag. 30, 272–284. https://doi.org/10.1111/sum.12112.

Carrubba, A., Scalenghe, R., 2012. The scent of Mare Nostrum: medicinal and aromatic plants in Mediterranean soils. J. Sci. Food Agric. 92, 1150–1170. https://doi.org/10.1002/jsfa.5630.
Castellini, M., Iovino, M., 2019. Pedotransfer functions for estimating soil water retention curve of Sicilian soils. Arch. Agron. Soil Sci. 65 (10), 1401–1416. https://doi.org/10.1080/03650340.2019.1566710.
Curtis, M.J., Claassen, V.P., 2009. Regenerating topsoil functionality in four drastically disturbed soil types by compost incorporation. Restor. Ecol. 17, 24–32. https://doi.org/10.1111/j.1526-100X.2007.00329.x.
Dane, J.H., Hopmans, J.W., 2002a. 3.3.2.2 Hanging water column. In: Dane, J.H., Topp, G.C. (Eds.), Methods of Soil Analysis, Part 4, Physical Methods, Number 5 in the Soil Science Society of America Book Series. Soil Science Society of America, Inc, Madison, WI, USA, pp. 680–683.
Dane, J.H., Hopmans, J.W., 2002b. 3.3.2.4 Pressure plate extractor. In: Dane, J.H., Topp, G.C. (Eds.), Methods of Soil Analysis, Part 4, Physical Methods, Number 5 in the Soil Science Society of America Book Series. Soil Science Society of America, Inc, Madison, WI, USA, pp. 688–690.
Dong, L., Zhang, W., Xiong, Y., Zou, J., Huang, Q., Xu, X., Ren, P., Huang, G., 2022. Impact of short-term organic amendments incorporation on soil structure and hydrology in semiarid agricultural lands. Int. Soil Water Conserv. Res. 10, 457–469. https://doi.org/10.1016/j.iswcr.2021.10.003.
Enea, 2017. Valorizzazione di risorse biologiche da Opuntia ficus indica. Prodotti innovativi bio-based da Opuntia ficus indica. Workshop Bilaterale Italia- Messico ENEA 20 Settembre 2017 – Roma.
Fan, C.C., Lu, J.Z., Chen, H.H., 2021. The pullout resistance of plant roots in the field at different soil water conditions and root geometries. Catena 207, 105593. https://doi.org/10.1016/j.catena.2021.105593.
Garbowski, T., Bar-Michalczyk, D., Charazińska, S., Grabowska-Polanowska, B., Kowalczyk, A., Lochyński, P., 2023. An overview of natural soil amendments in agriculture. Soil . Res. 225, 105462 https://doi.org/10.1016/j.still.2022.105462.
Głab, T., Zabinski, A., Sadowska, U., Gondek, K., Kopéc, M., Mierzwa-Hersztek, M., Tabor, S., Stanek-Tarkowska, J., 2020. Fertilization effects of compost produced from maize, sewage sludge and biochar on soil water retention and chemical properties. Soil . Res. 197, 104493 https://doi.org/10.1016/j.still.2019.104493.
Guo, H., Charles Wang Wai, N.G., Ni, J., Zhang, Q., Wang, Y., 2024. Three-year field study on grass growth and soil hydrological properties in biochar-amended soil. J. Rock. Mech. Geotech. Eng. https://doi.org/10.1016/j.jrmge.2023.08.025.
Guo, Z., Han, J., Li, J., Xu, Y., Wang, X., 2019. Effects of short-term fertilization on soil organic carbon mineralization and microbial community structure. PLoS ONE 14 (4). https://doi.org/10.1371/journal.pone.0216006.
Hillel, D., 1998. Environmental soil physics. Academic Press.
Ibrahim, A., Horton, R., 2021. Biochar and compost amendment impacts on soil water and pore size distribution of a loamy sand soil. Soil Sci. Soc. Am. J. 85, 1021–1036. https://doi.org/10.1002/saj2.20242.
IUSS Working Group WRB, 2022. World Reference Base for Soil Resources. International soil classification system for naming soils and creating legends for soil maps, 4th edition. International Union of Soil Sciences (IUSS), Vienna, Austria, p. 234.
Jury, A.W., Horton, R., 2004. Soil Physics. John Wiley and Sons.
Kranz, C.N., McLaughlin, R.A., Johnson, A., Miller, G., Heitman, J.L., 2020. The effects of compost incorporation on soil physical properties in urban soils - A concise review. J. Environ. Manag. 261, 110209 https://doi.org/10.1016/j.jenvman.2020.110209.
Larney, F.J., Angers, D.A., 2012. The role of organic amendments in soil reclamation: a review. Can. J. Soil. Sci. 92, 19–38. https://doi.org/10.4141/cjss2010-064.
Laudicina, V.A., Scalenghe, R., Pisciotta, A., Parello, F., Dazzi, C., 2013. Pedogenic carbonates and carbon pools in gypsiferous soils of a semiarid Mediterranean environment in South Italy. Geoderma 192, 31–38. https://doi.org/10.1016/j.geoderma.2012.07.015.
Laudicina, V.A., Dazzi, C., Delgado, A., Barros, H., Scalenghe, R., 2021. Relief and calcium from gypsum as key factors for net inorganic carbon accumulation in soils of a semiarid Mediterranean environment. Geoderma 398, 115115. https://doi.org/10.1016/j.geoderma.2021.115115.
Machado Vezzani, F., Anderson, C., Meenken, E., Gillespie, R., Peterson, M., Beare, M.H., 2018. The importance of plants to development and maintenance of soil structure, microbial communities, and ecosystem functions. Soil . Res. 175, 139–149. https://doi.org/10.1016/j.still.2017.09.002.
Matsuhiro, B., Lillo, L.E., Sáenz, C., Urzúa, C.C., Zárate, O., 2006. Chemical characterization of the mucilage from fruits of Opuntia ficus indica. Carbohydr. Polym. 63 (2), 263–267. https://doi.org/10.1016/j.carbpol.2005.08.062.
Minasny, B., McBratney, A.B., 2018. Limited effect of organic matter on soil available water capacity. Eur. J. Soil Sci. 69, 39–47. https://doi.org/10.1111/ejss.12475.
Myers, S.S., Smith, M.R., Guth, S., Golden, C.D., Vaitla, B., Mueller, N.D., Dangour, A.D., Huybers, P., 2017. Climate change and global food systems: potential Impacts on food security and undernutrition. Annu. Rev. Publ. Health 38, 259–277. https://doi.org/10.1146/annurev-publhealth-031816-044356.
Nasta, P., Kamai, T., Chirico, G.B., Hopmans, J.W., Romano, N., 2009. Scaling soil water retention functions using particle-size distribution. J. Hydrol. 374, 223–234. https://doi.org/10.1016/j.jhydrol.2009.06.007.
Nettleton, W.D., 1991. Occurrence, Characteristics, and Genesis of Carbonate, Gypsum, and Silica Accumulations in Soils. SSSA Special Publication Soil Science Society of America, Madison, WI, p. 149.
Ni, J.J., Bordoloi, S., Shao, W., Garg, A., Xu, G., Sarmah, A.K., 2020. Two-year evaluation of hydraulic properties of biochar-amended vegetated soil for application in landfill cover system. Sci. Total Environ. 712, 136486 https://doi.org/10.1016/j.scitotenv.2019.136486.
Nouri, H., Abdedayem, A., Hamidi, I., Najjar, S.S., Ouederni, A., 2021. Biosorption of lead heavy metal on cactus pear cactus biomaterial: kinetic, thermodynamic and regeneration studies. Cellul. Chem. Technol. 55, 919–932.
Paradelo, R., Basanta, R., Barral, M.T., 2019. Water-holding capacity and plant growth in compost-based substrates modified with polyacrylamide, guar gum or bentonite. Sci. Hortic. 243, 344–349. https://doi.org/10.1016/j.scienta.2018.08.046.
Peña, F., Torrent, J., 1990. Predicting phosphate sorption in soils of Mediterranean regions. Fert. Res. 23, 173–179. https://doi.org/10.1007/BF01073433.
Reynolds, W.D., Bowman, B.T., Drury, C.F., Tan, C.S., Lu, X., 2002. Indicators of good soil physical quality: density and storage parameters. Geoderma 110, 131–146. https://doi.org/10.1016/S0016-7061(02)00228-8.
Reynolds, W.D., Drury, C.F., Yang, X.M., Fox, C.A., Tan, C.S., Zhang, T.Q., 2007. Land management effects on the near-surface physical quality of a clay loam soil. Soil Tillage Res. 96, 316–330. https://doi.org/10.1016/j.still.2007.07.003.
Román Dobarco, M., Cousin, I., Le Bas, C., Martin, M.P., 2019. Pedotransfer functions for predicting available water capacity in French soils, their applicability domain and associated uncertainty. Geoderma 336, 81–95. https://doi.org/10.1016/j.geoderma.2018.08.022.
Rosskopf, U., Uteau, D., Peth, S., 2021. Effects of mucilage concentration at different water contents on mechanical stability and elasticity in a loamy and a sandy soil. Eur. J. Soil Sci. 73 (1), 14. https://doi.org/10.1111/ejss.13189.
Sadeghi, S., Ebrahimi, S., Zakerinia, M., 2014. The study of the parametric changes in water potential points by using waste manciple compost in three kinds of soils. Int. J. Basic Sci. Appl. Res. 3 (4), 254–260.
Scalenghe, R., Territo, C., Petit, S., Terribile, F., Righi, D., 2016. The role of pedogenic overprinting in the obliteration of parent material in some polygenetic landscapes of Sicily (Italy). Geoderma Reg. 7 (1), 49–58. https://doi.org/10.1016/j.geodrs.2016.01.003.
Schenk, H.J., Jackson, R.B., 2002. The global biogeography of roots. Ecol. Monogr. 72 (3), 311–328. https://doi.org/10.1890/0012-9615(2002)072[0311:TGBOR]2.0.CO;2.
Siedt, M., Schaffer, A., Smith, K.E.C., Nabel, M., Roß-Nickoll, M., van Dongen, J.T., 2021. Comparing straw, compost, and biochar regarding their suitability as agricultural soil amendments to affect soil structure, nutrient leaching, microbial communities, and the fate of pesticides. Sci. Total. Environ. 751, 141607 https://doi.org/10.1016/j.scitotenv.2020.141607.
Simonson, R.W., 1995. Airborne dust and its significance to soils. Geoderma 65, 1–43. https://doi.org/10.1016/0016-7061(94)00031-5.
Tóth, B., Weynants, M., Nemes, A., Mako, A., Bilas, G., Tóth, G., 2015. New generation of hydraulic pedotransfer functions for Europe. Eur. J. Soil Sci. 66, 226–238. https://doi.org/10.1111/ejss.12192.
Tóth, B., Weynants, M., Pásztor, L., Hengl, T., 2017. 3D soil hydraulic database of Europe at 250 m resolution. Hydrol. Process. 31, 2662–2666. https://doi.org/10.1002/hyp.11203.
Ullah, N., Ditta, A., Imtiaz, M., Li, X.M., Jan, A.U., Mehmood, S., Rizwan, M.S., Rizwan, M., 2021. Appraisal for organic amendments and plant growth-promoting rhizobacteria to enhance crop productivity under drought stress: a review. J. Agron. Crop Sci. 207, 783–802. https://doi.org/10.1111/jac.12502.

Wang, S., Zhao, X., Zhang, J., Jiang, T., Wang, S., Zhao, J., Meng, Z., 2023. Water retention characteristics and vegetation growth of biopolymer-treated silt soils. Soil. Res. 225, 105544 https://doi.org/10.1016/j.still.2022.105544.
Weber, J., Karczewska, A., Drozd, J., Licznar, M., Licznar, S., Jamroz, E., Kocowicz, A., 2007. Agricultural and ecological aspects of a sandy soil as affected by the application of municipal solid waste composts. Soil Biol. Biochem. 39, 1294–1302. https://doi.org/10.1016/j.soilbio.2006.12.005.
Weynants, M., Vereecken, H., Javaux, M., 2009. Revisiting Vereecken pedotransfer functions: introducing a closed-form hydraulic model. Vadose Zone J. 8 (1), 86–95. https://doi.org/10.2136/vzj2008.0062.
Yaalon, D.H., 1997. Soils in the mediterranean region: what makes them different? Catena 28, 157–169. https://doi.org/10.1016/S0341-8162(96)00035-5.

Hydrological response of a volcanic medium as a potential substrate for green roofs

Cristina Bondi
Department of Agricultural, Food and Forest Sciences
University of Palermo
Palermo, Italy
cristina.bondi@unipa.it

Vincenzo Alagna
Department of Agricultural, Food and Forest Sciences
University of Palermo
Palermo, Italy
vincenzo.alagna01@unipa.it

Massimo Iovino
Department of Agricultural, Food and Forest Sciences
University of Palermo
Palermo, Italy
massimo.iovino@unipa.it

Abstract **– This study aimed at evaluating the hydrological response of a volcanic medium (VM) obtained from ash deposition that followed the recent eruptions of Mount Etna (Italy). Due to its lightness and sustainability, this material appears appropriate for preparing "engineered soils" suitable as substrates for green roofs. Simulated rainfall experiments were conducted on microcosms to assess both detention and retention capacities of VM under dynamic conditions. Furthermore, to improve the physical and hydraulic properties of VM, the particle distribution was graded by artificially increasing or decreasing the coarse fraction. Starting from initial dry conditions, the green roof was able to detain from 19.3% to 46.0% of the total rain volume in line with the results of the literature. When initial wet conditions were considered, detention was reduced but anyway in the order of 10% of the total rainfall. Decreasing the VM coarse fraction reduced the distribution of macroporosity and increased that of mesoporosity thus enhancing the drainable water capacity with positive effects on the substrate's detention capacity.**

Keywords – Water retention; water detention; runoff delay; coarse fraction; engineered soil

I. Introduction

Green roofs represent one of the best management practices for reducing and attenuating stormwater runoff in cities [1]. A green roof is a plant system made on an impermeable structural support, such as floors or roofs, that typically consists of four main layers: a drainage layer, a filter layer that prevents the loss of soil particles, a substrate layer (or growing medium) and a vegetation layer [2].

Green roofs reduce the total runoff volume and mitigate the peak flow returned to the sewage system through two hydrological processes: the water retention capacity, i.e., the rainfall volume permanently stored by the substrate that is lost by evapotranspiration, and the detention of runoff, i.e., the transient precipitation storage resulting in a delay and reduction of the peak flood output [3] [4]. Both these processes are closely conditioned by the physical and hydraulic properties of the substrate, which represents the most important part of the green roof. Substrate is a porous media obtained by mixing in different proportions both mineral and organic components. In addition to the requirements of lightness and anchoring capacity for the roots, from the hydrological point of view it should offer high retention capacity, to constitute the water reserve necessary for plants, associated with a high drainage capacity to avoid surface ponding with consequent overload of the structures.

Detention and retention capacities can be evaluated experimentally through simulated rain tests, in which a controlled flow of water is applied to the surface of the green roof and the volumes of water retained and drained from the roof are measured [5] [6]. According to the conceptual model for green roof detention proposed by [7], runoff occurs only when the field capacity of the substrate is exceeded. Thus, detention is basically controlled by the gravity driven flow through the interconnected macropores [8]. On the other hand, retention is determined by micropores that characterize the matrix domain of the substrate [9]. Soil water retention curve (SWRC) can provide valuable insights on the impact of macro-, meso-, and micropores distribution on hydrological performance, also with the aim to provide "engineered soils" specifically designed to enhance both detention and retention capacities of a green roof substrate.

The main objective of this study was to quantify the hydrological response, in terms of retention and detention capacity, of a volcanic medium (VM), easily available from the street sweeping of areas surrounding Mount Etna (Italy), which have been affected by recent eruptions. The porous nature of the VM particles allows to limit the weight of the substrate favoring water retention, thus it represents a lightweight, sustainable material that aligns with the principles of the circular economy. Simulated rainfall experiments were conducted on VM microcosms to assess both detention and retention capacities under dynamic conditions. Then, in order to optimize the composition of a green roof substrate, VM particle size was graded by artificially increasing or decreasing the coarse fraction and the effects on pore size distribution evaluated from experimental assessment of SWRC.

II. Material And Methods

Laboratory tests were carried out at the Department of Agriculture, Food and Forest Sciences of the University of Palermo, Italy. The study employed an experimental setup (Fig. 1) consisting of a needle rain simulator with 45 hypodermic needles (22 Gauge, diameter of 0.7 mm) distributed over an area of 314 cm^2 and two load cells for continuous monitoring of substrate water content and drainage volume.

This study was carried out within the RETURN Extended Partnership and received funding from the European Union Next-GenerationEU (National Recovery and Resilience Plan – NRRP, Mission 4, Component 2, Investment 1.3 – D.D. 1243 2/8/2022, PE0000005)

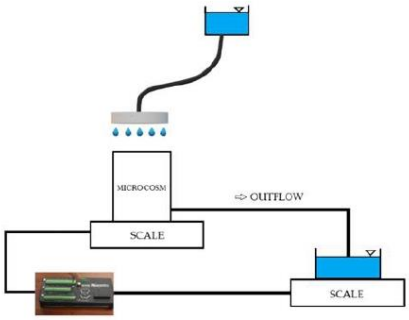

Fig. 1. Scheme of the experimental setup for simulated rain tests.

Data were acquired automatically through a CR1000 datalogger, produced by Campbell Scientific®, and registered with the software LoggerNet.

Green roof microcosms were prepared into plexiglass cylinders, with an internal diameter of 19.4 cm, equipped with a bottom drainage hole for outflow collection. Each microcosm consisted of a 10 cm layer of VM overlying a 4 cm drainage layer. The physico-chemical characteristics of VM are reported in table 1. Three drainage layers were considered including: a preformed stratified system called "MediDrain MD 25" (MD) produced by HARPO Verdepensile, a layer of expanded clay balls (EC) supplied by GEOLIA, and a mineral layer consisting of expanded perlite (EP) produced by "Perlite Italiana". A thin geotextile (<1 cm) made of polypropylene was used to prevent fine particles from the substrate from being washed into the drainage layer. The total height of microcosm was less than 15.0 cm, maximum limit for layering an extensive green roof. A single replicate was considered for each sample as the relatively high sampled volume (≈ 3000 cm^3) was considered representative of the real field conditions.

The microcosms were subjected to infiltration tests with a constant rainfall intensity of 60 mm h^{-1} with a duration of 1 h. A first simulated rain event was conducted on the initially air-dried sample to explore the hydraulic performance of green roof under very dry summer conditions. A second rain event was applied 24 hours later to examine the hydrological response of green roof in wet conditions close to the so-called "field capacity". Detention capacity was estimated as the volume of rainfall retained until the first appearance of water draining from the outflow. Retention capacity was estimated as the volume of water that remained stored into the microcosm after the drainage process practically stopped. This condition was assumed to be reached 1 h after the rainfall ended.

TABLE 1. Main physico-chemical characteristics of the volcanic medium: texture; bulk density, BD; porosity; pH; electrical conductivity, EC.

Texture*	BD (g cm^{-3})	Porosity (%V/V)	pH	EC** (ms m^{-1})
3-6-91	1.021	62	7.28	0.12

*Texture: clay-silt-sand as percent of the fine earth according to USDA.
**1:5 aqueous extract.

The reliability of the collected data was checked by applying the mass balance equation to verify that, in a given time interval, the change in water content stored into the substrate was equal the difference between rainfall input and drainage losses.

To evaluate the effects of the different pore size distributions on the soil water retention curves (SWRC), different parts by weight of the fine fraction (d < 2 mm) and the coarse fraction (d > 2 mm) of VM were arranged in five mixtures in which the coarse fraction was, respectively 0.25, 0.5, 1, 2, 4 times the coarse fraction, *c*, originally present into the natural VM. Starting from the air-dried medium, ten samples were prepared, two replicates for each mixture, compacted into metal cylinders with diameter of 5 cm and a height of 5 cm. Sample preparation was carried out following the methodology proposed by [10].

The SWRC was determined by the tension hanging water column apparatus [11], applying a drainage cycle consisting of a sequence of 10 pressure head values, h (m), applied in descending order. The volumetric water contents, θ (m^3m^{-3}), corresponding to potentials of –1, –3.3, –10, –30, and –150 m, were determined by the pressure method [12]. For each of the mixtures considered and for each potential, three samples with a diameter of 5 cm and a height of 1 cm were prepared.

Experimental data were fitted by SWRC fit software [13], with the van Genuchten model [14]:

$$\theta(h) = \theta_r + (\theta_s - \theta_r)(1 + |\alpha h|^n)^{-m} \quad (1)$$

in which θ_s (m^3m^{-3}) and θ_r (m^3m^{-3}) are the saturated and residual volumetric water contents, respectively, α is a scale parameter, n and m with $m = 1–1/n$ are shape parameters. The fitted van Genuchten water retention curves were used to estimate the macro- (p_{mac}), meso- (p_{mes}), and microporosity (p_{mic}) of the different mixtures.

$$p_{mac} = \theta_s - \theta_m \quad (2)$$

$$p_{mes} = \theta_m - \theta_{fc} \quad (3)$$

$$p_{mic} = \theta_{fc} - \theta_{pwp} \quad (4)$$

where θ_s (m^3m^{-3}) is the volumetric water content of the saturated medium, θ_m (m^3m^{-3}) is the volumetric water content of the matrix (h = –0.1 m), θ_{fc} (m^3m^{-3}) is the volumetric water content corresponding to so-called field capacity (h = –1 m) and θ_{pwp} (m^3m^{-3}) is the volumetric water content corresponding to the permanent wilting point (h = –150 m).

III. Results

The hydrological response of microcosms exposed to a simulated rainfall event with constant intensity of 60 mm h^{-1} was greatly affected by the initial moisture conditions (table 2). Starting from initial air-dried conditions, the microcosms detained a percentage of the total rainfall volume that ranged from 19.3% with MD drainage layer to 46.0% with EC drainage layer. The delay in runoff formation, i.e., the time lapse between the beginning of rainfall and the beginning of drainage, followed the same order of the detention capacity, being maximum for the VM-EC combination in which it amounted to 0.38 h.

TABLE 2. Hydrological performance of volcanic medium associated with different drainage layers.

Drainage layer	$T_{drainage}$ (h)	Detention (mm)	Retention (mm)
Dry			
MD	0.19	11.6	10.6
EP	0.28	20.8	18.6
EC	0.38	27.6	15.8
Wet			
MD	0.04	2.8	2.2
EP	0.10	6.2	5.8
EC	0.06	4.7	6.8

The retention capacity also depended on the drainage layer with a minimum of 17.7% of the total rainfall volume for MD layer and a maximum of 31.0% for EP. It is worth noting that detention and retention capacity showed a similar trend, given that EC drainage layer performed better in terms of detention and EP in terms of retention. For initial dry conditions the worst hydrological performance was obtained with MD drainage layer.

According to the literature, an extensive green roof can retain, on average, between 40% and 60% of the amount of rainwater [15] [16]. Taking into consideration that the microcosms lacked the vegetation layer responsible for additional water retention, our results aligned with this range.

When simulated rainfall started from initial wet conditions close to the field capacity, the delay in runoff formation was reduced as well as the detention and retention capacities (table 2). These results were expected given a large fraction of the total porosity was filled with water under wet conditions. It should be highlighted that the green roof retention capacity is a "dynamic" variable that depends on the initial moisture conditions, and it is different from the water retention capacity of the substrate that, instead, depends on the pore system arrangement and is a static property of the porous medium. Anyway, it may be interesting to note that the VM-EP and VM-EC combinations, even under wet conditions, showed an appreciable performance, retaining 9.7% and 11.3% of total rainfall volume, respectively. Also in this case, the worst performance was obtained for the VM-MD with a detention capacity that was two-fold lower and a retention capacity that was a factor of three lower than the other combinations.

The plots of hydrological response for microcosms formed by the VM-EC combination for both initial dry (Fig. 2a) and wet conditions (Fig. 2b) show how the green roof performance may undergo considerable changes depending on the initial moisture condition of the substrate. In agreement with [2], the amount of water retained, and the portion of runoff reduced by a green roof substrate is therefore greatly affected by the local climatic conditions and, specifically, by the season in which precipitation occurs.

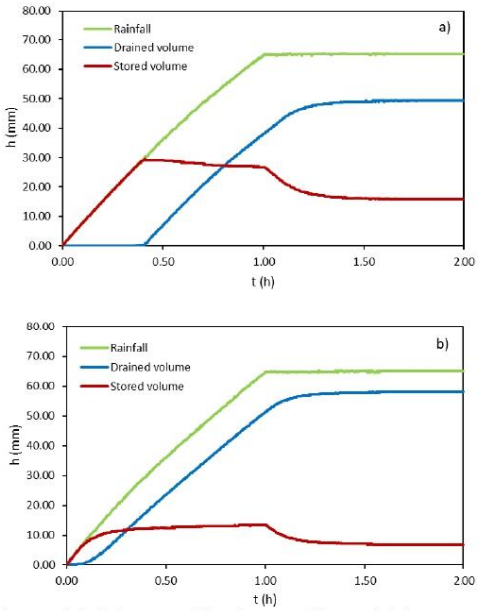

Fig. 2. Hydrological response of the microcosm with expanded clay, EC, as drainage layer, for a simulated rainfall event with a constant intensity of 60 mm h^{-1}: a) initial dry condition; b) initial wet condition.

Therefore, considering the local climatic context is important for evaluating the effectiveness of a green roof in retaining rainwater and reducing runoff.

In the design of a green roof, it is crucial to accurately determine the permanent load also considering that the various layers constituting the green roof can become saturated during intense rainstorms [17]. With this regard, table 3 reports the specific weight (kg m^{-2}) of each combination between substrate and drainage layer, during the simulated rain tests. The weights fell within the range of 70 to 250 kg m^{-2} that is typically considered operative for an extensive green roof.

Fig. 3 compares the different soil water retention curves obtained for the VM. The results clearly show how the water retention of the medium decreases as the coarse fraction *c* increases from 0.25 to 4.

TABLE 3. Specific weights (kg m^{-2}) of the considered microcosms at the start of simulated rainfall (initial), at the beginning of drainage (detention) and at the end of drainage (retention).

	Initial		Detention		Retention	
	Dry	***Wet***	***Dry***	***Wet***	***Dry***	***Wet***
MD	125.8	134.0	137.5	136.8	136.4	136.2
EP	135.8	149.7	156.6	155.9	154.3	155.6
EC	134.7	145.7	162.3	150.4	150.5	152.6

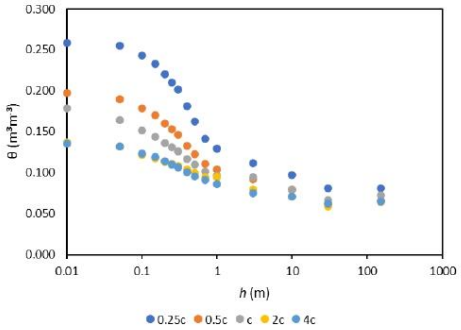

Fig. 3. Soil water retention curves of the mixtures with different parts by weight of fine fraction ($d < 2$ mm) and coarse fraction ($d > 2$ mm).

Increasing the coarse fraction, beyond 2c, did not lead to further decreases in θ, which remained approximately constant between 2c and 4c. It is also worth to note that θ variations, as a function of c, were more marked for the higher pressure heads, up to the field capacity ($h = -1$ m), while, for more negative pressure heads, up to the permanent wilting point ($h = -150$ m), the influence of the coarse fraction was weaker. Similar results were found by [18].

The water retention data were adequately fitted by the unimodal model of van Genuchten [14] as detected by the high correlation coefficients (mean $R = 0.9948$).
The volumetric water content at a given pressure head was negatively correlated with c, as detected by the Pearson's correlation coefficients, R. The values were significant ($p < 0.05$), except for the volumetric water content at the permanent wilting point, θ_{-150} (table 4).
This result further confirmed that the impact of the coarse fraction on the SWRC diminishes as the pressure head value becomes more negative.

The fitted soil water retention curves allowed to calculate the percentage distribution of macro-, meso-, and microporosity in the mixtures (Fig. 4).
Variations in the amount of coarse fraction did not result in appreciable changes in the percentage of microporosity, which is indicative of the plant available water content, *PAWC* [19]. However, both the percentage distributions of macro- and mesoporosity were influenced by such variations (Fig. 4).
Based on the capillary law, p_{mac}, p_{mes}, and p_{mic} correspond to pore diameters greater than 300 μm, between 30 and 300 μm, and between 0.2 and 30 μm, respectively.

TABLE 4. Pearson's correlation coefficients between volumetric water contents, θ, corresponding to selected pressure head values and the coarse fraction, c. Values in bold indicate statistically significant correlations ($p < 0.05$) ($N = 10$).

θ_s	$\theta_{-0.1}$	θ_{-1}	$\theta_{-3.3}$	θ_{-150}
-0.791	**-0.721**	**-0.763**	**-0.764**	-0.593

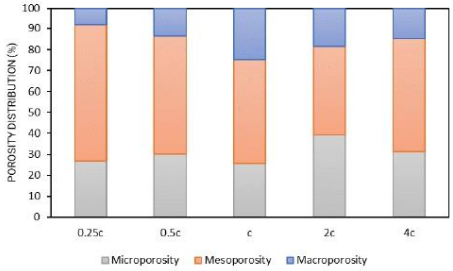

Fig.4. Percentage distribution of macro-, meso-, and microporosity of mixtures with different parts by weight of the fine fraction ($d < 2$ mm) and the coarse fraction ($d > 2$ mm).

Increasing the coarse fraction by 2c or 4c did not result in substantial differences, while decreasing it by 0.5c or 0.25c proportionally reduced the percentage distribution of macroporosity and increased that of mesoporosity. The latter is expressive of the drainable water capacity, which represents the soil water that is expected to drain below the growing substrate due to the combined effect of capillarity and gravity. Therefore, this result is of considerable practical importance for improving the detention capacity of the VM. In particular, it could be supposed that artificially decreasing the coarse fraction will result in an increased detention capacity of the volcanic substrate.

IV. Conclusions

Volcanic medium resulting from ash deposition that followed the recent eruptions of Mount Etna (Italy), represents a lightweight, sustainable material which can be used as "engineered soil" eventually after the physical and hydraulic characteristics are ameliorated.

The results indicated that the hydrological performance of extensive green roofs made with a 10 cm thick layer of VM associated with different commercial drainage layers greatly depended on the initial conditions. In particular, starting from initial dry conditions, the green roof was able to detain from 19.3% to 46.0% of the total rain volume, with the VM-EC combination that exhibited the largest detention capacity (28 mm), with a delay of 0.38 hour in the formation of outflow. Total rainfall volume permanently retained are comparable with those detained. Starting from initial wet conditions, detained and retained rain volumes were reduced, as expected due to the lower air-filled porosity. However, the VM-EP and VM-EC combinations showed appreciable performances, being able to retain about 10% of the total rainfall also in wet conditions.

Grading the particle size distribution of volcanic medium by artificially increasing or decreasing the coarse fraction resulted in variations in the soil water retention curve, and associated distributions of macro-, meso-, and microporosity. Specifically, the most relevant differences were observed when reducing the coarse fraction by 0.5 and 0.25, leading to an increase in the percentage of mesoporosity. These results showed the possibility of manipulating the particle size distribution to enhance the

drainable water capacity, thus improving the substrate's detention capacity.

Based on the results obtained, it is reasonable to conclude that volcanic medium represents an effective and sustainable option as a mineral component of a green roof substrate. When combined with a well-balanced mixture of organic materials such as compost, vermicompost or peat, it forms an optimal substrate for the growth of species like *Petrosedum sediforme* or *Sedum album,* commonly used for extensive green roofs under Mediterrenean climate.

Estimation of retention and detention capacity was conducted under the assumption that the water flow is basically one-dimensional and the drainage occurring at the bottom layer is suddenly transferred to the outlet of the green roof. This condition may partially differ under real conditions in which the green roof is positioned over a sloped surface and the travelling time could be larger due to the effect of horizontal flux. The next step of investigation will therefore involve the use of 2D modelling to assess the influence of the slope and length of the green roof on the retention and detention characteristics.

Further investigations are also required to evaluate the influence of rainfall intensity, as well as to assess the hydrological response of the substrate when the coarse fraction has been artificially modified.

REFERENCES

[1] M. Shafique, R. Kim, K. Kyung-Ho, 2018. Green roof for stormwater management in a highly urbanized area: the case of Seoul, Korea. Sustainability 10, pp. 584.

[2] J. Czemiel Berndtsson, 2010. Green roof performance towards management of runoff water quantity and quality: A review. Ecological Engineering 36(4), pp. 351–360.

[3] S. De-Ville, M. Menon, X. Jia, G. Reed, V. Stovin, 2017. The impact of green roof ageing on substrate characteristics and hydrological performance. Journal of Hydrology 547, pp. 332–344.

[4] Y. Li, R. W. Babcock, 2014. Green roof hydrologic performance and modeling: a review. Water Science & Technology 69.4.

[5] S. Huang, A. Garg, G. Mei, D. Huang, R. Balaji Chandra, S.G. Sadasiv, 2020. Experimental study on the hydrological performance of green roofs in the application of novel biochar. Hydrological processes, pp. 1–14.

[6] L. Gan, A. Garg, H. Wang, G. Mei, J. Liu, 2021. Influence of biochar amendment on stormwater management in green roofs: experiment with numerical investigation. Acta Geophysica 69, pp. 2417–2426.

[7] H. Kasmin, V. R. Stovin and E. A. Hathway, 2010. Towards a generic rainfall-runoff model for green roofs. Water Science & Technology - WST 62, pp. 898–905.

[8] C.Bondi, P. Concialdi, M. Iovino, V. Bagarello, 2023. Assessing short- and long-term modifications of steady-state water infiltration rate in an extensive Mediterranean green roof. Helyion 9, e16829.

[9] L. Lassabatere, S. Di Prima, S. Bouarafa, M. Iovino, V. Bagarello, R. Angulo-Jaramillo, 2019. BEST-2K Method for Characterizing Dual-Permeability Unsaturated Soils with Ponded and Tension Iniltrometers. Vadose Zone J. 18:180124.

[10] C. Bondi, M. Castellini, M. Iovino, 2022. Compost Amendment Impact on Soil Physical Quality Estimated from Hysteretic Water Retention Curve. Water 14, pp. 1002.

[11] J.H. Dane, J.W. Hopmans, 3.3.2.2 Hanging water column. In Methods of Soil Analysis, Part 4, Physical Methods, Number 5 in the Soil Science Society of America Book Series; Dane, J.H., Topp, G.C., Eds.; Soil Science Society of America, Inc.: Madison, WI, USA, 2002; pp. 680–683.

[12] J.H. Dane, J.W. Hopmans. 3.3.2.4 Pressure plate extractor. In Methods of Soil Analysis, Part 4, Physical Methods, Number 5 in the Soil Science Society of America Book Series; Dane, J.H., Topp, G.C., Eds.; Soil Science Society of America, Inc.: Madison, WI, USA, 2002; pp. 688–690.

[13] K. Seki, 2007. SWRC fit—A nonlinear fitting program with a water retention curve for soils having unimodal and bimodal pore structure. Hydrol. Earth Syst. Sci. 4, pp. 407–437.

[14] M.T. van Genuchten, 1980. A Closed-form Equation for Predicting the Hydraulic Conductivity of Unsaturated Soils. Soil Sci. Soc. Am. J. 44, pp. 892–898.

[15] V. Stovin, G. Vesuviano, H. Kasmin, 2012. The hydrological performance of a green roof test bed under UK climatic conditions. Journal of Hydrology 414, pp. 148–161.

[16] B.G. Gregoire, J.C. Clausen, 2011. Effect of a modular extensive green roof on stormwater runoff and water quality. Ecological Engineering 37, pp. 963–969.

[17] UNI 11235, 2007. Istruzioni per la progettazione, l'esecuzione, il controllo e la manutenzione di coperture a verde.

[18] J. M. Baetens, K. Verbist, W. M. Cornelis, D. Gabriels, G. Soto, 2009. On the influence of coarse fragments on soil water retention. WATER RESOURCES RESEARCH 45, W07408.

[19] W.D. Reynolds, C.F. Drury, C.S. Tan, C.A. Fox, X.M. Yang, 2009. Use of indicators and pore volume-function characteristics to quantify soil physical quality. Geoderma 152, pp. 252-263.

applied sciences

MDPI

Article

Hydraulic Characterization of Green Roof Substrates by Evaporation Experiments

Dario Autovino *, Vincenzo Alagna, Cristina Bondì and Massimo Iovino

Department of Agricultural, Food and Forest Sciences, University of Palermo, Viale delle Scienze, 90128 Palermo, Italy
* Correspondence: dario.autovino@unipa.it

Abstract: Green roofs can be a valid solution for stormwater management in urban environments. The objective of this study was to develop a laboratory procedure for the hydraulic characterization of artificial substrates, used in the realization of green roofs, based on transient evaporation and steady-state unit hydraulic gradient (UHG) experiments. The retention, $\theta(h)$, and hydraulic conductivity, $K(h)$, curves of two commercial substrates Terra Mediterranea® (TMT) and AgriTERRAM® (ATV) and a specifically developed substrate made by mixing peat, compost and sandy loam soil (MIX) were investigated. The unimodal van Genuchten–Mualem (VGM) hydraulic functions obtained by the direct evaporation method with different choices of the fitting parameters were compared with UHG measurements of $K(h)$ conducted close to saturation. A numerical inversion of the transient evaporation experiments performed by Hydrus-1D software was also conducted, assuming that the hydraulic properties could be expressed either by unimodal or bimodal VGM models. The results indicated that an appropriate a priori choice of the residual water content parameter improved the estimation of the water retention curve. Moreover, the water retention data estimated from the direct evaporation method were not statistically different from those obtained with the inverse Hydrus-1D. The unsaturated hydraulic conductivity estimations obtained by the direct and inverse methods were highly correlated and the use of the bimodal VGM model improved the estimation of $K(h)$ in the wet range. The numerical inversion of laboratory evaporation data with the hydraulic characteristics expressed by the bimodal VGM model proved to be a reliable and effective procedure for hydraulic characterization of artificial substrates, thus improving the reliability of simulated water fluxes in green roofs.

Keywords: green roof; evaporative method; Hydrus 1D; hydraulic characterization; retention curve; conductivity curve

Citation: Autovino, D.; Alagna, V.; Bondì, C.; Iovino, M. Hydraulic Characterization of Green Roof Substrates by Evaporation Experiments. *Appl. Sci.* **2024**, *14*, 1617. https://doi.org/10.3390/app14041617

Academic Editor: Ty P. A. Ferré

Received: 12 January 2024
Revised: 8 February 2024
Accepted: 15 February 2024
Published: 17 February 2024

1. Introduction

Green roofs are low-impact development measures aimed at mitigating the effects of flooding in urban areas [1]. Green roofs are able to reduce and delay the peak rate into the sewage system through two mechanisms: (i) the retention of rainfall and (ii) the detention of runoff. The retention capacity is the volume of rainfall that is stored by the growing medium and lost via evapotranspiration. Detention refers to the temporal delay occurring between rainfall that is not retained and emerges as runoff [2]. Considering that roofs may represent a large portion of the total impervious surfaces in urban areas, green roofs are one of the key options for hydrologic restoration and stormwater management [3].

Conceptual models for green roof hydrologic functioning, e.g., [4], include lumped parameters that are case sensitive and need to be calibrated against experimental data, thus limiting their general applicability [5,6]. Physically based models such as Environmental Protection Agency (EPA)'s Storm Water Management Model (SWMM) [6,7], Soil Water Atmosphere and Plant (SWAP) model [8] and Hydrus model [9–12] in either one-dimensional [13,14], two-dimensional [15,16] and three-dimensional versions [5] were

successfully applied to simulate the water balance and the hydrologic response of a vegetated roof. Knowledge of the hydraulic properties, i.e., the relationships between the soil water pressure head, h, the volumetric water content, θ, and the soil hydraulic conductivity, K, is necessary to apply simulation models based on the numerical solution of the Richards equation [8,14]. However, few studies have provided a comprehensive hydraulic characterization of green roof substrates. In most cases, the hydraulic properties of green roofs were highly simplified or limited to some specific soil characteristics (e.g., field capacity, wilting point, or particle size distribution) and generally focused only on the soil water retention curves. For example, in [13], only field capacity and wilting point were measured. These data, in conjunction with the bulk density and particle size distribution, were used to estimate the hydraulic properties of substrates using a pedotransfer function. Similarly, Refs. [8,17] assumed water retention parameters from the literature. Li and Babcock [15] acquired the shape parameters (α and n) of the van Genuchten model for water retention [18] from the hanging water column and saturated hydraulic conductivity from laboratory falling head experiments. A comprehensive estimation of both $\theta(h)$ and $K(h)$ functions for a mineral green roof substrate was conducted by [5] and [14] who used a simplified version of the evaporation method with an extended measurement range [19,20]. However, they assumed the saturated soil hydraulic conductivity, K_s, as a fitting parameter and their estimations of soil hydraulic conductivity function basically relies on measurements conducted in the dry range between 10 and 30% of volumetric water content.

In the range of θ values near to soil saturation, an accurate determination of $K(h)$ (or $K(\theta)$) is critically important for highly permeable porous media, like green roof substrates, given they must ensure rapid drainage and avoid water ponding on the surface even during intense precipitation. However, the high non-linearity of hydraulic functions represents a major difficulty as a small change in θ may change K by several orders of magnitude.

A very effective and rapid transient laboratory method for simultaneous determination of both $\theta(h)$ and $K(h)$ relationships for the same sample is the evaporation method, firstly proposed by Wind [21]. The water retention characteristic $\theta(h)$ is first estimated from the average water content and pressure head readings at several locations of the soil sample by an iterative procedure. Then, the unsaturated hydraulic conductivity function is determined from the pressure head profile and the changes in water content distribution. A simplified version of Wind's method was proposed by [22] in which tensiometers are installed at only two depths within a short soil column. However, the linearizing assumptions of the simplified method with respect to time, space and the water content–pressure head relationship could result in marked deviations from the true hydraulic properties for the coarse-textured pore media that are commonly used for green roof design [23].

Apart from this, other limitations may affect the evaporation method. Water cavitation in the tensiometers, typically occurring around −70 to −90 kPa, limits the measurement range on the dry end [19,20]. On the wet end, the major limitations arise from the inability to obtain accurate estimates of the hydraulic conductivity because the hydraulic gradients are too small and subject to uncertainties in tensiometric readings [19,24]. However, many hydrologic and agronomic studies require soil hydraulic property measurements at both lower and higher tensions. Therefore, the integration of evaporation data with independent measurements conducted for both the wet and/or the dry ends seems a valuable solution to improve the soil hydraulic functions' reliability. Water retention data at low pressure head values can be readily obtained by the pressure plate apparatus [25] whereas measurements of near-saturated hydraulic conductivity may be obtained from steady-state head-controlled infiltration experiments, like the unit hydraulic gradient (UHG) [26]. Although the combination of these two techniques is attractive, to our knowledge, measurements of near-saturated hydraulic conductivity on the same sample used for evaporation experiments were conducted only by [19,27]. Furthermore, provided that $\theta(h)$ and $K(h)$ data collected from the evaporation method are generally fitted by closed-form empirical functions like the van Genuchten–Mualem

(VGM) model [18], the consistency between modelled functions and additional steady-state measurements (pressure plate and UGH data) may be problematic and need to be specifically assessed. This is particularly true close to saturation where, due to the influence of the macropore domain, unimodal functions may be inappropriate to describe the hydraulic properties of green roof substrates [3,28–30].

Parameter optimization based on an inverse solution of the Richards equation has been largely used for soil hydraulic characterization (e.g., [31,32]). One of the advantages of the inverse method is the flexibility in modelling the hydraulic properties of the porous media. Though numerically more expensive, inverse modelling was considered preferable to simplified evaporation methods for coarse media with narrow pore-size distribution [33]. The optimization module of the Hydrus-1D model [9] was used to estimate the water retention curve and the hydraulic conductivity function of green roof substrates from simulated rainfall experiments [34–37] but the feasibility of estimating the parameters of the bimodal VGM [28] from an inverse approach was not explored.

The present study was performed with the main objective of developing a laboratory procedure for the hydraulic characterization of green roof artificial substrates based on evaporation and steady-state UHG experiments. The hydraulic properties of the substrates obtained with the direct Wind method were compared with those obtained by numerical inversion of the evaporation transient experiments performed by Hydrus-1D software. The agreement with independent near-saturated K measurements was assessed with the aim of establishing the reliability of unimodal and bimodal VGM models to describe the hydraulic properties of the considered artificial substrates. Specific aims were addressed, including the following: (i) evaluating the influence of fixing the parameters related to the dry portion of $\theta(h)$ and $K(h)$ functions, namely the residual volumetric water content θ_r and the shape parameter λ, and (ii) establishing the best approach to obtain mean $\theta(h)$ and $K(h)$ functions representative of several replicate samples.

2. Materials and Methods

2.1. Substrate Characteristics

Three green roof substrates were considered in this investigation, including two commercial substrates and a specifically developed growing substrate that showed good hydraulic characteristics for use in ornamental plant production [38]. The first commercial substrate is Terra Mediterranea® (TMT), manufactured by Harpo Verdepensile (Harpo spa, Trieste, Italy), consisting of a mixture of 80% mineral fraction (lapillus, pumice and zeolite) and 20% organic fraction (peat and compost). According to the technical specifications released by the manufacturer, the substrate dry bulk density, ρ_b, is 850–1000 kg m^{-3}, the saturated hydraulic conductivity, K_s, is larger than 1200 mm h^{-1} and the field capacity (i.e., water content at 100 cm suction), θ_{fc}, is 0.30–0.45 m^{3}m^{-3}.The second commercial substrate is AgriTERRAM® TV (ATV) manufactured by Perlite Italiana srl (Corsico, Milan, Italy). The mineral fraction (75–80%) includes lapillus, pumice and expanded perlite and the organic fraction (20–25%) includes peat, bark, coconut fiber and organic conditioners. Technical specifications certify that ρ_b = 400 kg m^{-3}, K_s > 780 mm h^{-1} and θ_{fc} > 0.50 m^{3}m^{-3}. The third growing substrate (MIX) was prepared by mixing on a volume basis 25% peat, 25% compost and 50% mineral soil. Commercial 100% sphagnum peat moss (Vigorplant, Fombio, Lodi, Italy) and 5-month-aged compost from orange juice processing wastes and garden cleaning [39] were used as organic fractions. The mineral fraction was obtained using 2 mm sieved sandy loam soil (Typic Rhodoxeralf, clay = 15.9%, silt = 27.2%, sand = 56.9%, USDA).

For each substrate, four replicated samples were prepared by compacting a given weight of material into plastic cylinders with a 9.3 cm inner diameter and 12 cm height. In order to avoid artefacts due to sample preparation, compaction was conducted in four successive steps by beating the substrates with five strokes from a height of 5 cm followed by five rotations with a pestle at each increment.

2.2. Evaporation and UHG Experiments

Given the evaporation method yields the drying branch of the unsaturated hydraulic functions (Figure 1a), the UHG experiment was performed prior to the evaporation experiment and following a descending sequence of applied pressure heads. A device similar to the one described by [26] was used (Figure 1b). Samples were saturated from the bottom on the porous plate of a glass funnel, with an air entry value of −40 cm, connected to an outflow tube that could be moved in height to establish a given h value at the bottom of the sample. A pressure head at the top of the sample was applied using a tension infiltrometer with an 8.5 cm diameter porous disk (Soil Measurement Systems, Tucson, AZ, USA). A thin layer of 2 mm sieved material was spread on the surface of TMT and ATV to ensure a good and stable hydraulic connection with the infiltrometer plate. The same h value was applied at both the upper and lower boundaries in order to establish and maintain a downward unit gradient flux. Under the assumption that the hydraulic gradient is a unit, the unsaturated hydraulic conductivity is equal to the measured downward steady-state flux. Steady-state conditions were considered to be achieved when the infiltration rate, at each imposed pressure head value, was constant with time. A sequence of pressure head values of −6, −12 and −18 cm was applied in succession.

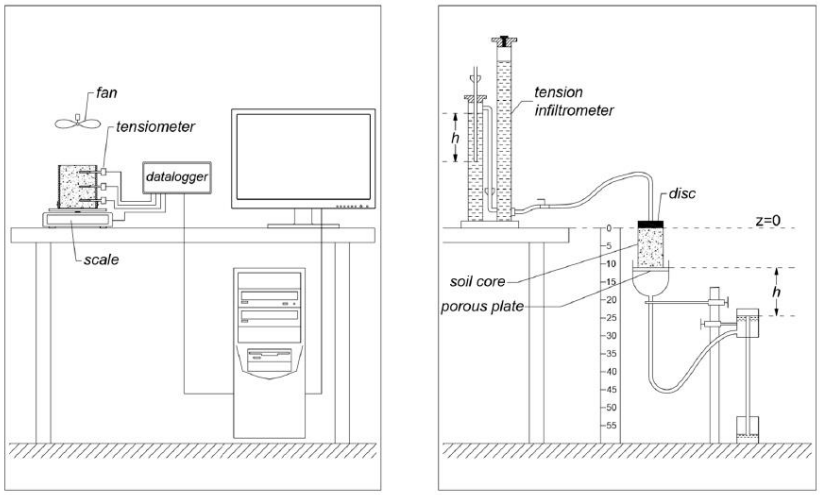

(**a**) (**b**)

Figure 1. Experimental setup for the Wind evaporation method (**a**) and apparatus for measuring unsaturated hydraulic conductivity with UHG method (**b**).

At the end of the UHG experiment, the sample bottom was sealed and three micro-tensiometers were horizontally inserted into holes drilled at 2, 6 and 10 cm heights in order to measure pressure head profiles during the evaporation experiment. The ceramic cups of 3 cm length and 0.6 cm outer diameter were connected to pressure transducers (SDEC, Reignac sur Indre, France). The soil core was then placed on a scale (maximum load 4000 g, resolution 0.1 g) and the evaporation process was allowed to start. Data from scales and tensiometers were automatically acquired and recorded by a CR1000 datalogger (Campbell Scientific, Shepshed, UK) at 1 min time intervals until the upper tensiometer stopped working properly. A blower was used to enhance the soil evaporation rate. For the entire duration of the evaporation experiments, the laboratory temperature was maintained at 22 ± 1 °C.

Depending on the characteristics of the tested substrates, the duration of evaporation experiments was from 72 to 170 hr for TMT, from 141 to 324 hr for ATV and from 222 to 489 h for MIX. The range of the explored pressure head values was rather limited, with the minimum measured h value equal to –282, –87 and –439 cm for TMT, ATV and MIX, respectively, but in line with the results obtained by [14] for TMT and [40] for coarse textured green roof substrates.

At the end of the experiment, the tensiometers were removed and the final water content of the substrate was determined by weighing the sample after oven drying at 105 °C. The average water contents of the soil sample at different times were backward calculated from recorded weights and final water content. For the calculation of hydraulic properties with the Wind iterative method [21], the soil core was divided into three compartments, centered on the tensiometer positions, with a constant thickness of 4 cm.

The volumetric water contents at a h value of −150 m, θ_{150}, were determined by the pressure plate extractors on three replicated samples of 5-cm diameter by 1 cm height [25].

2.3. Determination of the Soil Hydraulic Functions

On the assumption that the soil column is homogeneous, determination of the water retention characteristic involved the following iterative procedure:

1. An initial guess fitting of the van Genuchten [18] water retention curve was achieved from the mean values of the pressure head at the three depths, $\overline{h}_i = (h_{1,i} + h_{2,i} + h_{3,i})/3$ and the average sample water contents, $\overline{\theta}_i$, measured at the same time;
2. Using the fitted water retention curve, water contents, $\theta_{k,i}$, were estimated at depths and times at which the pressure heads were measured;
3. The estimated average water contents were compared with the measured water storages of the soil sample obtained from weighting and the differences equally redistributed among the three compartments;
4. From these $\theta_{k,i}$ vs. $h_{k,i}$ pairs, an updated water retention curve was obtained;
5. Steps 3 and 4 were repeated until the maximum absolute change in water storage values between two successive iterations was < 0.0001 $m^3 m^{-3}$.

In general, three iterations were sufficient to reach convergence.

Temporal changes in water content for each of the three compartments were used to compute hydraulic conductivity by means of a modified instantaneous profile method. During the time interval $\Delta t = t_{i+1} - t_i$, the water flux, q_k (L T^{-1}) from the compartment k upward in the compartment $k + 1$ is approximated by:

$$q_k = -\frac{(\theta_{k,\,i+1} - \theta_{k,\,i})\Delta z}{\Delta t} + q_{k-1,i} \quad (1)$$

in which Δz (L) is the compartment thickness (in this case Δz = 4 cm). The hydraulic conductivity, K (L T^{-1}), was consequently computed according to the Darcy equation as follows:

$$K_k\left(\overline{h}\right) = -\frac{q_k}{(\Delta h/\Delta z)_{k,k+1} + 1} \quad (2)$$

where $(\Delta h/\Delta z)_{k,k+1}$ is the average pressure head gradient between two consecutive compartments as measured from tensiometer readings at two consecutive times (t_i and t_{i+1}).

Corresponding h (or θ) values for the $K(h)$ (or $K(\theta)$) relationships were calculated from:

$$\overline{h} = \frac{h_{k,i} + h_{k,i+1} + h_{k+1,i} + h_{k+1,i+1}}{4} \quad (3)$$

$$\overline{\theta} = \frac{\theta_{k,i} + \theta_{k,i+1} + \theta_{k+1,i} + \theta_{k+1,i+1}}{4} \quad (4)$$

In view of the high uncertainty at low gradients due to the limited sensitivity of tensiometers, all K values obtained from hydraulic gradients lower than −0.2 m m^{-1} were excluded from the analysis.

2.4. Data Analysis

Coupled h vs. θ and K vs. h data obtained for each soil sample from the UHG and evaporation experiments were fitted by the unimodal van Genuchten–Mualem model [18] (VGM):

$$S_e = \frac{\theta(h) - \theta_r}{\theta_s - \theta_r} = \frac{1}{\left(1 + |\alpha h|^n\right)^m} \quad (5)$$

$$K(h) = K_s S_e^{\lambda} \left[1 - \left(1 - S_e^{\frac{1}{m}}\right)^m\right]^2 \quad (6)$$

where S_e is the effective water content, K_s (LT^{-1}), is the saturated hydraulic conductivity, θ_r and θ_s (L^3L^{-3}) denote the residual and the saturated water contents, respectively, λ is a pore connectivity parameter, and α (L^{-1}), n, and m (=$1 - 1/n$) are empirical parameters. Given that θ_r and λ influence the dry end of the soil hydraulic functions [41,42], it is likely that these parameters, when left unconstrained, could be poorly estimated. Therefore, it appeared worthwhile to evaluate if fixing θ_r and λ to an a priori fixed value could influence the quality of estimated $\theta(h)$ and $K(h)$ functions.

In order to verify the role of fixing/estimating θ_r and λ parameters, the following preliminary analyses were conducted:

6. The retention data obtained by the evaporation method were fitted using Equation (5) considering α, n, and θ_s as fitting parameters, whereas θ_r was either fitted or fixed at θ_{150};
7. The hydraulic conductivity data obtained by the evaporation method were fitted using Equation (6) considering α, n, θ_s and θ_r values obtained from the previous step, K_s as a fitting parameter and λ either fitted or fixed at $\lambda = 0.5$.

The quality of fitting was evaluated for each substrate sample in terms of the Root Mean Square Error (RMSE) and Nash–Sutcliffe Efficiency (NSE) [43,44]. When the estimates obtained considering a different number of fitted parameters were compared, the Akaike's information criterion (AIC) was also considered. The best fitting approach was selected as the one with the smallest value of AIC in order to penalize overfitting [5,45].

The possibility of estimating parameters of Equations (5) and (6) by the inverse method was also evaluated. To this aim, the sample weights and the pressure heads in the three compartments of the sample collected at 1 h intervals during the transient evaporation process were used as the input of the inverse method package of Hydrus-1D software [9]. Parameters α, n, and θ_s and K_s were estimated, while θ_r and λ were fixed at the optimal values obtained in the preceding step. Soil hydraulic properties obtained by the inverse method were compared with those obtained by the direct Wind method. Comparison was conducted either considering each replicated sample separately or the average $\theta(h)$ or $K(h)$ curves obtained by the four replicates. Specifically, average $\theta(h)$ or $K(h)$ curves were obtained by two approaches: (i) θ and K values were sampled at fixed h values (46 values for both θ and K) and averaged, the parameters of averaged $\theta(h)$ or $K(h)$ curves were then obtained by fitting the VGM model; (ii) the VGM parameters of the four samples were averaged and a curve corresponding to the average parameters considered.

Finally, the mean $K(h)$ relationships obtained from direct and inverse methods were compared with the mean near-saturated hydraulic conductivity values measured at -6, -12 and -18 cm by the UHG method. This last analysis aimed at evaluating the ability of the evaporation experiment when analyzed using the direct or inverse method to estimate accurate K values close to saturation. In order to increase the flexibility of $\theta(h)$ or $K(h)$ function to fit the measured data, the bimodal van Genuchten–Mualem model was used as follows [28]:

$$S_e = \omega_1 \left[1 + (\alpha_1 h)^{n_1}\right]^{m_1} + \omega_2 \left[1 + (\alpha_2 h)^{n_2}\right]^{m_2} \quad (7)$$

$$K_{(S_e)} = K_s \frac{(\omega_1 S_{e_1} + \omega_2 S_{e_2})^{\lambda} \left(\omega_1 \alpha_1 \left[1 - \left(1 - S_{e_1}^{\frac{1}{m_1}} \right)^{m_1} \right] + \omega_2 \alpha_2 \left[1 - \left(1 - S_{e_2}^{\frac{1}{m_2}} \right)^{m_2} \right] \right)^2}{(\omega_1 \alpha_1 + \omega_2 \alpha_2)^2} \quad (8)$$

where ω_1 and ω_2 are the weighting factors for the two flow regions (micro- and macropores), and α_i, n_i, m_i (=1 − 1/n_i), and λ are empirical parameters of the separate hydraulic functions (i = 1, 2).

3. Results

3.1. Estimation of Soil Hydraulic Functions by Direct Wind Method

The retention curves obtained for the different replicated samples of the three considered substrates are plotted in Figure 2. For both conditions (θ_r fitted or fixed at θ_{150}), the estimated retention curves effectively reproduced the measured *θ(h)* values and the two curves mostly overlapped in the measurement range. The estimated values of the volumetric water content at saturation, θ_s, ranged from 0.46 to 0.48 cm^3cm^{-3} and from 0.53 to 0.59 cm^3cm^{-3} for the TMT and MIX substrates, respectively. For these substrates, the differences in θ_s estimated with the two procedures were the most equal to 0.01 cm^3cm^{-3}. It was concluded that a close estimation of θ_s can be obtained independently of the considered estimation strategy. The only exception was for two samples of the ATV substrate in which the difference between the two estimated θ_s values reached 0.09 cm^3cm^{-3}.

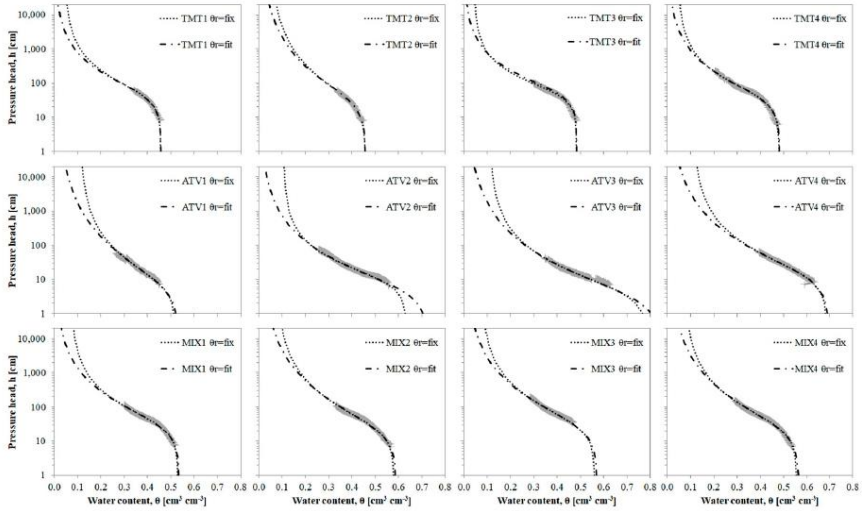

Figure 2. Retention curves obtained for each sample of the three substrates (TMT, ATV and MIX) by assuming θ_r was fitted (θ_r = fit) or fixed at θ_{150} (θ_r = fix). The grey dots represent the measured values.

For all the considered experiments (n = 12), when θ_r was estimated (θ_r = fit), the iterative Wind procedure yielded θ_r = 0 as the best solution and, therefore, θ_r was fixed at zero. Compared to the $\theta_r = \theta_{150}$ strategy, this resulted in a systematic underestimation of *θ(h)* in the dry range of the water retention curve. The goodness of fit for both strategies is indicated by the low RMSE values and the NSE value close to one. Specifically, the RMSE values ranged from a minimum of 0.002 to a maximum of 0.013 cm^3cm^{-3}, whereas the NSE index was always higher than 0.97.

For the TMT and ATV substrates, no clear preference for a specific estimation strategy could be claimed. For the MIX substrate, fixing the residual water content at the value measured for $h = \theta_{150}$ m generally yielded better estimates of the water retention curve (Table 1). From these findings, it can be deduced that the estimation of the retention curve carried out with the direct Wind method is more accurate if an appropriate choice of the θ_r parameter is made.

Table 1. Parameters of the retention curves obtained by the direct Wind method by assuming θ_r was fitted or fixed at θ_{150}.

Substrates	Sample	θ_r	θ_s	α	n	m	RMSE	NSE
		[cm^3 cm^{-3}]	[cm^3 cm^{-3}]	[-cm^{-1}]			[cm^3 cm^{-3}]	
TMT	1	0.04 *	0.46	0.020	1.61	0.38	0.002	1.00
	1	0.00	0.46	0.019	1.57	0.36	0.002	1.00
	2	0.04 *	0.46	0.031	1.40	0.29	0.003	0.99
	2	0.00	0.46	0.030	1.36	0.27	0.003	0.99
	3	0.04 *	0.46	0.030	1.41	0.39	0.003	1.00
	3	0.00	0.48	0.016	1.72	0.37	0.003	1.00
	4	0.04 *	0.48	0.023	1.61	0.38	0.007	0.99
	4	0.00	0.48	0.024	1.51	0.34	0.007	0.99
ATV	1	0.11 *	0.52	0.117	1.44	0.31	0.004	0.99
	1	0.00	0.53	0.138	1.30	0.23	0.004	0.99
	2	0.11 *	0.63	0.091	1.68	0.40	0.012	0.98
	2	0.00	0.72	0.177	1.41	0.29	0.013	0.97
	3	0.11 *	0.79	0.203	1.48	0.32	0.008	0.99
	3	0.00	0.85	0.332	1.33	0.25	0.008	0.99
	4	0.11 *	0.69	0.069	1.46	0.31	0.003	1.00
	4	0.00	0.70	0.076	1.35	0.26	0.002	1.00
MIX	1	0.07 *	0.53	0.029	1.56	0.36	0.005	0.99
	1	0.00	0.53	0.030	1.45	0.31	0.006	0.99
	2	0.07 *	0.58	0.037	1.43	0.30	0.006	1.00
	2	0.00	0.59	0.043	1.33	0.25	0.007	0.99
	3	0.07 *	0.56	0.029	1.49	0.33	0.003	1.00
	3	0.00	0.57	0.033	1.38	0.28	0.006	0.99
	4	0.07 *	0.55	0.033	1.47	0.32	0.004	1.00
	4	0.00	0.56	0.039	1.36	0.26	0.005	1.00

* θ_r fixed at θ_{150}.

The measured values of unsaturated soil hydraulics showed a large dispersion at higher pressure heads ($h > -30$ cm) particularly for the two commercial substrates (TMT and ATV) (Figure 3). The uncertainty in $K(h)$ measurements close to saturation is a known drawback of the evaporation method due to the influence of measurement errors when the hydraulic gradients are low. In the case of the commercial substrate, the measurement error influence is probably emphasized by the coarser nature of the material that makes the hydraulic contact with the ceramic cup of the tensiometers more problematic.

For both the considered conditions (λ fitted or fixed at 0.5), the estimated hydraulic conductivity curves overlapped the experimental $K(h)$ values in the measured range of pressure heads (Figure 3). The two estimated $K(h)$ relationships diverged for drier conditions (i.e., low h values). In this range, fitting of the λ parameter generally resulted in an underestimation of the unsaturated hydraulic conductivity function. This was the case for TMT, for which λ ranged from 1.51 to 6.57, sample 1 of ATV (λ = 3.0) and samples 1, 2 and 3 of MIX (λ = 1.32–1.77). Conversely, overestimated $K(h)$ functions in the dry range corresponded to fitted values of λ lower than 0.5 (samples 2, 3 and 4 of ATV and sample 4 of MIX). Due to the direct correlation existing between K_s and λ [32,46], higher estimated saturated hydraulic conductivity values corresponded to higher λ values (Table 2). Fitting a λ parameter greater than 0.5 resulted in an overestimation of K_s by a mean factor of

3.1. When fitted λ was lower than 0.5, K_s was underestimated by a mean factor of 0.87. Therefore, overestimation of K_s when λ was left unconstrained was a more frequent and relevant outcome than the opposite one (underestimation of K_s). It is worth noting that even an overestimation of K_s up to a factor of 2 was not able to fit the near saturated hydraulic conductivity values estimated from UHG experiments (Figure 3). The only exception was for sample 4 of TMT, for which K_s estimated with unconstrained λ was a factor of 12.4 larger than the one estimated with λ = 0.5.

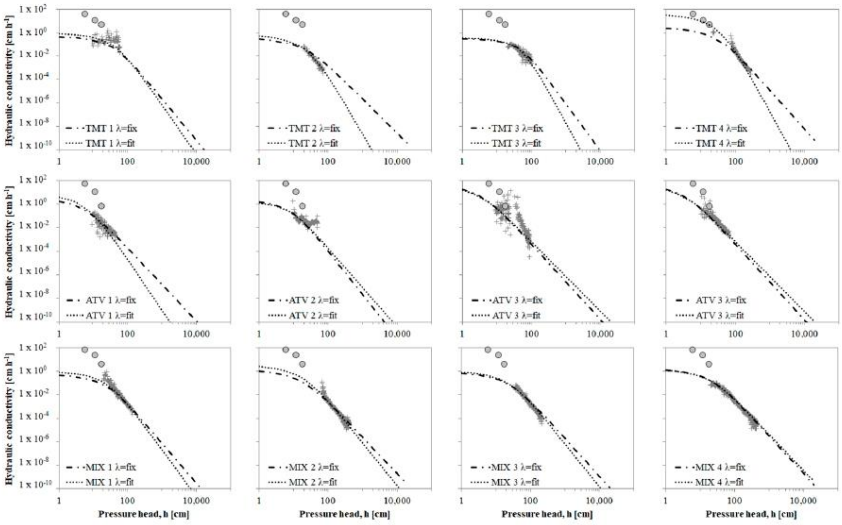

Figure 3. Hydraulic conductivity curves obtained for each sample of the three substrates by considering λ fitted (λ = fit) or fixed at 0.5 (λ = fix). The grey crosses and dots represent the values measured by direct Wind and UGH methods, respectively.

Table 2. Parameters of hydraulic conductivity curves obtained with the Wind iterative approach by assuming λ fitted or fixed at 0.5.

Substrate	Sample	K_s	λ	RMSE	NSE	AIC
		[cm^3 h^{-1}]		[cm^3 cm^{-3}]		
TMT	1	1.08	1.51	0.18	−1.64	0.04
	1	0.58	0.50 *	0.17	−1.50	0.02
	2	1.12	6.57	0.01	0.92	−0.38
	2	0.61	0.50 *	0.01	0.84	−0.17
	3	0.40	2.22	0.03	0.63	−0.22
	3	0.34	0.50 *	0.03	0.61	−0.11
	4	43.34	4.60	0.00	0.97	−0.44
	4	3.50	0.50 *	0.00	0.89	−0.19
ATV	1	10.74	3.30	0.03	0.53	−0.06
	1	4.52	0.50 *	0.03	0.51	−0.03
	2	1.94	0	0.03	0.35	−0.06
	2	2.30	0.50 *	0.03	0.34	−0.03
	3	48.11	0.00	0.14	0.46	0.03
	3	59.39	0.50 *	0.14	0.44	0.01
	4	4.62	0.00	0.07	0.54	−0.02
	4	5.11	0.50 *	0.07	0.53	−0.01

Table 2. *Cont.*

Substrate	Sample	K_s	λ	RMSE	NSE	AIC
MIX	1	1.08	1.51	0.00	0.96	−12.82
	1	0.58	0.50 *	0.00	0.94	−12.57
	2	4.31	1.77	0.00	0.97	−0.21
	2	1.74	0.50 *	0.00	0.96	−0.10
	3	1.25	1.32	0.00	0.90	−0.12
	3	0.97	0.50 *	0.00	0.88	−0.06
	4	1.85	0.26	0.00	0.95	−0.05
	4	1.99	0.50 *	0.00	0.95	−0.03

* λ fixed at 0.5.

The RMSE and NSE values indicated a very good estimation performance for the MIX substrate and a relatively good performance for the other two substrates (Table 2). Only sample 1 of TMT showed negative values of NSE and high values of RMSE. In terms of RMSE and NSE, the two considered estimation strategies (λ fitted or fixed at 0.5) were practically equivalent. For 10 out of 12 samples, the AIC values for fitted λ were lower than those for fixed λ. The two exceptions were sample 1 of TMT and sample 3 of ATV that showed poor RMSE and NSE values. Therefore, the strategy involving fitting of the λ parameter was considered preferable to that assuming a constrained λ value equal to 0.5.

3.2. Estimation of Soil Hydraulic Functions by Inverse Method

The retention and hydraulic conductivity curve parameters of three substrates estimated by the inverse method applied to the evaporation experiments are shown in Table 3. According to the results of the previous section, the θ_r parameter was set at θ_{150} and the λ parameter was estimated. Comparison between the mean soil hydraulic parameters obtained by the direct and inverse methods is reported in Table 4.

Table 3. Parameters of retention and hydraulic conductivity curves obtained by applying the inverse method approach.

Substrates	Sample	θ_r	θ_s	α	n	K_s	λ
		[cm^3 cm^{-3}]	[cm^3 cm^{-3}]	[cm^{-1}]		[cm h^{-1}]	
TMT	1	0.04	0.50	0.06	1.42	2.26	3.66
	2	0.04	0.46	0.04	1.36	0.73	3.10
	3	0.04	0.46	0.03	1.41	0.41	2.83
	4	0.04	0.49	0.03	1.58	10.10	1.54
ATV	1	0.11	0.45	0.09	1.51	1.61	0.09
	2	0.11	0.62	0.09	1.66	13.26	0.00
	3	0.11	0.69	0.12	1.49	21.13	0.00
	4	0.11	0.70	0.08	1.44	100.00	4.23
MIX	1	0.07	0.55	0.04	1.52	4.63	2.53
	2	0.07	0.61	0.05	1.42	4.15	0.97
	3	0.07	0.48	0.02	1.42	0.33	2.46
	4	0.07	0.58	0.05	1.43	17.78	2.11

The parameters of the water retention curves (i.e., α, n, and θ_s) obtained as the mean of the parameters of Equation (5) fitted to the individual samples were practically identical to those obtained by fitting Equation (5) to the mean water retention data. Minor differences in the two averaging approaches were found for hydraulic conductivity function parameters (K_s and λ). However, the differences in estimated K_s were reported within a factor of 0.96–1.04 that is negligible in practice. It was concluded that the two averaging approaches yielded coincident estimations of the substrate hydraulic properties as far as the unimodal VGM model is considered.

Table 4. Soil hydraulic parameters obtained by the direct Wind method and the inverse Hydrus-1D method by considering two averaging approaches.

Substrate	Method	Averaging Method	θ_s	α	n	K_s	λ
			[$cm^3\ cm^{-3}$]	[cm^{-1}]		[$cm\ h^{-1}$]	
TMT	direct	$\theta(h)$ and $K(h)$ curves	0.47	0.02	1.61	1.68	3.97
	direct	estimated parameters	0.47	0.02	1.60	1.62	6.60
	inverse	$\theta(h)$ and $K(h)$ curves	0.48	0.04	1.44	1.61	2.65
	inverse	estimated parameters	0.48	0.04	1.46	1.60	3.26
ATV	direct	$\theta(h)$ and $K(h)$ curves	0.66	0.12	1.51	8.90	0.24
	direct	estimated parameters	0.66	0.11	1.42	9.24	0.00
	inverse	$\theta(h)$ and $K(h)$ curves	0.61	0.09	1.52	14.56	0.03
	inverse	estimated parameters	0.61	0.10	1.51	14.62	0.30
MIX	direct	$\theta(h)$ and $K(h)$ curves	0.56	0.03	1.49	2.02	1.60
	direct	estimated parameters	0.56	0.03	1.49	2.01	1.65
	inverse	$\theta(h)$ and $K(h)$ curves	0.55	0.04	1.45	3.25	1.89
	inverse	estimated parameters	0.55	0.04	1.43	3.31	0.44

The retention curves and hydraulic conductivity functions obtained for the single samples of the three substrates with the direct and inverse method are compared in Figure 4. The plots confirm the good agreement of water retention curve estimates obtained by the direct and inverse methods with coefficients of determination, R^2, that ranged between 0.9768 and 1.00 (Table 5). On average, the best agreement between the water retention curve estimated by the two methods (i.e., direct and inverse) was observed for the MIX substrate (mean R^2 = 0.9997) and the worst for the TMT substrate (mean R^2 = 0.9973). The correlation for the hydraulic conductivity function was generally lower than the water retention curve, confirming that the two methods could yield different results for $K(h)$ (Table 5). The largest discrepancies were observed for substrate TMT with a mean R^2 of 0.9741. The remaining substrates were characterized by similar mean R^2 values (R^2 = 0.9915 for ATV and R^2 = 0.9916 for MIX). It is worth noting, however, that the worse correspondence observed for the TMT substrate is mostly determined by a single sample (sample TMT 1) that resulted in a very different estimation of λ parameters with the two approaches.

The results demonstrated how the two methods of analysis of the evaporation tests yielded similar results both in terms of the estimated water retention curve and unsaturated hydraulic conductivity functions. However, even with the inverse method, the marked tendency to underestimate the near saturated hydraulic conductivity measured with the UHG method was confirmed.

The bimodal VGM model was used in order to improve the predictive ability of the inverse Hydrus-1D method at high-pressure head values (Table 6). Due to the increased flexibility of the bimodal hydraulic functions, higher values of K_s were obtained that better approached the independently measured values. At the same time, larger λ values were estimated (Table 6). For the TMT substrate, K_s values estimated by the inverse method and the bimodal VGM model ranged from 54.1 to 473.4 cm h^{-1} with an average value of

182.4 cm h^{-1}. For the ATV substrate, estimated K_s values ranged from 75.3 to 315.7 cm h^{-1} with an average value of 235.4 cm h^{-1}. Finally, for the MIX substrate, the estimated K_s values were between 135.8 and 315.6 cm h^{-1} with an average value of 179.2 cm h^{-1}.

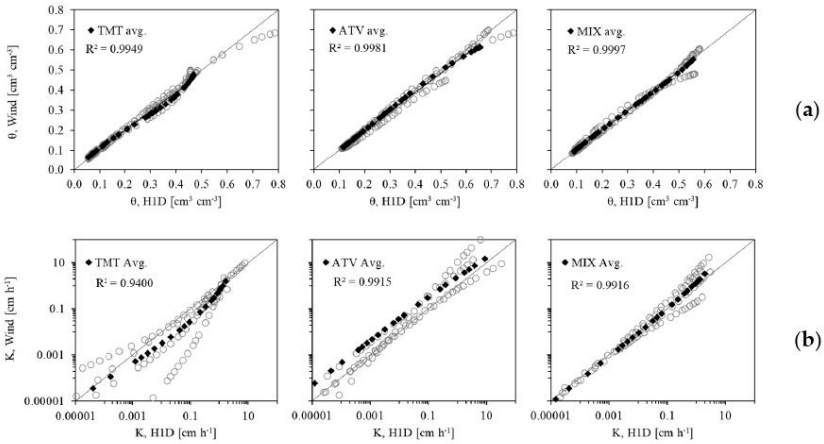

Figure 4. Comparison between (**a**) volumetric water content θ and (**b**) hydraulic conductivity K values estimated for a given h value by the direct Wind and inverse Hydrus-1D methods. Symbols in grey represent the individual samples, while symbols in black represent the average values.

Table 5. Correlation parameters for the water retention and hydraulic conductivity curves obtained from direct Wind and inverse Hydrus-1D methods.

		Water Retention Curve			Hydraulic Conductivity Curve		
Substrates	**Sample**	**Slope**	**Intercept** [cm^3 cm^{-3}]	**R^2**	**Slope**	**Intercept** [cm h^{-1}]	**R^2**
TMT	1	1.03	−0.01	0.9768	0.80	0.10	0.7453
	2	1.03	−0.01	0.9997	2.63	0.00	0.9939
	3	1.18	−0.02	0.9900	1.27	0.02	0.8958
	4	0.99	0.00	0.9992	0.79	0.05	0.9957
	Avg.	1.06	−0.01	0.9943	1.22	0.03	0.9467
ATV	1	1.15	−0.01	0.9992	1.60	−0.02	0.9767
	2	1.02	0.00	1.0000	0.26	0.00	0.9993
	3	1.08	−0.02	0.9889	4.72	−0.89	0.9675
	4	0.99	0.00	0.9997	0.06	0.04	0.9896
	Avg.	1.04	0.02	0.9977	0.59	−0.03	0.9948
MIX	1	1.00	0.00	0.9986	0.31	0.01	0.9848
	2	0.97	0.01	0.9976	0.76	0.02	0.9924
	3	1.19	−0.05	0.9831	4.75	−0.01	0.9924
	4	0.98	0.00	0.9976	0.16	0.04	0.9758
	Avg.	1.03	−0.01	0.9996	0.66	0.01	0.9930

The mean hydraulic conductivity curves obtained by the inverse method considering unimodal and bimodal unsaturated hydraulic conductivity functions are plotted in Figure 5. Compared to the unimodal model, the bimodal model was more effective in fitting the experimental data points obtained with the UHG method at a pressure head close to zero.

Table 6. Parameters of the van Genuchten bimodal water retention (Equation (7)) and hydraulic conductivity (Equation (8)) functions obtained by the inverse method.

Substrate	Sample	θ_r	θ_s	α_1	n_1	K_s	λ	ω_2	α_2	n_2
		[cm^3 cm^{-3}]	[cm^3 cm^{-3}]	[cm^{-1}]		[cm h^{-1}]			[cm^{-1}]	
TMT	1	0.04	0.50	0.062	3.07	54.12	2.15	0.168	0.003	1.100
	2	0.04	0.47	0.086	1.29	473.40	9.52	0.730	0.030	1.340
	3	0.04	0.46	0.010	1.30	121.30	5.44	0.105	0.010	1.100
	4	0.04	0.48	0.021	1.65	80.89	3.31	0.099	0.115	3.762
	Avg.	0.044	0.476	0.045	1.83	182.43	5.10	0.275	0.040	1.826
ATV	1	0.11	0.45	0.070	2.02	286.20	5.13	0.360	0.044	1.110
	2	0.11	0.60	0.075	2.08	263.10	3.67	0.380	0.058	1.300
	3	0.11	0.67	0.080	3.97	75.25	3.18	0.575	0.019	1.714
	4	0.11	0.66	0.031	1.42	315.70	6.09	0.392	0.090	1.877
	Avg.	0.106	0.595	0.064	2.37	235.06	4.52	0.427	0.052	1.500
MIX	1	0.07	0.55	0.068	5.54	135.80	7.74	0.894	0.030	1.519
	2	0.07	0.60	0.046	1.10	315.60	4.75	0.579	0.048	1.977
	3	0.07	0.46	0.013	2.38	155.30	10.11	0.067	0.072	5.000
	4	0.07	0.58	0.057	2.99	110.00	4.68	0.609	0.017	1.332
	Avg.	0.070	0.546	0.046	3.00	179.18	6.82	0.537	0.042	2.457

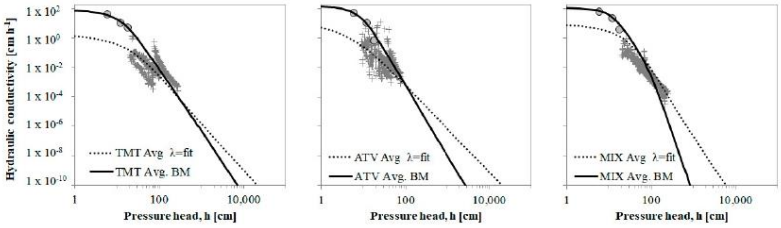

Figure 5. Hydraulic conductivity curves obtained by the inverse method considering unimodal (Equations (5) and (6), dot line) and bimodal (Equations (7) and (8), continuous line) VGM models. Lines represent the average of four replicated samples. Grey crosses and dots represent the measured *K(h)* values of individual samples measured by direct Wind and UGH methods, respectively.

4. Discussion

The direct Wind [21] evaporation method with a pressure head measured at three heights allowed an accurate description of the unimodal water retention curve of the three considered substrates, provided the θ_r parameter is fixed at the water content value measured at $h = -150$ m. Despite showing a relative larger dispersion at high h values, the measured unsaturated hydraulic conductivity data were adequately fitted by the unimodal VGM model when the λ parameter was left unconstrained. The direct Wind and the inverse Hydrus-1D methods yielded estimations of the water retention data that were practically coincident and highly correlated ($R^2 > 0.97$) estimations of *K(h)*. The experimental setup consisting of three tensiometers at 4 cm intervals seemed adequate to estimate the hydraulic properties of coarse green roof substrates that may be problematic with the simplified evaporation method, making use of only two tensiometers [23,33]. A very good estimation performance for the MIX substrate and a relatively good performance for the coarser TMT and ATV substrates was obtained, thus confirming that this sample schematization improved identification of the non-linearity of $h(t)$ profiles in the initial stage of the transient process and reduced errors caused by linearization and quasi steady-state assumptions [24]. However, for pressure heads higher than −30 cm, direct measurement of $K(h)$ was inaccessible due to the estimates of the hydraulic gradient that become too small. This is a well-known limitation of the evaporation method that can be overcome by

conducting UHG and evaporation experiments in succession on the same sample [20,27]. However, our results showed that this strategy was not enough in the case of green roof substrates that present a heterogeneous composition with a double order of pores of different sizes, i.e., micropores and macropores [30]. Indeed, the independently measured hydraulic conductivity values close to saturation were always underestimated.

When the inverse method with the hydraulic properties expressed by the bimodal VGM model was used, a close description of the $K(h)$ function in the range from saturation to the lower limit of the evaporation method was obtained. The effective benefit of using the bimodal VGM model was sometimes questioned. Peng et al. [3] and Liu and Fassman-Beck [29] showed that the bimodal VGM model improved the description of substrates' water retention but the hydraulic conductivity was effectively improved only when a three-modal function was considered. Turco et al. [30] showed that although the substrate could have a bimodal behavior, the differences between uni- and bimodal soil hydraulic characteristics had minimal effects on the hydrological functioning of a green roof, given the error in simulated runoff volume is less than 1%. They concluded that the unimodal model must be preferred instead of the bimodal due to the lower number of estimated parameters.

5. Conclusions

The knowledge of the substrate hydraulic properties, i.e., the relationships between the water pressure head, h, the volumetric water content, θ, and the hydraulic conductivity, K, of the porous medium, is crucial for the simulation of water fluxes in green roofs by mechanistic models. The evaporation method could be a very effective and rapid transient laboratory method for simultaneous determination of $\theta(h)$ and $K(h)$ relationships. In this study, we applied the Wind evaporation method supplemented by steady-state independent measurements of $K(h)$ conducted close to saturation to estimate the hydraulic properties of artificial substrates designed for green roof preparation. The results confirmed that the evaporation method, either direct or inverse, is inadequate to estimate the near saturated hydraulic conductivity of heterogeneous pore media like the substrates under study. A much better description of the $K(h)$ function could be obtained only when the inverse method with the bimodal VGM model was used. Therefore, this approach could be recommended as an effective strategy for green roof substrate characterization.

However, further investigation is necessary to assess the effectiveness of the bimodal models in improving the simulation of the hydraulic processes that occur in extensive green roofs subjected to natural rainfall and evapotranspiration.

Author Contributions: Conceptualization, M.I.; methodology, D.A., V.A. and C.B.; formal analysis, D.A. and V.A.; investigation, D.A., V.A. and C.B.; data curation, D.A. and M.I.; writing—original draft preparation, D.A. and M.I.; writing—review and editing, D.A., V.A., C.B. and M.I. All authors have read and agreed to the published version of the manuscript.

Funding: This research was funded by the European Union—FESR or FSE, PON Research and Innovation 2014–2020—DM 1062/2021 and PRIN 2022 PNRR "NBS4STORWATER", Next Generation EU, M4C2, CUP B53D23023760001.

Institutional Review Board Statement: Not applicable.

Informed Consent Statement: Not applicable.

Data Availability Statement: The raw data supporting the conclusions of this article will be made available by the authors on request.

Conflicts of Interest: The authors declare no conflicts of interest.

References

1. Czemiel Berndtsson, J. Green Roof Performance towards Management of Runoff Water Quantity and Quality: A Review. *Ecol. Eng.* **2010**, *36*, 351–360. [CrossRef]
2. Stovin, V.; Poë, S.; De-Ville, S.; Berretta, C. The Influence of Substrate and Vegetation Configuration on Green Roof Hydrological Performance. *Ecol. Eng.* **2015**, *85*, 159–172. [CrossRef]

3. Peng, Z.; Smith, C.; Stovin, V. The Importance of Unsaturated Hydraulic Conductivity Measurements for Green Roof Detention Modelling. *J. Hydrol.* **2020**, *590*, 125273. [CrossRef]
4. Kasmin, H.; Stovin, V.R.; Hathway, E.A. Towards a Generic Rainfall-Runoff Model for Green Roofs. *Water Sci. Technol.* **2010**, *62*, 898–905. [CrossRef] [PubMed]
5. Brunetti, G.; Šimůnek, J.; Piro, P. A Comprehensive Analysis of the Variably Saturated Hydraulic Behavior of a Green Roof in a Mediterranean Climate. *Vadose Zone J.* **2016**, *15*, vzj2016-04. [CrossRef]
6. Peng, Z.; Garner, B.; Stovin, V. Two Green Roof Detention Models Applied in Two Green Roof Systems. *J. Hydrol. Eng.* **2022**, *27*, 04021049. [CrossRef]
7. Krebs, G.; Kuoppamäki, K.; Kokkonen, T.; Koivusalo, H. Simulation of Green Roof Test Bed Runoff. *Hydrol. Process* **2016**, *30*, 250–262. [CrossRef]
8. Metselaar, K. Water Retention and Evapotranspiration of Green Roofs and Possible Natural Vegetation Types. *Resour. Conserv. Recycl.* **2012**, *64*, 49–55. [CrossRef]
9. Simunek, J.; Sejna, M.; Saito, H.; Sakai, M.; van Genuchten, M.T. *The HYDRUS-1D Software Package for Simulating the One-Dimensional Movement of Water, Heat, and Multiple Solutes in Variably-Saturated Media*; Version 4.08. HYDRUS Softw. Ser. 3; University of California-Riverside Research Reports: Riverside, CA, USA, 2009.
10. Simunek, J.; Van Genuchten, M.T.; Sejna, M. The HYDRUS Software Package for Simulating the Two- and Three-Dimensions Movement of Water, Heat, and Multiple Solutes in Variably-Saturated Media. *Tech. Man.* **2011**, *1*, 241.
11. Ghazouani, H.; M'Hamdi, B.D.; Autovino, D.; Bel Haj, A.M.; Rallo, G.; Provenzano, G.; Boujelben, A. Optimizing Subsurface Dripline Installation Depth with Hydrus 2D/3D to Improve Irrigation Water Use Efficiency in the Central Tunisia. *Int. J. Metrol. Qual. Eng.* **2015**, *6*, 402. [CrossRef]
12. Basile, A.; Albrizio, R.; Autovino, D.; Bonfante, A.; De Mascellis, R.; Terribile, F.; Giorio, P. A Modelling Approach to Discriminate Contributions of Soil Hydrological Properties and Slope Gradient to Water Stress in Mediterranean Vineyards. *Agric. Water Manag.* **2020**, *241*, 106338. [CrossRef]
13. Hilten, R.N.; Lawrence, T.M.; Tollner, E.W. Modeling Stormwater Runoff from Green Roofs with HYDRUS-1D. *J. Hydrol.* **2008**, *358*, 288–293. [CrossRef]
14. Palermo, S.A.; Turco, M.; Principato, F.; Piro, P. Hydrological Effectiveness of an Extensive Green Roof in Mediterranean Climate. *Water* **2019**, *11*, 1378. [CrossRef]
15. Li, Y.; Babcock, R.W. Modeling Hydrologic Performance of a Green Roof System with HYDRUS-2D. *J. Environ. Eng.* **2015**, *141*, 04015036. [CrossRef]
16. Brunetti, G.; Šimůnek, J.; Turco, M.; Piro, P. On the Use of Surrogate-Based Modeling for the Numerical Analysis of Low Impact Development Techniques. *J. Hydrol.* **2017**, *548*, 263–277. [CrossRef]
17. Palla, A.; Gnecco, I.; Lanza, L.G. Unsaturated 2D Modelling of Subsurface Water Flow in the Coarse-Grained Porous Matrix of a Green Roof. *J. Hydrol.* **2009**, *379*, 193–204. [CrossRef]
18. van Genuchten, M.T. A Closed-Form Equation for Predicting the Hydraulic Conductivity of Unsaturated Soils. *Soil Sci. Soc. Am. J.* **1980**, *44*, 892–898. [CrossRef]
19. Schindler, U.; Durner, W.; von Unold, G.; Müller, L. Evaporation Method for Measuring Unsaturated Hydraulic Properties of Soils: Extending the Measurement Range. *Soil Sci. Soc. Am. J.* **2010**, *74*, 1071–1083. [CrossRef]
20. Schindler, U.; Durner, W.; von Unold, G.; Mueller, L.; Wieland, R. The Evaporation Method: Extending the Measurement Range of Soil Hydraulic Properties Using the Air-Entry Pressure of the Ceramic Cup. *J. Plant Nutr. Soil Sci.* **2010**, *173*, 563–572. [CrossRef]
21. Wind, G.P. Capillary Conductivity Data Estimated by a Simple Method. In *Water in the Unsaturated Zone, Proceedings of Wageningen Symposium*; Institute for Land and Water Management Research: Wageningen, The Netherlands, 1969; Volume 1, p. 1.
22. Schindler, U. Ein Schnellverfahren Zur Messung Der Wasserleitfähigkeit Im Teilgesättigten Boden an Stechzylinderproben. *Arch. Acker Pflanzenbau Bodenkd.* **1980**, *24*, 1–7.
23. Peters, A.; Iden, S.C.; Durner, W. Revisiting the Simplified Evaporation Method: Identification of Hydraulic Functions Considering Vapor, Film and Corner Flow. *J. Hydrol.* **2015**, *527*, 531–542. [CrossRef]
24. Peters, A.; Durner, W. Simplified Evaporation Method for Determining Soil Hydraulic Properties. *J. Hydrol.* **2008**, *356*, 147–162. [CrossRef]
25. Dane, J.H.; Hopmans, J.W. Pressure Plate Extractor. In *Methods of Soil Analysis, Part 4, Physical Methods*; Dane, J.H., Topp, G.C., Eds.; Soil Science Society of America, Inc.: Madison, WI, USA, 2002; pp. 680–683.
26. Bagarello, V.; Castellini, M.; Iovino, M. Comparison of Unconfined and Confined Unsaturated Hydraulic Conductivity. *Geoderma* **2007**, *137*, 394–400. [CrossRef]
27. Sarkar, S.; Germer, K.; Maity, R.; Durner, W. Measuring Near-Saturated Hydraulic Conductivity of Soils by Quasi Unit-Gradient Percolation—2. Application of the Methodology. *J. Plant Nutr. Soil Sci.* **2019**, *182*, 535–540. [CrossRef]
28. Durner, W. Hydraulic Conductivity Estimation for Soils with Heterogeneous Pore Structure. *Water Resour. Res.* **1994**, *30*, 211–223. [CrossRef]
29. Liu, R.; Fassman-Beck, E. Pore Structure and Unsaturated Hydraulic Conductivity of Engineered Media for Living Roofs and Bioretention Based on Water Retention Data. *J. Hydrol. Eng.* **2018**, *23*, 04017065. [CrossRef]

30. Turco, M.; Palermo, S.A.; Polizzi, A.; Presta, L.; Pirouz, B.; Piro, P. The Assessment of the Effectiveness of the Unimodal and Bimodal Models to Evaluate the Water Flow through Nature-Based Solutions Substrates. *Water Sci. Technol.* **2023**, *88*, 932–946. [CrossRef] [PubMed]
31. Šimůnek, J.; van Genuchten, M.T.; Wendroth, O. Parameter Estimation Analysis of the Evaporation Method for Determining Soil Hydraulic Properties. *Soil Sci. Soc. Am. J.* **1998**, *62*, 894–905. [CrossRef]
32. Crescimanno, G.; Iovino, M. Parameter Estimation by Inverse Method Based on One-Step and Multi-Step Outflow Experiments. *Geoderma* **1995**, *68*, 257–277. [CrossRef]
33. Iden, S.C.; Blöcher, J.R.; Diamantopoulos, E.; Peters, A.; Durner, W. Numerical Test of the Laboratory Evaporation Method Using Coupled Water, Vapor and Heat Flow Modelling. *J. Hydrol.* **2019**, *570*, 574–583. [CrossRef]
34. Huang, S.; Garg, A.; Mei, G.; Huang, D.; Chandra, R.B.; Sadasiv, S.G. Experimental Study on the Hydrological Performance of Green Roofs in the Application of Novel Biochar. *Hydrol. Process* **2020**, *34*, 4512–4525. [CrossRef]
35. Wang, J.; Garg, A.; Liu, N.; Chen, D.; Mei, G. Experimental and Numerical Investigation on Hydrological Characteristics of Extensive Green Roofs under the Influence of Rainstorms. *Environ. Sci. Pollut. Res.* **2022**, *29*, 53121–53136. [CrossRef]
36. Bouzouidja, R.; Séré, G.; Claverie, R.; Ouvrard, S.; Nuttens, L.; Lacroix, D. Green Roof Aging: Quantifying the Impact of Substrate Evolution on Hydraulic Performances at the Lab-Scale. *J. Hydrol.* **2018**, *564*, 416–423. [CrossRef]
37. Gan, L.; Garg, A.; Wang, H.; Mei, G.; Liu, J. Influence of Biochar Amendment on Stormwater Management in Green Roofs: Experiment with Numerical Investigation. *Acta Geophys.* **2021**, *69*, 2417–2426. [CrossRef]
38. Gugliuzza, G.; Verduci, A.; Iovino, M. Water Retention Characteristics of Substrates Containing Biochar and Compost as Peat and Perlite Replacements for Ornamental Plant Production. *Acta Hortic.* **2021**, *1305*, 507–512. [CrossRef]
39. Bondì, C.; Castellini, M.; Iovino, M. Compost Amendment Impact on Soil Physical Quality Estimated from Hysteretic Water Retention Curve. *Water* **2022**, *14*, 1002. [CrossRef]
40. Sandoval, V.; Bonilla, C.A.; Gironás, J.; Vera, S.; Victorero, F.; Bustamante, W.; Rojas, V.; Leiva, E.; Pastén, P.; Suárez, F. Porous Media Characterization to Simulate Water and Heat Transport through Green Roof Substrates. *Vadose Zone J.* **2017**, *16*, 1–14. [CrossRef]
41. Nimmo, J.R. Comment on the Treatment of Residual Water Content in "A Consistent Set of Parametric Models for the Two-phase Flow of Immiscible Fluids in the Subsurface" by L. Luckner et Al. *Water Resour. Res.* **1991**, *27*, 661–662. [CrossRef]
42. Shinomiya, Y.; Takahashi, K.; Kobiyama, M.; Kubota, J. Evaluation of the Tortuosity Parameter for Forest Soils to Predict Unsaturated Hydraulic Conductivity. *J. For. Res.* **2001**, *6*, 221–225. [CrossRef]
43. Moriasi, D.N.; Arnold, J.G.; Van Liew, M.W.; Bingner, R.L.; Harmel, R.D.; Veith, T.L. Model Evaluation Guidelines for Systematic Quantification of Accuracy in Watershed Simulations. *Trans. ASABE* **2007**, *50*, 885–900. [CrossRef]
44. Duc, L.; Sawada, Y. A Signal-Processing-Based Interpretation of the Nash-Sutcliffe Efficiency. *Hydrol. Earth Syst. Sci.* **2023**, *27*, 1827–1839. [CrossRef]
45. Jarvis, N.; Koestel, J.; Messing, I.; Moeys, J.; Lindahl, A. Influence of Soil, Land Use and Climatic Factors on the Hydraulic Conductivity of Soil. *Hydrol. Earth Syst. Sci.* **2013**, *17*, 5185–5195. [CrossRef]
46. Weynants, M.; Vereecken, H.; Javaux, M. Revisiting Vereecken Pedotransfer Functions: Introducing a Closed-Form Hydraulic Model. *Vadose Zone J.* **2009**, *8*, 86–95. [CrossRef]

Heliyon 9 (2023) e16829

Contents lists available at ScienceDirect

Heliyon

journal homepage: www.cell.com/heliyon

Assessing short- and long-term modifications of steady-state water infiltration rate in an extensive Mediterranean green roof

C. Bondì [a], P. Concialdi [a], M. Iovino [a,*], V. Bagarello [a,b]

[a] Dipartimento di Scienze Agrarie Alimentari e Forestali, Università degli Studi di Palermo, Italy
[b] Centro Interdipartimentale di Ricerca "MIGRARE. Mobilità, differenze, dialogo, diritti", Università degli Studi di Palermo, Italy

ARTICLE INFO

Keywords:
Infiltration
Growing medium
Green roof
Detention capacity
Minidisk Infiltrometer

ABSTRACT

Green roof detention capacity is related to the steady-state infiltration rate, i_s, of the growing medium. With the aim to investigate short- and long-term modifications of the detention capacity of an extensive Mediterranean green roof, three mini-disk infiltrometer (MDI) measurement campaigns were conducted at construction, after one season and after five years of operation. A laboratory experiment was designed to separately measure i_s in the upper and the lower part of the substrate profile. During the first operating season, field i_s increased by a factor of 2.4 and 1.9 for near-saturated (applied pressure head, $h_0 = -30$ mm) and quasi-saturated conditions ($h_0 = -5$ mm), respectively. Similar rainfall height did not induce significant modifications in the upper layer of the laboratory columns, even if contribution of small pores to water infiltration tended to increase. Differently, i_s significantly decreased by a factor of 3.4–5.3 in the lower layer. After the simulated rainfall, the upper layer was less packed (mean bulk density, $\rho_b = 1.083$ kg m^{-3}) and the lower layer was more packed ($\rho_b = 1.218$ kg m^{-3}) as compared with the initial density ($\rho_b = 1.131$ kg m^{-3}) and the lower part enriched in small particles. Short-term modifications in the experimental plot were thus attributed to fine particles washing-off and bulk density decrease in the upper layer, yielding an overall more conductive porous medium. After five years of green roof operation, field i_s did not further increase thus showing that the washing/clogging mechanism was complete after one season or it was masked by counteracting processes, like root development and hydrophobicity.

1. Introduction

Green roof hydrological performance depends on the water retention capacity, i.e. the rainfall volume stored by the growing medium that is lost via evapotranspiration, and the detention of runoff, i.e. the transient storage of rainfall which reduces and delays the peak outflow rate [1,2]. Control of green roof detention properties is required to reduce the risks associated with pluvial flooding and/or combined sewer overflows. However, detention process is difficult to characterize as it combines the effects of plant, substrate and drainage layers as well as their interactions [3].

For the scopes of stormwater management, it is generally assumed that the potential of a green roof to retain and detain runoff remains constant over time. However, similarly to other natural or artificial porous media, the growing substrate may undergo temporal changes due to various biological and physical processes [3]. Root growth can reduce pore volumes due to local compaction

* Corresponding author.
E-mail address: massimo.iovino@unipa.it (M. Iovino).

https://doi.org/10.1016/j.heliyon.2023.e16829
Received 28 March 2023; Received in revised form 30 May 2023; Accepted 30 May 2023
Available online 2 June 2023

and pore filling [4,5]. The decay of dead roots leaves channels which may increase pore spaces and act as flow paths, increasing hydraulic conductivity [6]. Accumulation of suspended solids on the surface or in the void spaces of the porous media is responsible for clogging that reduces infiltration capacity [7,8]. Self-filtration, i.e., the process of particle mobilization and re-deposition within the porous medium, may result in a more compacted and less conductive lower layer [9].

Despite it can be expected that the age of green roof would influence hydraulic performances, specific studies are limited mainly because natural climatic variations tend to mask any subtle changes in the underlying hydrological characteristics of the system [10]. Getter, Rowe and Andresen [11] found that the pore volume doubled (from 41 to 82%) and the water-holding capacity increased from 17 to 67% after five years of usage. However, a review of data from 18 studies did not show any significant effect of green roof age on the annual runoff volume [12]. Seasonal variations of the detention performance of three different substrates were found to be more evident than annual trends due to time variable hydrophobicity of the substrate [13].

According to the conceptual model for green roof detention proposed by Kasmin, Stovin and Hathway [14], runoff occurs only when the field capacity of the substrate is exceeded. Thus, detention is basically controlled by the gravity driven flow through the interconnected larger pores of the growing medium that occurs for moisture content close to saturation. Monitoring the substrate steady-state infiltration rate under saturated or near-saturated conditions is therefore a potentially valuable tool for assessing modifications of detention capacity due to aging.

A relatively easy, rapid and inexpensive measurement of infiltration rate with a minimal disturbance of surface layer can be conducted by the MiniDisk Infiltrometer (MDI) [15]. Furthermore, field infiltration methods maintain functional connection of the conductive pore system with the surrounding medium [16]. Application of MDI allowed to investigate the seasonal variation in saturated and near-saturated hydraulic conductivity of the growing substrate of an extensive green roof plot established at the University of Palermo [17]. After only one growing season, the saturated hydraulic conductivity increased by a factor of 1.4 and the near-saturated hydraulic conductivity by a factor 3.0 compared to the initial values estimated on the new substrate at the time of green roof construction. The main cause of the observed differences was attributed to washing off of fine particles that accumulated in the lower layer. However, measurements of hydraulic conductivity in the lower layer of the growing medium were not conducted and the role of washing/clogging process was hypothesized on the basis of the observed modifications in particle size distribution and substrate bulk density.

This study was conducted to fill the gap of knowledge on the processes underlying the short-term modifications of green roof detention capacity. A laboratory MDI experiment was designed to detect modifications in steady-state infiltration characteristics of the growing substrate as a consequence of particle self-filtration operated by rainfall. Laboratory data were compared with field data obtained by Alagna, Bagarello, Concialdi, Giordano and Iovino [17] during the first year of operation of the extensive green roof plot. Furthermore, with the aim to investigate green roof aging at a longer temporal scale, in-situ MDI tests were replicated in the same full scale plot after five years of operation.

2. Materials and methods

2.1. Field experiments

The extensive green roof experimental plot at the Department of Agricultural, Food and Forest Sciences of University of Palermo is planted with *Sedum sediforme* and covers a plane surface of 18 m^2 (3 m wide by 6 m long). The green roof was constructed with the

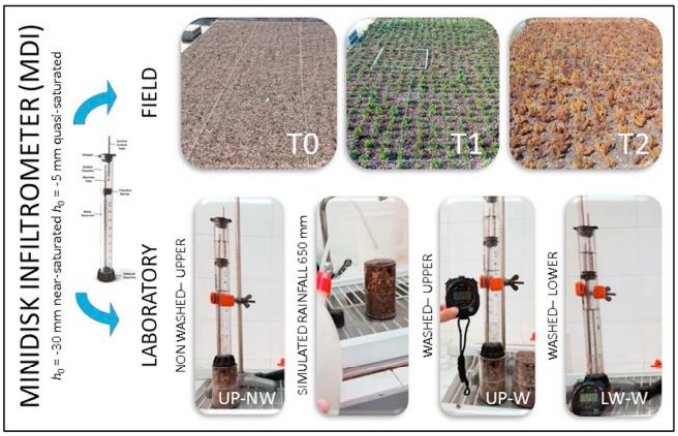

Fig. 1. Experimental setup.

"Mediterranean green roof system" supplied by HARPO Verdepensile (Trieste, Italy) that consists of a 3-cm-thick drainage and accumulation layer and a growing substrate (approximately 8 cm high) made by a mixture of 80% mineral fraction (lapillus, pumice and zeolite) and 20% organic fraction (peat and compost). According to the technical specifications released by the manufacturer, substrate dry bulk density, ρ_b, is 850–1000 kg m^{-3}, saturated hydraulic conductivity, K_s, is larger than 1200 mm/h and field capacity (i.e., water content at 100 cm suction), $\theta_{fc} = 0.30$–0.45 m^{3}m^{-3}.

Field infiltration experiments were conducted at the surface of the experimental plot in December 2017 (T0), at the time of green roof construction, and then in October 2018 (T1) at the end of the first growing season [17]. In summer 2022, i.e. after five years of green roof operation, the experimental plot was sampled again (T2), following the same experimental procedure, to assess long-term variations of the infiltration characteristics. A Minidisk Infiltrometer (MDI) manufactured by Decagon (Decagon Devices, Inc., Pullman, WA) having a disk diameter of 4.5 cm was applied by imposing pressure head, h_0, values of −30 and −5 mm (Fig. 1). The former value of h_0 was established to explore near-saturated conditions given that, according to the capillary law, only pores having an equivalent diameter, d_e, smaller than approximately 1 mm contribute to water flow whereas larger pores are empty. The latter value of h_0 was set to explore saturated (or quasi-saturated) conditions. A slight negative value of h_0 was selected to exclude the artefact due to porous plate resistivity on the assessment of infiltration rate when h is set to zero. In theory, a value of $h_0 = -5$ mm activates pores with equivalent diameter up to 6 mm therefore allowing assessment of substrate transmission properties closely related to the saturated condition. At each sampling date, 18 randomly selected sites were sampled for each of the two considered h_0 values. The surface layer of the experimental plot was also sampled at each measurement site to determine the initial gravimetric water content, U_i (g g^{-1}), after oven-drying at 105 °C for 24 h.

During time interval between T0 and T1, 638 mm rainfall occurred that is very close to the average year precipitation for the area of Palermo (from 637 to 755 mm in the period 2002–2018, depending on the rain gauge location). From T1 to T2, 1432 mm rainfall occurred mainly concentrated in fall-winter months. During the considered time interval (T0 - T2), no irrigation was performed and the vegetation was fed only by natural rainfalls.

For each of 108 infiltration experiments forming the considered dataset (18 locations x 2 pressure heads x 3 campaigns), the steady-state infiltration rate, i_s (mm h^{-1}), was estimated from the slope of the regression line fitted to linear portion of the cumulative infiltration, I (mm), vs. time, t (s), curve. A minimum of five consecutive I vs. t data was considered for regression and the maximum relative error between the estimated and measured I values in the linear portion of the infiltration curve was calculated.

2.2. Laboratory experiments

Nine soil columns were prepared by packing new substrate into plexiglass tubes (internal diameter, $D = 5.5$ cm; height $L = 10$ cm) made by two separate halves to split the soil sample into an upper (UP, 0–5 cm depth) and a lower (LW, 5–10 cm depth) part. A wire mesh (diameter 0.5 mm) and a nylon cloth was put at the bottom of the column to replicate a lower boundary condition similar to that of the experimental plot. The sample preparation was conducted following a repeatable procedure that consisted in filling the tube in four successive layers (each approximately 2.5 cm high) and compacting the sample by tapping it 10 times from a height of 2–3 cm. The mean dry bulk density ($\rho_b = 1.13$ g/cm^3, CV = 5.47%) was larger but not far from the one reported for the full scale green roof by Alagna, Bagarello, Concialdi, Giordano and Iovino [17].

Infiltration tests were performed by a MDI at the same imposed pressure heads of −5 mm and −30 mm at the soil surface. A small amount of 2-mm sieved substrate was spread onto the sample surface to fill the small depression and ensure a full hydraulic contact between the porous plate and the infiltrating surface. Given the dimension of the infiltration source was very close to the sample diameter, the hypothesis of one-dimensional (1D) water flow into the substrate was assumed. Water flow under laboratory conditions was therefore different form the field one. In the latter, a three-dimensional (3D) flux is expected due to the contribution of lateral capillarity as a consequence of unconfined infiltration [16]. However, the use of 1D infiltration experiments seemed appropriate as, under field conditions, the hypothesized self-filtration process activated by rainfall is a vertical process.

Similarly to field experiments, the steady-state infiltration rate, i_s (mm h^{-1}), was determined from the slope of the linear regression line fitted to $I(t)$ data. A minimum of five consecutive I vs. t data was considered for regression and the maximum relative error between the estimated and measured I values in the linear portion of the infiltration curve was calculated.

To simulate the effect of particle washing off operated by rainfalls, the following experimental procedure was followed (Fig. 1). After sample preparation, a first MDI run was performed on the sample surface with the pressure head $h_0 = -30$ mm applied first and $h_0 = -5$ mm after 24 h redistribution (non-washed columns, NW). The soil columns were then washed with 1500 cm^3 water applied in three steps of 500 cm^3 in three consecutive days to simulate the effect of a cumulative rainfall height of 650 mm, that is very close to the total rainfall amount recorded between T0 and T1. Soil columns were allowed to dry under laboratory conditions until an initial soil water content value close to the initial one was reached. A second MDI run was performed on the sample surface with the pressure head $h_0 = -30$ mm applied first and $h_0 = -5$ mm after 24 h redistribution (washed columns, W). Then, the soil columns were disassembled and dried to the same initial soil moisture content under laboratory conditions. A third MDI run was conducted on the surface of the lower part on the column following the same procedure (i.e., infiltration at $h_0 = -30$ mm followed by infiltration at $h_0 = -5$ mm after 24 h redistribution). Soon after the end of the MDI experiments, the upper (UP) and the lower (LW) parts of the soil columns (each having a thickness of 5 cm) were weighted and dried at 105 °C to determine final soil gravimetric water content and bulk density. Crushed samples were then sieved through a series of eight sieves (9.53, 6.0, 5.0, 4.0, 2.8, 2.0, 0.85, 0.25 mm) and the particle size distribution of both the total and the UP and LW parts of the columns determined.

2.3. Statistical analyses

The statistical frequency distribution of i_s data obtained from field and laboratory experiments was checked with the Lilliefors [18] test ($P = 0.05$), considering both a normal (NO) and a ln-normal (LN) distribution. For the field dataset, both the NO and LN distribution hypotheses were rejected for the second sampling date (T1) independently of the applied pressure head value. The LN distribution hypothesis was also rejected for experiments conducted at $h_0 = -30$ mm at third sampling date (T2). Therefore, the non-parametric Mann-Whitney U test [19] was applied to compare i_s data collected at the different field sampling dates ($P = 0.05$). A pairwise approach was applied to establish comparisons between i_s data in accordance with other investigations focused on sampling soil properties at different dates [20].

Both the NO and LN distribution hypothesis were never rejected for the steady-state infiltration rate collected at the two applied pressure heads on the laboratory repacked soil columns. Statistics of i_s were therefore calculated according to a NO distribution. Comparison between mean i_s values collected in the UP part of the column before and after simulated rainfall and between UP and LW parts of the column after water treatment were therefore conducted according to a paired t-test ($P = 0.05$).

A NO distribution was also assumed for U_i values measured at the three sampling dates in the experimental plot and statistical comparisons conducted by F-test and unpaired two-tailed t-test ($P = 0.05$).

3. Results and discussion

3.1. Field experiments

The experimental plot was sampled under different conditions of initial gravimetric water content (Table 1). The lowest mean U_i was measured for the summer sampling (T2) whereas the highest value corresponded to the T1 sampling that was conducted in October a few days after 40.8 mm rainfall occurred. Fall sampling was also characterized by the lowest spatial variability of U_i values. The winter (T0) and fall (T1) samplings showed similar maximum and minimum values but means differed by a factor of 1.36. It is worth noting that the maximum initial substrate water content in summer ($U_i = 0.019$ g g^{-1}) is far below the minimum value measured for the former two campaigns ($U_i = 0.136$ and 0.153 g g^{-1} for T0 and T1, respectively) thus showing the very dry conditions that may occur in the growing substrate during the summer season. The relatively high variability of U_i is line with the general guidelines proposed by Warrick [21] and other field investigations conducted on natural soils (e.g., Refs. [22,23]). However, further investigations need to be conducted to assess if the sampled substrate volume at each site (approximately 200 cm^3) can be considered representative for estimating the moisture content in heterogeneous media characterized by a large coarse fraction (52.3% by mass of particles were larger than 9.53 mm in size).

Independently of the sampling date, infiltration tests conducted at $h_0 = -30$ mm were on average 2.75 times longer than the corresponding tests conducted at $h_0 = -5$ mm. Following the theory, the infiltration rate was generally maximum at the initial stage of infiltration and then approached a steady-state condition [16]. A clear detection of a steady-state phase was always possible as showed by the single R^2 values that were always greater than 0.9848 (mean R^2 values equal to 0.9993 and 0.9992 for $h_0 = -5$ and -30 mm, respectively) and the low values of E_{max} (mean E_{max} equal to 1.2% and 1.5% for $h_0 = -5$ and -30 mm, respectively). Bagarello, Iovino and Reynolds [24] assumed a relative error of 2% between estimated and measured cumulative infiltration as a criterion to establish the onset of the steady-state stage but values up to 5% were considered acceptable [25]. In this investigation, the threshold of 2% was exceeded in 21 out of 108 experiments and the threshold of 5% never exceeded. Therefore, steady-state unconfined infiltration flux was always achieved during the experiments. Due to contribution of the pores with $d_e > 1$ mm, the mean steady-state infiltration rate for quasi-saturated conditions ($h_0 = -5$ mm) was on average 4.8 times larger than under near-saturated ($h_0 = -30$ mm) conditions.

For 3D infiltration into homogeneous soil, i_s depends on both soil hydraulic conductivity and sorptivity [26]. The former controls gravity flow whereas the latter, that depends on the initial soil water content, accounts for lateral expansion of the wetted bulb due to capillarity. The relative influence of the gravity over capillary flow can be detected from the shape of the cumulative infiltration curve, $I(t)$, in the initial transient stage on the infiltration process. A downward concavity indicates that the process is influenced by capillarity whereas a $I(t)$ curve that is linear with time indicates that the process is mainly driven by gravity, with limited or no influence of capillarity [16], and is therefore essentially 1D. An upward concavity of the $I(t)$ curve can occur in particular cases as for infiltration in water repellent soils [27–29]. In order to establish a comparison between field and laboratory infiltration tests, the influence of lateral capillary flow on the field measured infiltration process was preliminarily assessed by calculating the ratio between the mean

Table 1
Statistics of initial gravimetric water content, U_i (g g^{-1}), measured at the green roof plot for the different sampling dates.

	T0	T1	T2
N	18	18	18
min	0.136	0.153	0.007
max	0.304	0.316	0.019
mean	0.178 b	0.234 c	0.012 a
CV	23.3	14.7	25.4

Values followed by the same letter are not significantly different ($P = 0.05$).

infiltration rate, i_m, and the steady-state infiltration rate, i_s. An i_m/i_s ratio close to one identifies a cumulative infiltration curve that is linear with time. An $i_m/i_s > 1$ identifies a downward concavity whereas $i_m/i_s < 1$ an upward concavity.

The i_m/i_s ratio ranged from 0.94 to 1.39 with a mean value of 1.16 for the lower applied pressure head value ($h_0 = -30$ mm) and from 0.90 to 1.48 with a mean value of 1.14 for $h_0 = -5$ mm (Fig. 2). For a given sampling date, the set of i_m/i_s values collected under near-saturated and quasi-saturated conditions were not significantly different thus indicating that, under similar initial water content, the contribution of capillarity was not influenced by the applied pressure head. For both near-saturated and quasi-saturated conditions, Fig. 3 shows the normalized cumulative infiltration (I at any given time/cumulative infiltration at the end of the run, I_f) curves corresponding to the maximum (downward concavity) and the minimum (upward concavity) i_m/i_s values. The case of an infiltration curve with $i_m/i_s = 1$ (i.e., $I(t)$ curve linear on average) is also showed.

No i_m/i_s value lower than 1.0 was observed for the first two sampling dates (T0 and T1) (Fig. 2) and the slope of the regression line between i_m/i_s and U_i was not significantly different from zero, thus confirming that the initial moisture contents did not influence the contribution of lateral capillary flux for $U_i > 0.13$ g g^{-1}. Overall, the i_m/i_s values close to one indicate that the concavity of the measured infiltration curve was generally moderate and most of the infiltration curves showed steady-state conditions from the very beginning of the run. It was concluded that the lateral capillary flow had limited influence on the steady infiltration flux under unconfined field conditions. The steady-state infiltration rate can be therefore considered mainly dominated by gravity flow thus making it reasonable to compare the field MDI 3D tests conducted during the first operating season (T0 and T1 sampling dates) and the laboratory MDI 1D tests on repacked columns.

At the time of green roof construction (T0), the median steady-state infiltration rate was 37.5 mm/h under near-saturated conditions ($h_0 = -30$ mm) with an interquartile range (IQR) of 0.1 mm/h. For quasi-saturated conditions ($h_0 = -5$ mm), a median $i_s = 147.8$ mm/h was detected with an IQR of 35.2 mm/h (Table 2). Assuming the ratio between IQR and median value as a measure of the relative spatial variability of i_s, it was 0.003 at $h_0 = -30$ mm and 0.452 at $h_0 = -5$ mm. Field MDI experiments thus showed that initial packing of substrate resulted in a highly uniform distribution of pores with equivalent diameter, d_e, lower than 1 mm whereas relative spatial variability of larger pores ($d_e > 1$ mm) was two orders of magnitude higher. As documented by Alagna, Bagarello, Concialdi, Giordano and Iovino [17], following one operating season (T1), the steady-state infiltration rate significantly increased by a factor of 2.4 at $h_0 = -30$ mm and a factor of 1.9 at $h_0 = -5$ mm. Spatial variability increased for both small pores (IQR to median ratio = 0.395) and large pores (IQR to median ratio = 0.548). Therefore, during the first ten months following construction, the active pores underwent a rearrangement that yielded a more conductive growing substrate with increased spatial variability. Increased infiltration capacity for both near- and quasi-saturated conditions is expected to affect the detention capacity of the green roof as rainfall will flow more rapidly through the growing medium with increased outflow peak rate and reduced delay between rainstorm and runoff.

The field campaign conducted after five operating seasons yielded a median i_s value of 51.9 mm/h under near-saturated conditions ($h_0 = -30$ mm) and 267.7 mm/h under quasi-saturated conditions ($h_0 = -5$ mm) (Table 2). Compared to the values collected at the end of the first growing season (T1), median infiltration rate significantly decreased by a factor of 1.71 at $h_0 = -30$ mm but was practically unaffected under quasi-saturated conditions (i.e., i_s decreased by a not significantly factor of 1.02). At T2 sampling date, the maximum spatial variability of the considered monitoring period was observed, with a ratio between IQR and median values of i_s equal to 0.943 and 0.715 for $h_0 = -30$ and -5 mm, respectively (Fig. 4).

At $h_0 = -30$ mm, the long-term (T2) median i_s value was intermediate between the initial (T0) and the short-term (T1) median values. However, the maximum i_s at T2 was close to the maximum i_s value observed at T1 and around 28% of the i_s data collected at T2 were lower than the minimum value observed at T0 (Fig. 3). At $h_0 = -5$ mm, the long-term (T2) and short-term (T1) median i_s values coincided and 22% of long-term i_s data were higher than the maximum value observed at the end of the first operating season. In summary, long-term modifications increased variability but did not increased the average infiltration rate of the growing substrate as could be expected if the washing off process suggested by Alagna, Bagarello, Concialdi, Giordano and Iovino [17] had continued to

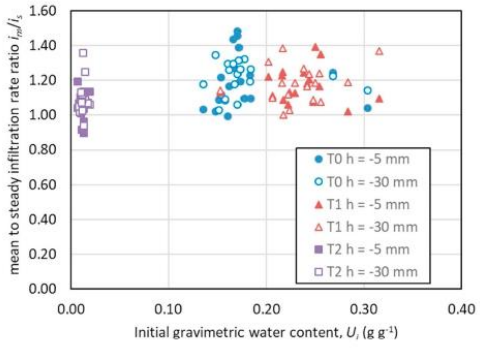

Fig. 2. Ratio between the mean infiltration rate and the steady-state infiltration rate, i_m/i_s, vs. initial gravimetric moisture content, U_i, of the experimental plot for field experiments conducted at the two pressure head values ($h_0 = -30$ and -5 mm).

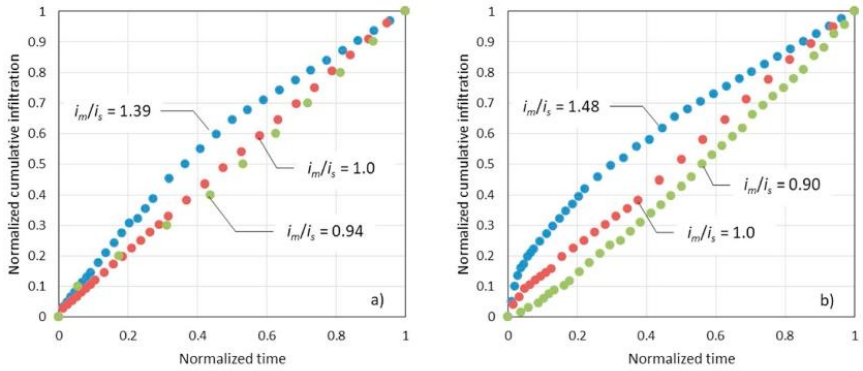

Fig. 3. Examples of normalized cumulative infiltration (I/I_f) curves corresponding to maximum, minimum and unity values of the ratio between the mean and the steady-state infiltration rates (I_f = cumulative infiltration corresponding to final time t_f); a) pressure head, $h_0 = -30$ mm, b) pressure head, $h_0 = -5$ mm.

Table 2
Statistics of steady-state infiltration rate, i_s (mm h^{-1}), for the different sampling dates and applied pressure heads.

	$h_0 = -30$ mm			$h_0 = -5$ mm		
	T0	T1	T2	T0	T1	T2
N	18	18	18	18	18	18
min	34.2	71.1	12.6	61.3	135.6	75.5
max	40.4	150.9	150.8	298.7	327.9	602.3
median	37.5 a	89.2 c	51.9 b	147.8 a	274.3 b	267.7 b
IQR	0.1	35.2	49.0	66.8	150.2	191.4

For a given pressure head value, values followed by the same letter are not significantly different ($P = 0.05$).

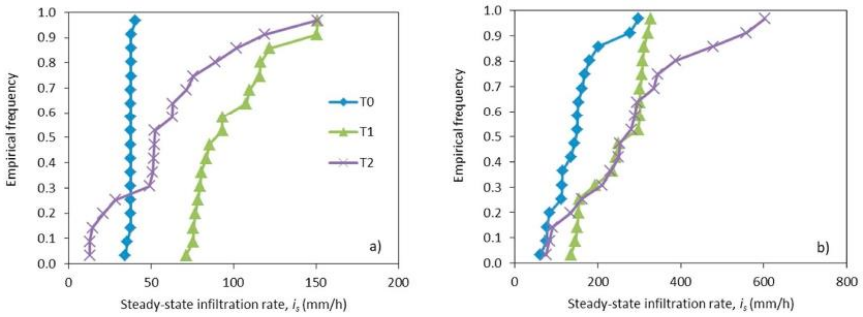

Fig. 4. Empirical frequency distributions of steady-state infiltration rate, i_s, determined at the two pressure head values ($h_0 = -30$ and -5 mm) for the three sampling dates; a) $h_0 = -30$ mm, b) $h_0 = -5$ mm.

operate in the spell from T1 to T2. The long-term detention capacity of the green roof is therefore relatively unaffected by aging and it should be expected that, following the decay of the first operating season, the hydrological performances will preserve with time. However, the increased heterogeneity of infiltration characteristics at T2 should be considered with caution given that, in specific spots of the vegetated roof, the detention properties could be severely jeopardized as a consequence of extremely high values of i_s under quasi-saturated conditions (Fig. 4).

Trying to explain the increased spatial variability of infiltration characteristics at T2, two possible phenomena could be invoked. One is the root growth that resulted in an uneven occlusion of conducting pores [5,30]. Another, is the onset of hydrophobicity due to vegetation exudates and decomposing materials [31,32]. Indeed, the characteristic upward concavity of the cumulative infiltration curve was observed only in four out of 36 infiltration runs conducted at T2 (Fig. 2). Both phenomena (i.e., root development and

hydrophobicity) can concur to reduce infiltration rate in smaller pores as they can be more easily occluded by roots and more affected by hydrophobicity than the large pores [33,34].

3.2. Laboratory experiments

The different initial water content of the soil columns affected the duration of the experiments. Near-saturated infiltration tests ($h_0 = -30$ mm) were conducted under substrate dry conditions as the initial gravimetric water content ranged from 0.019 to 0.024 g g^{-1} with a mean value of 0.022 g g^{-1} (coefficient of variation, CV = 5.47%). Average duration of the experiments was 1.35 h but a high variability was observed with a range between minimum and maximum duration of 4.10 h. Infiltration experiments at $h_0 = -5$ mm were conducted under much wetter conditions (mean $U_i = 0.342$, CV = 5.43%) and the total volume of the MDI reservoir (approximately 85 cm^3) took from 0.03 to 0.93 h to completely infiltrate into the soil column (mean duration 0.21 h). Independently of the applied pressure head at the column surface, a clear steady-state infiltration condition was always detected following a more or less prolonged transient stage. Coefficients of determination for the regression between measured and estimated $I(t)$ data were always greater than 0.9937 (mean $R^2 = 0.9986$). The average maximum relative error between the regression line and the measured I values was 2.1% and the threshold of 5% for E_{max} was exceeded only in two out of 54 infiltration experiments. The estimated i_s values can thus be considered representative of the steady-state 1D infiltration process in the repacked soil columns.

For both near-saturated ($h_0 = -30$ mm) and quasi-saturated ($h_0 = -5$ mm) conditions, the slope of the regression line between mean infiltration rate, i_m, and steady-state infiltration rate, i_s, was not different from unity ($P = 0.05$) and the mean ratio i_m/i_s was 1.24 and 1.22, respectively. Notwithstanding the different initial moisture content, the two mean i_m/i_s values were not statistically different thus confirming that the influence of capillarity was generally negligible for the substrate under study. The condition $i_m/i_s < 1$, indicating occurrence of hydrophobicity, was observed for a relatively high number of experiments (18 out of 54) mostly conducted under quasi-saturated conditions ($h_0 = -5$ mm). In particular, hydrophobic conditions ($i_m/i_s < 1$) were observed in 7 out of 9 experiments on non-washed (NW) samples.

The mean steady-state infiltration rate for the non-washed columns was 29.4 mm/h under near-saturated conditions (minimum $i_s = 1.9$ mm/h, maximum $i_s = 134.5$ mm/h) and 717.3 mm/h under quasi-saturated condition (minimum $i_s = 107.2$ mm/h, maximum $i_s = 1569$ mm/h) (Table 3). Increasing the surface pressure head from −30 to −5 mm thus determined, on average, more than one order of magnitude increase of the steady-state infiltration rate. Following simulated rainfall, the mean i_s increased by a factor of 1.50 at $h_0 = -30$ mm whereas it decreased by a factor of 1.25 for $h_0 = -5$ mm. In both cases differences were not significant.

Boxplot of i_s data estimated at $h_0 = -30$ mm for non-washed conditions (Fig. 5) highlighted the presence of an outlier, that is a single i_s data point that was more than twice the upper quartile value. When this outlier was disregarded, the mean i_s for UP-NW reduced to 16.3 mm/h and the difference between mean i_s values measured in the upper layer before and after washing resulted significant. Therefore, as a consequence of rainfall washing off, small pores contribution ($d_e < 1$ mm) tended to increase whereas large pores ($d_e > 1$ mm) contribution was practically unaffected (Fig. 5). This finding was not surprising given it is likely that prolonged leaching of samples mobilized the fine particles of the upper layer while the coarse ones, that are less mobile, remained in-situ. In agreement with this interpretation, variability of near-saturated i_s reduced (CV decreased from 141% to 87%) but remained almost the same for quasi-saturated i_s (Table 3).

Independently of the applied pressure head, after simulated rainfall the mean steady-state i_s of the bottom half of the columns was significantly lower than the upper one. The differences between the upper and the lower parts of the column were more pronounced for the experiments conducted under near-saturated conditions for which the steady-state infiltration rate decreased by a factor of 5.3 whereas under quasi-saturated conditions i_s decreased by a factor of 3.4. This result is also reasonable as it shows that small pores are more prone to the clogging phenomena determined by the fine particles washed off from the upper layer.

Seasonal modifications of green roof infiltration characteristics were more pronounced under field than laboratory conditions. In the time interval from T0 to T1, surface roof i_s increased by a significant factor of 1.9–2.4 depending on the applied pressure head (Table 2). Application of similar rainfall depth on the laboratory soil columns did not reveal significant changes in i_s or it suggested an increase on near-saturated i_s by neglecting a single data point (Table 3). Two counteracting factors likely contributed to the different findings for laboratory and field experiments: i) the mechanical compaction operated by rainfall; ii) the presence of plants. The total seasonal rainfall was applied in only three steps on laboratory soil columns thus promoting mechanical compaction of substrate that did not occur under natural rainfall. As a matter of fact, a small but significant change of ρ_b that increased from 1.13 to 1.15 kg m^{-3} (i.

Table 3
Statistics of steady-state infiltration rate for the upper (UP) and lower (LW) part of the substrate columns before (NW) and after the sample washing (W).

	near-saturated conditions $h_0 = -30$ mm			quasi-saturated conditions $h_0 = -5$ mm		
	UP–NW	UP–W	LW - W	UP–NW	UP–W	LW - W
N	9	9	9	9	9	9
min	1.9	6.2	2.5	107.2	150.4	15.2
max	134.5	129.7	24.3	1569.2	1265.7	384.3
mean	29.4 b	44.1 b	8.3 a	717.3 b	575.2 b	170.8 a
CV	140.7	86.6	78.3	75.8	69.8	90.8

For a given pressure head value, values followed by the same letter are not significantly different ($P = 0.05$).

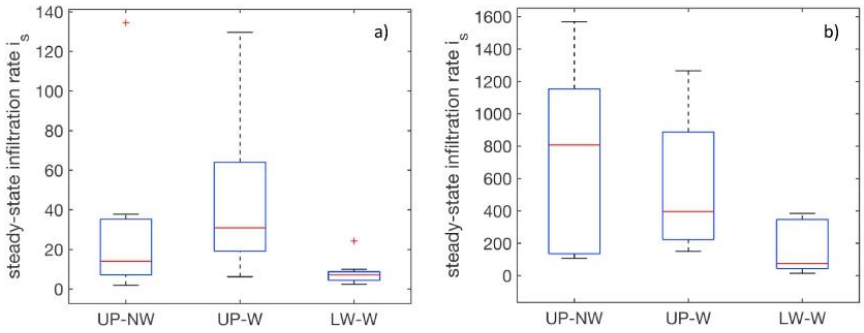

Fig. 5. Boxplot of steady-state infiltration rates collected for: a) near-saturated ($h_o = -30$ mm) and, b) quasi-saturated ($h_o = -5$ mm) conditions in the upper (UP) part of the columns before (NW) and after (W) simulated rainfall and in the lower (LW) part on the columns after simulated rainfall.

e., by a factor of 1.02) was observed for laboratory columns (Table 4). The substrate compaction, and the subsequent reduction of porosity, could have masked the effects of self-filtration thus yielding nearly stable or little variable i_s values in the upper layer of the columns. Conversely, under field conditions, plant canopy likely shielded the soil surface while roots contributed to maintain more conductive conditions in the upper layer of the growing media. Alagna, Bagarello, Concialdi, Giordano and Iovino [17] reported that the final bulk density of the upper layer was 0.85 times the bulk density at the time of roof construction thus showing that compaction due rainfall was not effective under field conditions. As a consequence, the self-filtration process was more effective in increasing the infiltration rates of field substrate.

Nevertheless, simulated rainfall modified the vertical distribution of substrate ρ_b with the upper layer of the soil column that was less compacted (mean $\rho_b = 1.083$ kg m^{-3}) and the lower layer that was more compacted (mean $\rho_b = 1.218$ kg m^{-3}) than the unwashed one (mean $\rho_b = 1.131$ kg m^{-3}) (Table 4). The observed changes in ρ_b were in agreement with changes in steady-state infiltration rate highlighting an increase of fine particle in the bottom layer and a decrease of fine particles in the upper layer.

Comparison of the relative proportions of the particles in a given texture class in the two halves of the columns (Fig. 6) showed that, after the simulated rainfall, the lower part of the sample enriched in small particles. Assuming that, for a given texture class, the initial vertical distribution of particle was uniform (i.e., 50% by weight of the particles in the upper part of the column and 50% in the lower part), the percentage of the fine particles tended to increase in the lower layer and decrease in the upper layer. This finding confirmed that the finest particles were mobilized from the upper layer and settled in the lower layer following the process referred to as self-filtration [9]. The phenomenon was particularly noticeable for particles with diameter smaller than 0.5 mm which likely were more mobile along the profile. For these fractions, the relative proportion in the lower layer increased up to 16%. Settling of fine particle determined phenomena of pore clogging in the lower layer of the soil columns that were considered the main cause of the observed reductions in steady-state infiltration rate.

4. Conclusions

Following artificial rainfall that mimicked the cumulative seasonal rainfall having occurred between the T0 and T1 sampling dates, the steady-state infiltration rate of the upper layer of the soil columns was not significant different from the initial one. In the field, the steady-state infiltration rate increased by a factor of 2.4 for near-saturated condition and by a factor of 1.9 for quasi-saturated condition. In agreement between the laboratory and the field experiments, signs were detected that, following simulated rainfall, contribution of small pores to water infiltration tended to increase as a consequence of prolonged leaching that mobilized the fine particles of the upper layer while the coarse ones, that are less mobile, remained in-situ.

A possible motivation of the observed differences between field and laboratory measurements of the upper layer i_s, may rely in the different combinations of compaction and self-filtration induced by natural and simulated rainfalls. Specifically, under field condition, plant canopy likely protected substrate surface, thus preventing compaction of the upper layer, and decay of dead roots improved the ability of the porous medium to transmit water. In this case, washing off of fine particles was particularly efficient in promoting the increase of porosity as confirmed by final bulk density (T1) that was 0.85 times the initial (T0) one. For laboratory columns, the two processes, i.e., mechanical compaction and washing of fine particles, played a counteractive role thus influencing the infiltration characteristics exclusively for the small pore system.

Simulated rainfall significantly affected the steady-state infiltration rates of the lower part of columns that were 3.4–5.3 times lower than the upper ones with larger reductions associated to the pore class that are activated for near-saturated condition ($d_e < 1$ mm). The hypothesized self-filtration process was confirmed by modifications in particle size distribution as the percentage of the fine particles tended to increase in the lower layer and decrease in the upper layer. It was concluded that rainfall can influence short-term infiltration characteristics of the green roof as a consequence of the detachment of fine particles from the top layer and clogging in the bottom layer. The detention properties of the green roof may be severely hampered as rainfall will flow more rapidly through the growing

Table 4
Statistics of the dry bulk density of the substrate columns before (NW) and after the simulated rainfall (W) and for the upper (UP) and lower (LW) parts following simulated rainfall.

	NW	W	UP-W	LW-W
N	9	9	9	9
min	1.025	1.059	0.994	1.091
max	1.227	1.243	1.174	1.320
mean	1.131 a	1.151 b	1.083 A	1.218 B
CV	5.47	4.94	6.89	6.68

Values followed by the same lowercase or uppercase letter are not significantly different ($P = 0.05$).

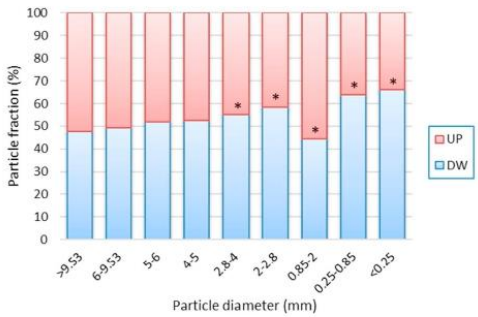

Fig. 6. Relative fractions of the particles in each considered diameter class after simulated rainfall.

medium due to increased steady-state infiltration rate close to saturation. Compared to the initial hydrological performance of the green roof, the outflow peak rate will be increased and delay between rainstorm and runoff reduced.

However, the field campaign conducted after five year of operation also showed that degradation of hydrological characteristics did not continue after the first growing season. Indeed, long-term modifications did not increase the average infiltration rate as could be expected if the self-filtration process had continued year after year. The lack of increases in i_s for quasi-saturated condition, or even the decrease for near-saturated one, was attributed to occlusion of small pores due to root development and onset of hydrophobicity due to vegetation exudates and decomposing materials. Uneven occurrence of both these phenomena explained the increased variability in infiltration characteristics.

Monitoring of infiltration characteristics is crucially important to detect modifications in green roof detention properties that could jeopardize most of their environmental benefits. Indeed, apart from the reduced ability to mitigate stormwater runoff, washing off of fine particle also reduces the retention properties of the growing medium thus hampering its ability to store water between two successive rainfalls. Therefore, plant water supply can be problematic for non-irrigated conditions. Also thermal properties of the vegetated roof may be affected with negative effects on building energy consumption. The simple and inexpensive MDI method proved to be effective in detecting both short- and long-term modifications of green roof hydrological properties directly in-situ and has the potential to be proposed as a routinely technique for temporal monitoring of aging phenomena that could compromise the benefits of the vegetated green infrastructures. A hydraulic characterization of the porous medium limited to its surface is not enough to properly describe its hydrological behaviour even if the thickness of the substrate is small.

Declaration of competing interest

The authors declare the following financial interests/personal relationships which may be considered as potential competing interests: Massimo Iovino reports financial support was provided by Government of Italy Ministry of Education University and Research. Vincenzo Bagarello reports financial support was provided by European Union Next-GenerationEU.

Acknowledgements

This study was carried out within the RETURN Extended Partnership and received funding from the European Union Next-GenerationEU (National Recovery and Resilience Plan – NRRP, Mission 4, Component 2, Investment 1.3 – D.D. 1243 August 2, 2022, PE0000005) and from Ministero dell'Istruzione, dell'Università e della Ricerca of Italy, project WATER4AGRIFOOD, contract "Tetto Verde", CON-0375, CUP B94I20000300005.

References

[1] Y. Li, R.W. Babcock Jr., Green roof hydrologic performance and modeling: a review, Water Sci. Technol. 69 (4) (2013) 727–738.
[2] V. Stovin, S. Poë, S. De-Ville, C. Berretta, The influence of substrate and vegetation configuration on green roof hydrological performance, Ecol. Eng. 85 (2015) 159–172.
[3] J. Czemiel Berndtsson, Green roof performance towards management of runoff water quantity and quality: a review, Ecol. Eng. 36 (4) (2010) 351–360.
[4] A.R. Dexter, Soil physical quality: Part I. Theory, effects of soil texture, density, and organic matter, and effects on root growth, Geoderma 120 (3) (2004) 201–214.
[5] K.M. Marcacci, J.M. Warren, E. Perfect, J.L. Labbé, Influence of living grass Roots and endophytic fungal hyphae on soil hydraulic properties, Rhizosphere 22 (2022), 100510.
[6] A. Schwen, G. Bodner, P. Scholl, G.D. Buchan, W. Loiskandl, Temporal dynamics of soil hydraulic properties and the water-conducting porosity under different tillage, Soil Tillage Res. 113 (2) (2011) 89–98.
[7] S. Le Coustumer, T.D. Fletcher, A. Deletic, S. Barraud, J.F. Lewis, Hydraulic performance of biofilter systems for stormwater management: influences of design and operation, J. Hydrol. 376 (1) (2009) 16–23.
[8] S. Lavrnić, V. Alagna, M. Iovino, S. Anconelli, D. Solimando, A. Toscano, Hydrological and hydraulic behaviour of a surface flow constructed wetland treating agricultural drainage water in northern Italy, Sci. Total Environ. 702 (2020), 134795.
[9] O. Dikinya, C. Hinz, G. Aylmore, Decrease in hydraulic conductivity and particle release associated with self-filtration in saturated soil columns, Geoderma 146 (1) (2008) 192–200.
[10] S. De-Ville, M. Menon, X. Jia, G. Reed, V. Stovin, The impact of green roof ageing on substrate characteristics and hydrological performance, J. Hydrol. 547 (2017) 332–344.
[11] K.L. Getter, D.B. Rowe, J.A. Andresen, Quantifying the effect of slope on extensive green roof stormwater retention, Ecol. Eng. 31 (4) (2007) 225–231.
[12] J. Mentens, D. Raes, M. Hermy, Green roofs as a tool for solving the rainwater runoff problem in the urbanized 21st century? Landsc. Urban Plann. 77 (3) (2006) 217–226.
[13] S. De-Ville, M. Menon, V. Stovin, Temporal variations in the potential hydrological performance of extensive green roof systems, J. Hydrol. 558 (2018) 564–578.
[14] H. Kasmin, V.R. Stovin, E.A. Hathway, Towards a generic rainfall-runoff model for green roofs, Water Sci. Technol. 62 (4) (2010) 898–905.
[15] V. Alagna, V. Bagarello, S. Di Prima, G. Giordano, M. Iovino, A simple field method to measure the hydrodynamic properties of soil surface crust, J. Agri. Eng. 44 (3s) (2013).
[16] R. Angulo-Jaramillo, V. Bagarello, M. Iovino, L. Lassabatere, Infiltration Measurements for Soil Hydraulic Characterization, Springer International Publishing, Cham, 2016, p. 383.
[17] V. Alagna, V. Bagarello, P. Concialdi, G. Giordano, M. Iovino, Evaluation of Green Roof Ageing Effects on Substrate Hydraulic Characteristics, Lecture Notes in Civil Engineering, 2020, pp. 89–97.
[18] H.W. Lilliefors, On the Kolmogorov-Smirnov test for normality with mean and variance unknown, J. Am. Stat. Assoc. 62 (318) (1967) 339–402.
[19] M.R. Spiegel, L.J. Stephens, Theory and Problems of Statistics, fourth ed. ed., McGraw-Hill, 2008.
[20] I. Mubarak, J.C. Mailhol, R. Angulo-Jaramillo, P. Ruelle, P. Boivin, M. Khaledian, Temporal variability in soil hydraulic properties under drip irrigation, Geoderma 150 (1–2) (2009) 158–165.
[21] A.W. Warrick, Appendix 1: spatial variability, in: D. Hillel (Ed.), Environmental Soil Physics, Academic Press, San Diego, CA, 1998, pp. 655–675.
[22] V. Bagarello, C. Di Stefano, M. Iovino, A. Sgroi, Using a transient infiltrometric technique for intensively sampling field-saturated hydraulic conductivity of a clay soil in two runoff plots, Hydrol. Process. 27 (24) (2013) 3415–3423.
[23] V. Bagarello, G. Caltabellotta, P. Concialdi, M. Iovino, Comparing two methods to perform a beerkan infiltration run in a loam soil at different dates, J. Hydrol. 617 (2023), 129095.
[24] V. Bagarello, M. Iovino, W.D. Reynolds, Measuring hydraulic conductivity in a cracking clay soil using the guelph permeameter, Trans. ASAE 42 (4) (1999) 957–964.
[25] L. Lassabatere, R. Angulo-Jaramillo, J.M.S. Ugalde, R. Cuenca, I. Braud, R. Haverkamp, Beerkan estimation of soil transfer parameters through infiltration experiments - BEST, Soil Sci. Soc. Am. J. 70 (2) (2006) 521–532.
[26] R. Haverkamp, P.J. Ross, K.R.J. Smettem, J.Y. Parlange, 3-Dimensional analysis of infiltration from the disc infiltrometer .2. Physically-based infiltration equation, Water Resour. Res. 30 (11) (1994) 2931–2935.
[27] M.R. Abou Najm, R.D. Stewart, S. Di Prima, L. Lassabatere, A simple correction term to model infiltration in water-repellent soils, Water Resour. Res. 57 (2) (2021), e2020WR028539.
[28] P. Concialdi, S. Di Prima, H.M. Bhanderi, R.D. Stewart, M.R. Abou Najm, M. Lal Gaur, R. Angulo-Jaramillo, L. Lassabatere, An open-source instrumentation package for intensive soil hydraulic characterization, J. Hydrol. 582 (2020), 124492.
[29] S.M. Beatty, J.E. Smith, Infiltration of water and ethanol solutions in water repellent post wildfire soils, J. Hydrol. 514 (0) (2014) 233–248.
[30] A.K. Leung, A. Garg, J.L. Coo, C.W.W. Ng, B.C.H. Hau, Effects of the roots of Cynodon dactylon and Schefflera heptaphylla on water infiltration rate and soil hydraulic conductivity, Hydrol. Process. 29 (15) (2015) 3342–3354.
[31] S.H. Doerr, R.A. Shakesby, R.P.D. Walsh, Soil water repellency: its causes, characteristics and hydro-geomorphological significance, Earth Sci. Rev. 51 (1–4) (2000) 33–65.
[32] M. Iovino, P. Pekárová, P.D. Hallett, J. Pekár, Ľ. Lichner, J. Mataix-Solera, V. Alagna, R. Walsh, A. Raffan, K. Schacht, M. Rodný, Extent and persistence of soil water repellency induced by pines in different geographic regions, J. Hydrol. Hydromechanics 66 (4) (2018) 360.
[33] P. Scholl, D. Leitner, G. Kammerer, W. Loiskandl, H.P. Kaul, G. Bodner, Root induced changes of effective 1D hydraulic properties in a soil column, Plant Soil 381 (1) (2014) 193–213.
[34] P. Nyman, G. Sheridan, P.N.J. Lane, Synergistic effects of water repellency and macropore flow on the hydraulic conductivity of a burned forest soil, south-east Australia, Hydrol. Process. 24 (20) (2010) 2871–2887.